DANMARKS OG GRØNLANDS GEOLOGISKE UNDERSØGELSE RAPPORT 2016/31

A reassessment of the Jameson Land Basin

Paul Knutz, Rasmus Rasmussen, Anders Mathiesen,
Pierpaolo Guarnieri, Morten Bjerager, Peter Japsen
& Jørgen Bojesen-Koefoed

GEOLOGICAL SURVEY OF DENMARK AND GREENLAND
DANISH MINISTRY OF ENERGY, UTILITIES AND CLIMATE

GEUS

DANMARKS OG GRØNLANDS GEOLOGISKE UNDERSØGELSE RAPPORT 2016/31

A reassessment of the Jameson Land Basin

Paul Knutz, Rasmus Rasmussen, Anders Mathiesen,
Pierpaolo Guarnieri, Morten Bjerager, Peter Japsen
& Jørgen Bojesen-Koefoed

Confidential report

Copy No.

Released 23-09-2024

GEOLOGICAL SURVEY OF DENMARK AND GREENLAND
DANISH MINISTRY OF ENERGY,UTILITIES AND CLIMATE

GEUS

Contents

EXECUTIVE SUMMARY

A reassessment of the Jameson Land Basin was carried out based on a new seismic interpretation study, including reprocessing of selected key seismic profiles, revised maturation modelling and fission-track analyses. The scope was to update the current knowledge on tectonic evolution, source rock development and play types within the license blocks held by Greenland Gas and Oil. The overall aim was to provide a sound basis for further derisking studies focussing on specific play targets in the license area

- The reprocessed seismic lines have improved the delineation of major seismic horizons, e.g. unconformities, fault structures and identification of depositional facies. Based on the regional seismic ties to the new data versions the non-reprocessed lines could be interpreted with higher confidence resulting in a more robust basin stratigraphy, except in the southern part of the area were data quality was inherently lower, probably related to the presence of sills/dykes. In addition to reprocessing the use of digital seismic data on modern interpretation platforms (Petrel) has enhanced the quality of interpretation significantly.

- In the previous study the post-Base Permian strata were interpreted as a relatively flat-lying package with no extensional basin development. Structural faults were inferred but linked to Carboniferous rifting. The new seismic–stratigraphic interpretation differs on several points: (1) It demonstrates a Triassic rift basin, trending NE-SW, with several fault-bounded depocentres, displaying thicknesses >2000 m, developed in the central and southwestern part of Jameson Land. (2) The post-Base Permian basin is much deeper displaying maximum depths of >8 km compared to 4.5 km in the old study. (3) Interpretation of the Jurassic units has provided more detailed knowledge on depth-structures and depocentre developments as well as depositional trends.

- Based on the current knowledge the prospectivity of the Jameson Land Basin relies on several high-quality source rocks (SR): Most importantly are (i) the marine Ravnefjeld Formation (Fm.) SR; (ii) the lacustrine Kap Stewart Group SR; and (iii) the marine Hareelv Fm SR. The latter two source rocks of the Jurassic succession are described from outcrops/boreholes within the licence area. The Ravnefjeld Fm. is known from outcrops north of the licence area but inferred to be widely present in the Permian basins.

- The revised basin modelling integrates the seismic interpretation with new maturity and apatite-fission track data. The key result is a thermal maturity assessment of the Jameson Land Basin that has focused further work towards relevant play types. This highlights the prospectivity of the Kap Stewart Group SR, but also several other potential source rock intervals that may have a significant potential for generating liquid hydrocarbons prior to the thermal alterations by volcanism. The updated basin model provides a framework for continued modelling that can test scenarios on timing and migration of petroleum generation to support the key play concepts.

- Of the four major play types considered in this study the early Jurassic post-rift and the Triassic syn-rift plays are the most relevant targets for further work. The criteria for this evaluation are primarily related to known source rock distribution, likelihood of high-quality reservoirs and burial depths in relation to assumed present-day oil window, which is strongly influenced by regional post-burial uplift/exhumation. Prospectivity of the Permian carbonate and the Late Jurassic clastic systems cannot be ruled out, but it is recommended that the Jurassic and Triassic plays be tested first in the process of derisking.

- The Early Jurassic clastic play (post-rift) is based on the presence of low-stand deltaic sandstone bodies that are interbedded and sealed by lacustrine anoxic mudstone of the Kap Stewart Group. The play area extends over the central-southern part of Jameson Land and is favoured by the alignment between the seismic interpretation and the sedimentological model of “forced regressions”. In addition, the play type is testable by shallow stratigraphic coring.

- In contrast to the local charge of the Early Jurassic play, the Triassic syn-rift play is more complex as it relies on hydrocarbons, derived from source rocks of the Permian Ravnefjeld Fm., having migrated updip through faults/fractures and accumulating in alluvial coarse-clastic deposits. The suggested trapping mechanism is a combination of up-dip stratigraphic pinch-out and structural closure along half-graben boundary faults. The crescent-shaped play area sheds focus on the north-northeastern basin margin where the seismic data favour structural traps, located up-section from potential Ravnefjeld Fm. strata. A major risks associated with the Triassic play is related to maturation history and migration pathways, which should be considered in further work.

- To accommodate the need for constraining critical parameters, e.g. source rocks levels, maturity gradients and reservoir properties, within the key play types, stratigraphic coring is recommended. Prime drilling targets are the Jurassic lake-to-marine transgressional sequence of the Kap Stewart and Neill Klinter groups, and if possible the uppermost interval of the Triassic rift sequence. Drilling localities have been suggested linked to key seismic profiles of the proposed play areas. Prior to a stratigraphic coring operation fieldwork should be accomplished to mitigate risks and facilitate site selection as well as drilling prognoses. In support of a fieldwork/drilling campaign it is suggested to carry out further reprocessing of relevant seismic lines, and perform a reservoir study of existing Triassic core material.

1. Introduction

Scope and objectives

The Jameson Land Basin (JLB) has traditionally been seen as an ”interior sag” or a graben-like feature, with faulted contacts to exposed basement towards the East and the West (Fig. 1.1) (Christiansen *et al.* 1991). Its northern limit is poorly defined and the southern limit is unknown since the basin fill is tilted gently towards the south where it continues beneath Scoresby Sund and under the plateau basalts of the Volquart Boon coast (Larsen & Marcussen 1992). The basin fill is thick, up to 17 km, consisting of Palaeozoic to late Mesozoic sediments. Up to seven potential source rock intervals have been presumed to be present or identified in the region, most importantly the Upper Permian (Ravnefjeld Fm), Late Triassic-Early Jurassic (Kap Stewart Group) and Upper Jurassic (Hareelv Fm). Within the sedimentary pile, intrusions of likely Paleogene age are common. Further to Neogene uplift (~Miocene), approximately 2 kilometres of presumably Upper Cretaceous sediments and Palaeogene volcanics have been removed by erosion.

According to the current petroleum strategy for Greenland, petroleum exploration in Jameson Land is underlain an ”open door” policy. In 2015 Greenland Gas and Oil acquired two license blocks covering about 2/3 of the Jameson Land Basin (total of 4,200 km^2) with a 10 year licence term and commitment to single well exploration. The scope of this report is to provide a re-evaluation of the petroleum potential of Jameson Land Basin that takes into account newly acquired data and recent developments on the tectonic evolution, including a suggested early Triassic rift phase (Guarnieri, 2015). To investigate further the implications of these findings, a new seismic-stratigraphic interpretation of the ARCO lines is considered of major importance. This involves a re-processing of key seismic lines with the aim to enhance visualisation of strata geometries, fault structures and sill/unconformity relationships. The revised tectonic-stratigraphic framework, combined with new information on source rock potential and uplift estimates, will provide input for a revised numerical modelling of the Jameson Land basin (Mathiesen et al., 1995) and update the play scenarios accordingly. The re-assessment will provide a sound basis for further de-risking studies focussing on specific play targets in the license area.

The report includes:

- Reprocessing procedure and outcome
- Stratigraphic framework
- Results from new seismic interpretation and mapping
- Revised tectonic model of the region
- Summary of source rocks
- Results from AFTA analyses
- Results from maturation modelling
- Play type characterisation and evaluation (play maps)
- Suggestions for further work

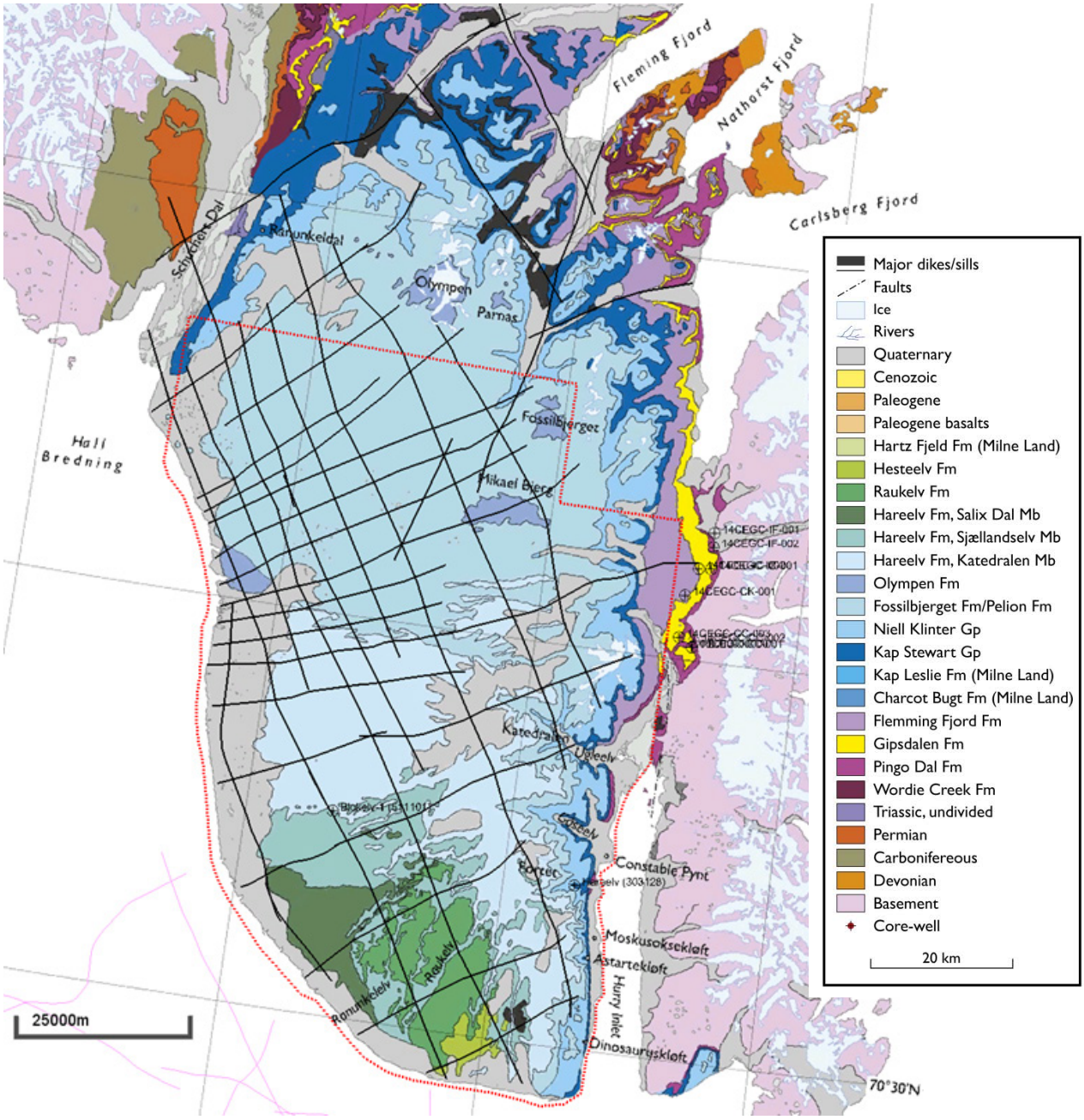

Figure 1.1. Geological map of Jameson Land and Liverpool Land with wells, ARCO seismic data (black lines) and GGO's licence area shown (red dotted line). GEUS boreholes Blokelv-1 and Hareelv-1 are indicated. Also shown are boreholes drilled by Avannaa in east Jameson Land south of Carlsberg Fjord (Klitdal area).

Exploration history

Initial systematic geological mapping of East and Northeast Greenland was carried out by a series of expeditions to the area over the year 1926 – 1958, all led by Lauge Koch. Through this remarkable pioneering effort the overall knowledge of the geology of the areas was established. Lauge Koch's work was primarily focused on areas north of 72°, but did to some extent also include Jameson. Over the years 1968-1972, the Geological Survey of Greenland (Grønlands Geologiske Undersøgelse, GGU, presently Geological Survey of Denmark and Greenland, GEUS) carried out a major mapping project in the greater Scoresbysund-area, through which our current understanding of Jameson Land was founded (Fig. 1.1). In addition to this, an important role has been played by the University of Copenhagen through which many different aspects of the geology of Jameson Land have been studied (Ineson & Surlyk, 2003). Other institutions include among others the Universities of Aarhus and Oslo as well as CASP (Cambridge Arctic Shelf Programme).

Petroleum geological investigations were carried out by the GGU in 1982-83, and in 1984 Atlantic Richfield Corporation (ARCO) was awarded a license in the area, after a dormant license from 1952 to Nordisk Mineselskab was nullified. ARCO initiated the work in 1985 by constructing a base and an air strip at Constable Pynt (Nerlerit Inaat). Vibroseismic surveys were carried out in the winters 1985-1986 and 1988-89, whereas seismic surveys using explosives were carried out in the summers of 1987, 1988, and 1989. In total approximately 1800 line-kilometres of seismics were recorded over the roughly 10.000 Km^2 large license area (Fig. 1.1). In addition, ARCO in collaboration with the GGU carried out various geological investigations, and drilled a number of shallow core-holes. In 1988 AGIP acquired 50 % of the license, but by as the first license term expired, the companies decided to relinquish the concession by the end of 1990.

In 2015 eight boreholes were drilled by Avannaa Exploration Ltd. in eastern Jameson Land, aimed at mineral exploration (Fig. 1.1). Penetration depths ranged from 62-513 m and a total of 1778 m was drilled, mainly recovering a Triassic sequence of mudstone with gypsum layers (Gipsdalen Formation) and coarse-clastic alluvial sediments (Pingo Dal Formation) (Holmes et al., 2014). An aeromagnetic survey (SkyTEM) was carried out to delineate structural features related to dykes and faults.

2. Reprocessing and data improvements

2.1 Data

A seismic data grid was collected 1986-1989 on Jameson Land (Fig. 1.1) by Atlantic Richfield Company (ARCO) resulting in approximately 1800 line km crossing an exposed Jurassic basin in central East Greenland. Some of the transects were collected in the summer season using dynamite as a source, while others were gathered during fall or spring based on a vibro-source. The data was analysed in the early 1990 in the context of understanding the basin development (Marcussen and Larsen, 1992) within the license area. Although the seismic data was generally of good quality the presence of sill intrusions presented a problem in maintaining a good signal response at depths greater than 1-2 s TWT, and consequently weakening the recognition of basin boundary faults, strata configurations and unconformities.

The scope of the present study was to attempt a new basic processing of the seismic data with the aim of improving the data quality which could benefit a new seismic interpretation of Jameson Land Basin. The primary data used for the seismic mapping in a Petrel seismic interpretation environment was 2D seismic lines collected by ARCO 1986-89. A subset of 4 line segments: ARC/JL86-6v, ARC/JL86-3v, ARC/JL87-3d and ARC/JL86-5v (approximately 280 km, Fig. 2.1), were selected for re-processing based on their basin coverage and importance in terms of providing outcrop ties (in the following the ARC/JL prefix will be omitted).

2.2 Recording parameters

Source:	vibroseis:	line 86-3v, 86-5v and 86-6v
		No. of sources: 4
		No. of sweeps: 16
		90 m between source points
	dynamite:	line 87-3d
		90 m between source points
		Avg. shot depth: 15 m
Recording parameters:		split spread (at trace no. 24 or trace no. 36)
		120 channels (24 geophones/channel)
		30 m group distance
		Offset range +/-(-900 m to 3150 m or -1110 m to 2550 m)
Near offset:		30 m for dynamite source
		300 m for vibroseis source
Recording length:		16 sec for vibroseis data (sweep length 10 sec)
		12 sec for dynamite data

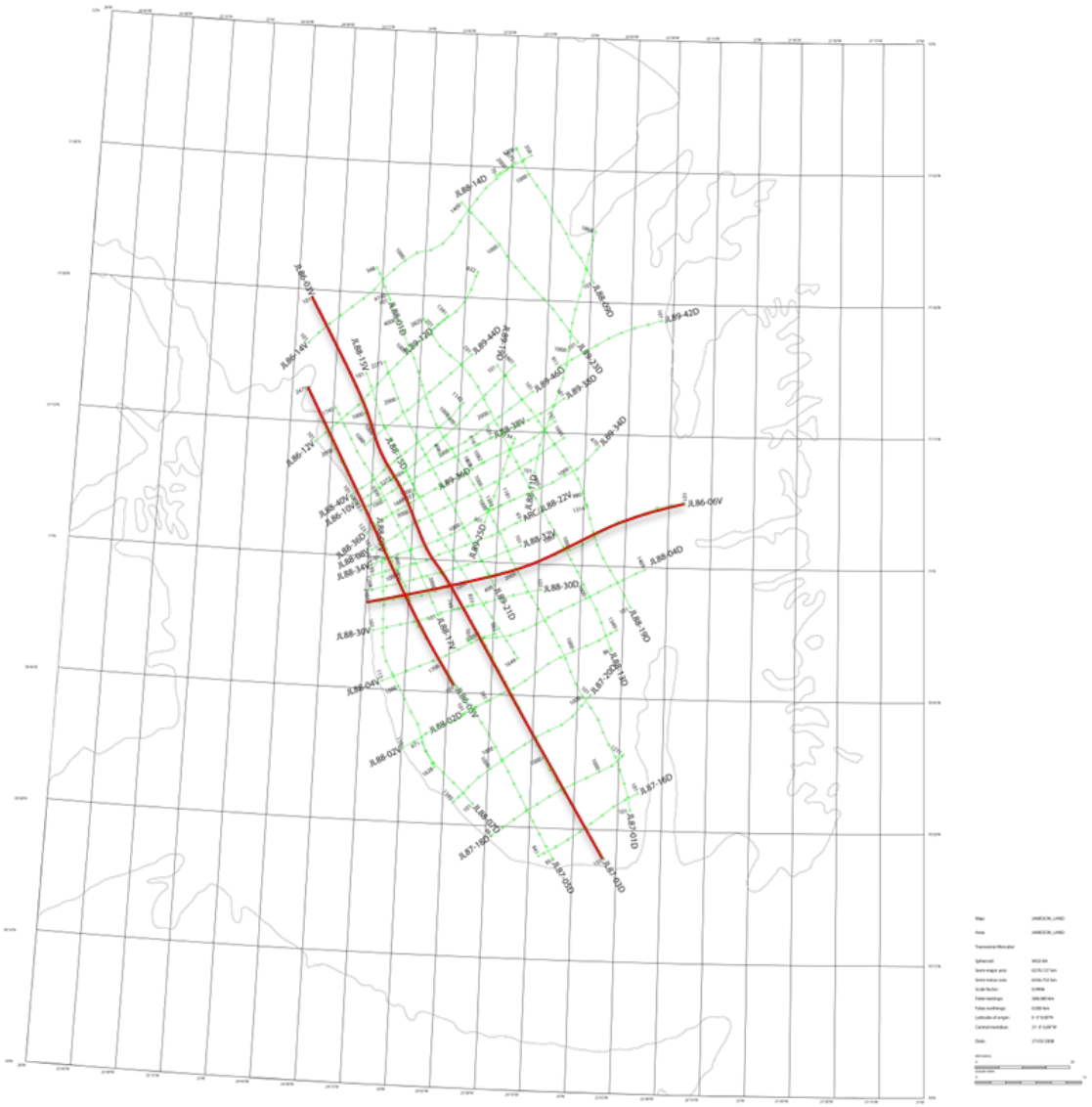

Figure. 2.1. ARCO data grid with reprocessed line sections shown in red.

2.3 Reprocessing testing and final processing sequence

The raw vibroseis acquisition data have been stored both in uncorrelated and correlated versions. For vibroseis line 86-5v and vibroseis line 86-6v the field correlated data versions have been used. For vibroseis line 86-3v the correlated version was incomplete, but by combining the raw uncorrelated and correlated data versions only the overlap zone between line 86-3v and 87-3d were affected, i.e. instead of full overlap between the two lines only taper zone data were available after combining raw correlated and raw

uncorrelated data for line 86-3v. For the 4 test lines only line 86-3v was influenced by missing raw data.

In principle the geometry setup is quite simple for the ARCO 1986-1989 datasets because of a fixed split-spread configuration for full line length. However, only the correlated vibroseis data contain trace header information for the station number. The uncorrelated vibroseis field data and the dynamite field data merely have the seismic field file identification (FFID) in the trace header. Consequently, for these data the station number identifier has to be picked manually from the paper-version observer logs.

For the reprocessing trial the complete processing sequence have been tested, but based on evaluation of the original dataset the main focus has been to improve the noise attenuation and to improve the seismic imaging.

FK-filtering in the shot domain is similar, but slightly weaker than the FK-filtering applied in the original processing. As opposed to the original processing the FK-shot domain filtering in the reprocessing work is followed by a relatively strong FK-filtering in the DMO-offset domain (trace distance 15 m). In addition to this time-frequency noise, attenuation of local noise bursts has been applied initially in the reprocessing (step 11 in the final processing sequence listed below). Finally, the FX-deconvolution process contributed substantially to the overall noise attenuation.

A 2-window surface-consistent deconvolution similar to the original processing has been chosen for the reprocessing trial. 2 ms was applied as the prediction distance (spiking) for the shallow application window, while 10 ms was applied below. The operator length is 200 ms for both deconvolution operators.

Similar to the original processing elevation static corrections (velocity 3300 m/s) to NMO processing datum and to final datum (860 m above MSL) has been applied. Other elevation velocities have been tested, but the test results confirmed the original choice of 3300 m/s for the elevation static correction. 3300 m/s elevation velocity is also supported by a generally good agreement with near-surface velocity measurements in the area. The original processing final datum start-time of the seismic data, corresponding to 860 m above MSL, has been kept in the reprocessing. A generalised hybrid/steepest ascent method has been used for the residual static correction.

The pre-stack Kirchoff time migration method has been tested against stack/post-stack migration and dip move-out (DMO/stack/post-stack migration) and was evaluated to be superior to these alternative approaches. To achieve the optimum result for the pre-stack time migration DMO-offset trace binning was tested. This indicated that the 15 m regular DMO-offset binning was superior to the coarser (and not equal trace distance) DMO binning.

In general the spacing between velocity locations is 6000 m, but depending on lateral complexity velocity picking down to 1000 m distance between velocity locations has been applied.

Final processing sequence:

1. Data loading of field data (and vibroseis correlation of the uncorrelated raw data used for line 86-3v)
2. Trace editing
3. -11 ms static shift of dynamite data for matching of dynamite and vibroseis data
4. 144 degree phase rotation of vibroseis data for matching towards original processing of the 1986-1989 surveys
5. Geometry setup inclusive DMO binning
6. Source/receiver consistency checking and trace QC
7. True amplitude recovery (0-2000ms: 15 dB/oct, 2000-3000 ms: 12 dB/oct, 3000-5000 ms: 3 dB/oct)
8. Spike and noise burst editing
9. Surface consistent amplitude scaling
10. Air blast attenuation (attenuation around 331 m/s)
11. Time frequency noise attenuation
12. Elevation statics to NMO datum (3300 m/s)
13. Two window surface consistent deconvolution (shallow depth:2-200, below 10-200)
14. FK-filtering in shot domain (velocities below 1800 m/s)
15. FK-filtering in DMO-offset domain (trace distance 15m, pass between +/-4 ms/tr)
16. Pre-stack time migration
17. Outer and inner trace mute
18. Residual statics
19. Stacking and static correction to final datum (860 m above MSL)
20. FX-deconvolution (window length: 500 ms, max frequency for filtering: 70 Hz)
21. TVF-filtering (low cut filters: 12-20, 5-12 and 3-8 Hz, high cut filters: 65-80, 55-70 and 45-60 Hz)
22. Robust AGC scaling in 1200 and 500 ms windows

2.4 Reprocessing results

In general important improvements have been obtained in the reprocessing (with a few exceptions for near surface data). Despite the general data improvements there is still a regional difference in data quality. In particularly the southern part of line 87-3d is noisy in comparison with the data quality further north.

In case of further reprocessing the processing sequence found in the present test study is expected to be directly applicable for all data from the ARC/JL surveys because the choice of processing parameters found for the test lines are expected to be representative for the survey area. Improvements in data quality for other seismic lines in the survey area are expected to be in good agreement with the improvements obtained in the present test study. Based on the knowledge gained in this study completeness of the archive data the ARC/JL seismic surveys should be checked at an early stage.

2.5 Improvements to seismic interpretation

In comparison with the previous study where interpretation was performed on paper-prints (Christiansen *et al.* 1991) the visualization of the digitized seismic data in Petrel already represents a significant advance in the potential for seismic-stratigraphic interpretation. Nevertheless, the old processing version is commonly marked by poor reflection continuity and noisy sections where reflections cross-cut, or become chaotic/erratic, notably along dipping or faulted sections (Figs. 3.2 – 3.5). The new pre-stack time-migrated (PSTM) processing versions of the subset seismic lines have improved the potential for interpretation based on seismic-stratigraphic concepts and recognition of strata terminations. The improvements are in particular seen by reduced noise and better horizon continuity, which has resulted in enhanced recognition of strata terminations, e.g. unconformities, and a better definition of reflection geometries, notably in the shallow part (<1500 ms). Moreover, definition of the basin boundaries and fault expressions have improved significantly,

An important task was to trace the Base Permian Unconformity, described as a regional peneplane (Ch. 5) from exposures northwest of Schuchert Dal and into the basin. This was potentially possible using lines 86-3v and 86-5v but on the old processing version the trace of the Base Permian was rather ambiguous (Fig. 3.2 and 3.3). The new seismic version afforded a much more robust interpretation of this unconformity, aided by software tools, e.g. horizon flattening. For the late Triassic – lower Jurassic package, tracing the laminar to sub-horizontal reflections, related to Top Fleming Fjord Fm and the Top Kap Stewart Group, was to some extent possible using the old data version. However, the new version provides a much more accurate representation of the strata and thus the bounding horizons can be traced with a high level of confidence from the outcrops and into the basin (Fig. 3.4 and 3.5). Despite the rather subdued nature of the basin bounding faults the reprocessing provided enhancements in the interpretation of fault structures (Figs. 3.2-3.5). An example of is seen in Fig. 3.5 were a fault is insinuated in the old processing version but a more robust interpretation relies on the new version. In summary, the more robust interpretation of the general basin geometry and seismic reflectors correlated to surface exposures based on the new PSTM profiles have strengthened the stratigraphic and tectonic interpretation of the entire area covered by the ARCO seismic data.

2.6 Conclusions

Reprocessing parameters differ from original processing by:

- FK- filtering both in source and offset domain in order to reduce strongly dipping noise (only source domain in the original dataset).
- Pre-stack time domain migration (DMO processing followed by post-stack migration for the original processing).
- The processing sequence derived in the present test study is expected to be directly applicable for all data from the ARC/JL surveys.

Improvements generated by new processing:

- Reduced noise, resulting in better horizon continuity and definition of seismic geometries.
- Enhanced recognition of major horizons, e.g. basin-wide unconformities.
- Improved definition of seismic facies linked with depositional processes.
- Improved fault tracing.

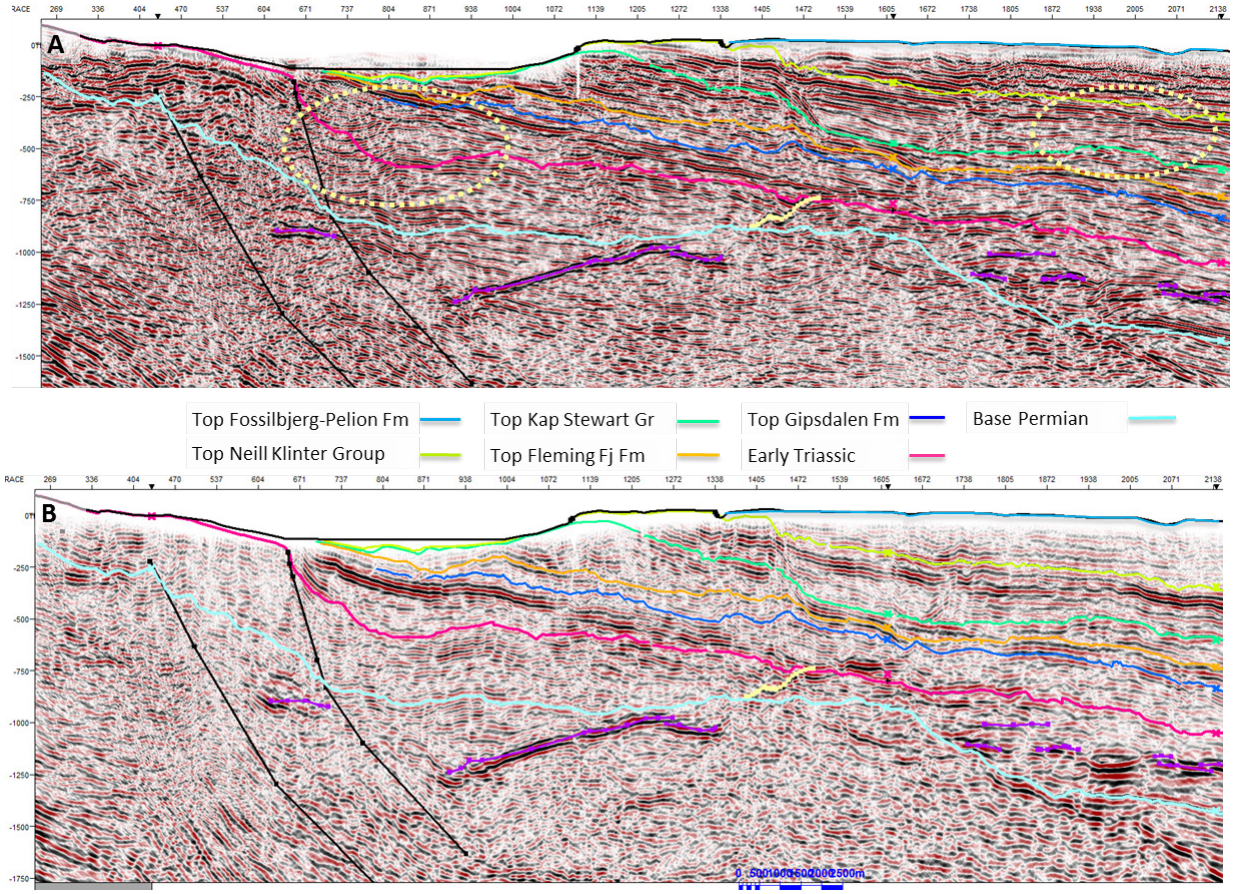

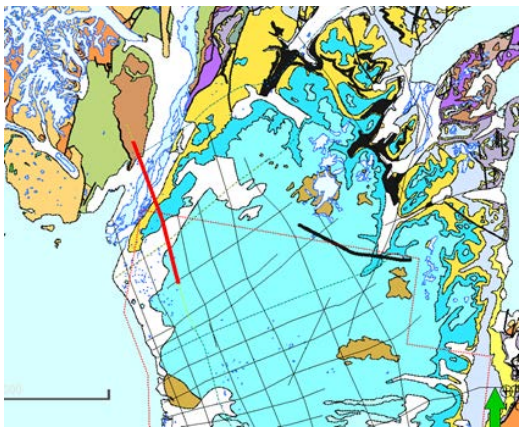

Figure 3.2. (a) Old processing version and (b) new processing version of line 86-3v. Horizons are interpreted based on the new version. Examples of improved reflection continuity are highlighted (yellow ellipsoides). Location of profile is shown on map.

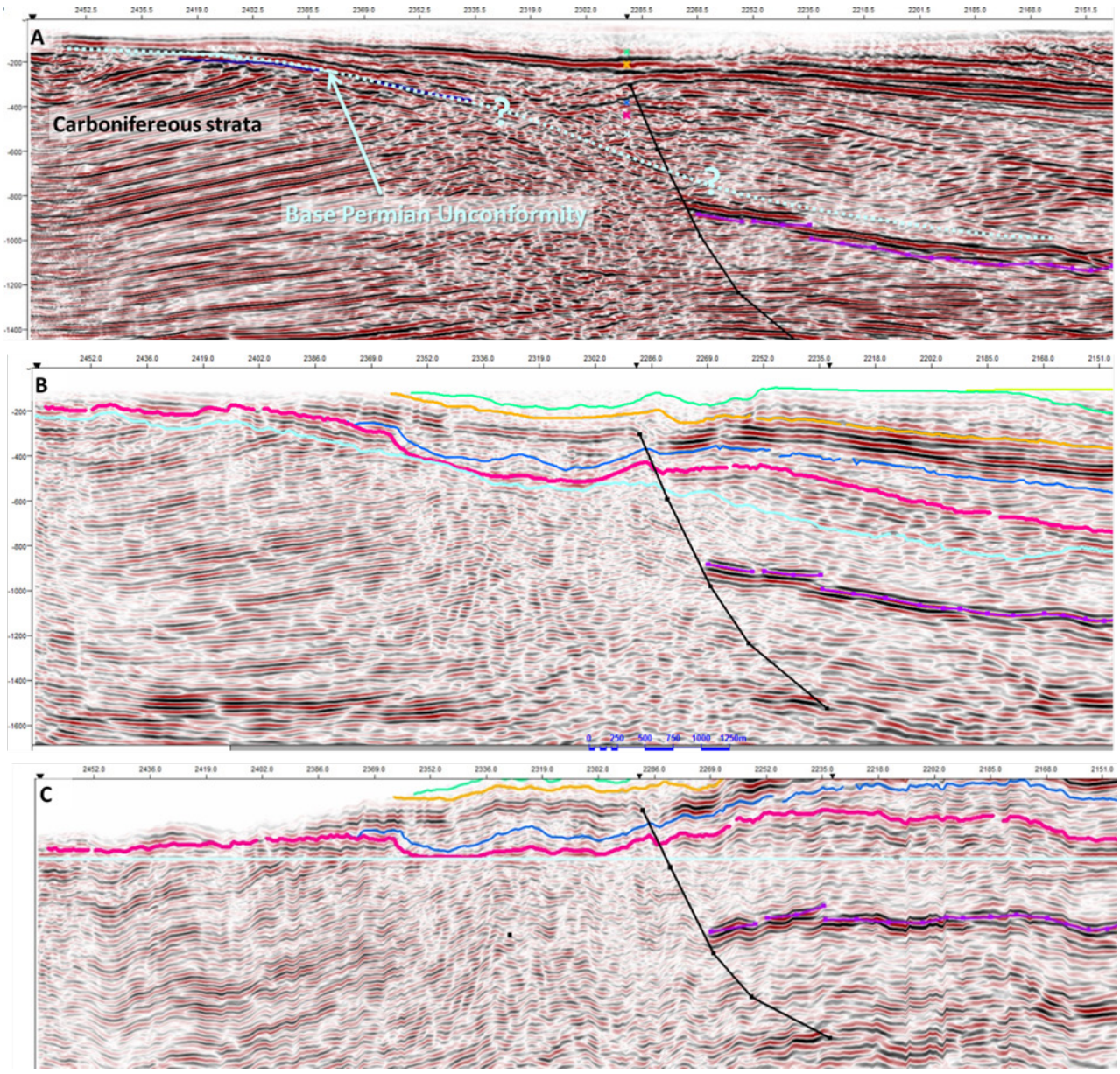

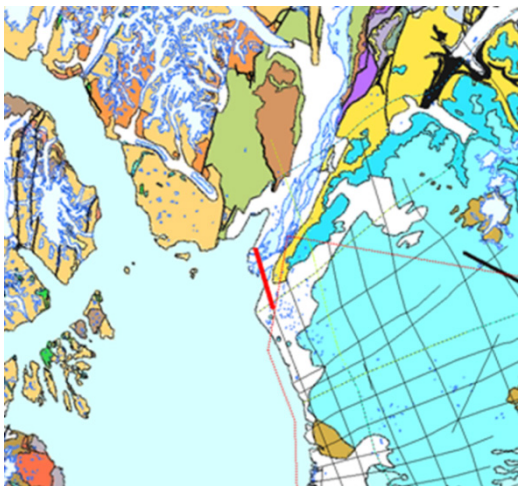

Figure 3.3. (a) Old processing version and (b) new processing version of line 86-5v at its northwest limit were seismic horizons can be groundtruthed to Carboniferous-Permian outcrops. Panel c show the new seismic processing flattened on the Base Permian unconformity. Location of profile is shown on map. Horizon names as in Fig. 3.2.

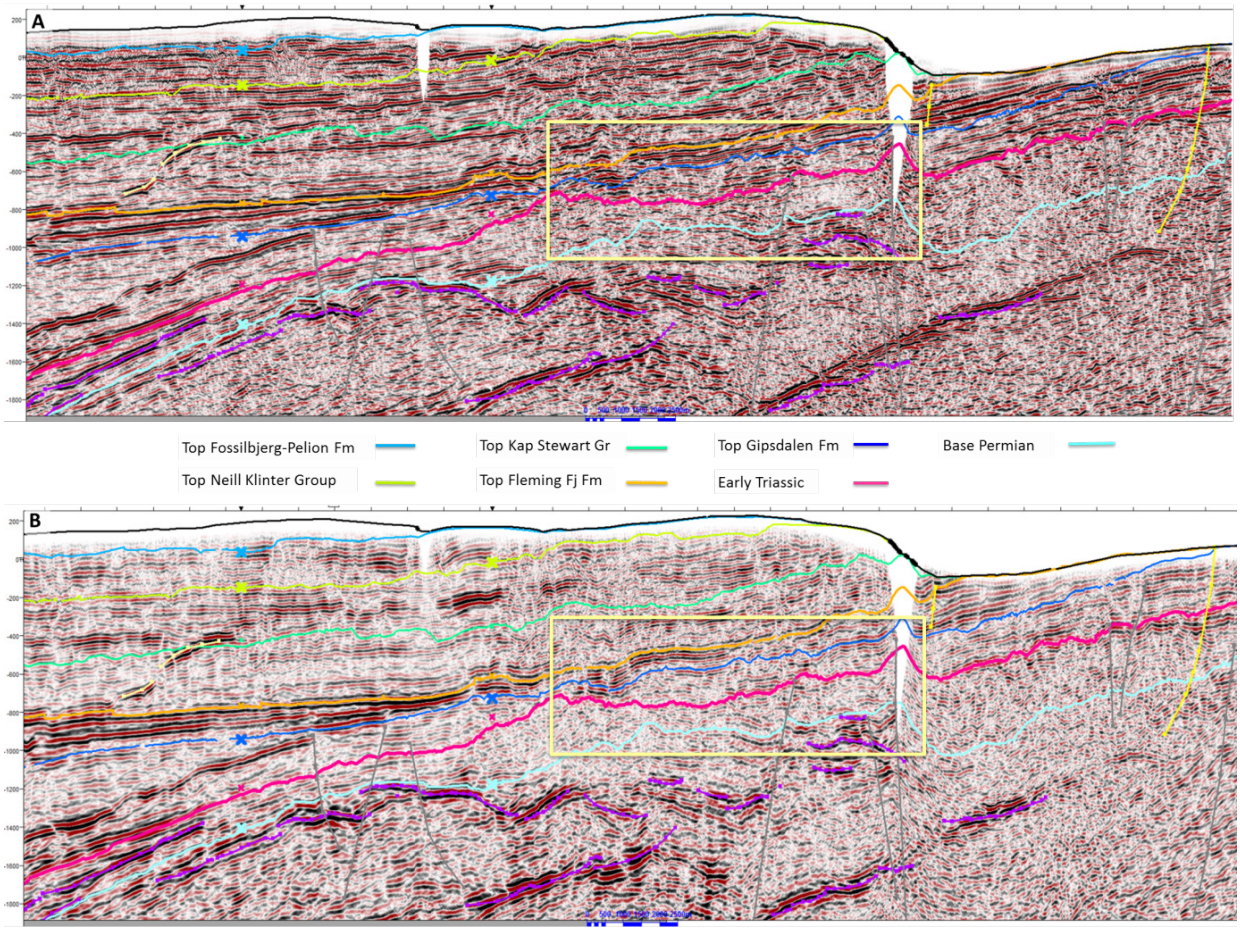

Figure 3.4. (a) Old processing version and (b) new processing version of line 86-6v at its eastern limit were seismic horizons can be verified in outcrop to Upper Triassic and Jurassic units. Yellow box indicate the detailed sections shown in Fig. 3.5.

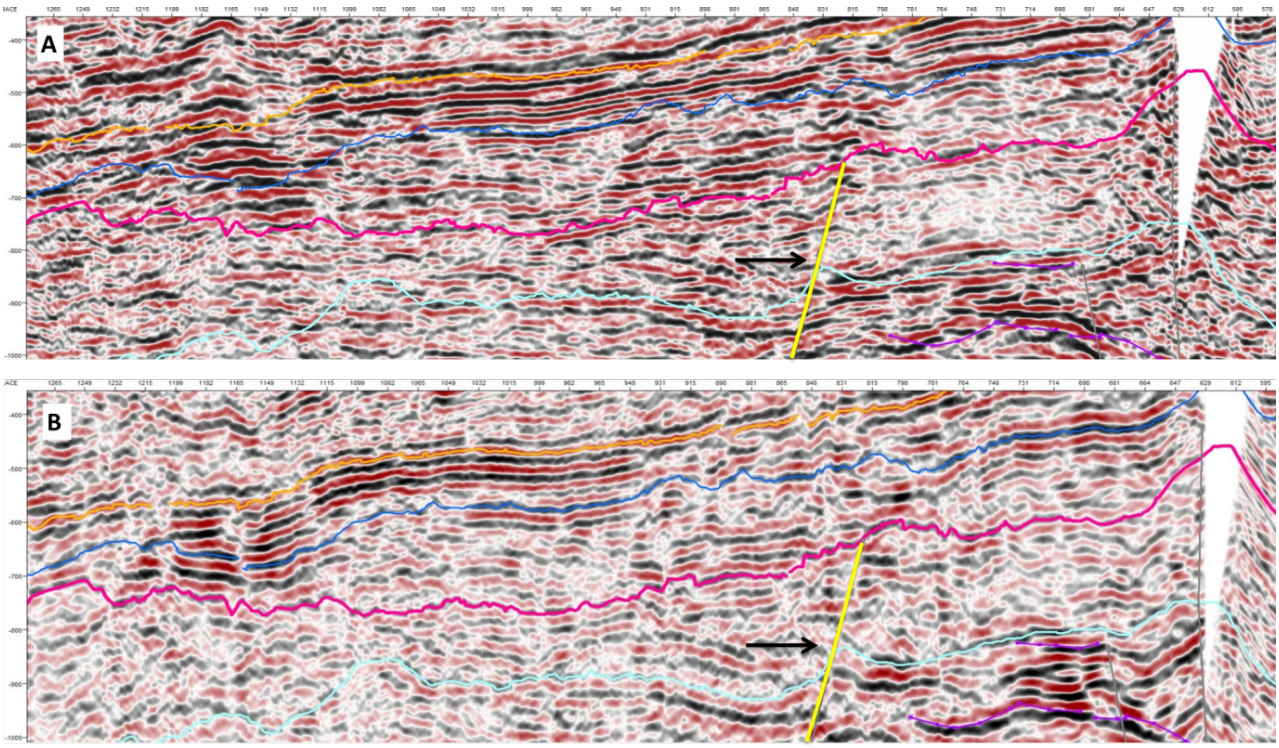

Figure 3.5. Detailed images representing (a) old and (b) new processing version of line 86-6v. See position in Fig. 3.5. Note the improvement of the fault trace interpretation showing displacement of the Base Permian unconformity with >60 ms.

:

3. Stratigraphy of the Jameson Land Basin

The Jameson Land Basin (JLB) represents a post-Caledonian record of Late Paleozoic – Mesozoic extensional basin formation, followed by oceanic breakup at the Paleocene–Eocene transition. The base Middle Devonian unconformity marks the change from Caledonian thrusting to initial Devonian rifting (extensional collapse of the Caledonian foldbelt) controlled by NNE–SSW trending extensional faults and N–S trending sinistral wrenching (Larsen et al. 2008). The latest Devonian–Carboniferous interval was characterized by formation of continental west-dipping narrow half-grabens (Stemmerik et al. 1991). The Late Carboniferous – early Permian uplift, erosion and formation of a regional peneplain in Northeast Greenland was followed by late Permian subsidence, minor rifting and a marine transgression (Surlyk et al. 1986). Late Permian–earliest Triassic rifting controlled marine-dominated deposition in mainly westerly-tilted half-grabens. A prominent earliest Triassic flooding resulted in a marine connection between East Greenland, Norway and Svalbard (Seidler et al. 2004; Bjerager et al. 2006). Rifting with borderland uplift events continued in the Early – Middle Triassic with mainly fluvial deposition, and followed by thermal subsidence and continued continental and lacustrine dominated deposition with a rift pulse in the Norian. Early–Middle Jurassic thermal subsidence in the JBL controlled deposition in terrestrial–lacustrine and shallow-marine environments (Surlyk 2003). This was succeeded by Middle Jurassic transgression with marine deposition that continued into the Early Cretaceous. Elsewhere in the region the Cretaceous period was characterised mainly by thermal subsidence with minor fault episodes (Whitham et al. 1999). This was followed by Late Cretaceous uplift whereas the offshore Danmarkshavn and Thetis Basins continued to subside and accumulate sediments (Hamann et al. 2005). The early Paleogene breakup unconformity is marked by extrusion of extensive flood basalts, especially south of Jameson Land. Intrusions of sills and dikes are prominent features in the JLB (Larsen & Saunders, 1998; Upton et al. 1995).

3.1 Devonian–Carboniferous

Devonian rocks are exposed in Canning Land and Wegener Halvø to the NE, and they are seismically interpreted in the deep buried parts of Jameson Land (Larsen et al. 2008). The exposed part is included in the Nathorst Fjord Group and comprises volcanics, c. 1 km thick, overlain by alluvial conglomerates, sandstones and siltstones, c. 3 km thick. Uppermost Devonian–Carboniferous sediments in the region are included in the Traill Ø Group (Vigran et al. 1999). It comprises an up to 3 km thick halfgraben succession subdivided into two overall units that are separated by a major mid-Carboniferous (Visian–Westphalian) angular unconformity. The lower unit is not exposed in Jameson Land, but northwards it consists of Tournasian–Visian fluvial and floodplain sediments. The upper unit (Westphalian and younger) comprise basin marginal alluvial fans that passes laterally eastward into fine flood plain deposits. The depositional systems were expanded and formations of new half-grabens with a basal unconformity against Devonian or older crystalline rocks are recorded in Jameson Land (Stemmerik et al. 1991).

Figure 3.1 (Next page) Stratigraphical scheme of the Jameson Land Basin

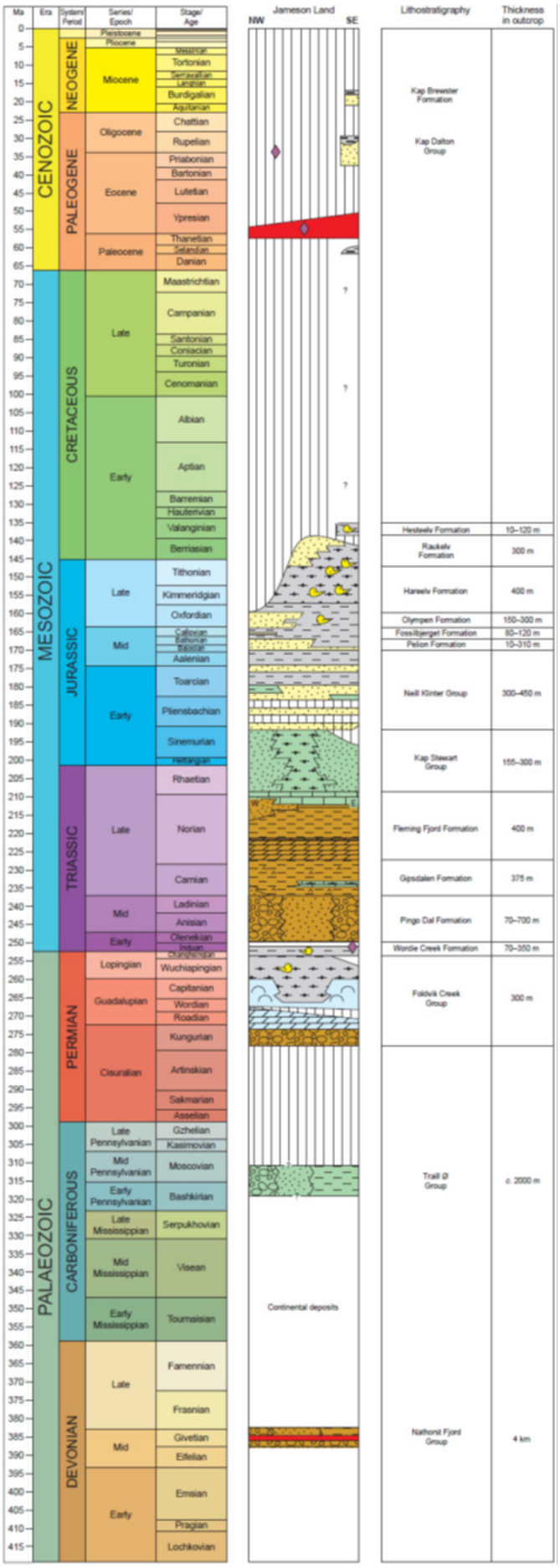
Ma
Era
System/ Period
Series/ Epoch
Stage/ Age
Jameson Land
NW
SE
Lithostratigraphy
Thickness in outcrop
CENOZOIC
MESOZOIC
PALAEOZOIC
NEOGENE
PALEOGENE
CRETACEOUS
JURASSIC
TRIASSIC
PERMIAN
CARBONIFEROUS
DEVONIAN
Pleistocene
Pliocene
Miocene
Messinian
Tortonian
Serravallian
Langhian
Burdigalian
Aquitanian
Oligocene
Chattian
Rupelian
Eocene
Priabonian
Bartonian
Lutetian
Ypresian
Paleocene
Thanetian
Selandian
Danian
Late
Maastrichtian
Campanian
Santonian
Coniacian
Turonian
Cenomanian
Early
Albian
Aptian
Barremian
Hauterivian
Valanginian
Berriasian
Late
Tithonian
Kimmeridgian
Oxfordian
Mid
Callovian
Bathonian
Bajocian
Aalenian
Early
Toarcian
Pliensbachian
Sinemurian
Hettangian
Late
Rhaetian
Norian
Carnian
Mid
Ladinian
Anisian
Early
Olenekian
Induan
Changhsingian
Lopingian
Wuchiapingian
Guadalupian
Capitanian
Wordian
Roadian
Cisuralian
Kungurian
Artinskian
Sakmarian
Asselian
Late Pennsylvanian
Gzhelian
Kasimovian
Mid Pennsylvanian
Moscovian
Early Pennsylvanian
Bashkirian
Late Mississippian
Serpukhovian
Mid Mississippian
Visean
Early Mississippian
Tournaisian
Late
Famennian
Frasnian
Mid
Givetian
Eifelian
Early
Emsian
Pragian
Lochkovian
Kap Brewster Formation
Kap Dalton Group
Hesteelv Formation
10–120 m
Raukelv Formation
300 m
Hareelv Formation
400 m
Olympen Formation
150–300 m
Fossilbjerget Formation
80–120 m
Pelion Formation
10–310 m
Neill Klinter Group
300–450 m
Kap Stewart Group
155–300 m
Fleming Fjord Formation
400 m
Gipsdalen Formation
375 m
Pingo Dal Formation
70–700 m
Wordie Creek Formation
70–350 m
Foldvik Creek Group
300 m
Traill Ø Group
c. 2000 m
Nathorst Fjord Group
4 km
Continental deposits

3.2 Permian

An isolated continental syn-rift conglomerate succession, c. 1 km thick, is represented by the Middle–Upper Permian Røde Ø Conglomerate in the Rødefjord area west of Milne Land. It has previously been considered Carboniferous or Lower Permian but new age data suggest, that it is contemporaneous with the Huledal Formation in Jameson Land (Stemmerik and Piasecki 2004).

The regional mid-Permian peneplain in Jameson Land is erosionally overlain by the Upper Permian Foldvik Creek Group, which is up to about 300 m thick. The basal conglomerate of the Huledal Formation is fluvial with a marine layer in the top. It is succeeded by shallow marine – hyper saline carbonates and evaporates of the Karstryggen Formation that is capped by a major sequence boundary. The following transgression resulted in deposition of fully marine carbonate buildups of the Wegener Halvø Formation along basin margins and intra basinal highs and contemporaneous organic rich shales of the Ravnefjeld Formation in basinal positions (Stemmerik 2001). The top of the Permian consists of basinal bioturbated mudstones and sandy turbidites of the Schuchert Dal Formation (Kreiner-Møller and Stemmerik 2001).

3.3 Triassic

A prominent Permian–Triassic boundary unconformity is recorded at basin marginal positions in East Greenland. The associated hiatus expands towards the north with evidence of subaerial exposure and much of the Upper Permian has been removed by erosion prior to deposition of the Early Triassic Wordie Creek Formation (Surlyk et al. 1986). In the deeper basinal areas in the south, a complete marine Permian–Triassic boundary interval is recorded in a marine mudstone succession (Stemmerik et al. 2001).

The Lower Triassic Wordie Creek Formation is exposed in the northern part of Jameson Land along the eastern and western margins and ranges here from 70–350 m in thickness Perch-Nielsen et al 1974). Further north in deeper parts of the basin the formation is up to 1 km thick. It consists of marine shales and sandy turbidites and shows an overall shallowing upward trend into shoreface and coastal plain sandstones and mudstones (Seidler et al. 2004; Bjerager et al. 2006). A marked unconformity terminated marine deposition in East Greenland and was followed by deposition of rift-related alluvial conglomerates and sandstones of the Pingo Dal Formation. The coarse-grained sediments attain a thickness of 600 m and they were sourced from the western (Post Devonian Main Fault area) and the eastern (Liverpool Land) basin margins (Clemmensen 1980a,b). The succession shows an upwards gradual transition into fine-grained flood plain, freshwater and saline lacustrine and aeolian deposits of the Upper Triassic Gipsdalen and Flemming Fjord Formations (Clemmensen 1980a,b). The Gipsdalen Formation includes a thin Carnian unit of lagoonal to lacustrine organic rich mudstones of the Gråklint Beds (Andrews et al. 2014).

3.4 Jurassic

The Triassic–Jurassic boundary marks a transition towards temperate and humid climate in the JLB, represented by the Rhaetian–Sinemurian Kap Stewart Group, about 600 m thick (Surlyk 2003). The group comprises alluvial (Innakajik Fm.), deltaic (Primulaelv Fm.), and organic rich lacustrine (Rhætelv Fm.) deposits. The base of the group is unconformably overlying the Flemming Fjord Formation along the southeastern basin margin. It is overlain by the marine Neill Klinter Group, which is 300–450 m thick and deposited in shoreface, restricted offshore and tidal embayment environments during an overall Pliensbachian–Early Bajocian transgression (Dam and Surlyk 1998). Shallow marine sandstones are represented in Rævekløft, Gulehorn and Ostreaelv Formations. Offshore mudstones of the Sortehat Formation form the uppermost part. A marked erosional unconformity is followed by the Vardekløft Group, up to 650 m thick, that represents the major westward and northward expansion of shallow marine deposition in the region. The group onlaps the crystalline basement at Milne Land. The lower part is represented by the sand-dominated shallow marine Bajocian–Bathonian Pelion Formation which is 50–400 m thick in S–N direction, and succeeded be the offshore mudstones of the Fossilbjerget Formation (Engkilde & Surlyk 2003). The overlying Callovian– Oxfordian Olympen Formation is represented by sandy shelf edge deltas and gravity flow units and minor offshore mudstone units (Larsen and Surlyk 2003). The Upper Oxfordian – Volgian (Tithonian) include the maximum flooding zone in East and Northeast Greenland with deposition of black organic rich mudstones and gravity flow sandstones of the Hareelv Formation in the Jameson Land.

3.5 Cretaceous

The Jurassic–Cretaceous boundary interval comprises the Raukelv Formation that represents a rapid sandy shelf progradation (Surlyk & Noe-Nygaard 1991). An erosional unconformity occurs at the base of the Lower Cretaceous Ryazanian–Valanginian Hesteelv Formation that is characterised by gravity flow deposits. The formation represents the youngest preserved Cretaceous deposits in Jameson Land. In Milne Land further west the Lower Cretaceous Valanginian – Hauterivian is represented by a shallow marine package about 200 m thick of the Hartz Fjeld Formation (Birkelund et al. 1984).

4. New seismic interpretation

4.1 Methods

Stratigraphic definition of the seismic horizons was based on tracing horizons away from formation outcrops in the eastern and northern part of the basin (Ch. 2). Initially the seismic horizons linked to exposed formation boundaries were identified and correlated to unconformable strata boundaries generally marked by onlap-downlap configurations and reflector truncations (Mitchum et al. 1977). Similar seismic-stratigraphic principles were applied to trace the horizons further into the basins. At depths >1500 ms twt the identification of unconformable strata boundaries was hampered by reduced seismic resolution and the influence of high-amplitude reflections linked to magmatic intrusions (sills). Apart from this general depth trend a noticeable reduction in data quality was observed in the southern part of Jameson Land, likely related to a more frequent presence of sills and dykes. The reprocessed seismic lines representing a more superior data quality were interpreted first and subsequently ties were made to the remaining part of the data. Care was taken to not to let the interpretation steered by the high-amplitude, hard-kick reflections representing sills. However, in some of the deeper sections crossing the basin margins it appeared that reflections interpreted as sedimentary strata was onlapping dipping sills. Results from other rifted margins have shown that sill intrusion preferentially follow weak strata, e.g. coal or organic-rich shale units, or boundaries between soft and indurated sediments, e.g. unconformities (Planke et al. 2005). In the deeper parts of the basin the Base Permian horizon is commonly interpreted as being concordant with highly-reflective sill systems, which may support the notion that the sills have preferentially intruded along strata boundaries marked by reduced lithological strength.

Depth conversion

The two-way time horizon grids were converted to metric depths using the seismic interval velocities extracted from unit intervals on the reprocessed lines 86-6v, 86-3v and 87-3d. This simple approach was validated by the close approximation of the time-depth picks to a polynomial regressional trend (Fig. 4.1). Outliers that lie below the general trend, e.g. showing greater metric depths for a given twt depth, are likely related to thin intervals, or intervals influenced by magmatic sills.

The polynomial function was applied to the time-depth picks based on final datum defined in the ARCO data set (+400m). The spread around the data points indicate an uncertainty +/- 5%. Beyond this analytical uncertainty the procedure of applying time-depth conversion solely based on seismic velocity extractions, e.g. in the absence of well-tie constraints, generates additional uncertainty in the depth structures maps. However, the results of Vp measurements on outcrop samples and plugs from Blokelv-1 (~3300 m/s), and the general knowledge of likely subsurface lithologies suggests that the time-depth trend is realistic. The polynomial best-fit display a progressive steepening so that at twt depth >3000 ms most of the points lie above the regression curve. Hence, to gain a better overall match in the deeper sections the function was modified to the 5% uncertainty limit (blue curve in Fig. 4.1). The reference datum for the ARCO data was by definition +860 so in order to

display the metric depth maps relative to MSL a static correction of this value was applied to the polynomial function.

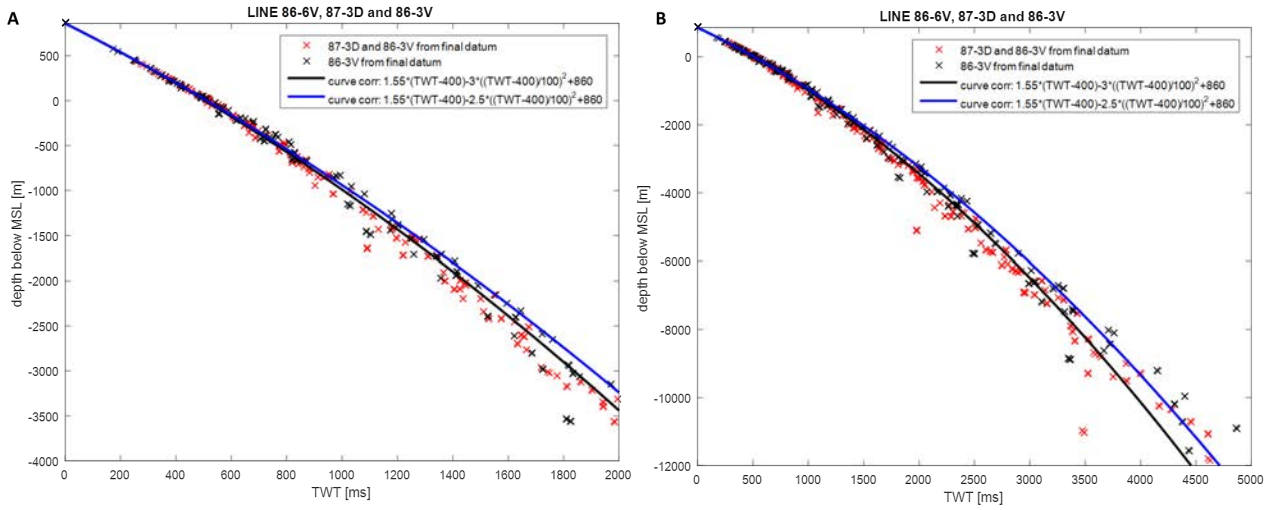

Figure 4.1. Time-Depth relationship plotted from 0-2000 ms (a) and down to 5000 ms (b) based on extracted seismic velocities from the reprocessed lines. The polynomial function displayed by the blue line was used in the time-depth conversion.

Seismic units/formations	***Max. thickness***	***Seismic geometries***	***Top horizon***
1, Hareelv Fm+E. Cret.	900 m	Plate shaped, basal onlap/downlap (low seis resolution)	Rugged
2, Fossilbjerg-Pelion Fm	800 m	Platy to mounded, aggrad. - progradational, basal onlap	Rugged
3, Neill Klinter Group	900 m	Saucer shaped, aggrad. - progradational, basal onlap/downlap	Smooth-rugged
4, Kap Stewart Group	800 m	Platy to mounded, aggrad. – progradational, basal onlap/ downlap	Smooth-rugged
5, Fleming Fjord Fm	1400 m	Saucer shaped (asymmetric), aggradational, basal onlap	Smooth
6, Gipsdalen-Pingo Dal Fm	3000 m	Bowl shaped, internal progradation, basal onlap/downlap	Rugged-smooth
7, Base Permian-E. Triassic	2200 m	Variable geometry, internal erosion, basal onlap/downlap	Rugged

Tabel 4.1. General characteristics of major seismic units that construct the post-Carboniferous Jameson Land Basin. Maximum thicknesses are conservative estimates and disregards local anomalies around line crossings.

4.2 Seismic-stratigraphic horizons and units

Eight seismic horizons were identified based on recognition of unconformable reflection terminations and changes in seismic facies (Mitchum et al. 1977). The horizons subdivided the sedimentary package occupying approximately the upper 3.8 s twt of the seismic data into 7 units shown in Tabel 1. The acoustic basement was defined by a change in reflectivity between 3-6 s twt which generally followed the early study reported by Marcussen & Larsen (1992). The seismic interpretation based on the reprocessed lines is generally robust although in the southern part of Jameson Land the data quality diminishes to the extent that tracing seismic horizons/discontinuities becomes difficult and recognition of seismic facies impossible. Consequently, there is an increase in the uncertainty of the seismic interpretation toward the southeastern part of the Jameson Land Basin, which in particular affects the deep-lying units/horizons (Units 6-7, Base Permian and Early Triassic horizons, see Table 4.1).

As far as possible, horizons have been named according to the formation boundary they intersect at surface exposures or in vicinity of outcrops. A lower Cretaceous unit, corresponding to Hareelv, Raukeelv and Hesteelev formations, was recognised in southern Jameson Land but because of its thin appearance (<200 ms) and low seismic quality on the southernmost line segments covering the lower Cretaceous formations it was not mapped in detail.

The seismic data of the JLB is markedly influenced by magmatic intrusions/sills (Larsen & Marcussen 1992). These features are observed as high-amplitude, linear-curvature reflections that tend to follow the seismic layering and occasionally cross-cut reflections considered to be sedimentary strata. Bright reflectors related to sills are most frequent in the deeper section at or below the Base Permian unconformity. The sills tend to follow the overall geometry of the basins and hence they become more inclined and shallow toward the northern and eastern margins (Fig. 4.2 and 4.3). Bright reflections are also seen in the Jurassic interval although these are less frequent, thinner (close to seismic resolution) and tend to cross-cut strata at steeper angles displaying upward inclined curvatures (yellow signature, Fig. 4.3).

Depth and thickness maps converted to meters (based on seismic interval velocities, Ch. 4.1) are shown as appendices A1.1-A1.7 and A2.1-A2.6, respectively. The maps also show coastline, localities of stratigraphic boreholes, and perimeter of the GGO licence area. A one-point smoothing step was performed to reduce bulls-eyes and unwarranted detail on the isobaths curves. Note that calculated elevation depths have mean sea-level (MSL) as reference datum in order to harmonize with the basin modelling.

4.2.1 Unit 7: Late Permian - Early Triassic

The twt structure map of the Base Permian unconformity displays a marked increase from terrain level to more than 4000 ms in the southwestern part of the basin (Fig. 4.3). Converted to metre depth domain this corresponds to a maximum depth of around 9-10 km and only along the fringe of the basin is the Base Permian located at depths <3000 m (A1.1). The maximum depths are, however, subject to a high uncertainty due to (1) the

difficulty of interpreting the Base Permian through the southern sector marked by poor data quality, and (2) the lack of well constraints on seismic velocities within the study area. The gridded map indicates several intra-basinal highs covering areas on the order of 10-30 km^2 although only the structure in the northern part of the licence area, encircled by the 3200 m contour line (A1.1), is defined by more than one line. A ridge-like structure is indicated by several lines crossing the deep basin. A separate basin development is seen in the northeast; hereafter referred to as the "northern Permian sub-basin" (depths <2000 m). The metre thickness map, shown as A2.1, indicate a rather uniform distribution of the Upper Permian-early Triassic unit over the northern part of Jameson Land, e.g. mainly in the range of 800-1000 m thickness. In the central-southern parts apparent thicknesses reach >2200 m although this value should be treated with some caution (cf. reasons stated above).

On the northern and eastern basin margins, at relatively shallow depths (<1500 ms), the Late Permian-Early Triassic unit show discontinuous reflections forming aggradational-mounded shapes over the Base Permian horizon (Fig. 4.4). The northern segments of line 86-3v and 5v are connected to the Karstryggen Fm (Fig. 3.2) so in these sections it is most likely that this facies pattern reflects carbonate platform deposits with local reef build-ups. Similar aggradational-mounded seismic patterns are observed on the eastern margin (line 86-6v), and although it lacks a direct tie to Permian outcrops, this may suggests that limestone formations occur widespread along the basin margins.

The upper part of Unit 7 displays a semi-continuous reflection pattern with enhanced amplitudes that onlaps, or drapes over, the underlying positive seismic topography (Fig. 4.5). On the basin margins this semi-continuous seismic facies is typically 100 ms thick (e.g. ~200 m) (Figs. 4.2 and 4.3). Based on settings and geometries described for the Late Permian outcrops north of the JLB the onlapping semi-continuous reflections in the upper part of Unit 7 may correspond to the Ravnefjeld Fm. However, considering the lack of direct ties and distance to Ravnefjeld Fm this interpretation should be regarded as tentative, requiring further testing.

The top of Unit 7 represents an unconformable surface that in the basin is downlapped by clinoform wedges of Unit 6. In the basinal parts the top of Unit 7 may correspond to the early Triassic Wordie Creek formation that is exposed in the northern part of Jameson Land where it displays thicknesses in excess of 350 m (Figs. 1.1 and 2.1). Wordie Creek Fm is generally described as a deep-water marine sediment with intraformational turbidite sands and basin-floor fan developments (Ch. 2). Hence, it is expected to be present in the thicker and deeper parts of Unit 7, where it may contribute significantly to the unit thicknesses.

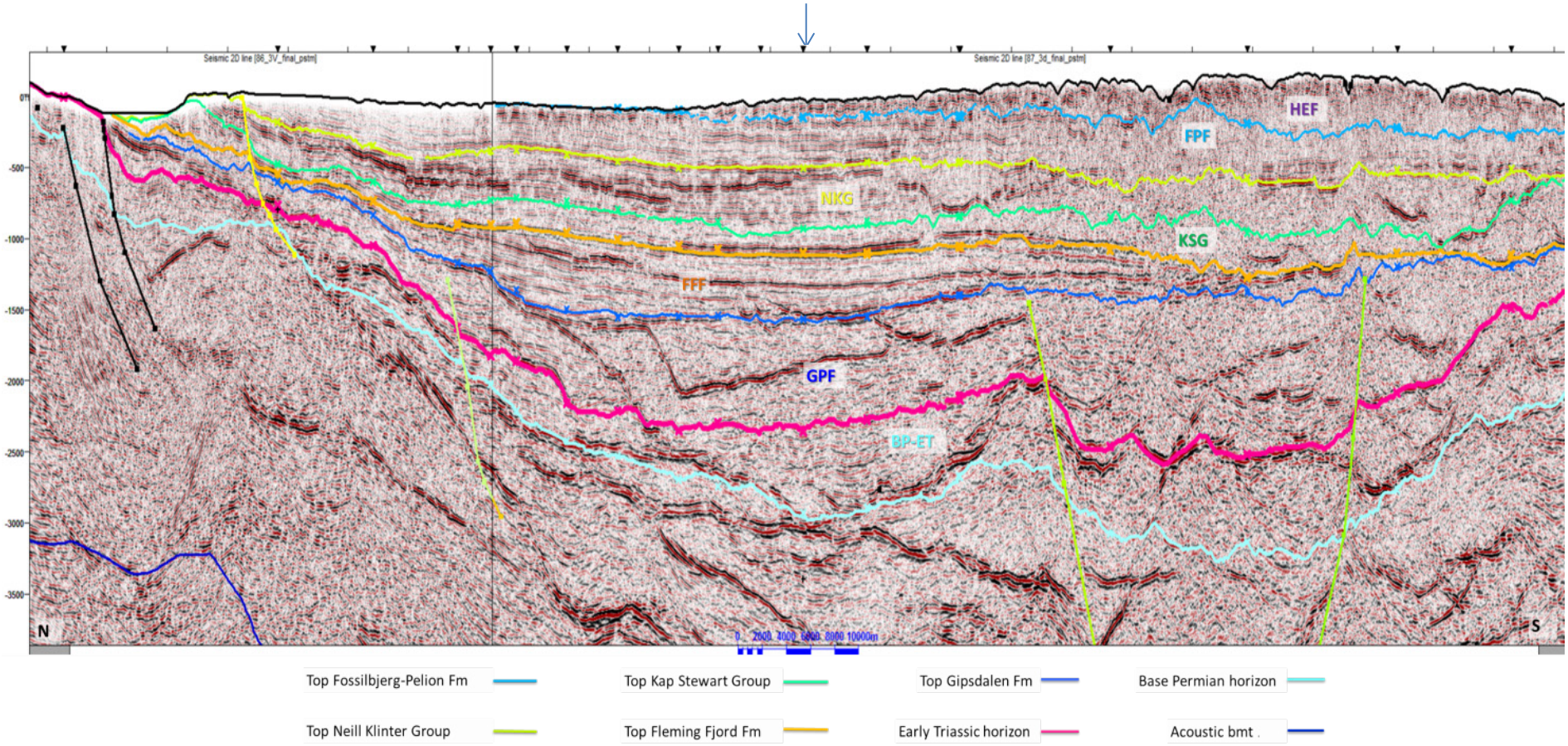

Figure 4.2. Line 86-3v and 87-3d (reprocessed versions, position shown on Fig. 3.1) with interpreted seismic horizons and faults. HEF = Hareelv Fm (+ thin Cretaceous), FPF = Fossilbjerget/Pelion Fm, NKG = Neill Klinter Group, KSG = Kap Stewart Group, FFF = Fleming Fjord Fm, GPF = Gipsdalen/Pingo Dal Fm, BP-ET = Base Permian-Early Triassic interval. Arrow indicates crossing point of 86-6v.

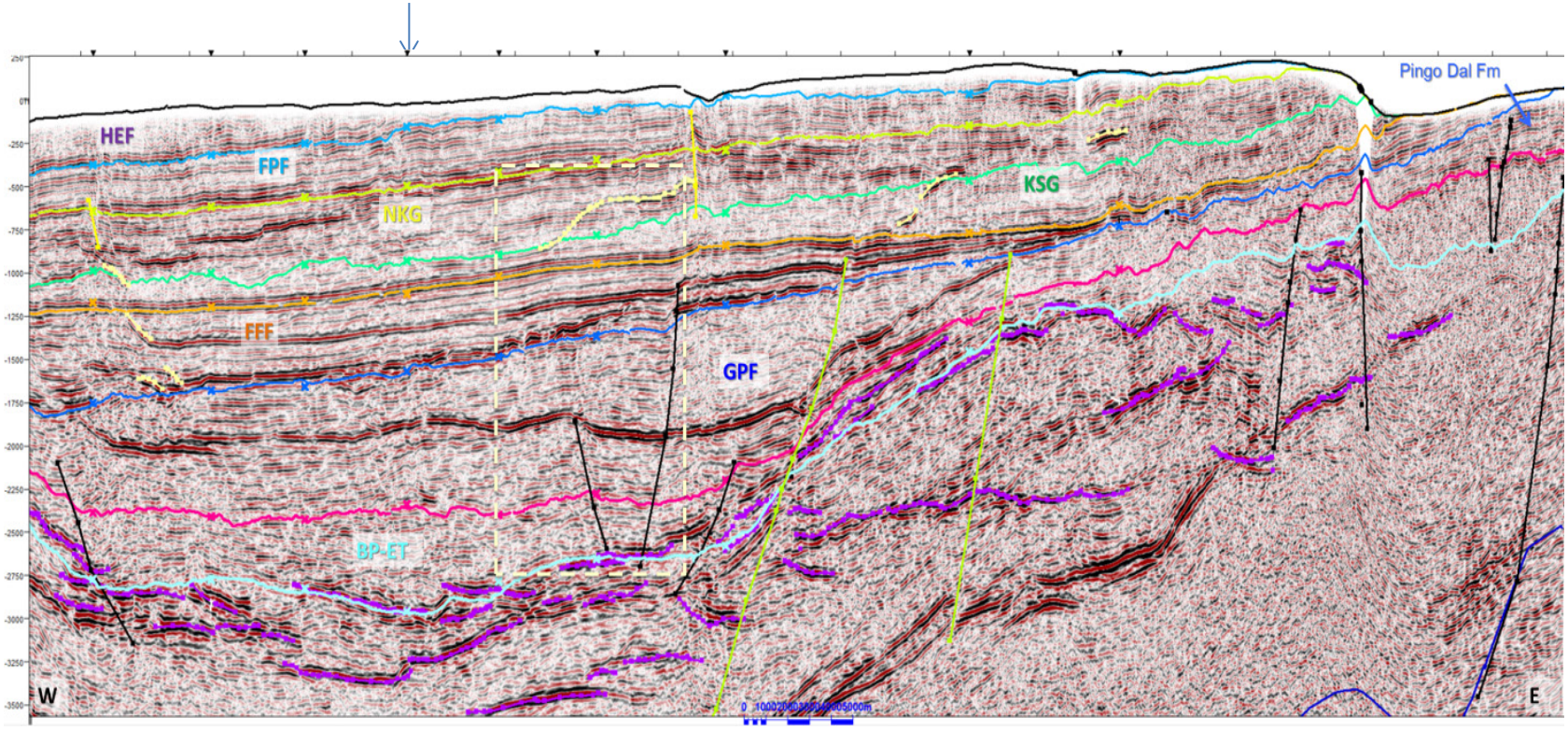

Figure 4.3. Line 86-6v (reprocessed, position shown on Fig. 3.1) with interpreted seismic horizons and faults. Arrow indicate crossing point of 87-3d. Position of detailed section in Fig. 4.13 is indicated by box. Deep-lying reflections interpreted as major magmatic intrusions are highlighted (purple). Shallow cross-cutting sills are also marked (yellow). Prominent reflector intersecting GPF is interpreted as a major sill (not marked) that may provide a source for the shallow sill/dyke systems.

A sedimentary body reminiscent of a submarine fan, potentially equivalent to Wordie Creek Fm, has been interpreted on the two crossing lines 86-6v and 87-3d, situated between the Early Triassic horizon and an interval erosional surface within Unit 7 (Fig. 4.6). The fan unit is up to 400 ms thick (~1000 m), show progradation from north to south and is apparently confined to the deep basin (>1500 ms twt). Commensurate with the Permian sections observed at more shallow depths semi-continuous onlapping reflections are inferred as possible Ravnefjeld Fm analogues.

In the northeastern part of the study area Unit 7 thickens into a separate basin that contains enhanced stratification of laterally continuous, high-amplitude reflections (Fig. 4.7 and A2.1). This part of Unit 7 thus shows a gross seismic signature that is different from the main basin, from which it is separated by internal erosional discontinuities toward west and south (e.g. lines 88-13d and 89-44d). However, interpretation is difficult since only a few seismic lines of vintage-quality processing cross this basin sector. It is possible that the strata succession represents a distal basin-infilling component to a carbonate-clastic sedimentary system that is conceptualized in the sequence-stratigraphic model shown in Fig. 7.3. Consequently, marine mudstone units equivalent to the Ravnefjeld Fm. may form part of the northeast Permian basin package where, however, only the southernmost part is covered by the licence area (Figs. 4.4 and 4.7).

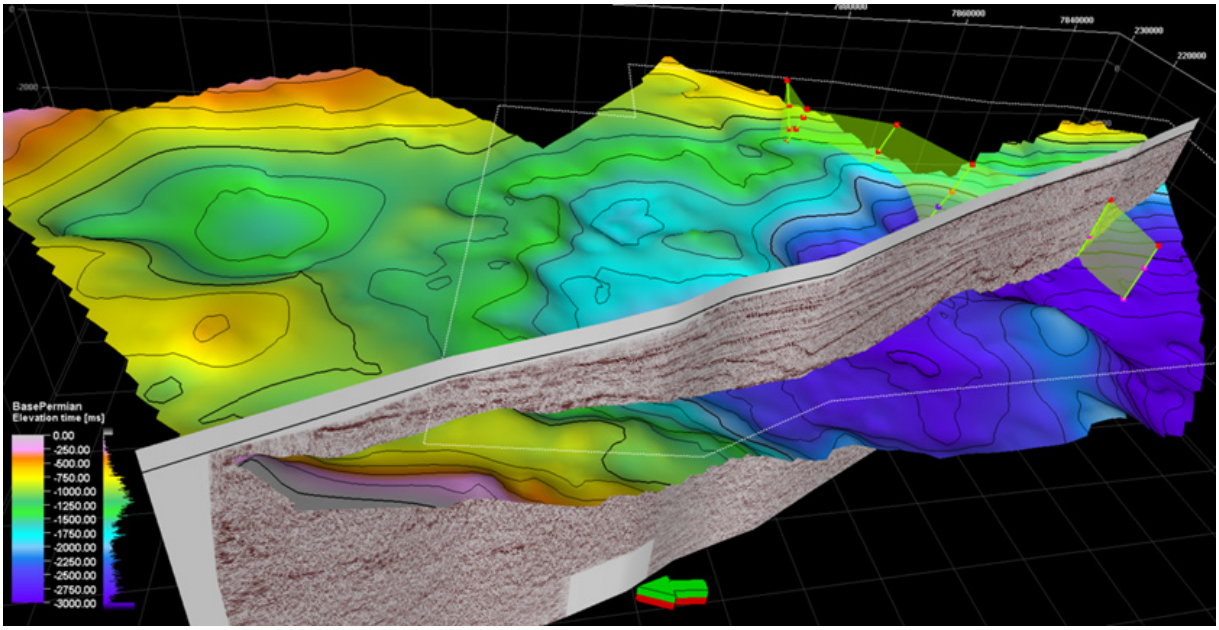

Figure 4.4. Twt surface (ms) of the Base Permian Unconformity intersected by the composite lines 86-3v/87-3d. Major fault planes along the southeast basin boundary are indicated.

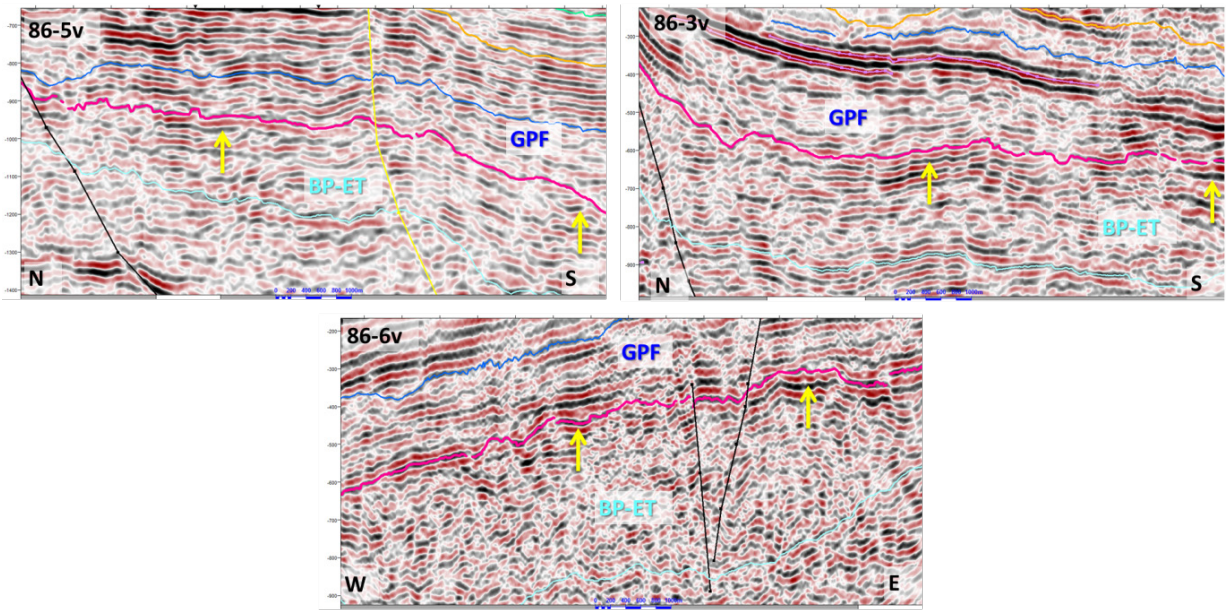

Figure 4.5. Seismic facies expressions of Unit 7 (Base Permian-Early Triassic) and Unit 6 (Gipsdalen-Pingo Dal Fm) at shallow locations (<1000 ms). Potential seismic analogs to Ravnefjeld Fm are marked by yellow arrows. Twt scale displayed with 100 ms intervals.

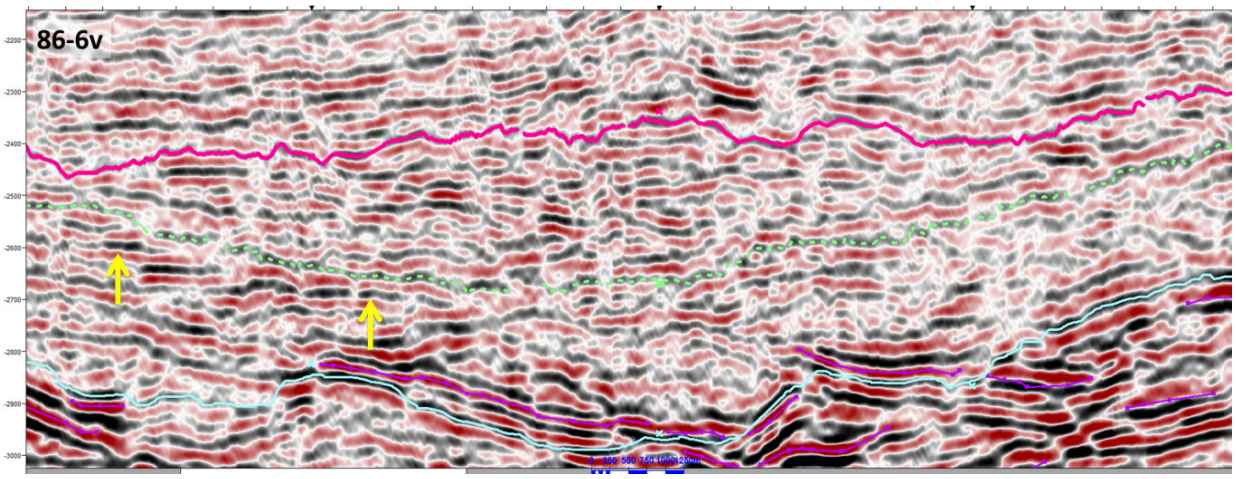

Figure 4.6. Seismic facies expressions of Unit 7 (Base Permian-Early Triassic) and Unit 6 (Gipsdalen-Pingo Dal Fm) in the central basin (line 86-6v). The depositional infill between the Early Triassic horizon (red) and the incised surface (green dotted line) within Unit 7 is interpreted as a submarine fan, possibly equivalent with the Wordie Creek Formation. Reflections below the incised surface, displaying horizontal onlap (yellow arrows), may correspond to mudstone units equivalent to Ravnefjeld Fm. The mounded-aggradational features overlying sills (purple) that are concordant with the Base Permian horizon (blue) is inferred as potential carbonate build-ups. Twt scale is displayed with 100 ms intervals.

4.2.2 Unit 6: Gipsdalen/Pingo Dal Fm

The Early Triassic horizon forming the base of Unit 6 reaches depths of >6000 m in the southwestern part of the Jameson Land Basin. The horizon display a marked relief (gradients ranging from 5-15°), most pronounced across the eastward flanks of the basin, where it rises steeply to depths above 2000 m (A1.2). In the northern part of the licence area the Early Triassic horizon form a prominent ridge approximately 6 km wide and 20 km long. In contrast, the top of Unit 6 (Top Gipsdalen Fm), display a more even surface with gradual changes in depth isobars reflecting the termination of a major basin-filling stage (A1.3).

The definition of the top bounding horizon of Unit 6 is based on tying this seismic profile to the intersection between Fleming Fjord Fm. and Top Gipsdalen Fm. In addition, the presence of Klitdal Member, e.g. part of Pingo Dal Fm., is inferred based on the correlation to the Avannaa boreholes (Fig. 4.8).

Unit 6, correlated to the Early-Late Triassic sequence of Gipsdalen-Pingo Dal Fm, shows several depocentres with thicknesses up to 3600 m in the southern sector, although thicknesses of >3000 m are only indicated by two lines (Fig. 4.9 and A2.2). The depocentres and the basin bounding faults are orientated toward SW and SSW trending along the structural lineament of Fleming Fjord and Nathorst Fjord. Configurations of asymmetric depocentres bounded against extensional faults are suggestive of half-graben formations in the central and southern parts of JLB (Figs. 4.2 and 4.3). The southeastward basin bounding faults are, however, rather vaguely defined and difficult to trace on the original seismic data.

A half-graben basin is also indicated on a single line north of the licence area (89-23d), toward Fleming Fjord, superimposed on the northern Permian sub-basin (A2.1 and A2.2). In the eastern part of Jameson Land Unit 6 appear to form a minor depocentre, corresponding to the Klitdal Basin, which is only crossed by line 86-6v (Fig. 4.2). Judging from this profile the Klitdal Basin is separated from the main JLB by a broad structural high, which is consistent with the tectonic model shown in Fig. 5.6.

The internal seismic geometries are variable but progradational clinoform features and dipping wedges trending south and west are common (Figs. 4.2, 4.3, 4.5 and 4.6). Over the margin highs the units thin out due to depositional onlap. The lower and presumably major part of the Unit 6 is likely to represent coarse-clastic sedimentation associated with Pingo Dal Fm/Klitdal Member while the uppermost part presumably contains lacustrine mudstone and evaporites of Gipsdalen Fm.

Unit 6 is intersected by an extensive sill system that can be traced as a positive (red) high-amplitude reflector across the basin (Figs. 4.2-4.3). Estimation of the sill thickness is difficult but it is likely to be at least 20 m. The basin-wide sill within Unit 6 is possibly the source to the smaller and more inclined sill features observed in the Jurassic units above. In an eastward direction the sill gradually turns to a more shallow position towards, following the general geometry of the sedimentary package. It is probable that the sill system provided the magmatic source for the horizontal extrusions observed along the valleys west of Hurry Inlet (Fig. 4.10).

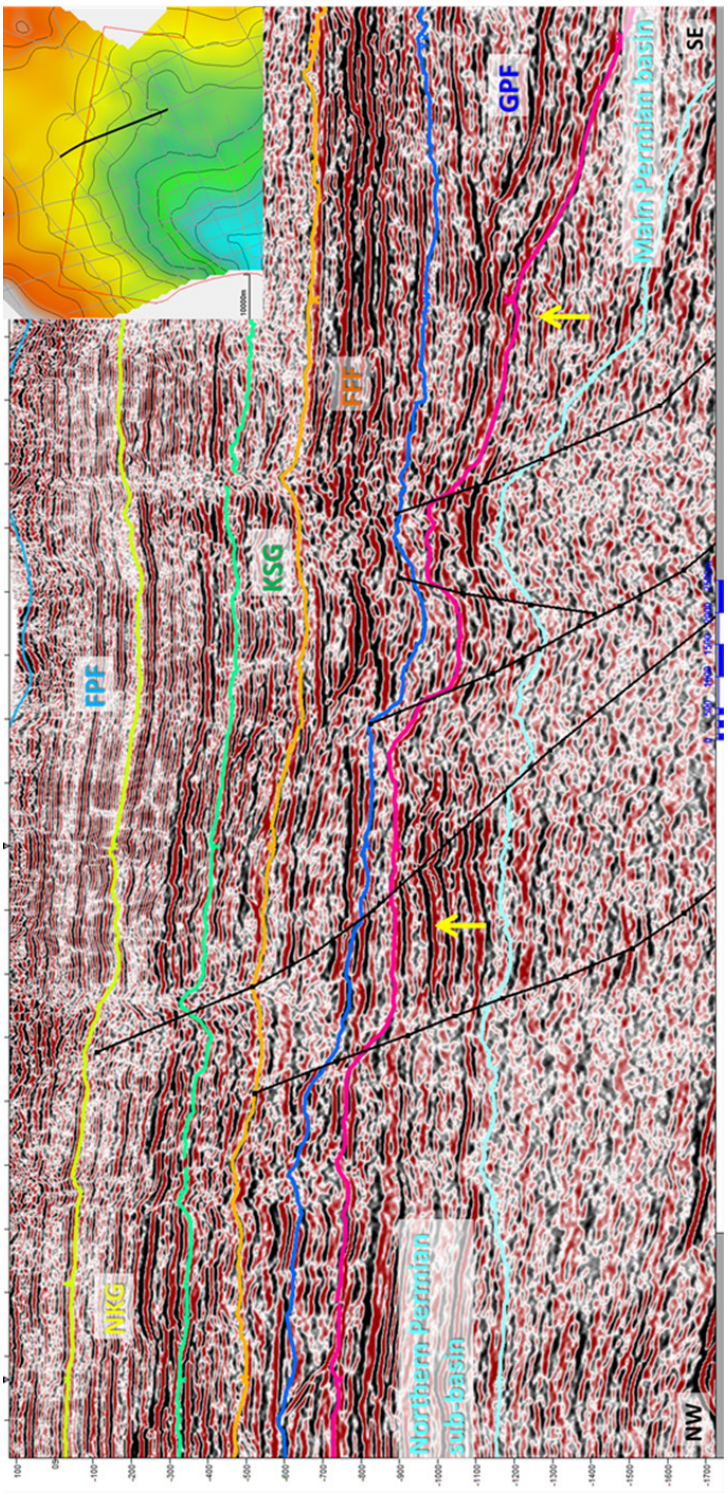

.

Figure 4.7. Seismic section (line 88-13d) across the rifted margin in the northeastern part of the license area, displaying structural features related to southward dipping extensional faults. The profile illustrates the transition between the main Permian basin and the sub-basin to the north (see twt structure in Fig. 4.4). The extensional faults linked to Triassic rifting appear with throws of up to 80 ms. Possible strata equivalents to Ravnefjeld Fm are indicated (yellow arrows). Line position is shown on map with depth structure of Fleming Fjord Fm (FFF) as background (A1.4). Mounded wedges seen within the FFF are related to a late rifting/subsidence phase.

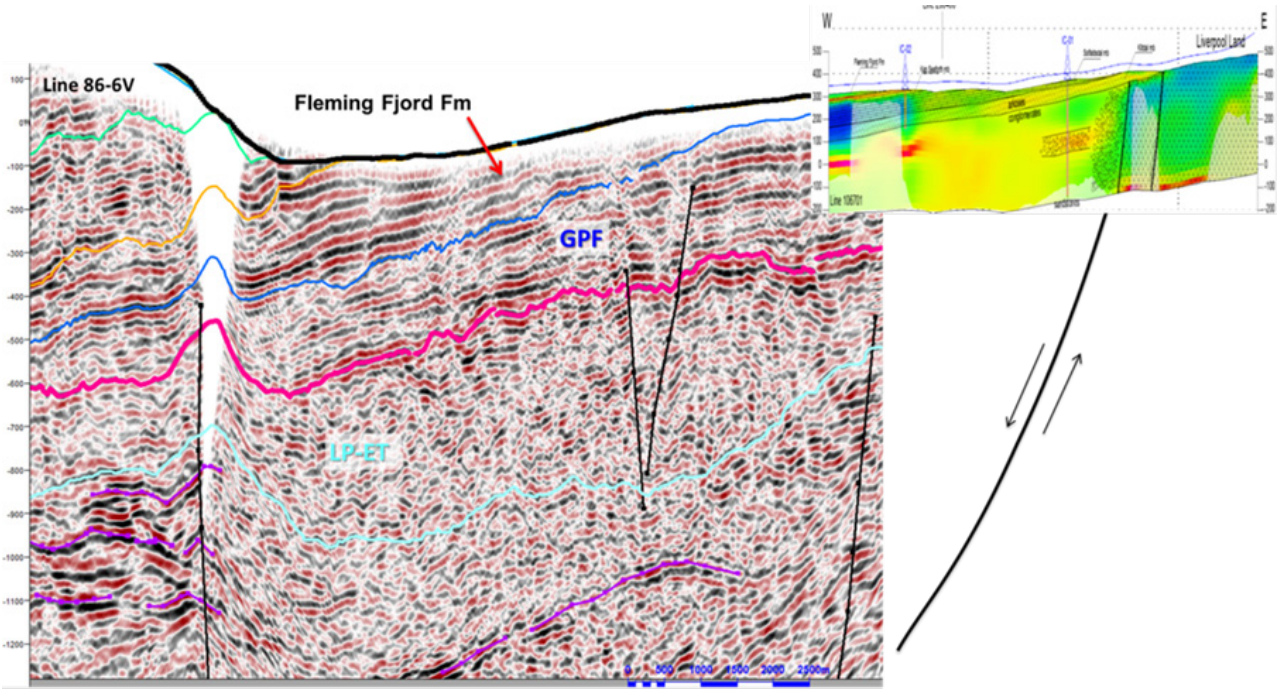

Figure 4.8. Seismic tie to Avannaa boreholes (IC-1 and IC-2) and electromagnetic profile (SkyTEM) across the Klitdal Basin. The seismic geometries suggest the presence of a structural high situated below the escarpment truncating the Jurassic formations. The age of the conglomerates above the basement fault drilled at site IC-1 below Klitdal Member is unknown, but this layer may form part of an alluvial wedge associated with early Triassic rifting. See also Ch. 5. GPF = Gipsdalen-Pingo Dal Formation. BP-ET = Base Permian-Early Triassic interval.

4.2.3 Unit 5: Fleming Fjord Formation

The top of Unit 5, Top Fleming Fjord Fm (A1.4), display a surface that is generally tilting toward south- west, with a gentle inclination in the basinal region (1-2°) but steepening along the eastern and northern periphery (5-8°). The thickness of Unit 5 is rather uniform over northern and eastern parts of JLB, e.g. 200-600 m. Depocentres with thicknesses up to about 1600 m are observed in the western sector, with a marked asymmetric development of the northern depocentre aligned SW-NE presumably continuing below Hall Bredning (A2.3, Fig. 4.2). The strata show depositional onlap onto Top Gipsdalen Fm. The unit is considered as mainly mud-prone due to the flat infilling seismic character and the correlation to the generally fine-grained Fleming Fjord Fm. However, coarse-grained alluvial deposits of the Ørsted Dal Member may be present within the asymmetric depocentre which might reflect a late rifting stage. The top bounding horizon is seen as strong continuous reflection which likely reflects the seismic impedance transition from Kap Stewart Group mudstone to lacustrine limestone beds (Tait Bjerg Beds, see Ch. 3). Internally the unit is marked by strong semi-parallel reflections that thin-out toward the depocentre. Some of the high-amplitude reflections may, however, be due to sills intruding into parallel-laminated mudstone.

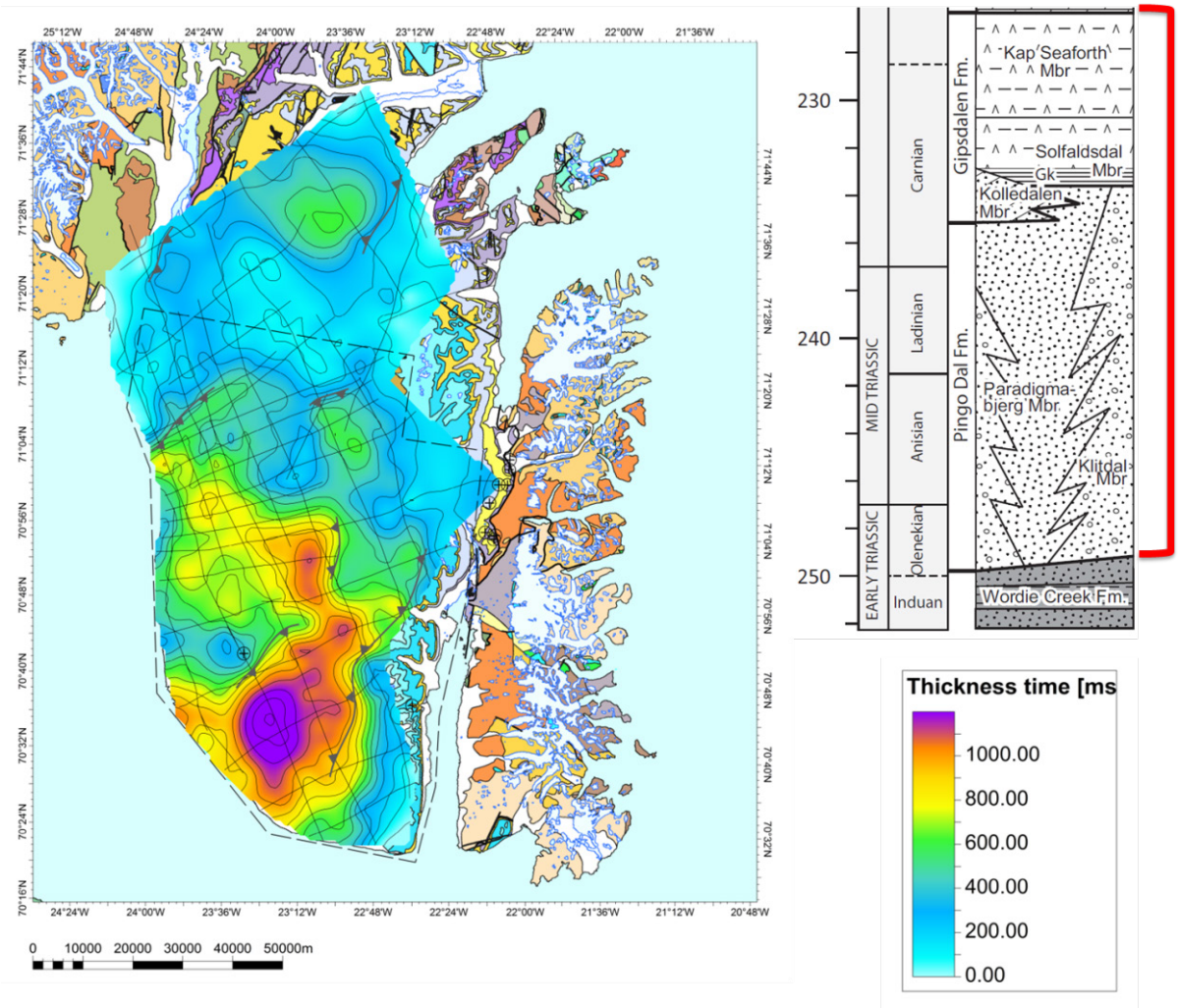

Figure 4.9. Isochore thickness map (ms twt) of Unit 6. Basin boundary faults are indicated. The unit is considered to be equivalent to the Early-Late Triassic succession represented by Pingo Dal and Gipsdalen formations (Andrews et al., 2014).

4.2.4 Unit 4: Kap Stewart Group

The Top Kap Stewart Group (depth map range from surface levels (around +400 m) to about -2500 m below MSL in the south-western part. It has a general saucer-shaped geometry but with structural developments in the form of prominent ridges extending from east to west in central-southern part of JLB (A1.5). The elongate topographic features are associated with depocentres displaying thicknesses between 600-900 m (A2.4). In between these accumulation areas the Unit 4 is generally between 400-600 m but in some places down to about 200 m. The region north of the licence area generally shows thicknesses of 200-400 m.

The depocentre localities of Unit 4 are characterised by disrupted-irregular seismic facies often with slightly mounded geometries and vaguely defined downlap configurations towards south and west (Fig. 4.11). This pattern is intercalated with medium-amplitude parallel, semi-continuous reflections often showing internal onlap. Outside the

depocentres (e.g. <600 m thickness) the unit is dominated by uneven-to-parallel, semi-continuous facies. This strata appears to continue along the base of the unit depocentres, e.g. immediately overlying the prominent horizon of Top Fleming Fjord Fm. High amplitude continuous and cross-cutting reflections are likely associated with sills. In agreement with the extensive outcrop studies (Surlyk, 2003) Unit 4 is interpreted as a deltaic-lacustrine succession with the major depocentres representing fluvial-deltaic input sources along the basin fringes. The onlapping parallel reflections are interpreted as lacustrine mudstone deposits that may have source-rock potential.

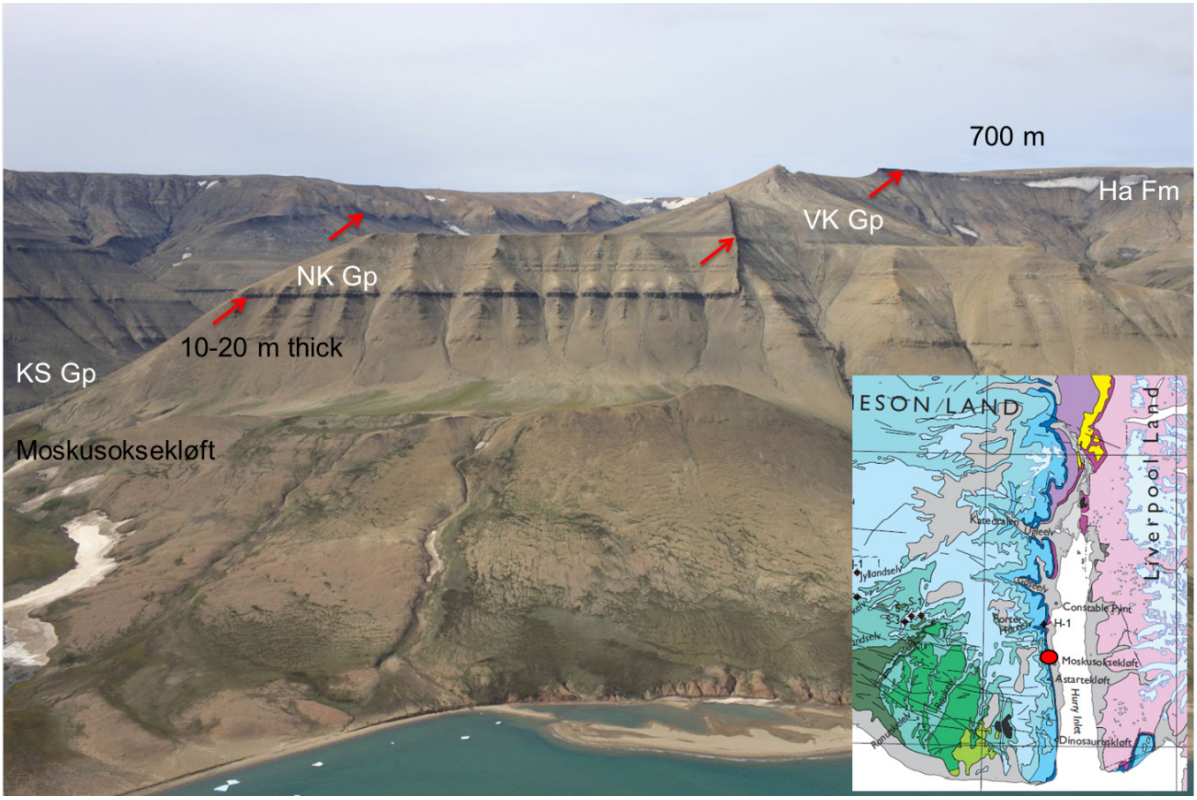

Figure 4.10. Magmatic sills, 10-20 m thick, intruding the Jurassic strata exposed along the southwest margin of JLB.

4.2.5 Unit 3: Neill Klinter Group

The Top Neill Klinter Group (NKG) surface reaches maximum depths of around 1700 m in the southwest (A1.6). The isopach map display marked thickness variations forming three depocentres: A central and southern accumulation with thicknesses up to 1000 m, and a smaller accumulation in the north (A2.5). The thickness distribution of the Unit 3 is generally incongruent to that of Unit 4 (Kap Stewart Group), in particularly observed by infilling of the distal Kap Stewart lake basin by the Neill Klinter Group. Conversely, the NKG thins over the central-eastern parts of Jameson Land where the KSG is relatively thick.

The basal part of Unit 3, notably at the location of depocentres (Figs. 4.11 and 4.12), show continuous parallel reflections that onlap the top KSG (see also Fig. 4.2). It is possible that this reflects the onset of marine transgression (e.g. first high-stand). Alternatively, the onlapping strata at the base of NKG is a continuation of the Kap Stewart lake sequence, in which case unrecognised source rock intervals may be present in Unit 3. Seismic geometries indicate stacked prograding sedimentary systems interconnected by mounds/ridges in the distal parts (Figs. 4.11-4.12). These systems tend to move westward infilling the lake basin, and may be associated with a tidally-dominated prograding coastline, equivalent to Rævekløft, Gulehorn and Ostreaelv Formations of the Neill Klinter Group (Ch. 7). Unit 3 is commonly intersected by strata-crossing and high-amplitude reflections related to sills.

4.2.6 Unit 2: Fossilbjerg/Pelion Fm

The Top Fossilbjerg/Pelion Fm (FPF) horizon follows the general trend of deepening toward southwest (A1.7). However, this stratigraphic level designates a change in the geometry of isobaths from a N-S trend to a NW-SE alignment. The isopach map of Unit 2 display a rather even thickness distribution within the licence area, typically 500-700 m (A2.6). Poorly defined depocentres >800 m are seen in the western part. In the northern part of the peninsula (north of 71 °N) the FPF is at surface position and thus the thickness map may to some extend be influenced by surficial erosion.

The seismic expression of Unit 2 is dominated by even, continuous and generally high-amplitude reflections, some of which can be traced across the basin (except the southern part where resolution is poor) (Figs. 4.2, 4.3, 4.11 and Fig. 12). The unit show low-angle onlap at the base while downlapping reflections are seen in the top parts. Internal onlap surfaces are commonly observed (Fig. 4.12). Small-scale progradational features are occasionally observed which may correspond to low-stand wedges of shallow marine sandstones of the Pelion Formation.

4.2.7 Unit 1: Hareelv Fm + Early Cretaceous.

These units are mainly present in the southern part of the licence area where the seismic quality is poor (Figs. 4.2 and 4.12). Hence, a more detailed mapping and subdivision of this interval has not been carried out as part of this study.

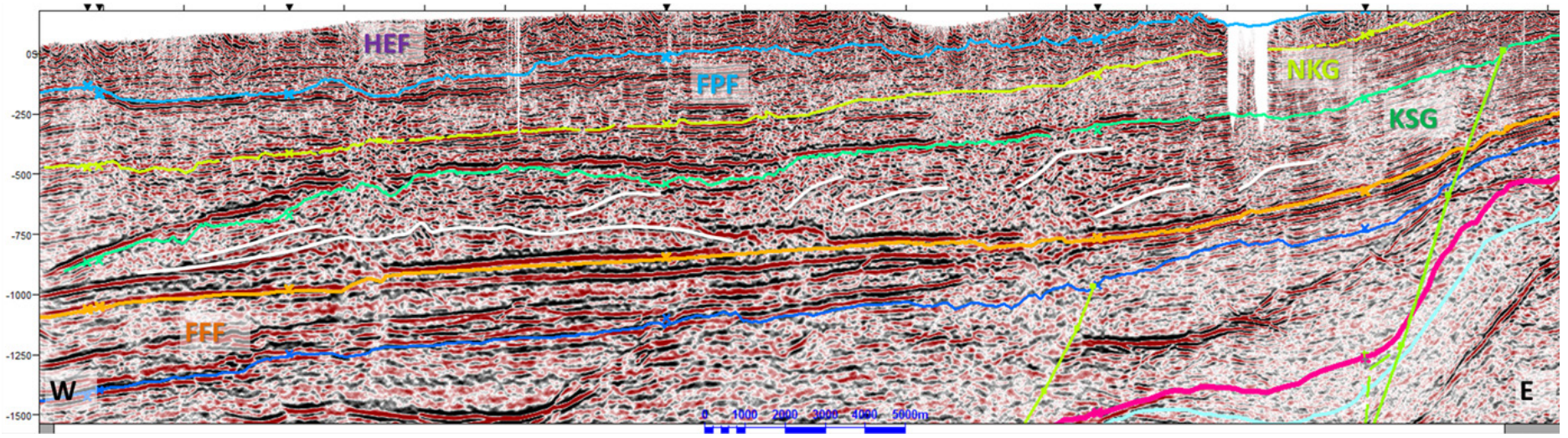

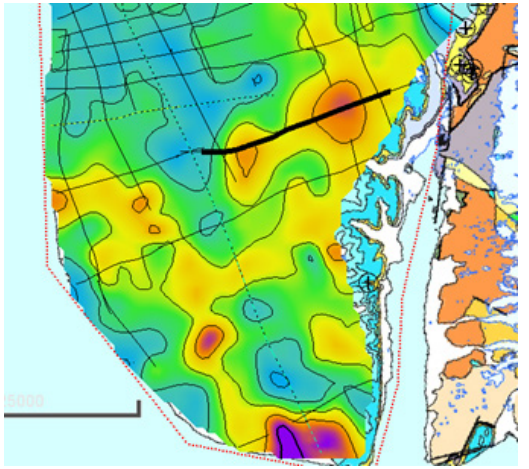

Figure 4.11. Seismic profile (88-4d) displaying one of the elongate depocentres of the Kap Stewart Group (central JLB). Notice continuous to semi-continuous parallel reflection patterns developed within and along the base of the unit. Clinoform signatures and basal mounded features are indicated. Map displays KSG thickness (see A2.4).

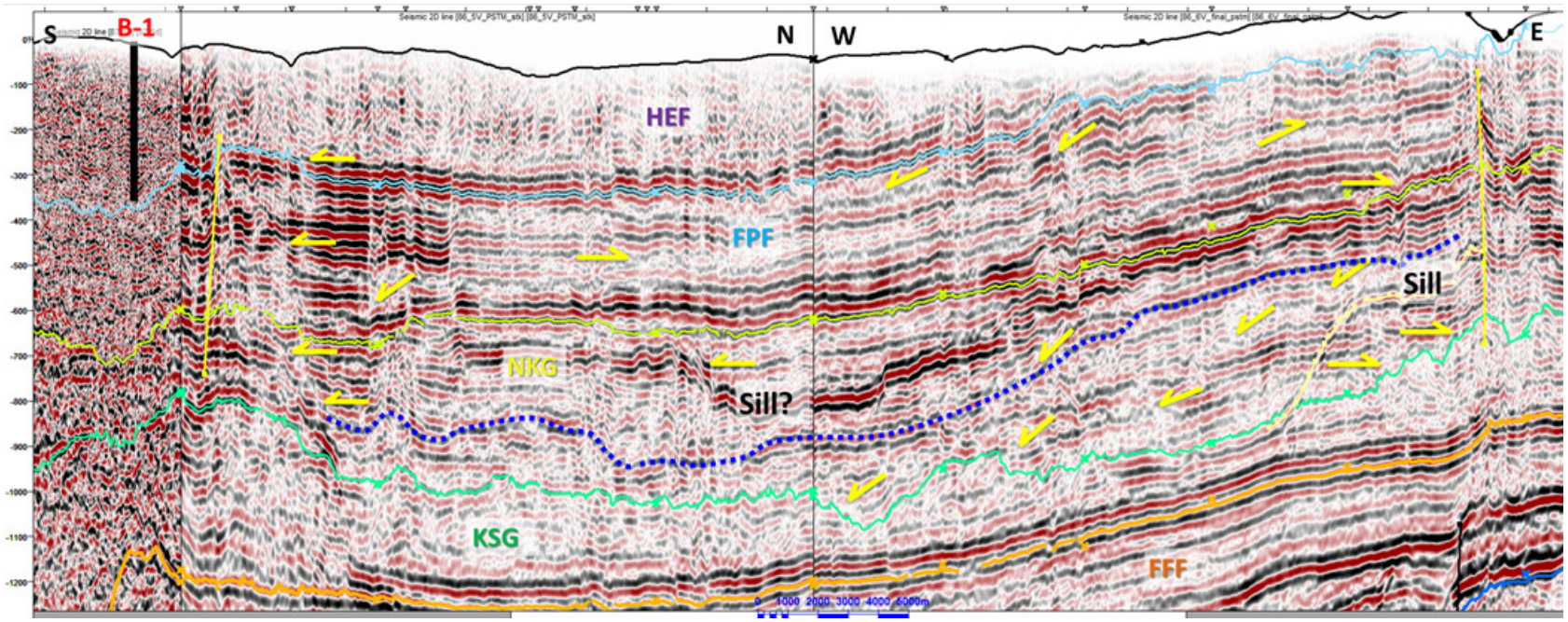

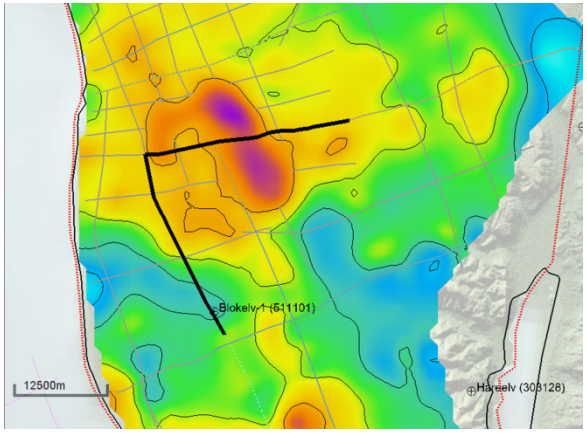

Figure 4.12. Composite section E-W (86-6v) and N-S (86-5v, 87-5d) displaying the Jurassic sedimentary package in the central parts of the Jameson Land. Configurations of strata termination, e.g. onlap-downlap, are indicated with arrows. The top of a prograding-mounded unit within the Neill Klinter Group is highlighted (blue punctuated line). The position of Blokelv-1 is projected on the seismic profile 87-5d, which has a poor seismic resolution compared to the reprocessed data. Legend as in Figs. 4.2-4.3. The map shows thickness in meters of the Neill Klinter Group (see A2-5).

4.3 Constraints from gravity and magnetic data

A way of testing the robustness of the seismic interpretation was to compare the gross basin thickness/geometries with gravity and magnetic anomaly data (Fig. 4.13). The magnetic anomaly map shows a pronounced high that extends from Liverpool Land and across JLB in a northwest direction. This feature correlates with reduced sedimentary thicknesses associated with an intra-basinal high that is demarcated by the Base Permian unconformity on E-W lines (Fig. 4.3). The structure may represent an inverted component of the Devonian-Carboniferous basin although the causal tectonic phase is illusive. The extensive presence of sill intrusions in the pre-Permian strata that is apparent from the seismic data, may explain the pronounced magnetic response. Comparing the rift basin isopachs with free-air gravity it is seen that the V-shaped basin development in the southern part of Jameson Land coincides with a gravity-low of a similar geometry. A pronounced gravity-low is seen in the central-northern part of Jameson Land, which may be linked with the northern Permo-Triassic sub-basin. However, here sedimentary thicknesses here are much lower than in the south, and hence there may be other factors than the Triassic rift that produces this anomaly.

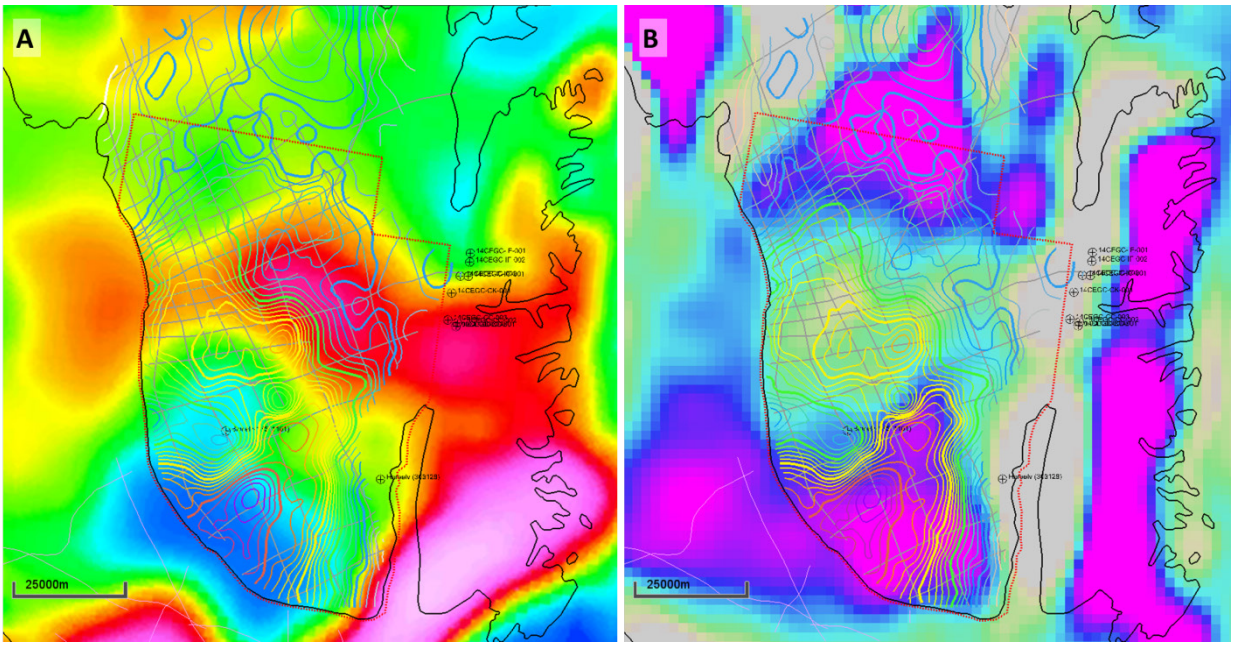

Figure 4.13. (**a**) Magnetic anomaly map and (**b**) free-air gravity (100 km filtering) overlain by contours representing the total thickness of the Permo-Triassic basin (Base Permian-Top Fleming Fjord Fm.). Isopach contours are shown with 300 m intervals. Greatest thicknesses are displayed by red contouring. The bold yellow contour represents 4500 m depth.

4.4 Comparison with previous interpretation

Seismic horizons interpreted as part of the previous study only exist in an analog format, e.g. as they are drawn on the seismic prints, and shown in the GEUS report (Christiansen et al., 1991). A comparison was made by using some of the seismic examples and maps from the report (Fig. 4.14). The two versions are seen to differ substantially, in particular for the Base Permian and Early Triassic markers, which in the new study lie deeper. In the example from line 86-6v the position of the Early Triassic horizon (previously named “Base Triassic”) differ with >1 s twt. It is also seen that the onlapping parallel stratified Unit 5 that is now interpreted as the Late Triassic Fleming Fjord Fm. was previously regarded as a condensed Permian-middle Triassic interval. As a result the Base Permian now reaches depths of up to 10 km in the southwest compared to 4.5 km in the vintage study. The result of the new mapping produces a bowl-shaped geometry of the Base Permian and Early Triassic compared to a plate-shaped signature of the old interpretation. In the northwestern part of the JLB the differences in seismic interpretation are less marked but still significant (line 88-13D), for example the early Jurassic Top Kap Stewart Group is positioned about 300 ms deeper in the new study. Deviations in the tracing of fault structures are also apparent.

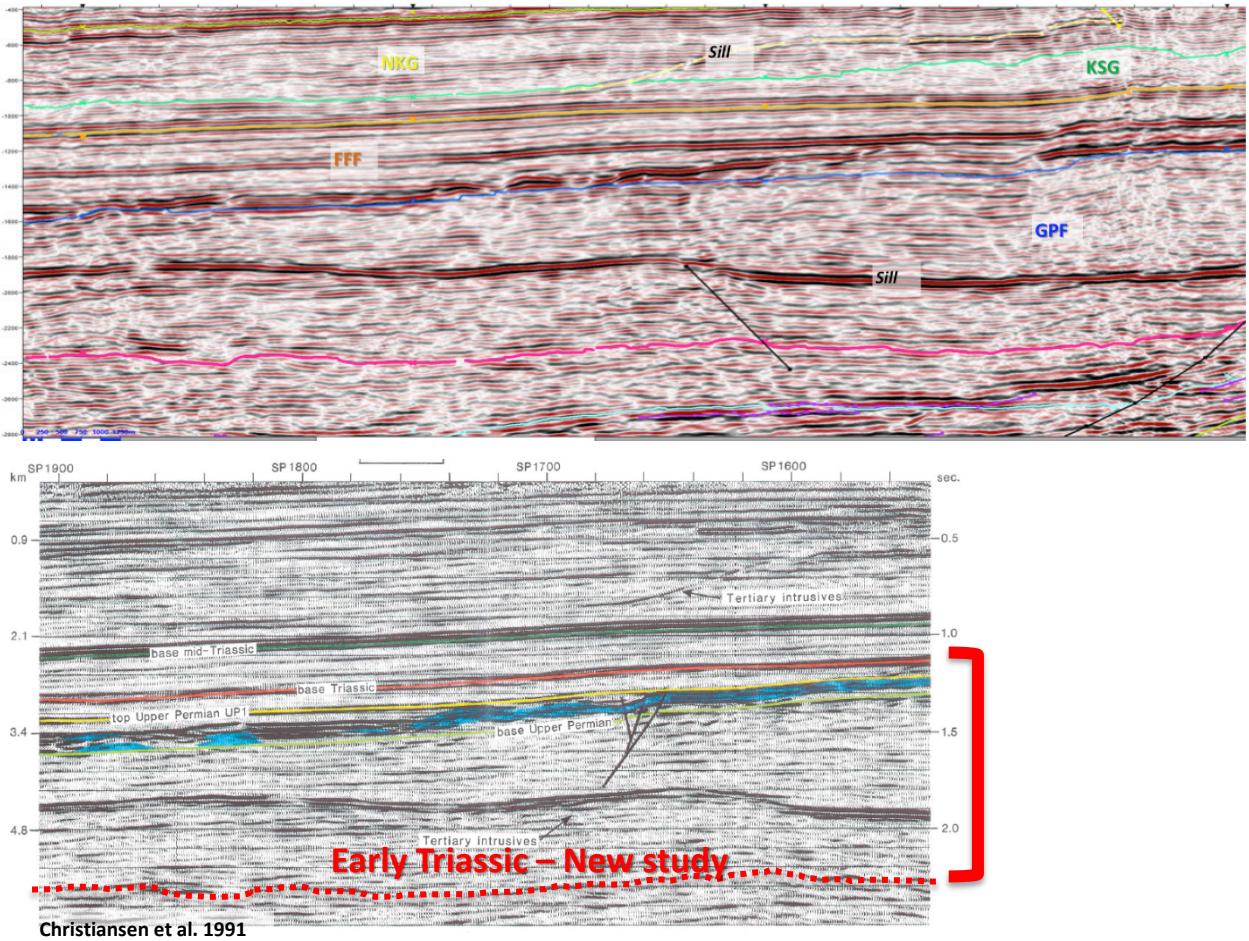

Figure 4.14. Comparison between new (upper panel) and old (lower panel) horizon interpretations on line 86-6v.The location of the section is shown in Figure 4.3. The red bar illustrates a >1 s difference in the interpretation of the Early Triassic horizon (“Base Triassic” in the old study).

4.5 Conclusions

- The new seismic interpretation differs substantially from the initial study reported in Christiansen et al. (1991). This is notably seen for the Base Permian horizon which reaches depths of >6 km compared to 4.5 km in the old study. The post-Base Permian package was divided into 7 mega-units correlated to outcrop formations of the Foldvik Creek Group, Gipsdalen-Pingo Dal Fm, Fleming Fjord Fm, Kap Stewart Group, Niell Klinter Group, Fossildalen-Pelion Fm, and Hareelv Fm (the latter including lower Cretaceous strata).

- Several types of seismic facies are recognised on the reprocessed seismic data above the Base Permian horizon, which are likely related to carbonate build-ups and basinward mudstone deposition, possible equivalent to the Ravnefjeld Fm.

- Development of several depocentres of >2 km thicknesses within the Triassic interval is linked to a continental rift phase occurring prior the Jurassic transgression. The sedimentary accumulations display a NE-SW trend aligned with the Fleming Fjord and Nathorst Fjord systems. Half-graben formed against extensional faults are seen on some of the seismic profiles crossing the eastern and northern basin margin. Interpretation of the Triassic system is supported by recent borehole information in east Jameson Land (see also Ch. 5).

- The lower Jurassic Kap Stewart Group show multiple local depocentres of >700 m thickness with topographic reliefs of up to 200 m in the eastern and central-southern parts of the basin. The strata geometries are reminiscent of delta-fan deposits that prograded into the central parts of the basin, mainly from east and southeast. Parallel, semi-continuous reflections are particularly common in between the depocentres and may reflect lacustrine mudstone deposits with possible source rock potential.

- The Neill Klinter Group infills the central parts of the basin onlapping the Kap Stewart Group. Parallel strata at the base of this unit may signify mudstone units (lacustrine-marine?) deposited in the deepest part of the Jurassic basin, thus harbouring a further potential for source rock deposition. Seismic patterns indicate that sediments generally filled the basin from east to west.

- Emplacement of sills is notably evident in the pre-Triassic succession although several major sill systems can be traced laterally throughout the Triassic-Jurassic interval. The timing of sill emplacement is not well constrained but likely to be early Tertiary (~Eocene). The major sills tend to intrude along unconformable strata boundaries and thus their presence and distribution appears to reflect the overall basin geometries.

5. Tectonic model

5.1 Evidence for Triassic rifting and basin development

During Triassic time East Greenland was affected by a major phase of basin margin uplift and rapid fault-controlled basin subsidence leading to the sedimentation of coarse-grained red alluvial fan sequences, up to 600 m thick (Clemmensen 1980a,b, Clemmensen et al. 1998). The coarse-grained sequence passes laterally into sandy floodplain deposits with longitudinal drainage towards the north. A major barchanoid dune field was developed along the western margin, while extensive inland sabkhas formed in the central parts of the basin. Aeolian dune sands continued to be deposited in the western part while variegated gypsiferous sandstone-mudstone cycles characterized the eastern part. Fault activity documented during the Early Triassic was associated with incised submarine canyons described in the Wordie Creek Formation at Wegener Halvø (Seidler 2000; Seidler et al. 2004). The N-S trend of the Liverpool Land, constituting the east border of the Jameson Land Basin is interpreted as a N-S trending horst structure developed in Triassic time.

New geological and structural data supported by detailed aeromagnetic, electro-magnetic and drill-core data show that the Triassic rift has a NNE-SSW to NE-SW trend, oblique to the N-S trends that are inherited from the Late Carboniferous tectonics.

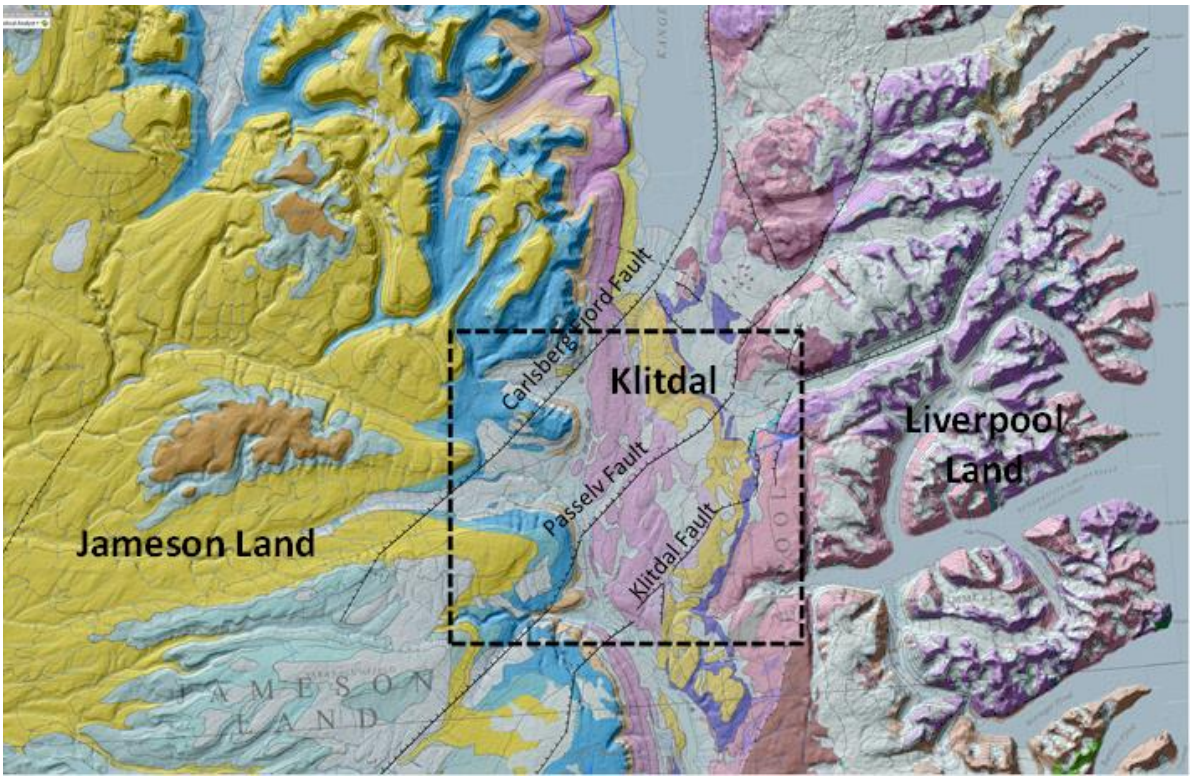

Figure 5.1 (previous page)**.** Geological Map of the Jameson Land Basin with the NE-SW trending Triassic faults. Inset = Figure 5.5. Grey dashed line=Figure 5.6.

5.1.1 Geological and structural data

Fieldwork along the East margin of the Jameson Land Basin highlighted the presence of NE-SW trending fault escarpments offsetting the Permian peneplain and the coarse-grained deposits of the Pingo Dal Formation (Klitdal member) (Figs 5.2 to 5.3).

Three major faults were mapped (Fig. 5.5) in the Klitdal area, defining what is called the Klitdal Basin filled in with more than 500 m of syn-rift coarse grained sandstones and conglomerates in half-graben structures (Fig. 5.6).

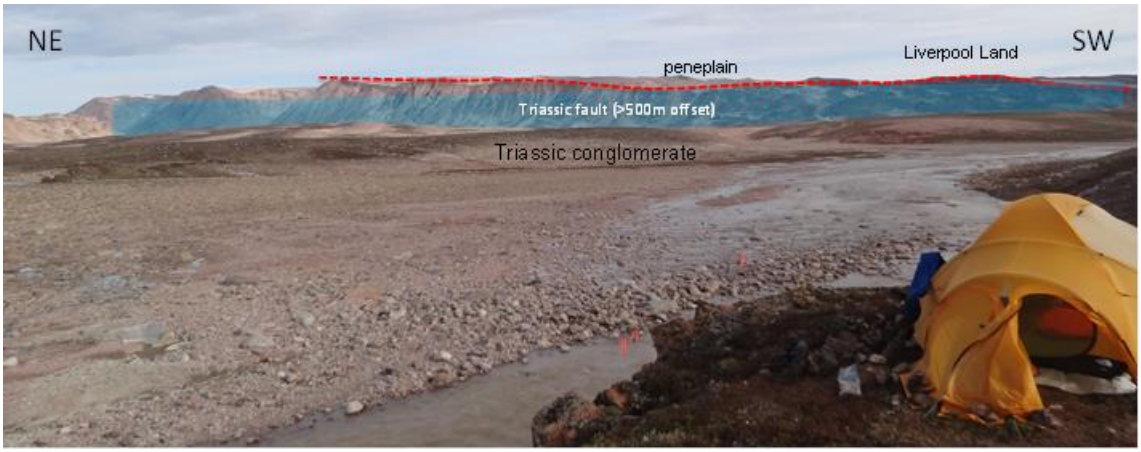

Figure 5.2. Panoramic view from the NW toward the Liverpool Land showing a NE-SW trending fault escarpment (Passelv Fault) offsetting the gently dipping Permian peneplain (red line) and the Triassic conglomerate of the Klitdal member (Pingo Dal Formation).

Figure 5.3. Fault escarpment along the NE-SW trending Klitdal Fault.

Figure 5.4. Slickensides on a fault plane showing dip-slip normal movement.

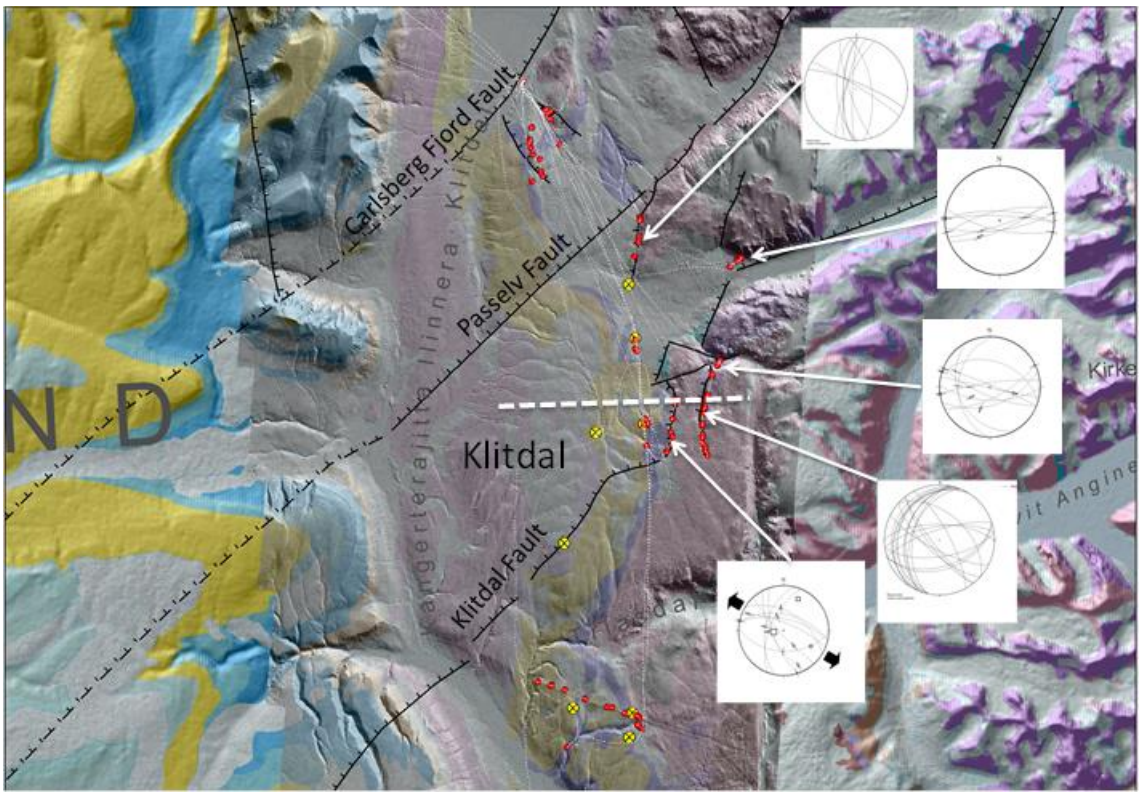

Figure 5.5. Structural map of the Klitdal area with major faults and kinematic data along with palaeostress reconstruction derived from inversion of fault-slip data showing NW-SE extension (black arrows). Yellow dots=drill cores; red dots way-points of visited localities; dashed line=Figure 5.8.

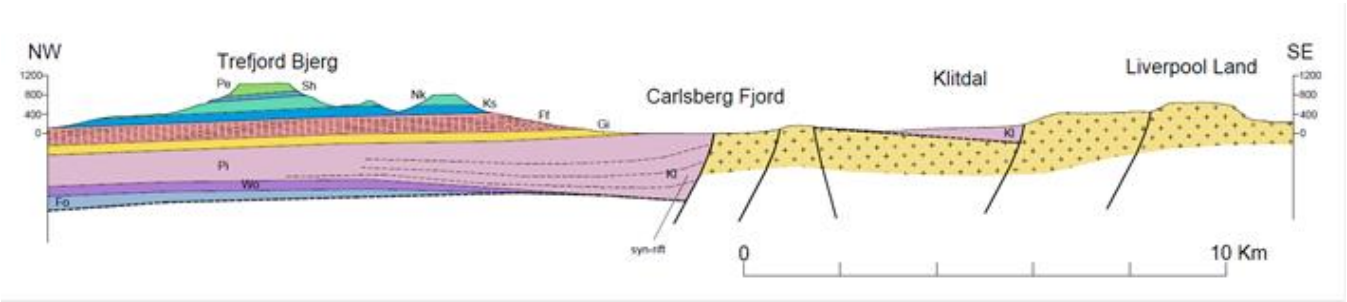

Figure 5.6. Geologic cross-section from Trefiord Bjerg to Klitdan showing the SE-ward tilted blocks hosting the Klitdal Basin bounded by the Klitdal Fault, Passelv Fault and the Carlsberg Fjord Fault. Location shown in Figure 5.1.

5.1.2 Aeromagnetic data

Between May 22nd and June 6, 2013, Fugro Airborne Surveys conducted a high resolution gradient magnetic survey of the Klitdal and Wegener-Halvø Blocks on behalf of Jameson Land Resources A/S, a JV partnership between Anglo American Exploration plc and Avannaa Logistics Aps. Using Constable Point, Greenland as the base of operations, a total of 10,171 line kilometres of data was collected using a Cessna 208B airplane. The survey data were processed and compiled in the Fugro Airborne Surveys Ottawa office. A total of 293 traverse lines were flown ranging in length from 4 km to 85 km, with a spacing of 200 m between lines (100 m for the Klitdal infill area), and 76 tie lines were flown with a spacing of 2,000 m between tie-lines totalling 10,171 km for the complete survey.

One of the most important magnetic trends corresponds to the NE-SW lineament separating the high magnetic susceptibility of the Liverpool Land characterized by metamorphic rocks from the low magnetic signal corresponding to the Triassic sediments (Fig. 5.7). This evidence supports the presence of a major fault along that trend.

5.1.3 SkyTEM and Drill-core data

A high-resolution dual moment, i.e. Low Moment (LM) and High Moment (HM) airborne time-domain electromagnetic survey (SkyTEM) was conducted along the eastern margin of the Jameson Land basin in central East Greenland to explore for base metals. The survey was followed by a drilling campaign to investigate the presence of copper mineralization in the Triassic sandstone and conglomerate of the Pingo Dal Formation (Fig. 5.8).

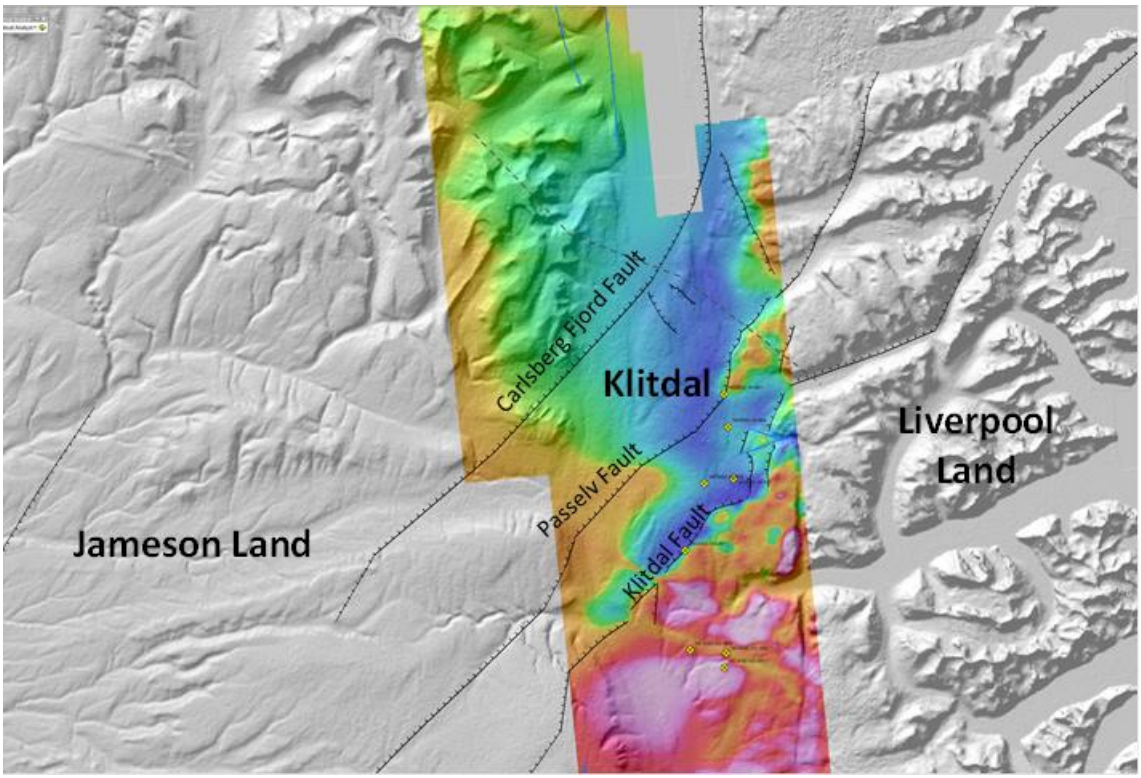

Figure 5.7. The Fugro aeromagnetic survey showing the correspondence between mapped faults and magnetic trends in the Klitdal area.

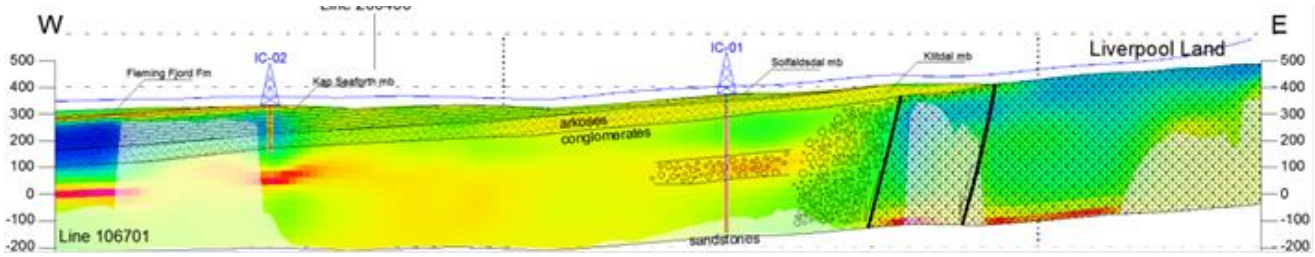

Figure 5.8. Conductivity section (1D-inversion EM data from SkyTEM survey) (Fig. 5.7). Note the faults in the eastern part between the basement and the sediments as well as the 512m deep drill hole IC-01 which does not reach the basement.

5.2 Difference between old and new tectonic model

The summary report on the petroleum potential of Jameson Land by Christiansen et al. 1991 assumed the following tectonic evolution of the basin:

- Crustal extension (E-W) of the order of 30-40 km during the Devonian by displacement along an eastward dipping detachment zone.

- Extension (NW-SE?) of the order of 10-15 km with antithetic faulting and rotation of fault block in the late Devonian to early Carboniferous time, associated with transpression along the basin margins and major halfgraben formation that filled tectonic relief.

- Dominantly thermal subsidence with no crustal extension in the Permian through Tertiary time.

- Early Tertiary igneous activity with emplacement of sills but no faulting of the basin.

- Tertiary uplift of the region.

The tectonic history inferred from the new structural and seismic study differs substantially from the previous one:

1. The combination of NE-SW trending fault escarpments offsetting the Base Permian horizon and similarly orientated depocentres of thicknesses of >2 km between the Base Permian and upper Triassic horizons supports the presence of a major Triassic rift phase in the Jameson Land Basin (Fig. 5.9).

2. The Triassic depocentres display a general NE-SW orientation aligned with the Fleming Fjord and Nathorst Fjord systems. This trend follows the axis of the Vøring Basin on the conjugate Norwegian margin. The pattern of accumulation suggests that extension was not uniform across the basin and possibly influenced by structural elements inherited from the Late Carboniferous tectonic phase (Caledonian).

3. The Permo-Triassic basin development occurred in three stages defined by four seismic-stratigraphic horizons which are generally seen as unconformities: Base Permian, Early Triassic, Top Gipsdalen Fm. and Top Fleming Fjord Fm. Although uncertainty is associated with the timing of rifting the main rift phase is likely early-middle Triassic. Half-graben geometries developed against northeasterly trending extensional faults are seen on some of the seismic profiles.

4. The seismic unit representing Fleming Fjord Formation indicates late Triassic subsidence in central parts linked to thermal cooling. However, asymmetric basin developments in the west and northwest sector of the licence area (A2.3) may reflect a late extensional phase.

5. The Triassic rift phase was replaced by more regional subsidence associated with a widespread transgressional phase across the North Atlantic region, resulting in the overall plate-shaped sedimentary geometries of the Jurassic units.

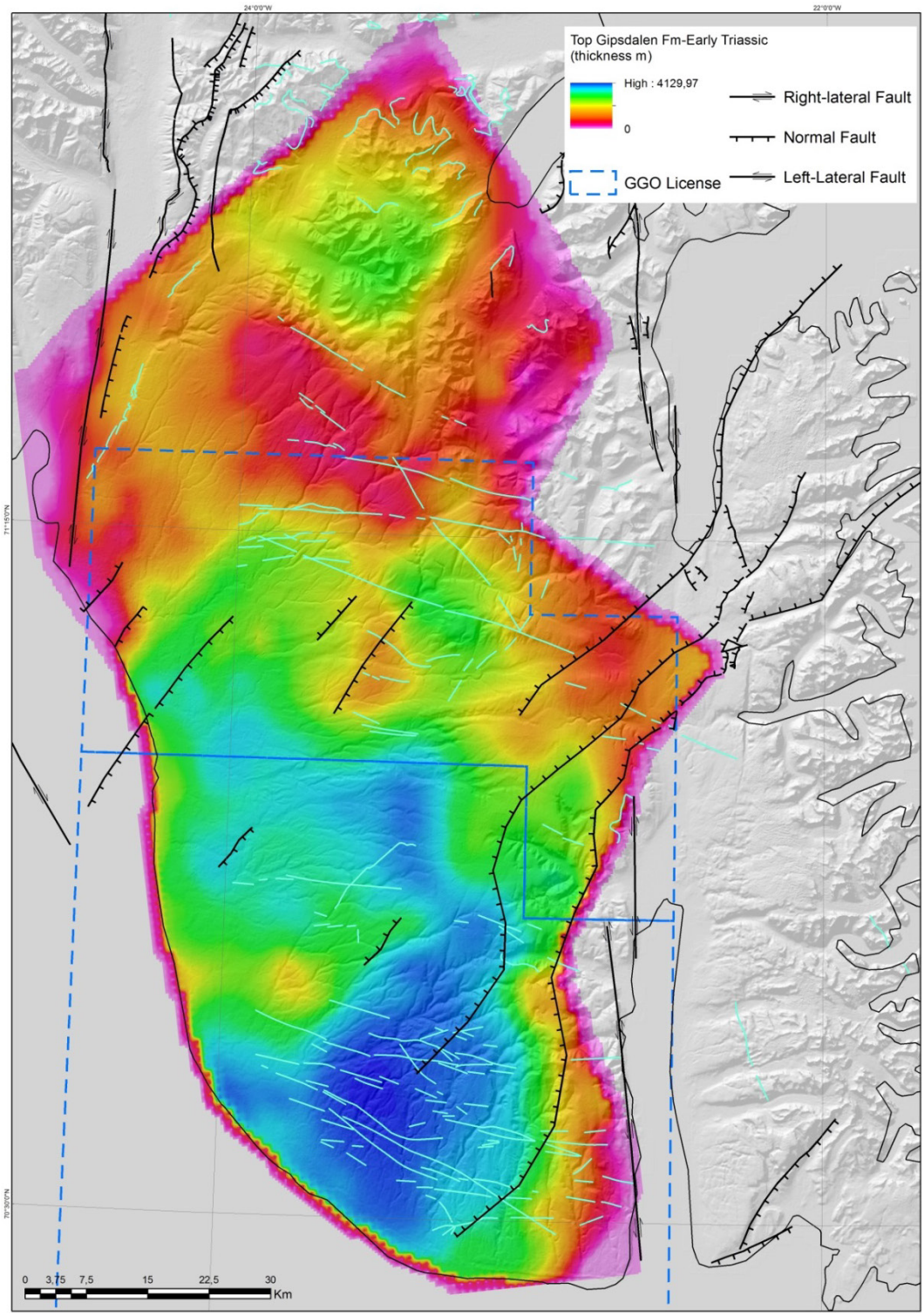

Figure 5.9. Structural map of the Jameson Land Basin showing Triassic normal faults (extrapolated into basin from outcrop positions) overlain on the thickness map of the Triassic syn-rift package. Light blue=Tertiary sills and dikes.

6. Potential source rock intervals

6.1 Ravnefjeld Formation (Upper Permian)

Key references include Surlyk et al. (1986), Piasecki & Stemmerik (1991), Christiansen et al. (1990, 1992, 1993), Stemmerik (2001a,b). Marine organic-rich shales of the Upper Permian Ravnefjeld Formation are widespread in East and Northeast Greenland, including Jameson Land. The shales were deposited in the axis of a more than 400 kilometres long and at least 80 kilometres wide marine basin, surrounded by shallow water carbonate platforms. The sedimentology, stratigraphy and organic geochemistry of the Ravnefjeld Formation has been described in detail by Surlyk et al. (1986), Piasecki & Stemmerik (1990) and Christiansen et al. (1992, 1993). Permian deposits equivalent to the Ravnefjeld Formation have been encountered in shallow core-wells drilled off mid-Norway (Bugge et al. 2002).

Within the Ravnefjed Formation, organic-rich shales with petroleum source potential occur in two distinctive units with a cumulative thickness of 15–20 m, separated by a bioturbated unit (Piasecki & Stemmerik 1993). The laminated organic-rich shales show good to excellent generation potential with values of TOC sometimes close to 10 % and Hydrogen indices near 700 (Fig 6.1, Table 6.1). The shale units have been traced throughout the basin for more than 400 kilometres along strike. Based on average values of TOC and Hydrogen Index (Table 6.1) in combination with the distribution of TOC and Hydrogen Index within the sample set (Fig. 6.2), recommended parameters for basin modelling are estimated at TOC: 4%, Hydrogen Index 400 with a source rock thickness of 15m.

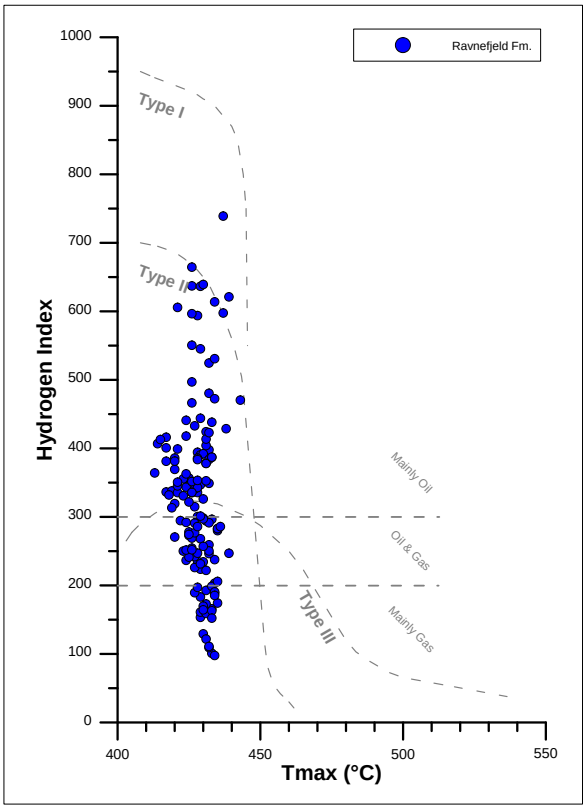

Selected data, source rocks only:
TOC>1%, S2>2mg/g

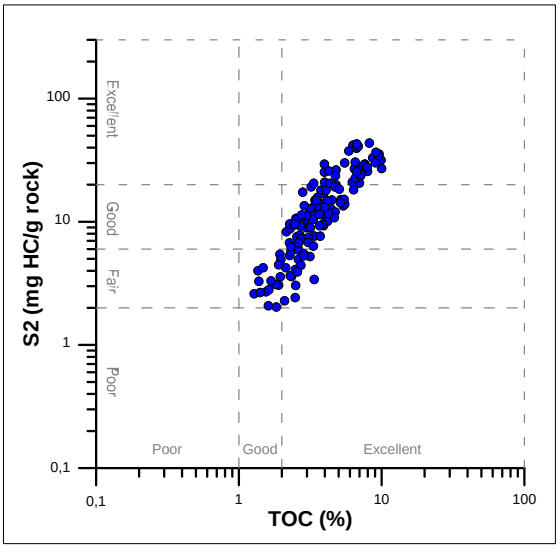

Figure 6.1 (previous page). Standard plots of Rock-Eval-type pyrolysis data for 145 samples of the Ravnefjeld Formation, collected over most of Northeast Greenland, including Jameson Land. Many samples show excellent generation characteristics.

Ravnefjeld Fm., Permian, selected samples, TOC>1%, S2>2 mg/g	TOC (wt-%)	S2 (mg/g)	Hydrogen Index	# samples
Minimum	1,28	2,03	98	
Maximum	10,00	43,52	739	
Mean	**4,06**	**14,42**	**332**	**145**

Table 6.1. Minimum, maximum and average values of Total Organic Carbon content, S2 pyrolysis yield and Hydrogen index.

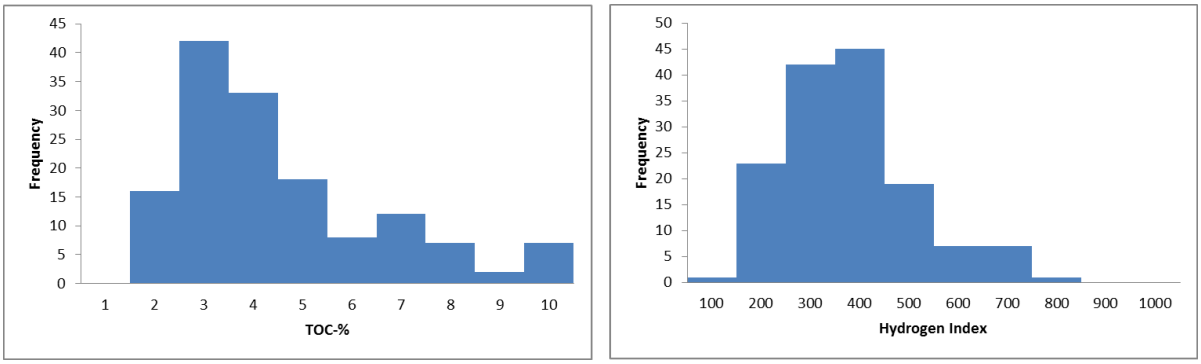

Figure 6.2. Distribution of TOC (left) and Hydrogen Index (rigth) in samples of the Ravnefjeld Formation (U. Permian), selected samples, TOC>1%, S2>2mg/g.

6.2 Gråklint Beds of Gipsdalen Formation (Upper Triassic)

Key References include Clemmensen (1980a,b), Clemmensen et al. (1998) and Andrews et al. (2014). The petroleum generation potential of Upper Triassic lacustrine shales referred to the Gråklint Beds, Solfaldsdal Member, Gipsdalen Formation (Jameson Land, Traill Ø) is largely speculative. However, a recent publication by Andrews et al. (2014) points to the presence of possible petroleum potential within the Gråklint Beds. However, the dataset is very small, samples are scattered, and little is known about the thickness of the prolific deposits relative to non-productive deposits within the Gråklint beds. Increasing thickness and/or stacking of prolific source beds within the newly discovered Triassic-age rift in Jameson Land cannot be ruled out, and this possibility should thus not be ignored, despite the scarcity of factual information. Some of the organic-rich lacustrine shales show good to excellent generation potential with values of TOC sometimes up to >6 % and Hydrogen indices near 500 (Fig 6.3, Table 6.2). Based on average values of TOC and

Hydrogen Index (Table 6.2) in combination with the distribution of TOC and Hydrogen Index within the sample set (Fig. 6.4), recommended parameters for basin modelling are estimated at TOC: 3.5%, Hydrogen Index 350 with a source rock thickness of 1m.

Figure 6.3. Standard plots of Rock-Eval-type pyrolysis data for 10 samples of the Gråklint Beds, Gipsdalen Formation, collected in Jameson Land. Several samples show excellent generation characteristics.

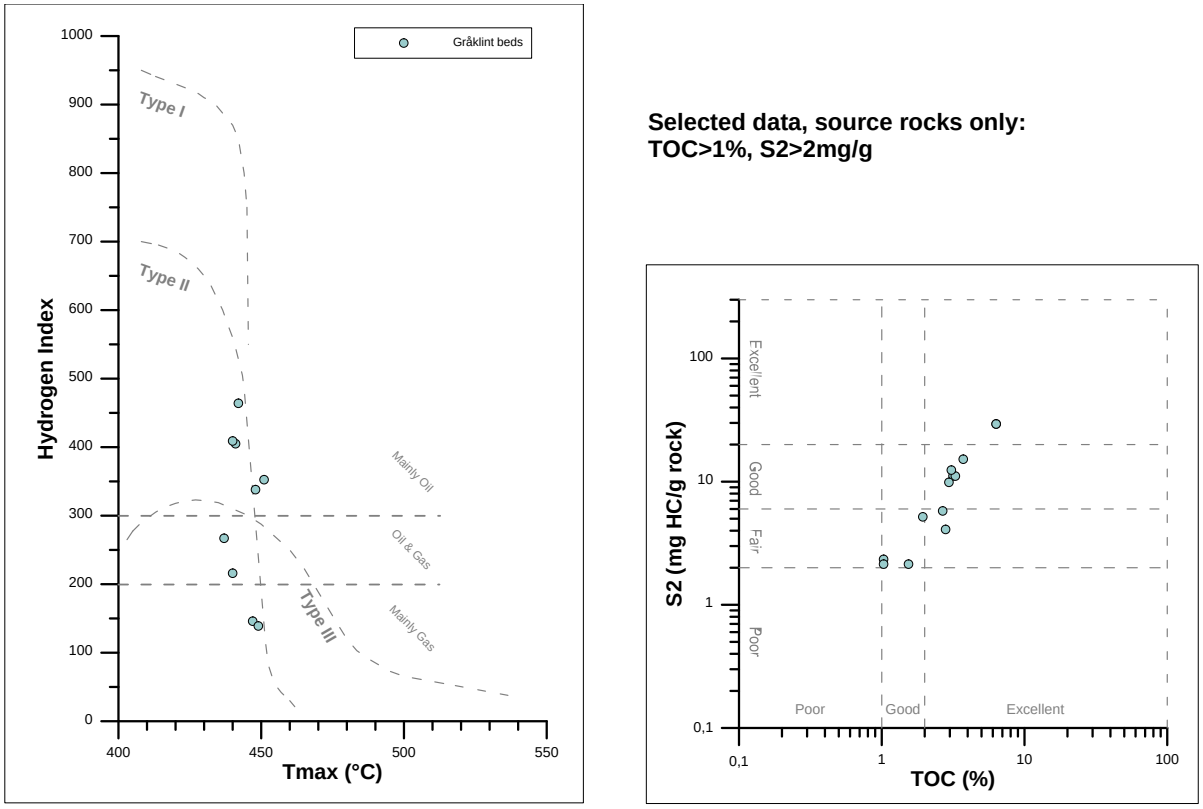

Gråklint beds, Triassic, selected samples, TOC>1%, S2>2 mg/g	TOC (wt-%)	S2 (mg/g)	Hydrogen Index	# samples
Minimum	1,03	2,14	139	
Maximum	6,33	29,36	464	
Mean	**2,95**	**9,88**	**296**	**10**

Table 6.2. Minimum, maximum and average values of Total Organic Carbon content, S2 pyrolysis yield and Hydrogen index.

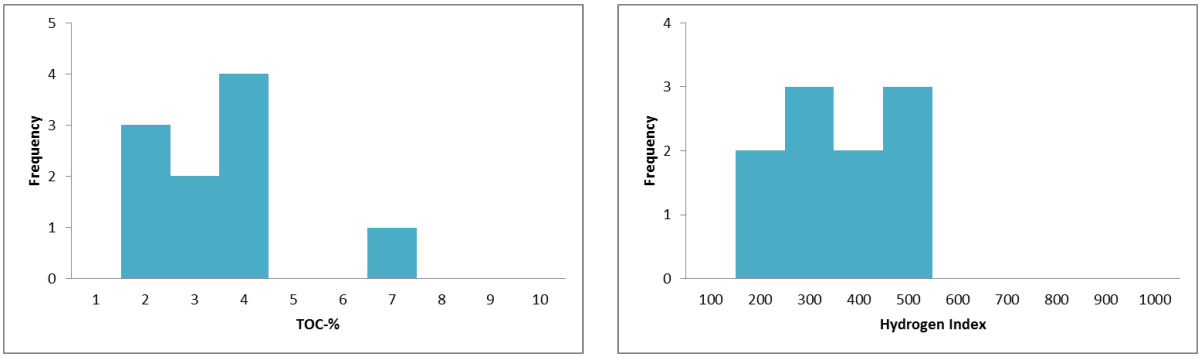

Figure 6.4. Distribution of TOC (left) and Hydrogen Index (rigth) in samples of the Gråklint Beds, Gipsdalen Formation (U. Permian), selected samples, TOC>1%, S2>2mg/g.

6.3 Kap Stewart Group (Lower Jurassic)

Key references include Dam & Christiansen (1990), Christiansen et al. (1992), Dam & Surlyk (1992, 1993), Surlyk (2003). Uppermost Triassic – Lower Jurassic lacustrine shales with source potential are widespread in Jameson Land. The Kap Stewart lake covered more than 12 000 km^2, and organic-rich shales seem to have had an almost basin-wide distribution during high lake level. Outcrops of the Kap Stewart Group sediments are found along the inferred paleomargins of the lake over most of Jameson Land. The thickest exposed organic-rich shale with generative potential for liquid hydrocarbons is 10–15 metres thick, but it is likely that much thicker, oil-prone shales are present in the deeply buried, central part of the lake basin. The sedimentology, stratigraphy and organic geochemistry have been described by Dam & Christiansen (1990), Dam & Surlyk (1992, 1993), Dam et al. (1995) and Krabbe (1996) who propose a fresh-water lacustrine depositional environment for the mudstones. Organic geochemical screening data (TC/TOC/Rock-Eval) on the Kap Stewart Group shales show wide scatter, probably reflecting different depositional environments in the lake. Values of TOC may be very high and coals may even occur, and pyrolysis yield likewise very high. However, for the more prolific deposits values of TOC in the range 5–10% and HI values between 350 and 700 are common (Fig. 6.5, Table 6.3). The level of thermal maturity is generally low, immature to early oil window mature, but in the deeply buried central parts of the basin, the level of thermal maturity is probably higher. Based on average values of TOC and Hydrogen Index (Table 6.3) in combination with the distribution of TOC and Hydrogen Index within the sample set (Fig. 6.6), recommended parameters for basin modelling are estimated at TOC: 6%, Hydrogen Index 500 with a source rock thickness of 30m.

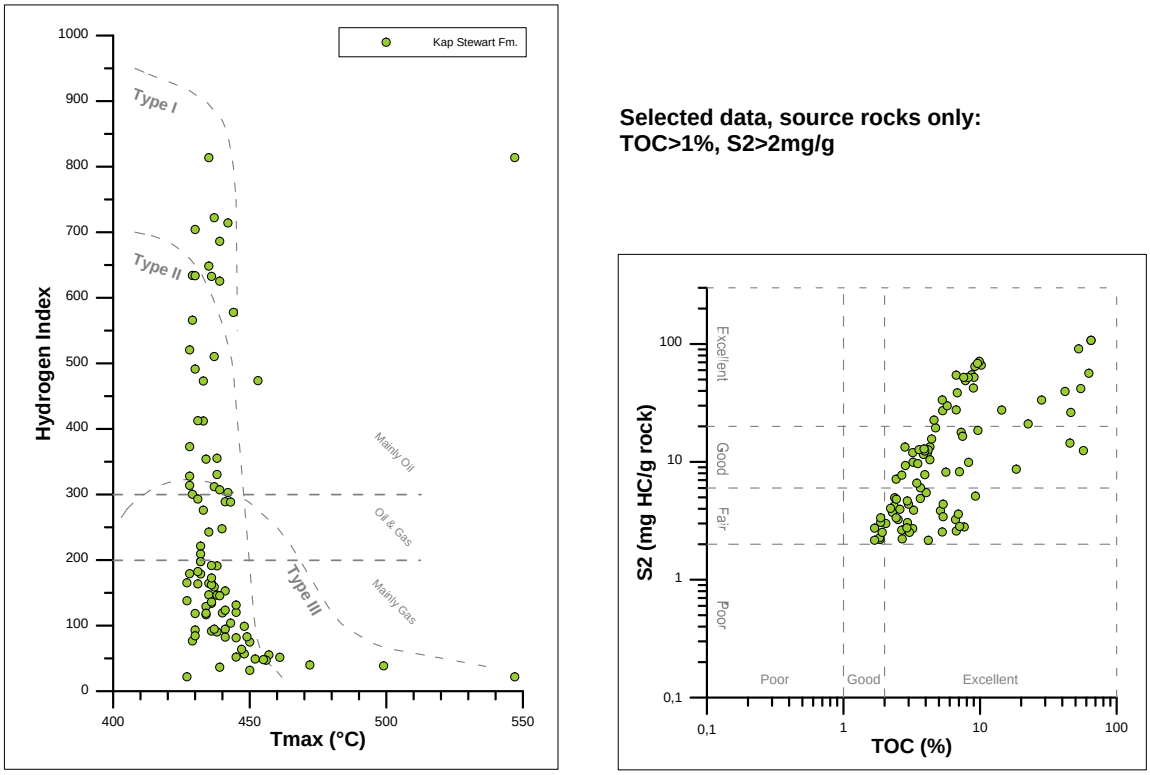

Figure 6.5. (previous page). Standard plots of Rock-Eval-type pyrolysis data for 92 samples of the Kap Stewart Group collected in Jameson Land. Many samples show excellent generation characteristics.

Kap Stewart Fm. Tr/J, selected samples, TOC>1%, S2>2 mg/g	*TOC (wt-%)*	*S2 (mg/g)*	*Hydrogen Index*	*# samples*
Minimum	*1,69*	*2,16*	*22*	
Maximum	*64,90*	*107,28*	*814*	
Mean	***9,64***	***18,47***	***248***	***92***

Table 6.3. Kap Stewart Formation. Minimum, maximum and average values of Total Organic Carbon content, S2 pyrolysis yield and Hydrogen index.

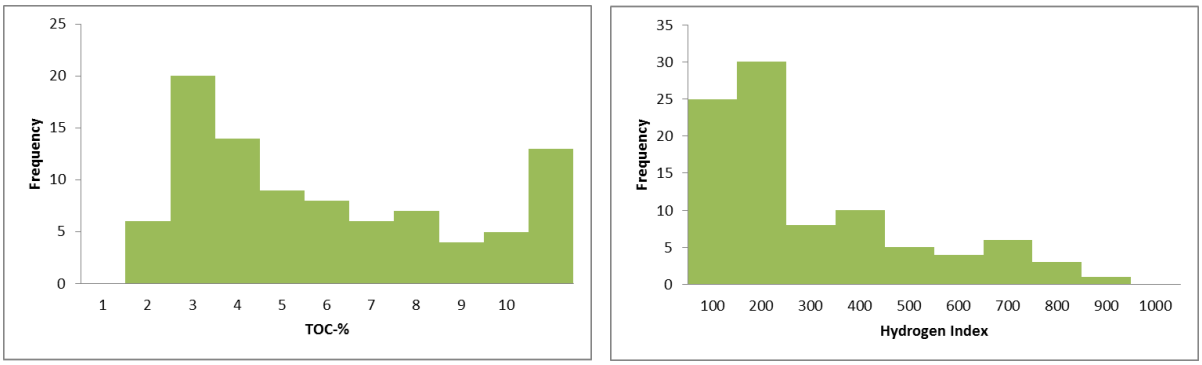

Figure 6.6. Distribution of TOC (left) and Hydrogen Index (rigth) in samples of the Kap Stewart Group Lower Jurassic), selected samples, TOC>1%, S2>2mg/g.

6.4 Additional potential source rocks

In addition to the three units briefly discussed above, Jameson Land hosts a number of additional potential petroleum source rock successions. Foremost, the Upper Jurassic – Lower Jurassic Kimmeridge Clay Formation equivalent succession referred to the Hareelv and Hesteelv formations. The succession is drilled by the Blokelv well, data from which form the basis for the maturity parameters used in the maturity modelling described herein, but otherwise, the succession is considered less relevant for the present purpose in that it is exposed or very shallowly buried over most of Jameson Land.

Marginal source rocks are also found in the Aalenian Sortehat Formation, but again, although these may perhaps serve as a supplementary source for hydrocarbons, they are regarded as unimportant in the present context.

Deeply buried lacustrine petroleum source rocks are presumably present within the Devonian and Carboniferous successions. However, such source rocks have never been documented in Jameson Land and their presumed presence relies solely on their presence in areas further north. In the present context they have been left unconsidered, since little is known about their distribution, thickness and quality. Moreover, they can be expected to be overmature if present.

Additional data and relevant references on these units can be found in Bojesen-Koefoed et al. (2009).

7. Characterization of play types

The main play described by ARCO was the Upper Permian carbonate build-ups with lateral and overlying organic shales as source rock and seal. No exploration well was drilled to evaluate the play and the concession was terminated in 1990. An exploration report was completed by GGU in 1991 based on the oil geological studies including shallow core holes by GGU during the 1980´ties and the concession work of ARCO (Christiansen et al 1991). The exploration report presented three conceptual play types:

1. A Devonian-Carboniferous structural play with rotated fault blocks of lacustrine Carboniferous shales as source rocks and Devonian – Permian sandstones as reservoir rocks and intraformational and overlying lacustrine mudstones as seals.

2. The Upper Permian carbonate play as described above by ARCO.

3. A Lower Jurassic play with lacustrine mudstones as source rock and seal, and intraformational delta front sandstones as reservoirs.

In this report we re-evaluate the play types based on the new seismic interpretation of the reprocessed data, maturity data from shallow core drillings and recent fieldwork of Upper Permian – Jurassic strata. The conceptual play types are presented in geological order, i.e. they are not ranked according to risk assessment.

7.1 Upper Permian carbonate play (Foldvik Creek Group)

- Source rock: Marine mudstone of the Ravnefjeld Formation

- Primary reservoir units: Platform and reef carbonates, Karstryggen Formation and Wegener Halvø Formation

- Secondary reservoir units: Turbidite sandstones of Schuchert Dal (Upper Permian) and Wordie Creek Formations (Lower Triassic)

- Primary seal: Marine shales of the Schuchert Dal Formation/Wordie Creek Formation
- Trapping mechanism: Combination of stratigraphic and structural closure

- Prime risks: Burial history and migration pathways (e.g. overmature in basin setting); porosity and permeability of potential carbonate reservoir units

The play presented in Christiansen et al. (1991) was based on seismic interpretation of carbonate buildups centrally in Jameson Land (Fig. 7.1). The new seismic interpretation suggests that the Permian interval is buried much deeper in the central and southwestern part of the basin (Ch. 4). Aggradational-mounded seismic features inferred as carbonate buildups are observed on the reprocessed lines, two of them with direct ties to Karstryggen Fm. (Fig. 4.4), which may suggest that carbonate deposits of the Foldvik Creek Group are

widely distributed along the northern and eastern margins of the basin. Similar features overlying the Base Permian horizon on line 86-6v (Fig. 4.5) implies that buildups are also present in the deep part of the basin (pre-rift stage). However, the wider basinal distribution of Permian carbonate deposits is difficult to interpret at the present level of seismic resolution (notably in the southern part of JLB). A better understanding of how the carbonate system is distributed could be gained by additional reprocessing of ARCO lines.

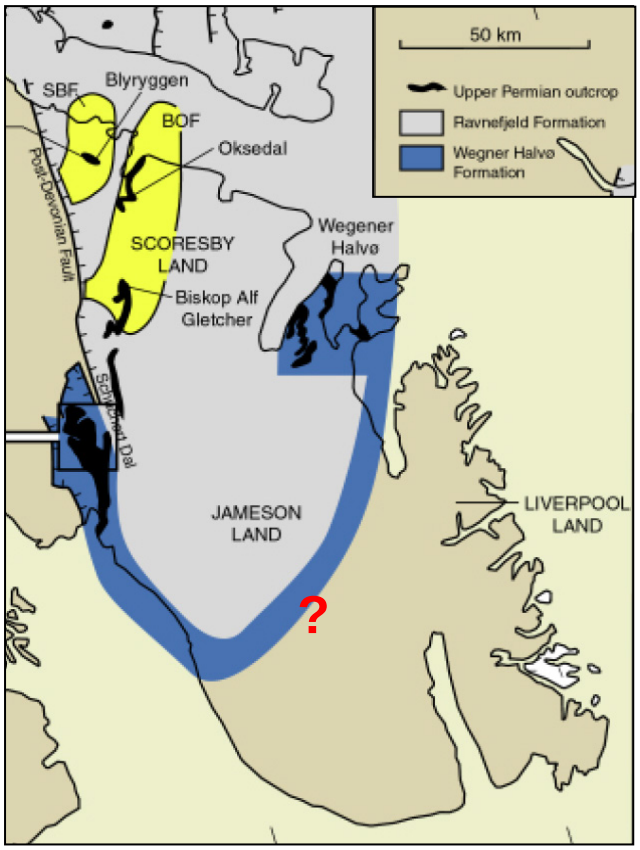

Figure 7.1 Palaeogeographic reconstruction of the Late Permian in the Jameson Land Basin Wegener Halvø – Ravnefjeld Formation times (Stemmerik 2001a). Carbonate platforms are distributed along the basin margins and over structural highs based on outcrop studies and previous seismic interpretations. The present seismic interpretation differs entirely from the old study were the Permian was inferred to be at a much shallower level. With the new interpretation it is likely that Ravnefjeld Fm or equivalent mudstone units are more wide spread than suggested in the old study. Lowstand turbidite fans as part of Wordie Creek Fm, exposed in the proximal western part of Jameson Land, may have contributed to the great thicknesses of the Permian unit in the central and southern parts (see also sequence stratigraphic section in Fig. 7.3).

Platform carbonates of the Karstryggen Formation range 10 – 150 m in thickness, and contain potential reservoir units described in outcrop studies and core data along the NW and NE basin margins (Scholle et al. 1993). The quantitative porosity and permeability of the units are not well known, but extensive karst- and breccia related secondary porosity are reported (Scholle et al. 1993). Porosity reducing characteristics include widespread calcite cementation, neomorphic and mineralogical replacements. The carbonate buildups of the Wegener Halvø Formation show composite thicknesses of up to 100 m. Porosity of the carbonates are presently low, generally <2%, but were likely magnitudes higher at the time of hydrocarbon migration (>10%, Stemmerik 2001).

The marine shales of the Ravnefjeld Formation that provides the principle Permian source rock show thickness variations from a few metres in proximal settings and up to 100 m in basinal settings. Intervals of excellent petroleum generation potential have been identified with a cumulative thickness of up to 20 m (Ch. 6, Christiansen et al., 1992, 1993). The formation interfingers with the Wegener Halvø Formation carbonates in the lower part and

towards the basin margins. A seismic facies consisting of semi-continuous, onlapping reflections seen in the upper part of seismic Unit 7, is interpreted as potential equivalents to Ravnefjeld Fm mudstone (Figs. 4.4-4.5). As for the Permian buildups further reprocessing of seismic lines would provide a better constrain on the distribution of seismic facies linked to source rock.

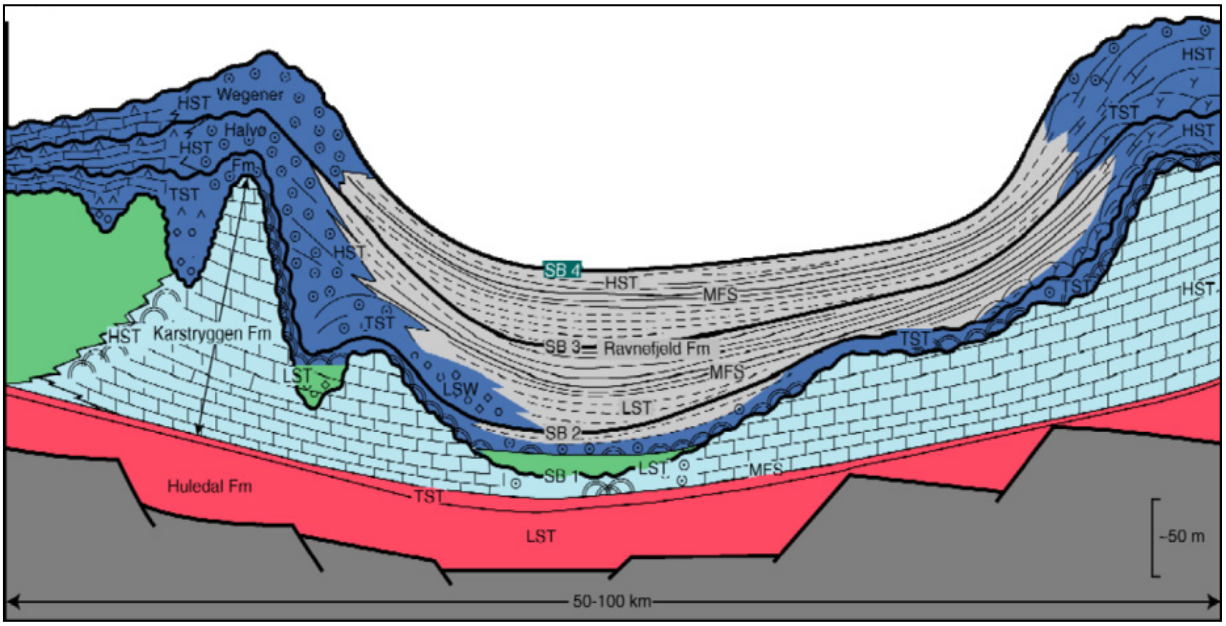

Figure 7.2. Schematic cross-section of the East Greenland Permian basin fill showing major lithostratigraphic units and depositional sequences. From Stemmerik (2001a).

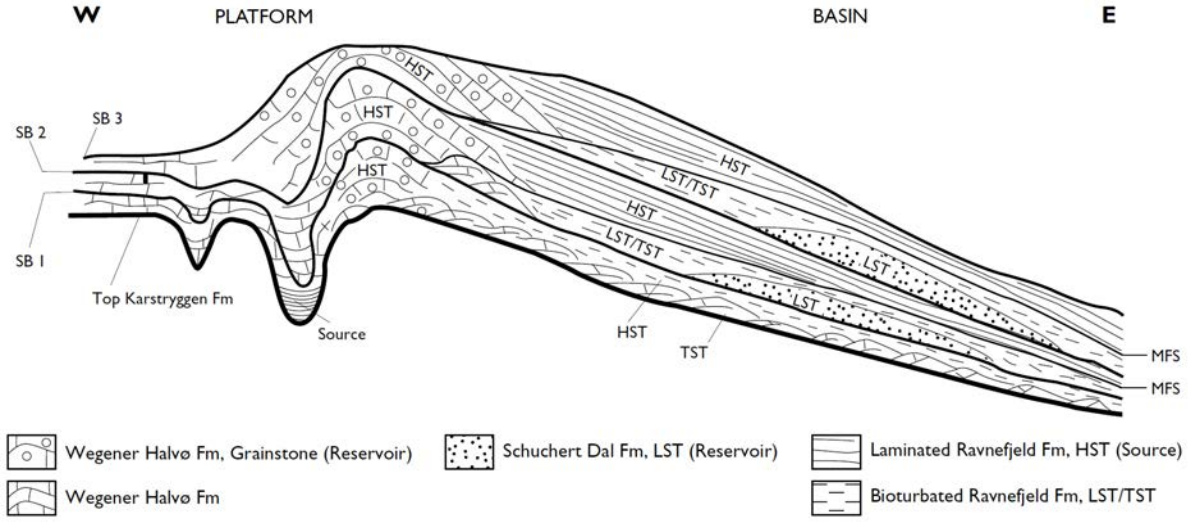

Figure 7.3. Sequence stratigraphic model of the Upper Permian Wegener Halvø, Ravnefjeld and Schuchert Dal Formations in Jameson Land. Potential source and reservoir rocks are indicated. SB: sequence boundary; MFS: maximum flooding surface; LST, TST and HST: lowstand, transgressive and highstand systems tracts (Stemmerik et al. 1998).

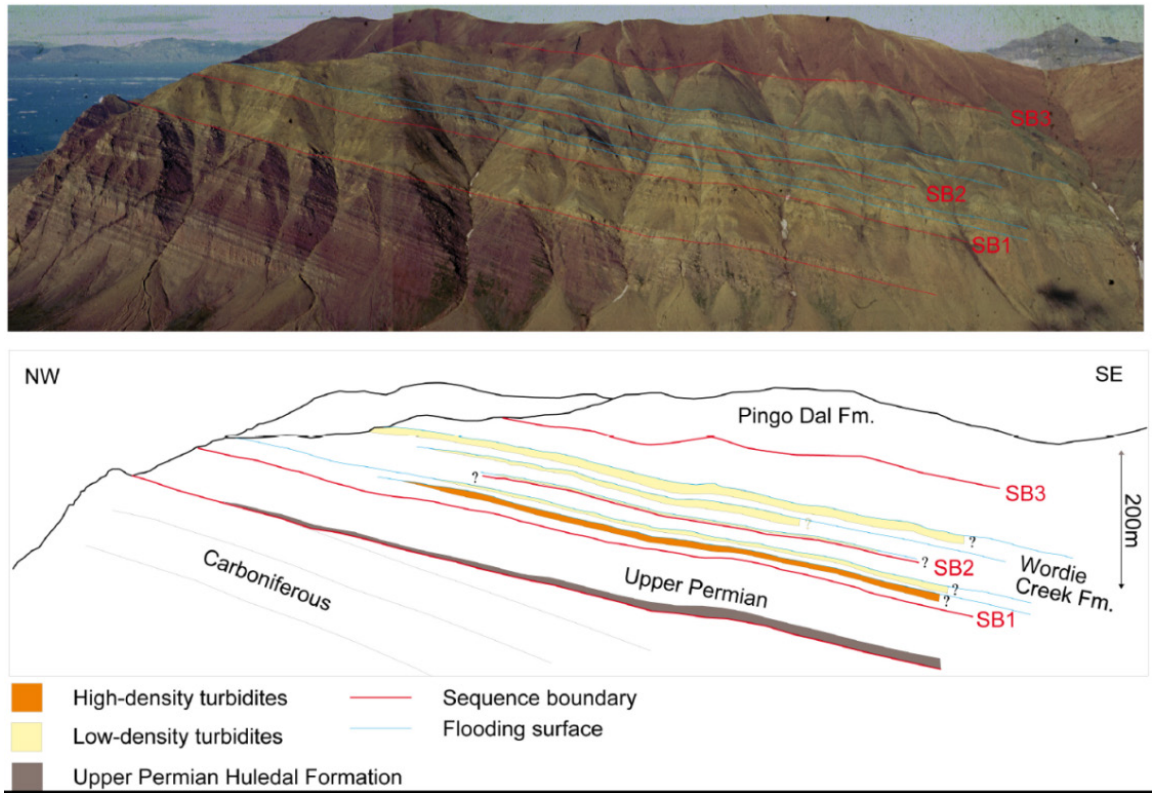

Figure 7.4. Depositional strike section of a tilted fault-block in the northern part of Jameson Land. Lower Triassic turbidites of the Wordie Creek Fm pinch out towards the crest of the tilted fault-block. The SB3 (Griesbachian– Dienerian) is developed as an angular unconformity related to augmented tectonic tilting during the Late Griesbachian rifting event. The Early Triassic seismic horizon is correlated to this erosional event.

In basinal settings additional Upper Permian reservoir units may occur in lowstand sandy turbidites of the Schuchert Dal Formation (Fig. 7.3). The primary seal comprise mudstones of the Schuchert Dal Formation which attains a maximum thickness of up to 300 m in the northern Jameson Land. The unit comprise marine mudstones and three intercalated turbidite sandstone units (Kreiner-Møller & Stemmerik 2001).

Additional seal unit comprises mudstones of the Lower Triassic Wordie Creek Formation. Seismic signatures inferred as a submarine fan accumulation that appears to prograde from north-northwest into the basin (Fig. 4.5), is likely a correlative to Wordie Creek Formation, which shows intraformational turbidite sandstones and fan developments with thicknesses up to 50 m in the northern part of Jameson Land (Fig 7.4, Seidler 2000, Seidler et al. 2004, Bjerager et al. 2006).

The trapping mechanism of the Permian play type is a combination of stratigraphic and structural closure. The carbonate buildups form potential closed stratigraphic structures sealed by overlying mudstones. The prime risks are related to the burial history and

migration pathways. At the present the Ravnefjeld Fm is considered to be overmature in most of the basin and hence the play type relies on updip migration of hydrocarbons during the main burial stage into reservoirs on the shallow fringes of the basin (maturation modelling in Ch. 9).

7.2 Triassic rift phase

- Primary source rock: Marine mudstone of the Ravnefjeld Fm.
- Additional source rock: Lagoonal – lacustrine mudstones of Gråklint Beds (Gipsdalen Fm)
- Primary reservoir: Sandstone and conglomerates, Pingodal Formation
- Secondary reservoirs: Wordie Creek Formation, Ørsted Dal Member of the Fleming Fjord Formation
- Primary seal: Mudstones of Fleming Fjord Formation
- Trapping mechanism: Combination of up-dip stratigraphic pinch-out and structural closure
- Prime risks: Timing of maturation and charge, top seal along the basin margin, reservoir quality

The new play is based on the present interpretation of the reprocessed seismic data that is correlated with recent shallow core-drillings and fieldwork along the eastern basin margin (Ch. 5). The Triassic play comprises rift-controlled wedges of alluvial clastics that fill into grabens developed along NE orientated extensional faults (seismic Unit 6: GPF in Figs. 4.2, 4.3 and 4.6). The clastic wedges, interpreted as equivalents to Pingo Dal Fm, are buried/ sealed by upper Triassic mudprone sediments of the Gipsdalen and Fleming Fjord Formations. These graben structures were earlier poorly defined and tentatively suggested to comprise Carboniferous clastic formations that included Devonian–Carboniferous lacustrine source rocks (Christiansen et al. 1991). In light of the new interpretation the Ravnefjeld Formation provides the primary source rock of the Triassic rift play.

The primary reservoir unit are alluvial sandstones and conglomerates of the Klitdal Member (Pingo Dal Formation) (Fig. 7.5-7.6). In outcrops along NE and NW fringes of the JLB these deposits form sedimentary prisms more than 600 m thick (Fig. 3.1). Aeolian sandstones of the Kolledalen Member (Gipsdalen Formation) form an additional potential reservoir unit, 90–190 m thick, along the western basin margin. A prominent rift fault zone is identified along the eastern margin of JLB (Klitdal Basin) with faults trending NE–SW (Ch. 5) with coarse clastic deposits on the hanging wall attaining thicknesses of >500 m decreasing to <50 m on the footwall to the east and draped by Upper Triassic sediment of the Gipsdalen Formation.

Fluvial sandstones and conglomerates of the Ørsted Dal Member may represent intraformational deposits of the Upper Triassic Fleming Fjord Formation, displaying thicknesses of >1200 m along the western basin margin. The Ørsted Dal Member is erosionally overlain by sandstones of the Kap Stewart Group along its proximal settings and fine-grained calcareous sediments of the Tait Bjerg Beds of the Fleming Fjord Fm farther basinwards (Clemmensen, 1980). The Ørsted Dal Member may thus form an additional reservoir unit to the Triassic rift play or to the Kap Stewart Group play type as described below. Equivalent sand-prone sediments may be present within the elongate depocentre of seismic unit 5 (~ Fleming Fjord Fm) in the northwestern part of the study area (A2.3). Farther eastward the Upper Triassic package is influenced by several deep-seated faults that extend into the Jurassic interval, thus implying a marked structural influence on the Triassic rift play (Fig. 4.6). In general terms, the suggested trapping mechanism is a combination of up-dip stratigraphic pinch-out and structural closure along half graben boundary faults. The primary exploration risks of the Triassic Rift Play is related to timing of maturation and charge from the Ravnefjeld Formation, integrity of top seal along the basin margin and reservoir quality. It is emphasized that multiple reservoirs exist for this play type, and in the northeast it may be closely linked to the lower Jurassic system (see below) via the structural setting.

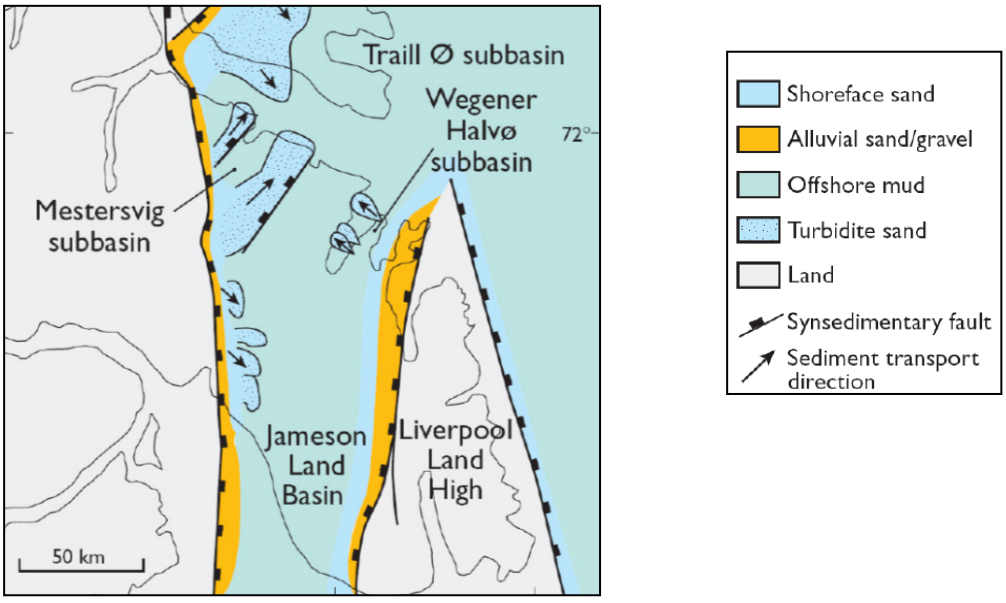

Figure 7.5. Palaeogeographic reconstruction of the Early Triassic (from Seidler et al. 2004). This contrasts the new interpretation displaying a series of segmented rift basins that opens up and deepens toward southwest (Figs. 4.9 and 5.9).

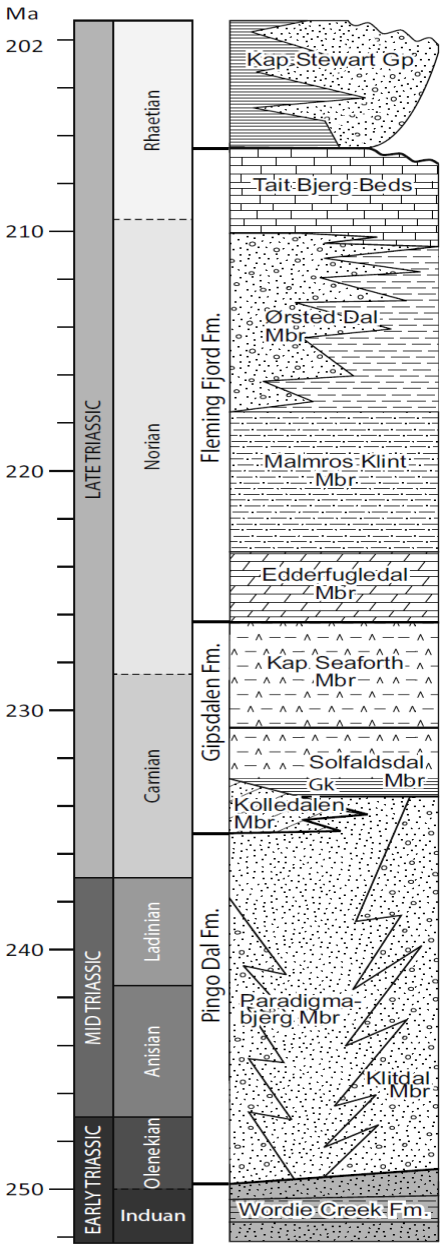

Figure 7.6 Stratigraphic scheme of the Triassic in Jameson Land. From Andrews et al. (2014).

7.3 Late Triassic – Lower Jurassic clastic systems (post-rift)

- Source rock: Anoxic lacustrine sediments, Kap Stewart Group
- Additional sources: Migration from deeper SR systems (Triassic-Permian?).
- Primary reservoir: Deltaic sandstones (low-stand delta sheets and wedges)
- Secondary reservoirs: Marine transgressive sands, Neill Klinter Group and Pelion Formation
- Primary seal: Mudstone facies of the Neill Klinter Group
- Trapping mechanism: Mainly stratigraphic
- Migration pathways: Direct charge of isolated sandstone bodies, low-angle up-dip migration into fluvial-deltaic deposits, fault-controlled in some places
- Prime risk: Top seal along the basin margins, filling history and reservoir quality.

The play is also described in the exploration report by Christiansen et al. (1991) based on the ARCO seismic and extensive geological fieldwork with during 1980´ties. Further fieldwork with data collection and analytical works were performed in the 1990´ties and onwards with focus on stratigraphy, sedimentology and organic geochemistry (Christiansen et al. (1992), Dam & Christiansen (1990), Dam and Surlyk (1992, 1993), Dam et al. (1995), Krabbe (1996) (Figs. 7.7-7.9)

The revised interpretation of this study differs significantly from the previous mapping (Dam et al. 1995) by showing a different thickness distribution across the basin. In the original study greatest thicknesses of the Kap Stewart Group were located in the western part of the basin whereas in the present analyses the main depocentres are located in the eastern and southern parts (Fig. 7.9).

Westward into the basin more isolated to semi-isolated and elongate depocentres are observed. On some lines the easternmost part of the KSG is influenced by reactivated extensional faults but a distinct depositional control by NW-SE trending faults suggested by Dam et al. (1995) is not observed. The new mapping also displays a more detailed depth-structure (to the extent allowed by the seismic grid) and internal seismic geometries, e.g. progradational features and parallel strata, which enhances the play characteristics.

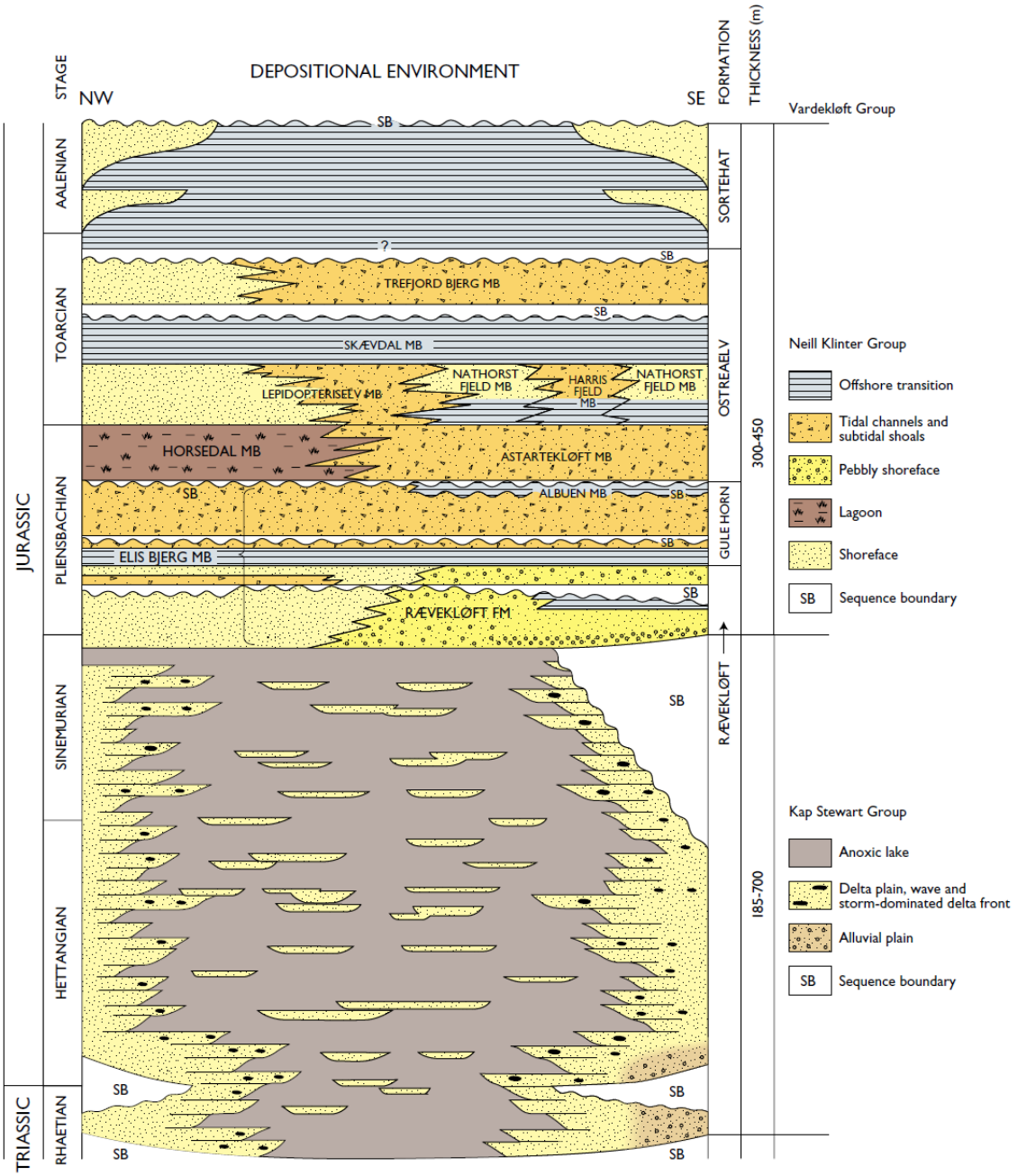

Figure 7.7 Stratigraphical scheme of the Kap Stewart and Neill Klinter Groups (From Dam and Surlyk 1998, and Stemmerik et al. 1998).

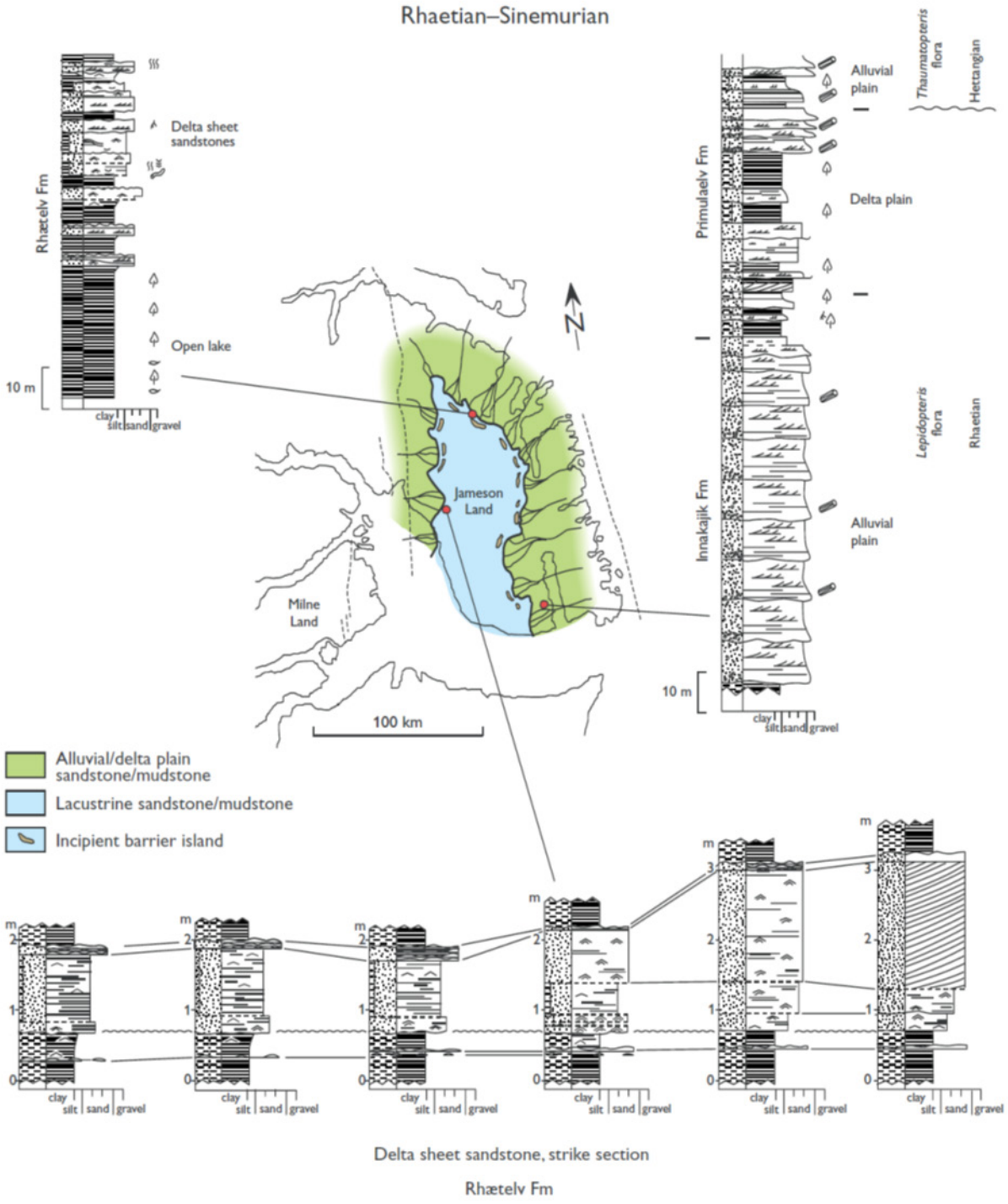

Figure 7.8 Palaeogeographic map of the Rhaetian–Sinemurian fluvio-lacustrine Kap Stewart Group. Characteristic sections through lacustrine, deltaic and alluvial plain deposits shown. Based on Dam & Surlyk (1993).

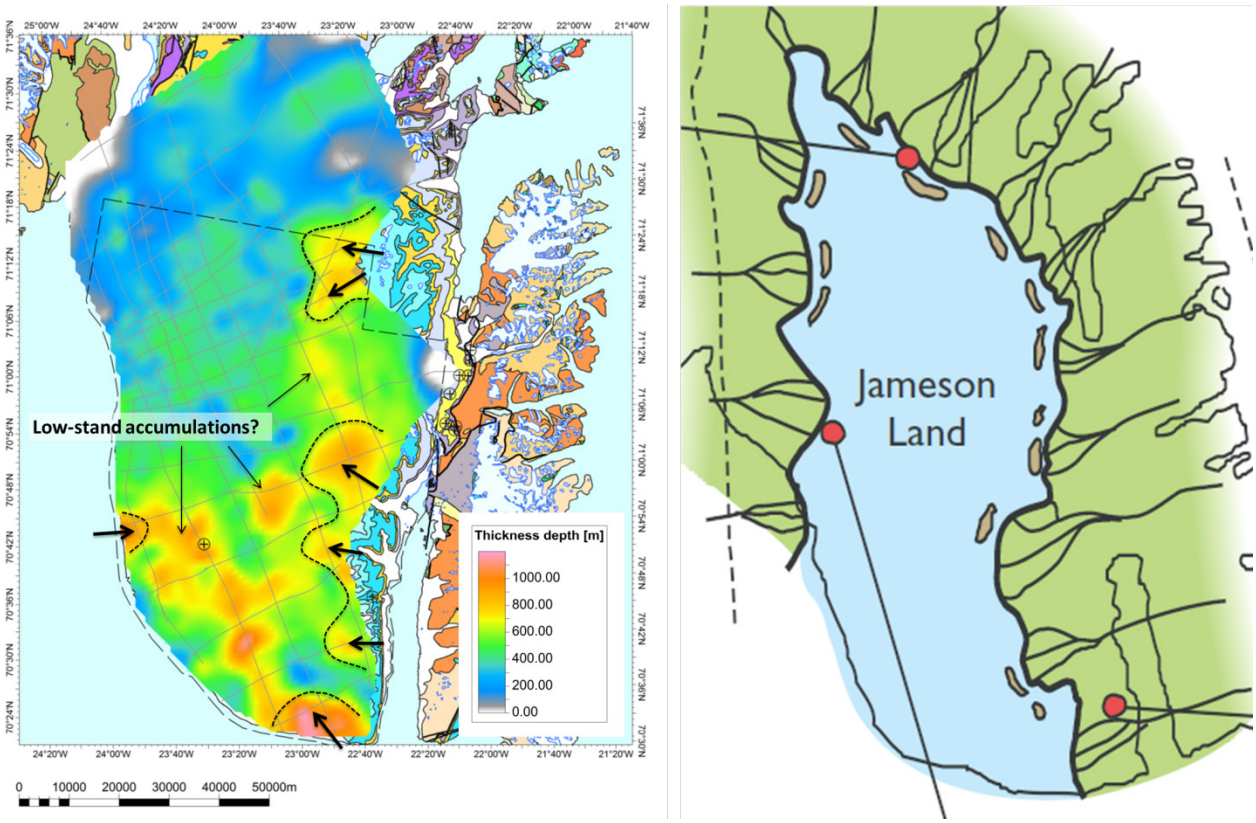

Figure 7.9 Thickness map of the KSG showing depocentres with indications of deltaic progradation (thick arrows) and inferred low-stand sand-prone accumulations (wedges, ridges). The map to the left shows the interpretation based on outcrop studies (from Surlyk 2003). The location of the major deltaic source areas in eastern Jameson Land is largely consistent. The barrier island formations interpreted in sedimentological profiles are below the present seismic resolution.

The uppermost Triassic – Lower Jurassic lacustrine source rock (Ch. 6) is exposed along the margins of the basin. The outcrop studies indicate a composite interval of 10–15 m thickness with a generative potential for hydrocarbons. This source rock thickness probably increases significantly towards the central parts of the JLB basin that likely corresponded to deepest parts of the Kap Stewart lake, presumably covering an area of around 12 000 km^2 (Dam & Surlyk 1993).

Potential reservoir rocks include alluvial sandstones of the Innakajik Formation which shows thicknesses between 10 and 140 m in outcrops (Fig. 7.8). Further basinward these deposits may correlate with sandy Gilbert-type prograding delta front units, inferred from prograding clinoforms that are evident on the digitalized seismic profiles (Fig. 4.11). Of particular interest is the presence of isolated/semi-isolated depositional bodies in the central parts of the basin. These features may be linked to low-stand events in the lake system, manifest by sand sheets considered to represent forced-regression cycles by Dam & Surlyk (1992, 1993). The reservoir units related to cyclic low-stands, described from outcrops in the northwest sector, range in thickness from a few metres to a few tens of metres thick (Ranunkel dal, Fig. 7.10). These units are probably below seismic resolution

but they may represent fairways/pathways along which sand is transferred to the intrabasinal depocentres. The agreement between seismic observations and the depositional development interpreted based on outcrop studies (Fig. 7.9) adds value to this play type.

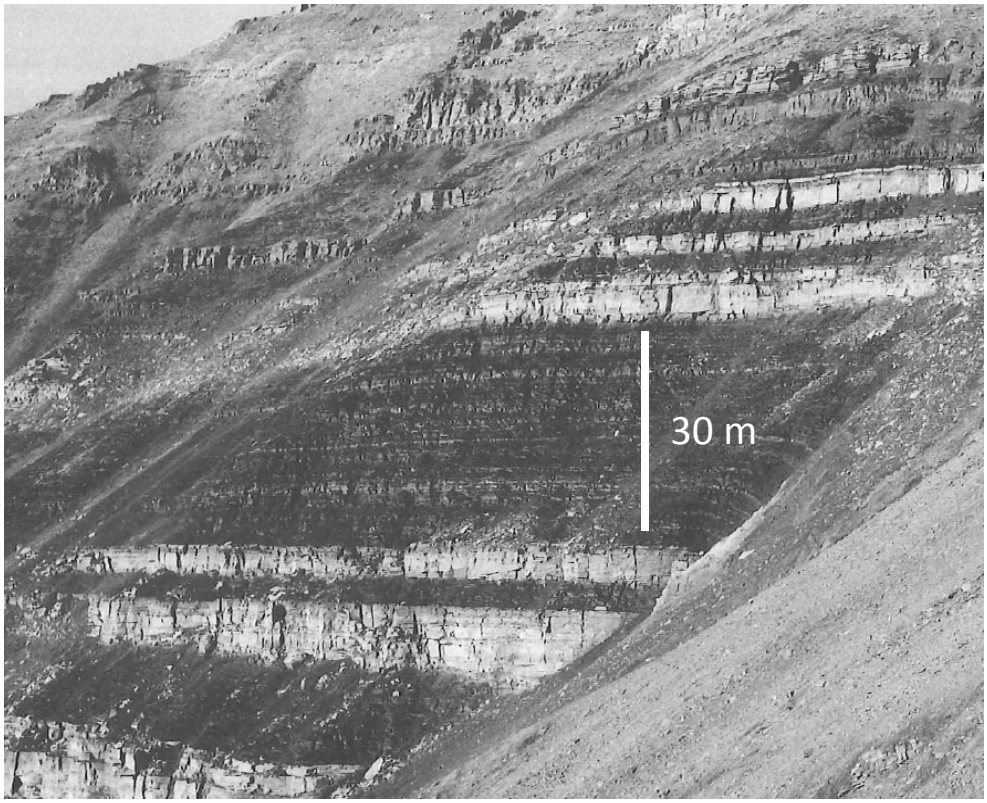

Figure 7.10 Lacustrine anoxic mudstones and interbedded lowstand sand sheets of the Kap Stewart Group at Ranunkeldal (Dam & Surlyk 1993).

Internal organic mudstone units within the Kap Stewart Group act as direct source rocks as well as seals. Development of the early Jurassic play will depend on identification of these types of stratigraphic traps within the Kap Stewart Group. Additional reservoir potential exists in the Neill Klinter Group with shallow marine and tidal sandstones of the Rævekløft, Gule Horn and Ostreaelv Formations (Figs 7.7, 7.11). These units show considerable reservoir thicknesses from outcrop studies (Table 7.1).

Seismic mapping of the Neill Klinter Group show several depocentres distributed in the north-northeast and central parts of the basin (Ch. 4, A2.5), which may contain stratigraphical traps formed by shoreface deposits (e.g. Gule Horn Fm). However, further analyses aimed at resolving the internal stratigraphic relationships of the Jurassic units should be based on reprocessed seismic data. Intraformational marine mudstones, e.g. Elis Bjerg and Skævdal Members, or the overlying mud-prone Sortehat Formation may act as potential seals.

Bajocian lowstand wedges of shallow marine sandstones from the lower part of the Pelion Formation of the Vardekløft Group may form an additional reservoir unit. The unit is up to 30 m thick in exposed section along the eastern margin of the basin (Engkilde & Surlyk 2003). A stratigraphic trap is considered for this additional play with the overlying mudstones Fossilbjerget Formation as a seal.

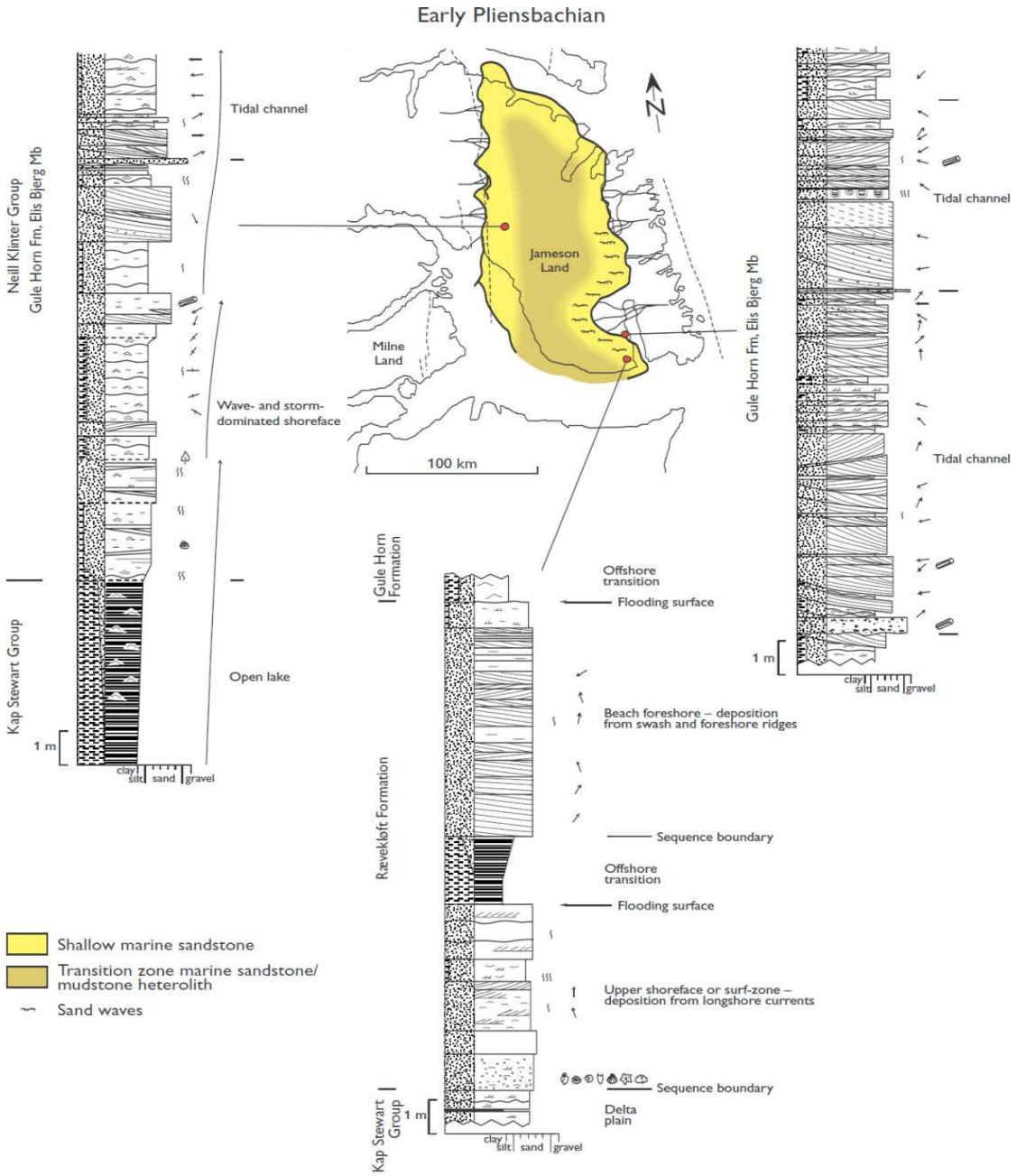

Figure 7.11. Early Pliensbachian palaeogeography represented by the Rævekløft Formation and basal Gulehorn Formation (Dam & Surlyk 1998, Surlyk 2003).

Reservoir unit	Depositional setting	Thickness
Rævekløft Formation	Marine shoreface sandstones	9–20 m
Gulehorn Fm	Marine shoreface and tidal channel sandstones and heteroliths	90 – 185 m
Astartekløft Member (Os Fm)	Subtidal sandstones	18–43 m
Nathorst Fjeld Member (Os Fm)	Shoreface sandstones	29–37 m
Harris Fjeld and Lepidopteriselv Members (Os Fm)	Tidal sandstones	34–60 m
Trefold Bjerg Member (Os Fm)	Tidal channel, subtidal shoals, and wave and storm-dominated shoreface sandstones	21–45 m

Table 7.1. Potential reservoir units in the Pliensbachian– Aelenian Neill Klinter Group (Os, Ostreaelv).

7.4 Late Jurassic deep marine sandstones

- Source rock: Anoxic marine shales of the Hareelv Formation
- Primary reservoirs: Gravity flow sandstones (Hareelv Formation) and shelf edge sandstones (Raukelv Formation)
- Primary seal: marine shales of the Hareelv Formation
- Trapping mechanism: Stratigraphic
- Migration pathways: Direct charge of isolated sandstone bodies and low-angle up-dip migration
- Prime risk: Maturity level, top seal along the basin margins, filling history, reservoir quality and compartmentalisation

The play is developed based on the new data and analytical results from the Upper Jurassic Blokelv-1 core drilling in the southern central part of Jameson Land (Bjerager et al. 2010). The interval is poorly expressed in the seismic data from ARCO, which is probably due to the occurrence of magmatic intrusions/dykes. The play is only relevant in the southern part of Jameson Land and probably further southwards in Scoresby Sund where the interval is interpreted overlain by Cretaceous sediments (Larsen & Marcussen 1992). The depositional setting of the Hareelv Formation is interpreted as a giant sandstone injection complex (Surlyk et al. 2007). A multi-proxy petroleum geological study of the formation is presented in Bjerager et al. (2010) based on the Blokelv-1 core drilling.

The source rock comprises anoxic marine shales of the Hareelv Formation, which is exposed in the central and southern part of Jameson Land. In the Blokelv-1 core in the central part of the basin the shale units attain a combined thickness of >100 m and they are intercalated with potential reservoir units of gravity flow sandstones and injectites that

similarly comprise a combined thickness of >100 m. Individual units are a few cm to several metres thick and show large variation in porosity and permeability; between 6–26 % in porosity and 0.05–400 mD in permeability. Outcrop studies east of the Blokelv-1 drilling location show individual sandstone units up to 50 m in thickness and due to the injective nature they form geometrically complex successions (Fig. 7.12). The sandstones may serve as conduits /carrier beds up dip into shelf edge sandstones of the overlying Raukelv Formation laterally extensive distributed.

The main risks are related to the presently shallow burial of the Hareelv Formation, which has implications for maturity level, filling history and seal integrity.

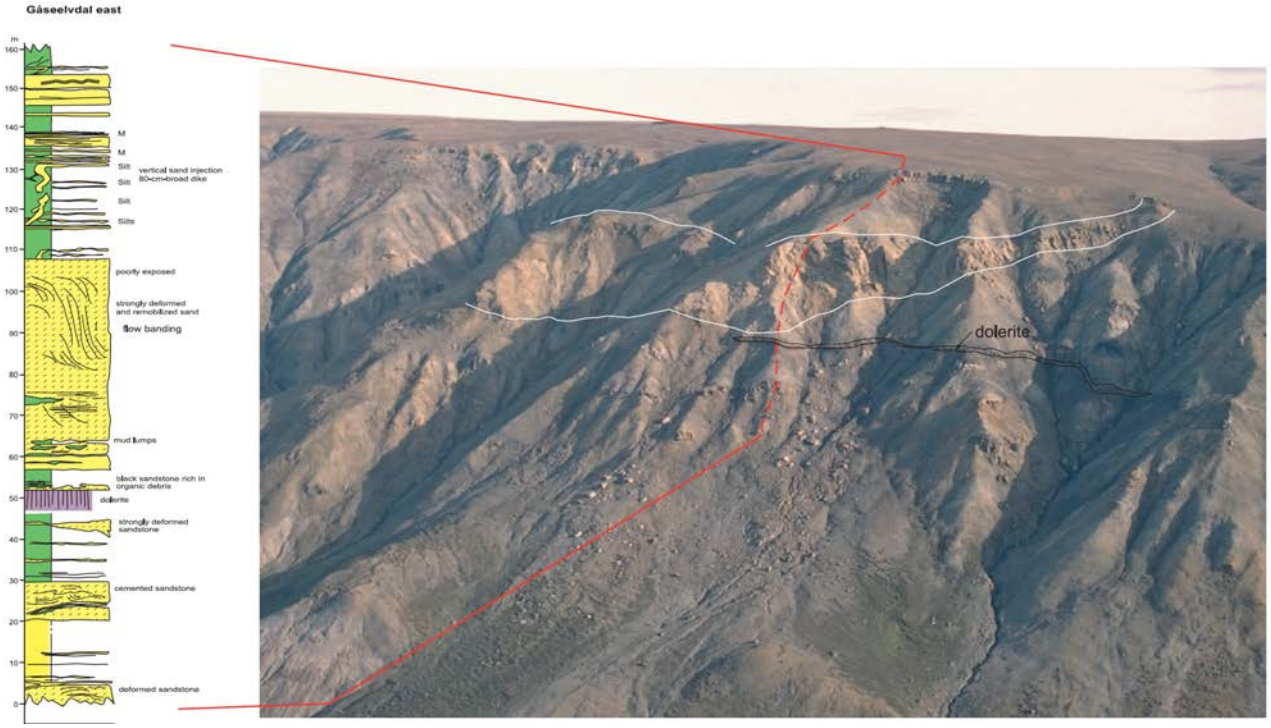

Figure 7.12 Sedimentary section and outcrop of the Hareelv Formation at Gåseelv (Surlyk et al. 2007).

8. Results from apatite-fission track analyses

8.1 Thermal history interpretation of the AFTA data

Five Jurassic sandstone samples provided high yields of apatite suitable for analysis, and the quality of these apatite grains is generally high. Quantitative interpretation of the AFTA data in each sample is summarised in Table 8.1, and full analytical details are presented in Geotrack Report GC1194 (that accompanies this GEUS report). Sample locations are shown in Fig 8.1.

Two samples from the Blokelv borehole (GC1052-1, -2), Jameson Land, have previously been analyzed for AFTA. Since then, refinement of Geotrack's interpretive methods has led to improved definition of three cooling events from AFTA data in a single sample. Consequently, it was decided to reassess the AFTA data in the Blokelv samples for this study (Table 8.1).

AFTA data from all samples provided highly reliable thermal history constraints (parameters defining a range of palaeotemperatures from which the sample cooled within a time interval). Measured fission-track ages in both samples were significantly less than predicted from the Default Thermal History (i.e. the history calculated from the assumption that all units throughout the well are currently at their maximum temperatures since deposition). This shows that the sampled units have been much hotter than present-day temperatures at some time after deposition. The principles of AFTA were recently described in detail by Green et al. (2013).

AFTA data in samples GC1194-1 and -2 require three discrete post-depositional palaeo-thermal episodes to explain all aspects of the data, while data in samples GC1194-4, -5 and -6 can each be explained in terms of two post-depositional episodes of heating and cooling, combined with additional fission tracks formed in sediment provenance regions (Table 8.1). Assuming that the AFTA data reflect synchronous cooling episodes, results in the five samples define three discrete post-depositional episodes of heating and subsequent cooling which began in the interval illustrated by the vertical columns in Figure 8.2a1 (see also Table 8.2). When the cooling ended is not constrained by the data.

The revised interpretation of the two Blokelv-1 borehole samples defines three discrete post-depositional episodes of heating and subsequent cooling (Fig. 8.2a2). The results point to a Cenomanian–Turonian (beginning between 95 and 90 Ma) event of cooling identified only tentatively in the previous study (see below). This interpretation is consistent with the new results samples GC1194-1 and -2 which suggests cooling from >115˚C during the Cenomanian–Turonian episode. The timing constraints on the second episode identified in the two Blokelv-1 samples correlate with the late Eocene (37-35 Ma) regional cooling episode when these samples cooled from palaeotemperatures around 95 to 105˚C. Similarly, the timing of the most recent cooling episode in each of the two samples from the Blokelv borehole correlates with the late Miocene (~10 Ma) regional cooling episode when both samples cooled from palaeotemperatures around 80˚C. In this revised

interpretation of data from the Blokelv borehole, the early Eocene episode is not detected in the AFTA data.

The timing of the major post-Jurassic cooling episodes identified in previous studies (GEUS report 2012/87; Japsen et al. 2012) is compared with those identified in the AFTA data from samples analysed for this study (Fig. 8.2a3). There is consistency between the three sets of constraints (time intervals during which each of the samples cooled), and based on the assumption that the AFTA data reflect synchronous cooling episodes across the region, we infer that the new results represent those regional episodes identified in previous studies: **Cenomanian–Turonian**, **early Eocene**, **late Eocene** and **late Miocene**, in which cooling began in the intervals highlighted in Table 8.2. In addition to the palaeothermal episodes discussed above, an early Miocene episode (beginning between 20 and 18 Ma) is focussed in the northern part of Jameson Land where palaeotemperatures in this event exceed 110°C at locations around Mestersvig and Wegener Halvø and slightly lower further inland around Schuchert Dal.

8.2 Regional synthesis

Four maps of palaeotemperatures in each of the episodes discussed here in samples from previous studies and from this study are shown in Figure 8.3. Results from the Blokelv borehole are represented by the shallower of the two samples, GC1052-1.

Cenomanian–Turonian (95-90 Ma) cooling: Previous studies identified this event in samples to the west and north of the present study region. The results of this study, including the reassessment of data from the Blokelv borehole (Fig. 8.3a) suggest that this cooling/exhumation phase also affected the Jameson Land Basin. Combining the two new data points with evidence from the wider East Greenland region it appears that Late Cretaceous uplift may have affected a vast area of the margin, extending to at least 78ºN and over 200 km inland, and all Mesozoic samples cooled from maximum palaeotemperatures in this event or later. Consequently, this event represents the termination of hydrocarbon generation over large parts of the onshore Mesozoic basins.

Early Eocene (55-48 Ma) cooling: This phase has been identified sporadically, largely restricted to certain areas where intrusive bodies of similar age are present. The extent of these effects overlaps with that of intensive Palaeogene intrusive activity and the timing correlates with the age of c. 53 Ma for dykes and sills in the Jameson Land Basin (Hald and Tegner, 2000). Palaeotemperatures are generally around 100°C or above, and show erratic variation with elevation. On this basis the palaeotemperatures characterising this episode are interpreted to be due either to contact or hydrothermal effects associated with igneous activity. The mapped extent of early Eocene intrusive bodies (Larsen & Marcussen 1992), particularly the sills, follows the pattern of early Eocene palaeotemperatures in Figure 8.3b and it seems likely that the presence of shallow-dipping sills has produced profound effects on the thermal history of the Jurassic rocks at outcrop across the region. Moreover, the effect of hydrothermal heating may have been higher in the southern part of Jameson Land (e.g. south of Blokelv-1) due to the increase in frequency of shallow sills (Ch. 4) and the marked presence of dykes on the surface (Fig. 5.8). No convincing evidence for any regional Palaeocene to Eocene exhumation has been

identified for samples in the area around Jameson Land, and the geological record south of Jameson Land documents that subsidence and burial dominated at the Palaeocene–Eocene transition (Brooks 2011).

Late Eocene (37-35 Ma) cooling: This episode is identified chiefly in a zone close to the present-day coast except for samples from the Blokelv borehole (Figure 8.3c), and is interpreted as representing the initial phase of post-breakup exhumation of the margin that led to the formation of the dominant planation surface along the East Greenland margin (Bonow et al. 2014). The evidence of this cooling episode in samples close to the coast gives the impression that exhumation in this event was focused within this narrow region. AFTA data from two vertical transects in northern Jameson Land and on Liverpool Land provide constraints on the palaeogeothermal gradients in this episode and show that it is close to present-day values (GEUS report 2012/87). This implies that elevated heat flow along the margin cannot explain the apparently localized nature of evidence of this event. The event is recognised in AFTA data in samples along most of the East Greenland margin, both north and south of 70°N, and results from an ODP borehole off SE Greenland indicate strong, mid-Cenozoic uplift of the inner margin (Larsen et al. 1994).

Late Miocene (~10 Ma) cooling: The palaeotemperatures linked to this episode echo the results of recent studies in showing fairly uniform values across the region (Fig. 8.3d). Late Miocene palaeotemperatures around 70-80ºC over most of the region and around 90ºC in the south generates difficulties in resolving the earlier events, notably the timing of onset-of-cooling. Effects of the late Miocene cooling episode are identified in all regions of the margin studied to date, from 70ºN to 78ºN, and also in the published study of Japsen et al. (2014) extending southwards to 68ºN. This episode is interpreted as representing the onset of the uplift that resulted in the present-day high elevations along continental margin of East Greenland.

Paleo-thermal gradient

With no constraints available on palaeogeothermal gradients in any of the main palaeo-thermal episodes, it is not possible to provide rigorous estimates of the amounts of section that has been removed during the various phases of exhumation. Table 5.1 in Geotrack report GC1194 provides some general estimates of the amount of additional burial required to heat rocks to palaeotemperatures between 60 and 130°C, for a range of palaeogeothermal gradients. In broad terms, Cenomanian–Turonian palaeotemperatures around 100 to 115ºC or more require burial by an additional 2.7 to 3 km or more for a palaeogeothermal gradient around 30ºC/km or around 1.5 km for a palaeogeothermal gradient around 50ºC/km. Late Miocene palaeotemperatures around 70ºC correspond to burial by an additional 1.7 km for a gradient of 30ºC/km or ~1 km for a gradient of 50ºC/km.

Relative variation of the magnitude of the evens across Jameson Land

The results suggest that the effects of Cenomanian–Turonian exhumation dominate in the west but are overtaken by the effects of late Eocene exhumation moving eastwards towards the present-day margin. It is therefore likely that Cenomanian–Turonian and the

late Eocene exhumation events affected the entire region with differing magnitude in different regions, with both events of similar magnitude around the vicinity of the Blokelv-1 borehole and samples GC1194-1 and -2, which mark the location where one event supplants the other. The interplay between these events is complicated further by variation in the magnitude of the early Eocene episode, which seems to be of similar magnitude at this location.

The magnitude of the two Eocene events differs by only ~10ºC between sample GC1194-1 and -2. Neither of the Eocene events are resolved in the data from samples GC1194-4, -5 and -6 presumably because of the high late Miocene palaeotemperatures in those samples. The histories for the locations of samples GC1194-1 and -2 and also that for samples GC1194-5 and -6, combined with results from the Blokelv borehole, suggest that the two Eocene events are of broadly equal magnitude and the detection of each event in the AFTA data will depend on the details of the locality (Fig. 8.1).

Figure 8.4 provides a schematic illustration of the burial and exhumation history of the Jurassic rocks now at or near outcrop in southern and central parts of Jameson Land. To the west and in central Jameson Land, Cenomanian–Turonian exhumation from burial depths of around 3 km followed by late Miocene exhumation of lesser magnitude dominate the history (Fig. 8.4a). Moving eastwards, palaeotemperatures exceeding 110˚C were reached in the early Eocene, and it is thus not possible to constrain palaeotemperatures in earlier events; e.g. during the Cenomanian–Turonian exhumation that most likely also affected the eastern part of the basin (Fig. 8.4b). Here maximum Cenozoic burial depths (also up to 3 km or more) were reached in the late Eocene.

As illustrated by Figure 8.4, the interplay between the Cenomanian–Turonian, the late Eocene and the late Miocene exhumation events shows that burial continued through Cretaceous times (145–90 Ma), Late Cretaceous – Eocene times (90-35 Ma) and Oligocene–Miocene times (35–10 Ma).
Cenomanian–Turonian palaeotemperatures for Upper Jurassic sediments are likely to reflect burial below Jurassic – Turonian strata.

Late Eocene palaeotemperatures are likely to reflect burial below Upper Cretaceous – Paleocene strata and basalts erupted during and after breakup along the margin as well as Eocene sedimentary units that are well known from region south of Scoresby Sund (Brooks 2011). Maximum Cenozoic palaeotemperatures in the late Miocene event (Fig. 8.4a) are likely to reflect burial below Upper Cretaceous – Eocene strata as well as sedimentary units of Oligocene–Miocene age.

8.3 Discussion

There are several lines of evidence that indicate that a significant tectonic event affected the margins of East Greenland (where outcrops of Upper Cretaceous sediments are scares) and NW Europe in the earliest Late Cretaceous. On Traill Ø, north of the Jameson Land Basin, Surlyk and Noe-Nygaard (2001) defined the Månedal Formation with a tentative Late Turonian – Early Coniacian age. According to these authors, the conglomerates and sandstones of this formation were also associated with sliding of older

sediments that overlie a mid-Turonian unconformity. Lien (2005) mapped a Turonian succession of fairly uniform thickness (1–2 sec TWT) across the Møre and Vøring Basins that were located immediately east of the Jameson Land basin prior to break-up. Doré et al. (1997) discussed the importance of the regional mid-Cenomanian unconformity in the Vøring Basin and reported a late Turonian to Coniacian input of sand that is widely recognizable along the eastern Vøring and Møre Basin margins, with gross thicknesses ranging up to 150 m. Recently, Stoker and Ziska (2011) reported a regional unconformity centred on the Turonian in the Faroe-Shetland Basin.

Mathiesen et al. (2000) investigated the denudation history of the Jameson Land Basin using basin modelling constrained by apatite fission-track data. They concluded that the Upper Jurassic sediments now exposed were buried below a 2–3 km thick succession of Cretaceous to Palaeogene rocks. This magnitude of exhumation is in agreement with the estimates presented here. Mathiesen et al. (2000) estimated that the exhumation of the Jameson Land Basin accelerated after the Palaeogene, volcanic eruptions. The AFTA study performed as part of the Jameson Land reassessment points to two main stages of uplift and exhumation: A Mesozoic phase beginning in the Cenomanian–Turonian and a Cenozoic phase beginning in the late Eocene. The results presented here, thus narrows down the timing for the onset of the Cenozoic exhumationfrom being post-Palaeocene (<56 Ma) to being late Eocene (~35 Ma). Evidence for a Cenomanian–Turonian exhumation phase has previously only been presented in GEUS report 2012/87.

Our estimate of the magnitude of the section removed from the basin (~3 km) fits also with the results of Bonow et al. (2014) and Japsen et al. (2014) in their studies of the area between Milne Land and Kangerlussuaq (68–71°N) based on integration of evidence from stratigraphic landscape analysis, thermochronology and the stratigraphic record. These authors argued that the present-day high elevation in East Greenland is the result of three tectonic phases of uplift and erosion during the Cenozoic (late Eocene, late Miocene and Pliocene) that followed the eruption of voluminous flood basalts at the Paleocene–Eocene transition (Larsen and Saunders 1998; Brooks 2011).

Analysis of further samples may be useful for resolving the discrepancies between interpretations derived from AFTA data and VR values, which are generally lower than expected on the basis of the AFTA data. Our experience is that in the absence of suppression effects in organic-rich, source-rock facies organic matter, the two techniques give consistent results and these measurements would constitute a valuable step in confirming the thermal history of Jurassic rocks in the Jameson Land Basin.

8.4 Conclusions

The results of this study reveal a complex pattern of variation in the thermal history of Jurassic sedimentary rocks across Jameson Land. The palaeotemperatures derived from the AFTA data are interpreted as representing the combined effects of deeper burial followed by successive episodes of exhumation in the Cenomanian–Turonian, late Eocene and late Miocene, combined with localised early Eocene heating due either to contact heating or hydrothermal effects associated with intrusive activity. The AFTA study points to

two main stages of uplift and exhumation: A Mesozoic phase beginning in the Cenomanian–Turonian and a Cenozoic phase beginning in the late Eocene. The results presented here, thus narrows down the earlier estimates of the onset of the Cenozoic exhumation from post-Palaeocene (<56 Ma) to late Eocene (~35 Ma).

For the central parts of the Jameson Land Basin, we find that Jurassic sediments at – or near – the surface were buried below a ~3 km thick cover during maximum burial that most likely occurred in the Cenomanian–Turonian and that that cover consequently consisted of Upper Jurassic – Turonian sediments (assuming a palaeogeothermal gradient 30°C/km and likely temperatures at the surface).

Along the eastern margin of the basin, the Jurassic sediments were buried below a cover of similar thickness in the late Eocene. Maximum burial may have occurred in the Cenomanian–Turonian, but early Eocene palaeotemperatures exceeding 110˚C makes it impossible to define palaeotemperatures in earlier events. It is possible that the Cenomanian–Turonian and the late Eocene exhumation events affected the entire region with differing magnitude in different areas, with both events being of similar magnitude in the central parts of the basin. The interplay between these events is complicated further by the sporadic variation in the magnitude of the early Eocene episode which may equal that of the late Eocene episode. Where the late Miocene palaeotemperatures are high, neither of the Eocene events are resolved. As no Cenozoic units are preserved across the region, the amount of section removed between each phase of exhumation cannot be constrained due to uncertainty about the magnitude of any intervening episodes of reburial.

Further AFTA work may assist in elucidating the extent of the cooling episodes identified in this study and also in providing further constraints from within the Jameson Land Basin, so that a firmer link may be established with the regional evidence. Paired AFTA and vitrinite reflectance (VR) samples from wells drilled in the basin, combined with studies of sedimentary petrology/diagenesis, may help to constrain the thermal basin history and define paleogeothermal gradients.

Sample No.	Source number	Strati-graphic age	Max palaeo-temper-ature *2	Onset of cooling *2	Max palaeo-temper-ature *2	Onset of cooling *2	Max palaeo-temper-ature *2	Onset of cooling *2
GC1194-		(Ma)	(°C)	(Ma)	(°C)	(Ma)	(°C)	(Ma)
1	292016	161-145	109-79	89-99	73-35	57-75	18-0	109-79
2	333054	175-161	>115	97-71	89-101	70-40	65-79	24-8
4	405501	161-145	>110	574-346	94-99	189-44	61-90	20-0
5	461209	200-145	>110	>300	99-107	267-59	86-94	25-3
6	139163	175-161	>110	>300	95-100	191-36	73-93	30-8
GC1052-		(Ma)	(°C)	(Ma)	(°C)	(Ma)	(°C)	(Ma)
1	-	159-146	>110	111-60	95-103	54-31	68-80	16-6
2	-	159-146	>110	100-51	95-105	50-27	77-87	14-7

*[1]Present temperature estimates based on an assumed surface temperature of 20°C. Thermal history interpretations are insensitive to this parameter.
*[2]Thermal history interpretation of AFTA data based on assumed heating and cooling rates of 1°C/Myr and 10°C/Myr, respectively. Quoted ranges for palaeotemperature and onset of cooling correspond to ±95% confidence limits.

[x1]Japsen et al. (2014) related an event of cooling with overlapping timing (55–50 Ma) in southern East Greenland to the emplacement of the Kangerlussuaq Intrusion.

Table 8.1. Palaeotemperature analysis summary: AFTA data in 5 outcrop samples from Jameson Land (Geotrack Report #1194, where full analytical details are found). Also shown is reassessment of 2 drill core samples from Blokelv-1 (Geotrack report #1052). Pre-depositional events are shown in red type.

Onset of cooling (Ma)				
Five Jameson Land samples, this study	97–79	70–40		18–8
Two Blokelv-1 samples (reassessment)	100–60		50–31	14–7
Study A, NEG	95–90	55–48[x1]	37–35	~10
Study B, SEG		[x1]	40–35	~10
Preferred regional timing	**95–90 Cenomanian-Turonian**	**56–45 early Eocene**	**37–35 late Eocene**	**~10 late Miocene**
Inferred mechanism of cooling	Exhumation	Cooling after intrusive heating	Exhumation	Exhumation

Table 8.2. Intervals defining the onset of post-Jurassic episodes of cooling from AFTA data. Study A: 220 outcrop samples interpreted by Geotrack as part of a regional GEUS study from of North-East Greenland (NEG), north of 70°N (GEUS report 2012/87; Japsen et al. 2012). Study B: 90 samples from outcrops and drillholes in a regional study of southern East Greenland (SEG) focussed between 68 and 70°N (Japsen et al., 2014).

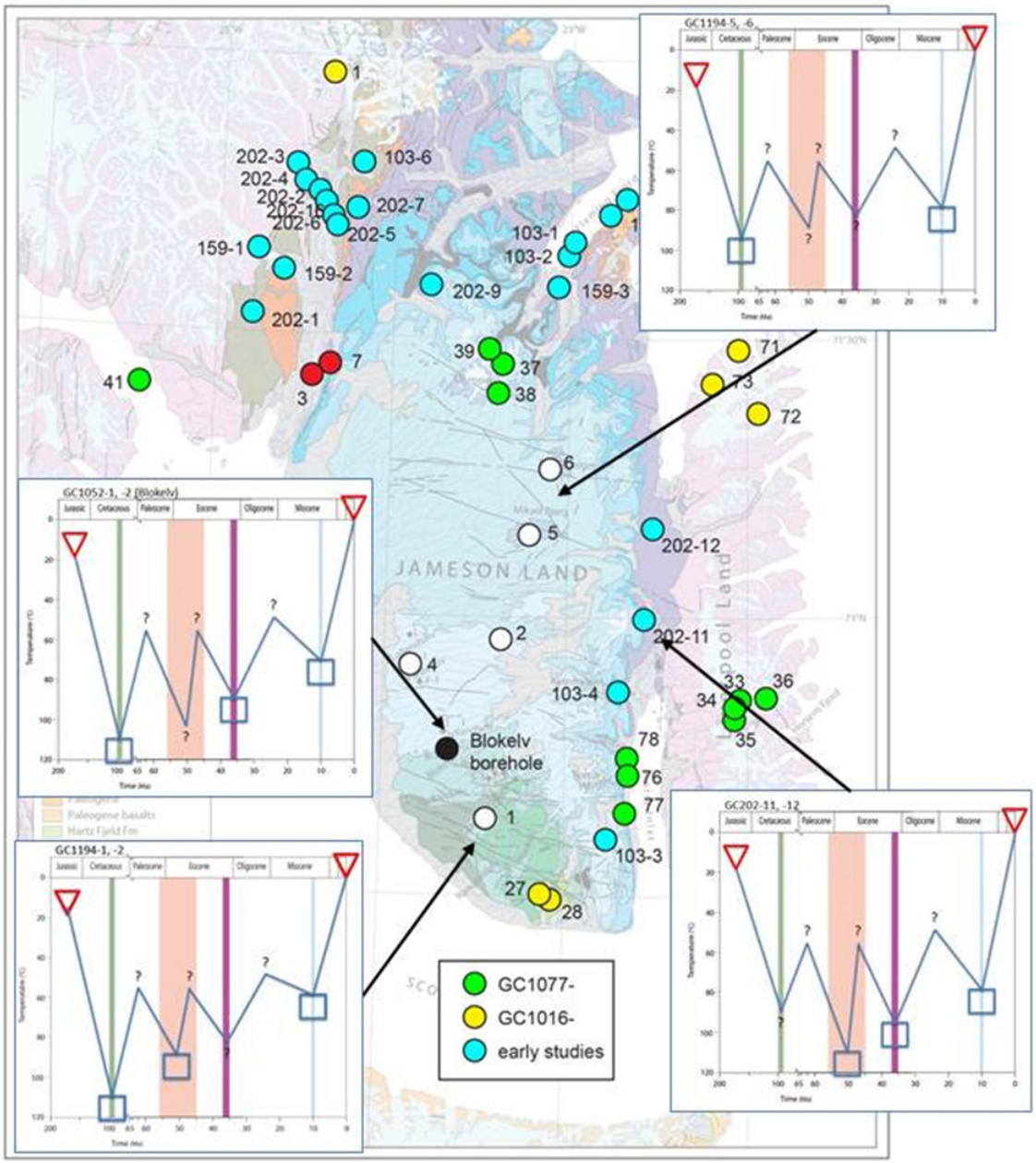

Figure 8.1. Location of samples analyzed for this (GC1194) and previous studies. The map is overlain with a summary of interpreted regional variation in thermal history styles based on AFTA data in samples of Jurassic sandstones from Jameson Land. White symbols: samples that yielded apatite. Red symbols: Samples that failed to yield apatite. AFTA data in many samples north of the study area are dominated by the effects of early Miocene intrusions.

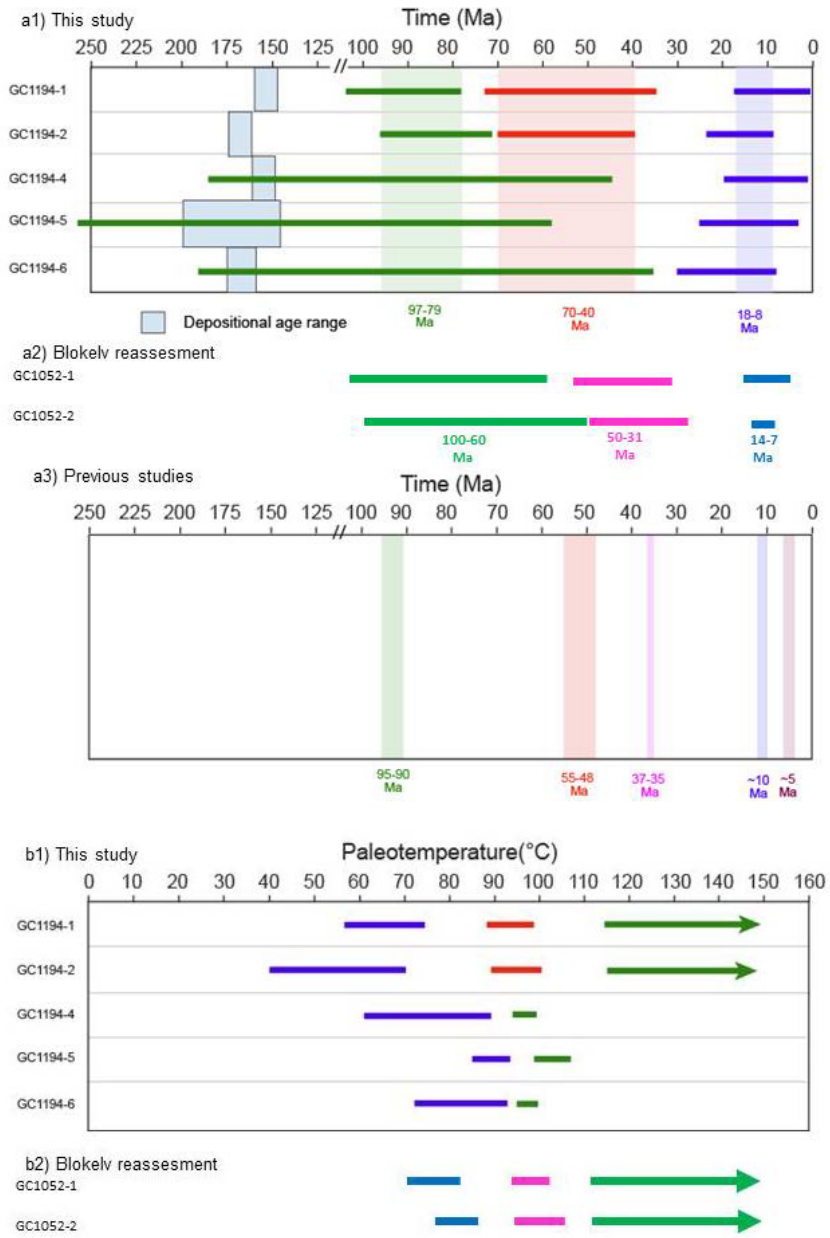

Figure 8.2. Thermal history solutions from AFTA data in five outcrop samples (this study; GC1194) and two samples from the Blokelv borehole (GC1052) the regional constraints on the timing of cooling events. a: Timing constraints on the onset of cooling derived from AFTA data in individual samples (Table 8.1) compared with depositional ages and the regional constraints on the timing of cooling events defined from AFTA data in in previous Geotrack studies for GEUS (GEUS report 2012/87; Japsen et al. 2012) (a3). b: Maximum or peak palaeotemperatures from which samples cooled at the times shown in a), with colour coding consistent between the two plots (arrows indicate temperatures with no maximum limit). Regional palaeo-thermal episodes: Cenomanian-Turonian (95-90 Ma), early Eocene (55-48 Ma), late Eocene (37-35 Ma) and late Miocene (~10 Ma) are indicated by vertical colour bands. The ~5 Ma event is also not recorded in this study. Note time-scale break in x-axis of a1 and a2.

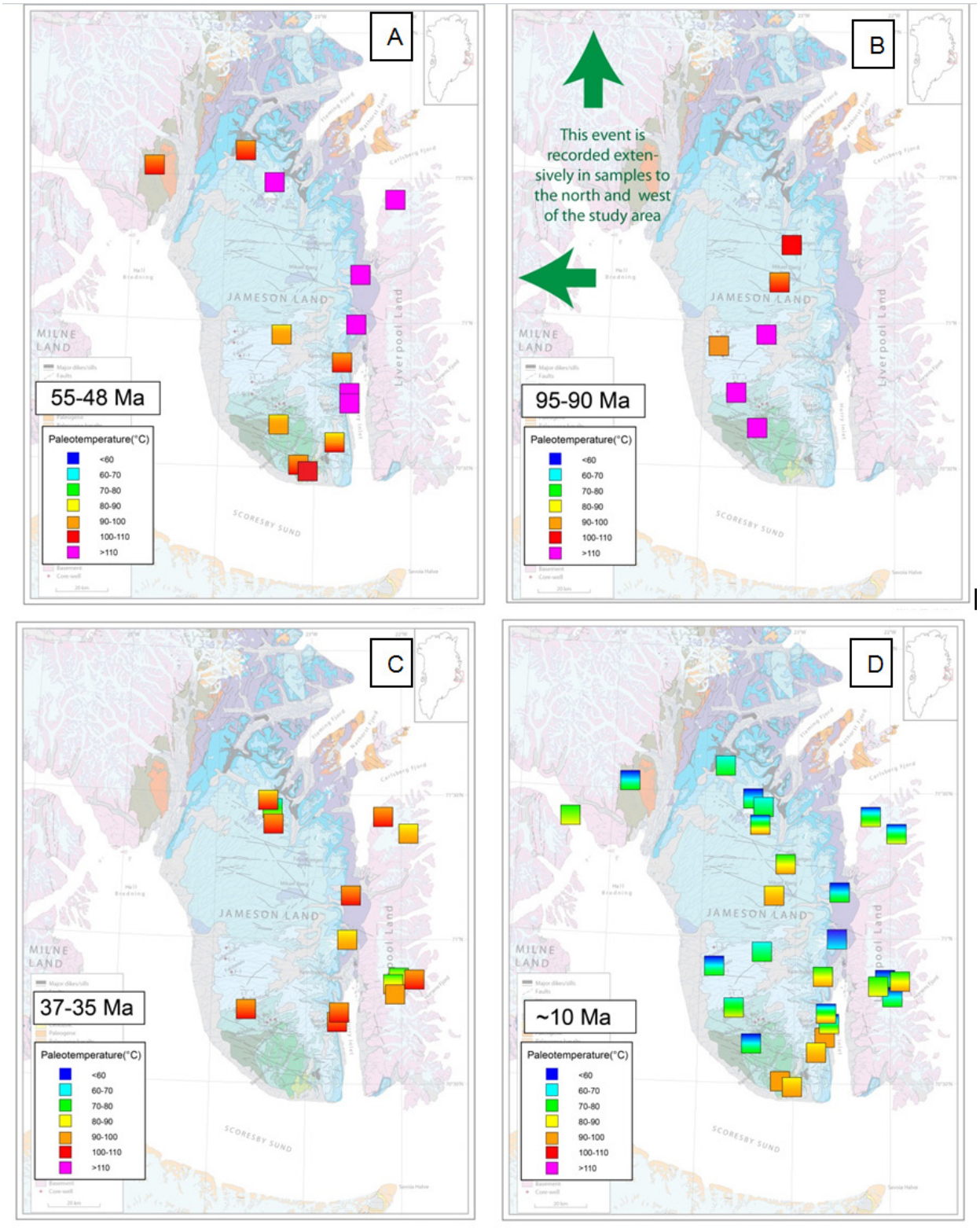

Figure 8.3. Paleotemperatures in four events derived from AFTA data in outcrop samples from Jameson Land in this study and previous studies of the region (including samples from the Blokelv borehole), Figs A–D: 95–90 Ma (Cenomanian–Turonian), 55-48 (early Eocene), 37–35 Ma (late Eocene), ~10 Ma (late Miocene). Note that the Cenomanian–Turonian event is recorded extensively in samples to the north and to the west of the study area.

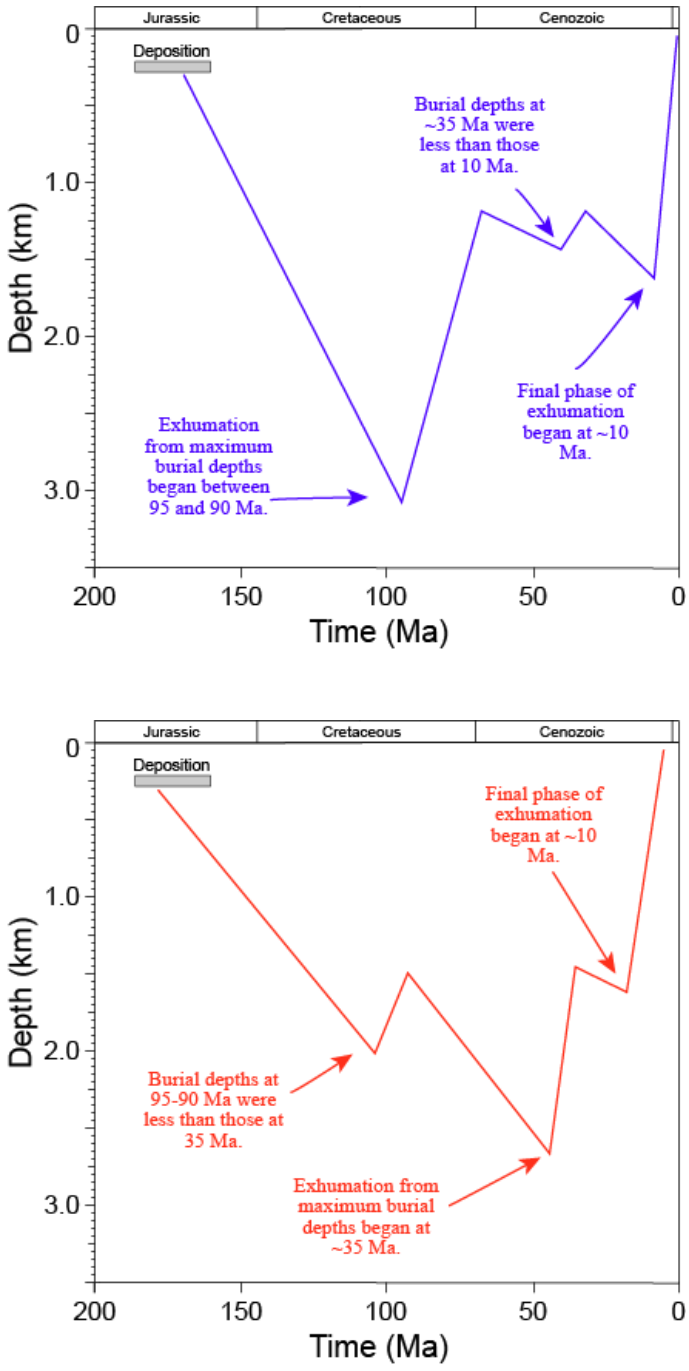

Figure 8.4. Schematic illustrations of inferred burial/exhumation histories for Jurassic sandstones at two locations in Jameson Land based on the results presented here. Upper: Central Jameson Land (near samples GC1194-1 and -2). Lower: Eastern Jameson Land (near samples GC202-11 and -12). Depths are only approximate and are shown only to provide a generalised impression of the overall history in each region. Note that in the eastern part of the basin, palaeotemperatures exceeding 110˚C were reached in the early Eocene (Fig. 8.3) which may have obscured an earlier Cenomanian–Turonian exhumation event.

9. Maturation modelling

The aim of basin modelling study is to investigate maturity of potential source rock shales in the Jameson Land area of East Greenland. The timing and extent of source rock maturation is crucial to understanding petroleum systems and predicting hydrocarbon accumulations (e.g. Magoon & Dow, 1994). The used basin modelling software is a tool to integrate dynamic geologic data into a conceptual model that contains all of the key elements, to organise and integrate results and to conduct sensitivity studies on import parameters (e.g. depth/thickness and heat flow models).

The basin modelling study is carried out in order to:

- Test ideas for the petroleum system obtained during the geological analysis.
- Provide the most realistic assessment of the maturation history, including the extent of maturation.
- To shed light on critical parameters that should receive special attention in future studies, e.g. migration from the most important potential source rocks.
- Justify a working petroleum system in the Jameson Land as a plausible assumption.
- Assess the sensitive of the most important boundary conditions (heat flow history, lithology and Paleogene and Cenozoic erosion).

The current understanding of the Jameson Land Basin (JLB) and revised exploration potential can to a certain extent be tested by numerical modelling. However, the model precision relies on the data and parameters it is based upon. The basin modelling may be used as a guideline to test possible scenarios/concepts, involving thermal maturity and timing of petroleum migration from possible source rocks, as a means of supporting/developing potential play types.

9.1 Background

In Mathiesen et al. (1995, 2000) a 1D basin model was applied using all available shallow core data, compiled field data and knowledge and thermal calibration constrained by maturity data and apatite fission track data. On the basis of this integrated approach combining maximum-burial (estimates of removed overburden based on maturity modelling) and fission tracks (temperature and cooling history based on fission track modelling) it was possible to outline consistent erosion, and to some extent, uplift history for the JLB.

The **updated model concept** used in the following study is based on this previously geological concept, but has been updated by integrating the revised timeframe (Ch. 3), new maturity data from the Blokelv-1 and new fission track data (Chapters 6 and 8). Based on these new data the model runs have been performed to evaluate if the previous model concept is still valid for the Jameson Land area.

In the present study 1D basin modelling was used to update the 21 pseudo wells compiled in Mathiesen et al. (1995, 2000). A preliminary 2D modelled transect of the W-E trending 86-6V seismic line, was used as to further evaluate the general maturity from west to east (Fig. 9.1). 2D modelling results have not been included in this report, but future work on the 2D transect together with other transects can be used to test possible scenarios/concepts to support potential play types near the transects. Stacking and migration velocities is available from all interpreted lines allowing individual depth-conversion of each transect (Chapters 2 and 4). The 86-6V seismic line has a stratigraphic resolution adequate to interpret potential source rock intervals and roughly estimate gross-lithologies. Furthermore, a preliminary 3D regional model of the Jameson Land Basin based on the depth-converted seismic maps described in Chapter 4 was used as background for generating the play maps in Chapter 10.

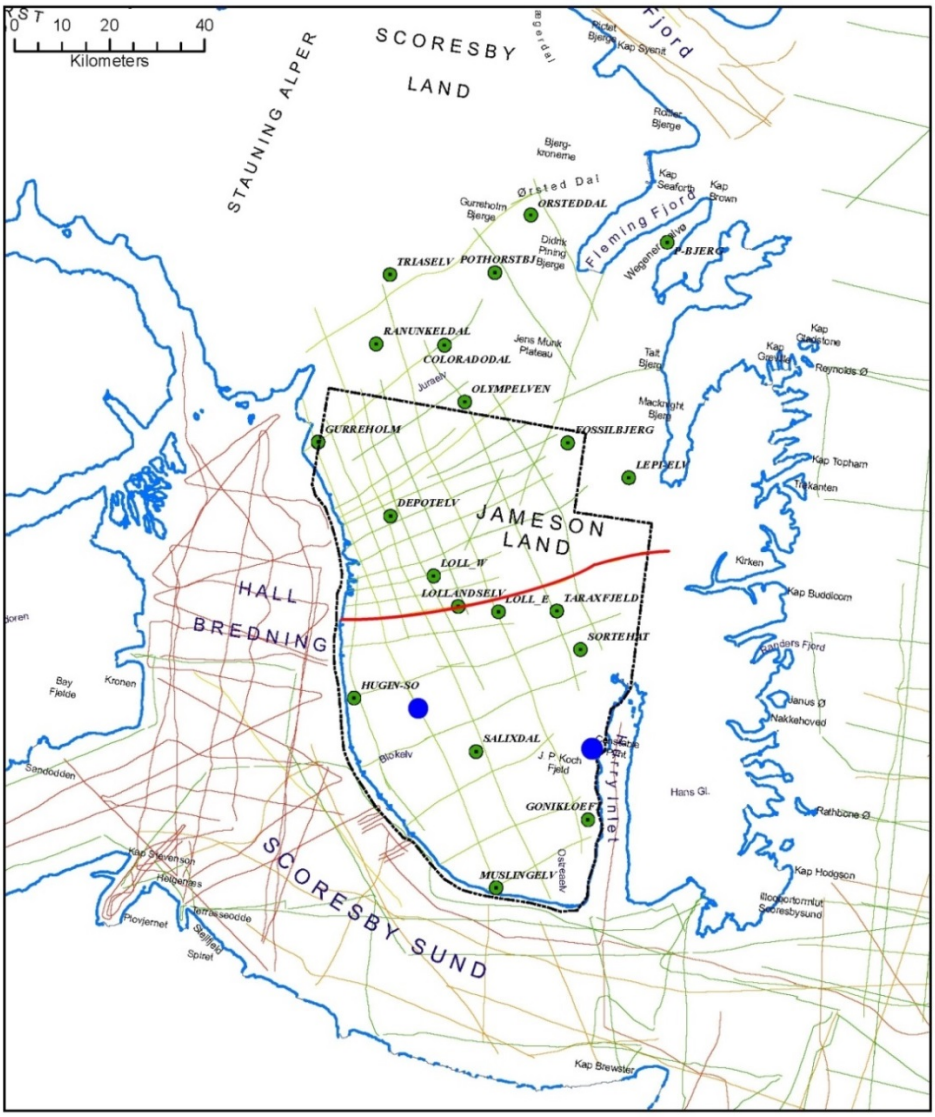

Fig. 9.1 Location of the 21 pseudo wells and license area. Notice the Blokelv and the Primulaelv pseudo well locations (enlarged blue dots), and the 86-6V seismic line used for the 2D model (red line).

Modelling of oil migration pathways and evaluation of potential traps has not been part of the task for this report. Furthermore, the effect of local heating from sill-dyke complexes, the effect of retrograde diagenesis and development of secondary porosity has not been part of this study.

9.2 The model concept

The IES PetroMod® 1D/2D/3D software (v14) (Schlumberger, Integrated Exploration Systems 2013) is forward modelling program that quantifies and describes all important basin processes as a function of time based on a defined tectonic-stratigraphic framework (i.e. model layers or events). This means that the program starts simulation of the geological development from the base of the sedimentary section and performs a calculation forward in time of parameters such as formation thickness, pressure, temperature, vitrinite reflectance, sterane- and hopane-isomerisation ratios and hydrocarbon generation. In order to constrain the modelling results, the calculated values for the present day situation are compared with measured data.

In this study 1D, 2D and 3D models have been compiled where each modelling is based on the 'most likely' input parameters. These modelling results demonstrated the changes in maturity, and hydrocarbon generation in time and depth for potential source rocks. Standard kinetic models with a standard set of kinetic parameters have been used.

The software models maturity using EASY %Ro (Sweeney & Burnham, 1990) based on the thermal evolution of the basin. The temperature history is based on standard mathematical approximations of heat flux through time, surface temperature through time, composition and thickness of sedimentary infill, potential erosion and timing. The resulting temperature history in combination with the interpreted geological outline of the seismic transect are used as input for the kinetic models to estimate maturation of presumed source rock intervals and can – at a later stage – be used to assess more detailed oil and gas generation, and expulsion, migration and potential accumulation.

The workflow of the petroleum systems modelling usually works through four steps:

1. Establishing a conceptual model (reconstructing the basin history and subdividing the geologic history into "events": deposition/hiatus/erosion).
2. Setting up a numerical model (assigning absolute values to the events: real thickness/erosion; absolute ages; rock properties incl. thermal conductivity, compressibility; source rock properties; special models incl. salt movement, igneous intrusion; thermal boundary conditions through time (surface temperature and basal heat flow).
3. Calibration of model to observations, e.g. from wells and outcrops incl. temperature profile, vitrinite reflectance, biomarkers, fluid inclusions, apatite fission track analysis, formation pressures and porosity measurements.
4. Prediction of maturity, timing of maturity, migration and trapping of hydrocarbons.

The following sections describe the most important input parameters used in this study.

9.3 Definition of Events

The chronostratigraphy and event definition is based on compiled geological data from the Jameson Land Basin and is a revised version that was used for modelling of 21 pseudo wells (Mathiesen et al., 1995, 2000).

Layer	Top [m]	Base [m]	Thickness [m]	Eroded [m]	Depo. Start [Ma]	Depo. End [Ma]	Erosion Start [Ma]	Erosion End [Ma]	Lithology	PSE	TOC [%]	Kinetic	HI [mgHC/gTOC]
ICE	0	0	0	1000	0.50	0.10	0.10	0.00	Ice	Overburden Rock			
EarlyMio-LateMio	0	0	0	5	13.00	12.00	12.00	10.00	Siltstone (organic lean)	Overburden Rock			
Tertiary Volcanics II	0	0	0	300	53.00	52.00	52.00	20.00	Basalt (normal)	Overburden Rock			
Tertiary Volcanics I	0	0	0	600	55.00	53.00	20.00	13.00	Basalt (normal)	Overburden Rock			
Pre-Volcanics	0	0	0	50	66.00	63.00	63.00	55.00	Shale (organic lean, silty)	Overburden Rock			
Upper Cretaceous	0	0	0	450	100.00	66.00	10.00	7.00	Shale (organic lean, silty)	Overburden Rock			
Aptian - Albian (Undiff)	0	0	0	500	126.00	100.00	7.00	4.00	Shale (organic lean, silty)	Overburden Rock			
Hauter.-Barrem (Undiff)	0	0	0	300	139.00	126.00	4.00	2.00	Shale (organic lean, silty)	Overburden Rock			
Raukeelv Fm	0	0	0	300	155.00	139.00	2.00	0.75	Sandstone (clay rich)	Overburden Rock			
Hareelv Fm, Up, SjlandMb	0	50	50	150	157.00	155.00	0.75	0.50	Sandstone (clay rich)	Overburden Rock			
Hareelv Fm Lower, SR	50	250	200		161.00	157.00			Shale (organic rich, 8% TOC)	Source Rock			
Olympen Fm	250	364	114		164.00	161.00			Sandstone (clay rich)	Reservoir Rock			
Fossilbjerget Fm	364	664	300		166.00	164.00			Shale (organic lean, silty)	Reservoir Rock			
Pelion Mb	664	1078	414		169.00	166.00			Sandstone (clay rich)	Reservoir Rock			
Sortehat Fm	1078	1178	100		174.00	169.00			Shale (organic lean, sandy)	Reservoir Rock			
Neil Klinter Fm	1178	1480	302		192.00	174.00			Sandstone (clay rich)	Reservoir Rock			
Kap Stewart Fm, Upp	1480	1795	315		197.00	192.00			Siltstone (organic lean)	Reservoir Rock			
Kap Stewart Fm, SR	1795	1845	50		200.00	197.00			Shale (organic rich, 8% TOC)	Source Rock	6.00	Pepper&Corvi(1995)_TII(B)	500.00
Kap Stewart Fm, Low	1845	2251	406		205.00	200.00			Siltstone (organic lean)	Reservoir Rock			
Flemming Fjord Fm	2251	3044	793		230.00	205.00			Shale (organic lean, sandy)	Reservoir Rock			
Gipsdalen Fm	3044	3780	736		240.00	230.00			Sandstone (clay rich)	Reservoir Rock			
Pingo Dal Fm	3780	4180	400		250.00	240.00			Sandstone (arkose, clay rich)	Reservoir Rock			
Wordie Creek Fm	4180	4470	290		252.00	250.00			Sandstone (arkose, clay rich)	Reservoir Rock			
Schuchert Dal Fm	4470	4626	156		257.00	252.00			Sandstone (arkose, clay rich)	Reservoir Rock			
RavneFjeld Fm	4626	4666	40		260.00	257.00			Shale (organic rich, 8% TOC)	Source Rock	4.00	Pepper&Corvi(1995)_TII(B)	400.00
Wegener Halvø Fm	4666	4706	40		267.00	260.00			Sandstone (arkose, clay rich)	Underburden Rock			
Karstryggen Fm	4706	4736	30		275.00	267.00			Sandstone (arkose, clay rich)	Underburden Rock			
Huledal Fm	4736	4766	30		279.00	275.00			Sandstone (arkose, clay rich)	Underburden Rock			
Low.Permian (Undiff)	4766	5166	400	10	300.00	290.00	290.00	279.00	Coal (silty)	Underburden Rock			

Figure 9.2. 1D Timeframe, event-split and Facies definition.

A total of 29 events were chosen to describe a consistent, isochronous frame of the geological development from the Upper Permian until present time. The event-split, i.e. the number of events was chosen as a compromise between the geological details included in the model and the calculation time for the models. The model has been extended down to basement based on information derived from years of geological fieldwork and the new interpretation of seismic data (Section 4).

Sensitivity modelling has shown that a simplified event-split of the Mesozoic and Cenozoic sequence does not lead to major differences between the modelled and measured values of temperature and vitrinite reflectance compared with results obtained using detailed event-split based on detailed sequence stratigraphy. The standard lithology used here is based on published or unpublished sources on depositional facies variation as e.g. information on porosity is very limited.

9.4 Calibration data

Only a rough calibration of maximal burial and subsequent post volcanic Paleogene and Cenozoic uplift and erosion history is possible due to the presence of scattered maturity

data derived from shallow- and gravity cores with relatively limited difference is sample altitudes. Besides the new Bloklev-1 data highly sensitive surface data is scattered throughout most of Jameson Land, which makes it difficult to calibrate the 1D models. The basin modelling software is only sensitive to changes over ranges of more than 1000 m. Thus, the new Blokelv-1 core data provide limited constraints on the palaeo-heat flow, and consequently, calibration of thermal maturation of potential source rock intervals therefore remains uncertain.

Geographically, the highest density of maturity data are from the northwestern and southeastern basin margins while relatively few data are available from the basin centre. The maturity pattern of the surface samples is believed to be relatively simple (Mathiesen et al., 1995, 2000). Most of central and southern Jameson Land has immature surface sediments, the only exceptions are a few abnormal zones in the vicinity of dolerite dykes and sills. In northernmost Jameson Land, several areas have postmature surface sediments, which is due in part to the effect of large mid-Tertiary intrusions. In others, such as Wegener Halvø, the high maturity of the Upper Permian is the result of deep burial combined with circulation of hydrothermal fluids (e.g. Surlyk et al. 1986; Christiansen et al. 1990; Mathiesen et al., 1995, 2000).

Available isomerisation of steranes and hopanes, Tmax and vitrinite reflectance (VR or %Ro) have been applied to optimize the subsidence, uplift and thermal history. Surface sections with a difference in altitude of up to 800 m have provided recognisable gradients in some areas; however, in this study most work has concentrated on calibrating the revised model against the new Blokelv-1 data, even though the limited depth-ranges of max. ca. 250 m prevent a good match (see also Fig. 9.4 and Section 9.7).

Blokelv-1 corehole maturity data

In general, the level of thermal maturity of the Upper Jurassic Hareelv succession penetrated by the Blokelv-1 corehole is close to or within the early stages of the oil-generative window, with incipient petroleum generation actually taking place in the vicinity of magmatic intrusions (Section 7). A number of independent types of thermal maturity data are all in perfect agreement showing a clearly increasing trend with depth, and with the transition to the 'oil-window' as defined by Tmax>435°C and %Ro>0.55% located somewhere in the interval around 120 m (green dot in Fig. 9.4).

Normally a clear %Ro gradient is not observed over such narrow depth interval as represented by the ~234 m long core. This implies that a significant thickness of overburden has been removed by erosion since the deposits were at their maximum depth of burial. It is estimated that between 2 and 3 kilometres of Cretaceous sediments and Paleogene volcanics have been removed due to Paleogene and Neogene uplift and erosion, which is supported by the new fission track data (Section 9.6). Hence, with a removed section of 2–3 kilometres, the Upper Jurassic succession was close to or within the oil-generative window at its maximum depth of burial, assuming only a small increase of the geothermal gradient during volcanic activity at the time of maximum burial.

9.5 Boundary conditions and other important input parameters

In frontier areas boundary conditions (i.e. palaeo-water depth, palaeo-surface-temperature and heat flow history) and other input parameters are initially kept fixed and source rock generation characteristics are assumed to follow standard kinetic models. Besides the boundary conditions, described below, other model input assumptions include:

1. Simple bulk source rocks kinetics (see also Ch. 6):

    a. The **Upper Permian Ravnefjeld Fm** is believed to have net source rock thickness of between 15 and 20 m and is regionally distributed throughout East and Northeast Greenland. The initial TOC averages close to 4% with an initial average HI of 400 (type II kerogen). This source rock was deposited in restricted marine basins fringed by carbonates. Kinetics: Pepper & Corvi, 1995, Type_II(B); TOC = 4 %; HI = 400 mgHC/gTOC (Fig. 9.2).

    b. The **Lower Jurassic Kap Stewart Gr.** has a net source rock thickness between 30 and 50 m with an initial average TOC of 6% and initial average HI of 500 (type I/II kerogen). The source rock was deposited in a large freshwater lacustrine lake that covered most of Jameson Land. Kinetics: Pepper & Corvi, 1995, Type_II(B); TOC = 6 %; HI = 500 mgHC/gTOC) (Fig. 9.2).

2. The oil window being defined as EASY %Ro= 0.55–1.3%, and gas window as Easy Ro =1.3–4.0%.

3. No faults were included at this stage.

Overburden and excess heat may have an effect on oil window depth and vitrinite reflectance pressure retardation. Delayed source rock maturation may therefore occur, e.g. in high-pressure areas. In the lack of deep wells in the Jameson Land area, information on the pressure regime through time is lacking. The fast late Cretaceous and Paleogene deposition and the presence of volcanics and shale may have promoted overpressure during periods in some areas and intervals. However, Paleogene and the later Cenozoic uplift and erosion in the region would probably have worked towards normalizing the pressure regime in much of the area. In the modelling a normal pressure regime has been assumed in the lack of other information.

9.5.1 Palaeo-water depth

The palaeo-water depths are average estimates based on general geological considerations following Mathiesen et al. (1995, 2000). Estimates of palaeo-water depth were based on in-house work. The palaeo-water depth values used here has no

implications on the 1D modelling maturation results (Fig. 9.3) but in case of more detailed 2D and 3D modelling the accuracy should be reassessed.

9.5.2 Palaeo-surface-water temperature

The palaeo-surface-temperature (SWIT) is the average temperature of the sediment-water interface during a particular event, i.e. at time of deposition. Estimates of palaeo-temperature were derived from palaeo-climatic models included in the software (Wygrala, 1989) for 71^{o}N (Fig. 9.3).

9.5.3 Heat flow model

The basin models require several initial input parameters, based on assumptions and qualified speculations. Reasonable geological heat flow histories - used for calibrating the maturity - can be constructed based on assumptions on the palaeo-heat flow regime. Low heat flow (35–40 mW/m^2) is generally associated with a cold, thick lithospheric setting (e.g. subduction trenches). Higher heat flows (80–90 mW/m^2) are normally associated with hot, thin lithospheric settings (e.g. back-arc basins and active rifting). Intra-cratonic failed-rift setting, such as offshore North-East Greenland, is usually in the range of 60–70 mW/m^2.

The heat flow model used for the simulations is based on assumed minor rifting and volcanic activity in the region, with a small increased heat flow during the early-middle Triassic rifting phase and during the volcanic episode, and lower (and generally decreasing) values in tectonically stable periods with slow and uniform subsidence (Ch. 5 and Fig. 9.3). Due to lack of calibration data in the Jameson Land area the 1D models were tested over a heat flow range of 35–65 mW/m^2 assuming a simple heat flow history (Figs 9.4 and 9.9). Based on analogues from the Barents Sea and the general geological setting, the palaeo-heat flow values is most likely to lie around 60–65 mW/m^2 (Ohm et al., 2008; Cavanagh et al., 2006). However in order to match the Blokelv-1 data palaeo-heat flow values around 45 mW/m^2 are needed to achieve a reasonable match (Fig. 9.4a, bottom). The lower palaeo-heat flow values (ca. 50 mW/m^2) during the Triassic rifting event will not have much effect on the maturity of the potential Upper Permian source rock. The need for a heat flow model with lower values than expected is at present not fully understood and is difficult to elucidate with the limited calibration data. The effect of sills/dykes or of hydrothermal fluid on maturity is only believed to have local influence as seen in the Blokelv-1 data and is at present only believed to have impact on the maturity trend along the eastern margin. Heating effects due to the existence of sills/dykes and hydrothermal fluid should be considered when the modelling is focused towards more specific play type.

The heat flow model applied varies slowly both in time and space, except for a short period of volcanism (~ 55–52 Ma). During this short interval of 2–3 my, the palaeo-heat flow values used in the models was allowed to vary in order to match the maximum temperature without having to change the thickness of overlying layers. This is based on the assumption that the sills and dykes acted as long-lived conduits for transporting magma and that there were permeable sediments to transport heat by convection. The presence of

sills has allowed for increasing the heat flow peak value in the eastern part of the basin. The short period of increased heat flow is justified by numeric modelling of cooling around sills in a sedimentary section (Mathiesen et al., 1995).

The inferred heat flow history was then modified to match vitrinite reflectance data, but constrained to result in smooth heat flow variations in time and space. To assess the sensitivity of the heat flow model, two models with respectively, a uniform constant heat flow model of 42 mW/m^2 and of 60 mW/m^2 were applied for assessing the effect on maturity and timing (Fig. 9.4).

The heat flow used in the modelling is regarded as the heat that was transmitted into the base of the sedimentary succession (typically at a depth of 10 km or less). The heat flow at this level is influenced by transient effects from sedimentation, volcanics and erosion, in contrast to the background heat flow from the upper mantle. It can therefore change faster than the background heat flow.

Fig. 9.3 Palaeo-water depth (PWD), Palaeo-surface-water temperature (SWIT), Heat flow model (HF) assuming rifting during early-middle Triassic and with a 3 my extensive volcanic event comprising the main Paleogene volcanic pulse.

9.6 Model for uplift and erosion

The updated model concept used for assessment of the maturity modelling has been tested against maturity data to consider if it was possible to determine which of the burial and exhumations/uplift models based on AFTA data (Ch. 8) that are preferable.

To further assess possible uplift scenarios in Jameson Land a series of 1D modelling were carried out using maturity data from Blokelv and Primulaelv pseudo well locations to optimise the models. It should be noted that vitrinite reflectance is much more sensitive to temperature than to time and therefore mainly dependent on maximum temperature and not on the time when this temperature was reached, i.e. when the sediments were at maximum burial.

The new AFTA data and fission track modelling supports the general assumption that uplift and erosion took place after volcanic eruption and increased from late Miocene. Furthermore, the AFTA study supports previously quantified amounts based on the earlier integrated basin modelling study (Mathiesen et al. 1995, 2000).

A possible scenario of the AFTA results is that a maximum burial of Mesozoic sediments was reached at 100–90 Ma, and thus, before the volcanic episode (at c. 55–52 Ma) and prior to the Neogene uplift and erosion. However, this scenario, with an earlier maximum burial, cannot be modelled to match the VR gradient and the general model concept for the Jameson Land area. This discrepancy between results from the new AFTA modelling and the maturity data is at present not fully understood. Moreover, the AFTA data indicate higher maximum palaeo-temperatures than measured in the Blokelv-1 vitrinite reflectance and Tmax data, a difference that is likewise not resolved. Based on the preliminary assumptions and maturity modelling, the timing of erosion subsequent to maximum burial at c. 52 Ma is, at present based on the general geological understanding and a Late Paleocene and Neogene uplift and erosion with an increasing amount of erosion from 15–12 Ma.

9.7 Summary of modelling results

The basic concept described in Sections 9.2–9.6 has been used to optimize the models by varying the thickness of the removed Upper Cretaceous marine shales and of the Lower Tertiary volcanics. It was assumed that the depositional rate was relatively constant throughout the Cretaceous and that the Tertiary volcanics were extruded as horizontal flows (see Mathiesen et al., 1995, 2000 for further details).

1D basin modelling based on the previous concept has been updated, based on the new seismic interpretation, for the original 21 pseudo well locations and for the new Blokelv pseudo well location in order to assess the impact on the maturity and hydrocarbon generation. The detailed Blokelv-1 maturity data represents a location in the central part of Jameson Land Basin while the Primulaelv pseudo well location represents a location in the eastern margin of the basin (se Fig. 9.1). These two representative locations are in the following used for this assessment (Figs. 9.4–9.12). Notice that the volcanic thickness at the two pseudo well locations is assumed to be around 800–900 m.

Figure 9.4 shows the optimised 1D model at the Blokelv pseudo well locations calibrated against vitrinite reflectance and biomarker data. Figure 9.4 show the results of four calibrated models using different heat flow histories in order to assess the sensitivity of the possible heat flow models. The original and the new updated model concept results in a

better match than the uniform heat flow histories when comparing the match of models (Fig. 9.4). When using at uniform heat flow history of 60 mW/m^2 there is no calibration match and the model becomes to 'hot' (Fig. 9.4b, bottom).

Figure 9.5 and 9.6 show subsidence plots with modelled hydrocarbon and vitrinite reflectance zones at the Blokelv and Primulaelv pseudo well locations. Notice that Figure 9.5 show the hydrocarbon generation for at kerogen Type-II and Type-I at the Blokelv pseudo well location, respectively, assuming Pepper & Corvi (1995) kinetics (Figs. 9.5a and 9.5b). The vitrinite reflectance is divided and coloured in maturity zones according to general accepted maturity boundary values for kerogen Type-II (see legend in figures):

0.20—0.55	:	Immature	(light blue)
0.55—0.70	:	Early Oil	(light green)
0.70—1.00	:	Main Oil	(green)
1.00—1.30	:	Late Oil	(dark green)
1.30—2.00	:	Main Gas	(red)
> 2.00	:	Postmature	(orange)

Thus, onset of oil generation is taken at a vitrinite reflectance of 0.55 %R_o, whereas the peak oil generation is conventional set to between 0.7 and 1.0 %R_o. The threshold values will vary with kerogen type and thermal maturation history (e.g. Figs. 9.5a and 9.5b).

The modelling shows that the Kap Stewart source rock at the Blokelv pseudo well location entered the oil window during Early Cretaceous, prior to volcanic extrusions and after extrusions stayed in the late oil – gas window until present day. At the Primulaelv pseudo well location the Kap Stewart source rock entered the oil window during the volcanic extrusions (c. 52 Ma) and stayed in the oil window until present day. Thus, the modelling indicates that at the Primulaelv location the Kap Stewart source rock is at present day in the oil window at a depth of ~350–300 m assuming c. 2500–3000 m of post-volcanic uplift (Fig 9.6).

Before the generated hydrocarbons can be expelled the rock matrix must be saturated and a continuous hydrocarbon-phase formed. In the Jameson Land area little is known on the source rock kinetics and consequently, the Pepper & Corvi (1995) kinetics has been used (Ch. 9.5). Based on these assumptions for a Type-II-kerogen figure 9.11 shows the transformation ratio and oil and gas generation potential against time for the two potential source rocks. The potential Kap Stewart source rock has generated oil since Paleocene, while only gas is generated from the potential Ravnefjeld source rock at present (Fig. 9.11).

Beside the inferred heat flow model, source rock kinetics is among the most sensitive input parameters. The choice of kinetic parameters and kinetic models may have a dramatic impact on the modelling results and thus, timing of generation and expulsion of hydrocarbons. Uncritical use of a single set default values may lead to erroneous conclusions regarding petroleum systems, where few or no calibration data exists.

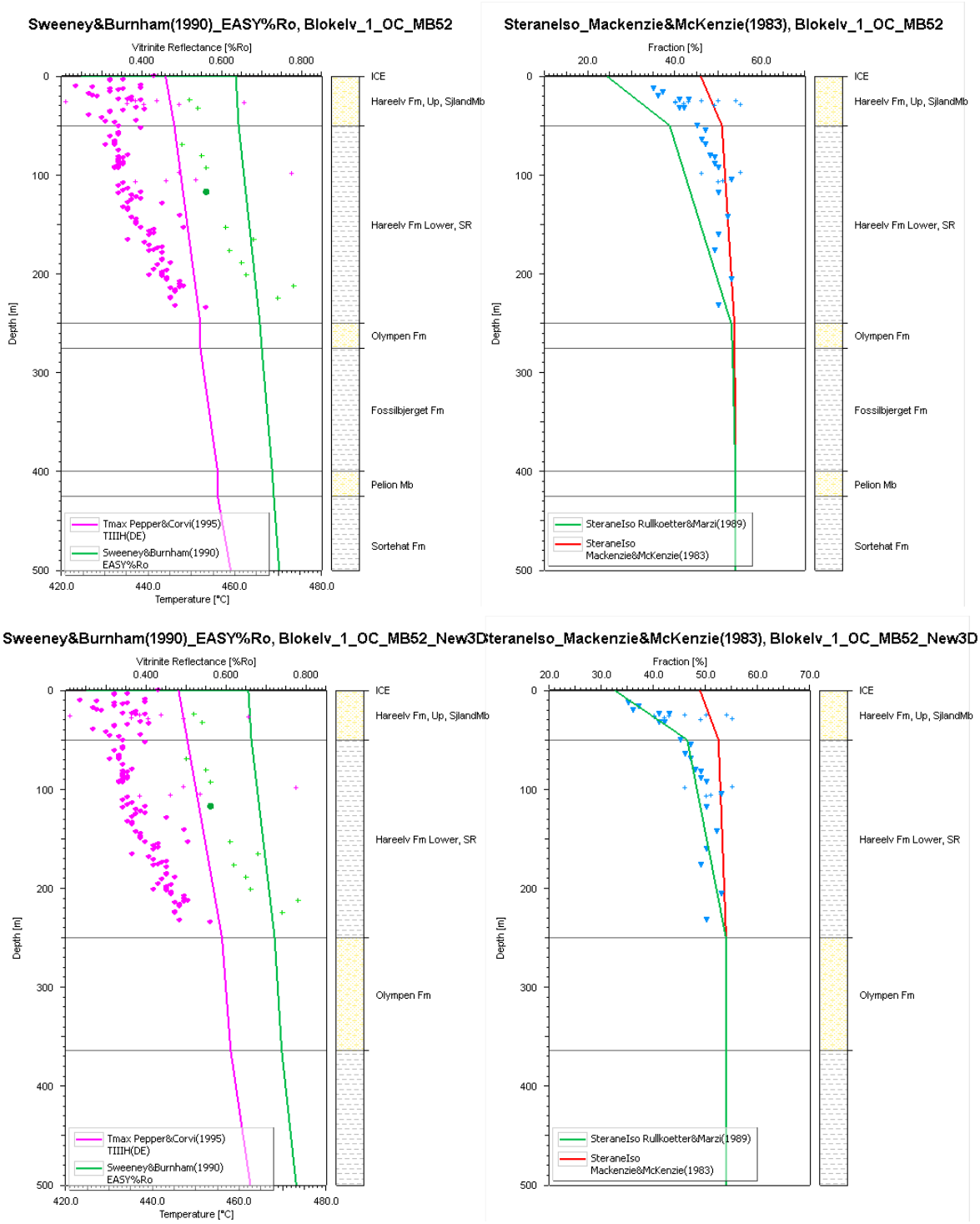

Figure 9.4a. Plots at the Blokelv pseudo well location with Blokelv-1 maturity data (symbols) showing matching of different three different 1D model maturity models (**Top:** original model concept; **Bottom:** updated model concept. Modelled %Ro, Tmax and biomarker models are shown as solid lines. Notice that the 'oil-window' (defined as Tmax>435°C and %Ro>0.55%) is marked with a green dot at a depth of ca. 120 m (green dot on the %Ro plots to the left).

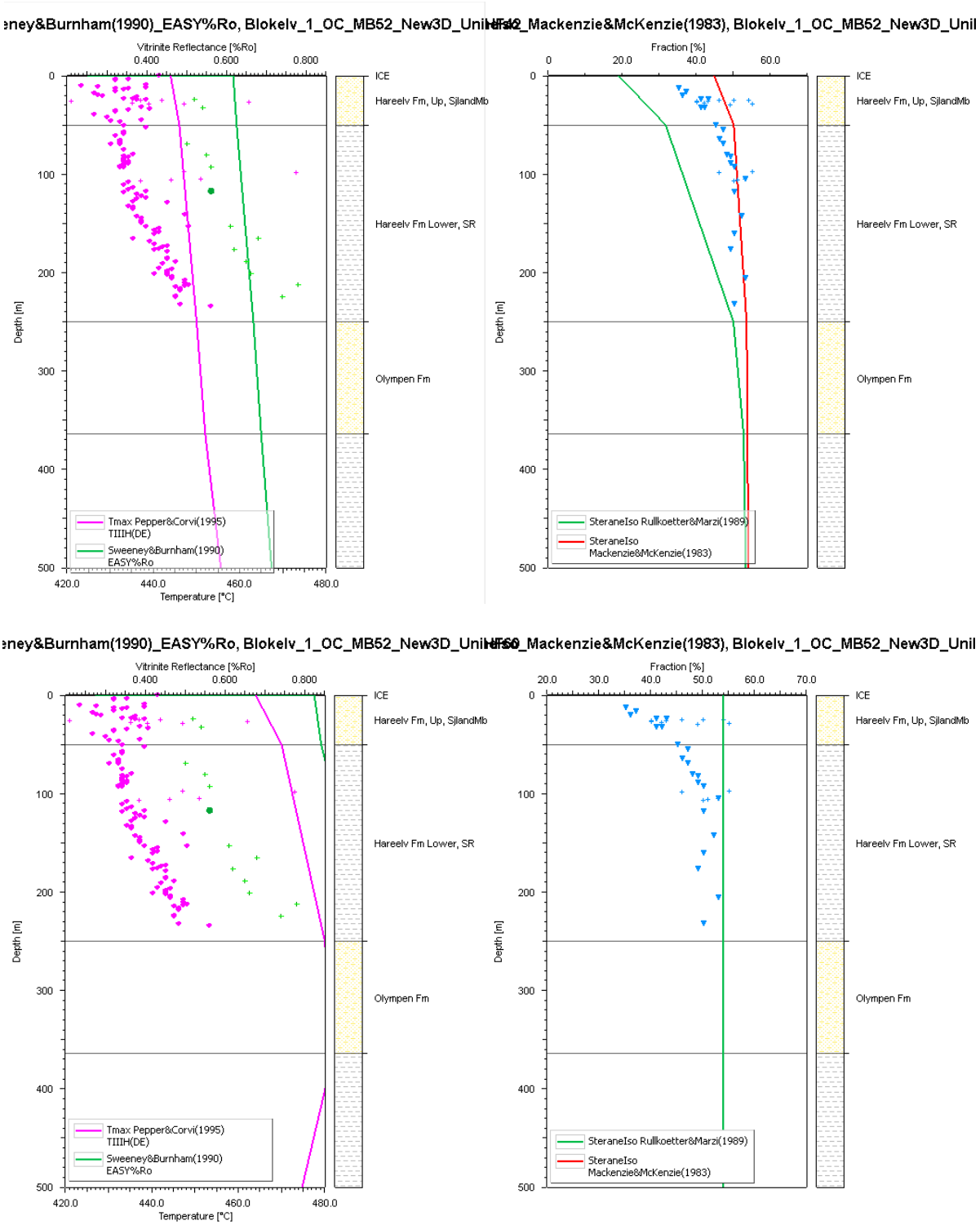

Figure 9.4b. Plots at the Blokelv pseudo well location with Blokelv-1 maturity data (symbols) showing matching of different three different 1D model maturity models (**Top:** model with uniform heat flow history of 42 mW/m^2; **Bottom:** model with uniform heat flow history of 60 mW/m^2). Modelled %Ro, Tmax and biomarker models are shown as solid lines. Notice that the 'oil-window' (defined as Tmax>435°C and %Ro>0.55%) is marked with a green dot at a depth of ca. 120 m (green dot on the %Ro plots to the left).

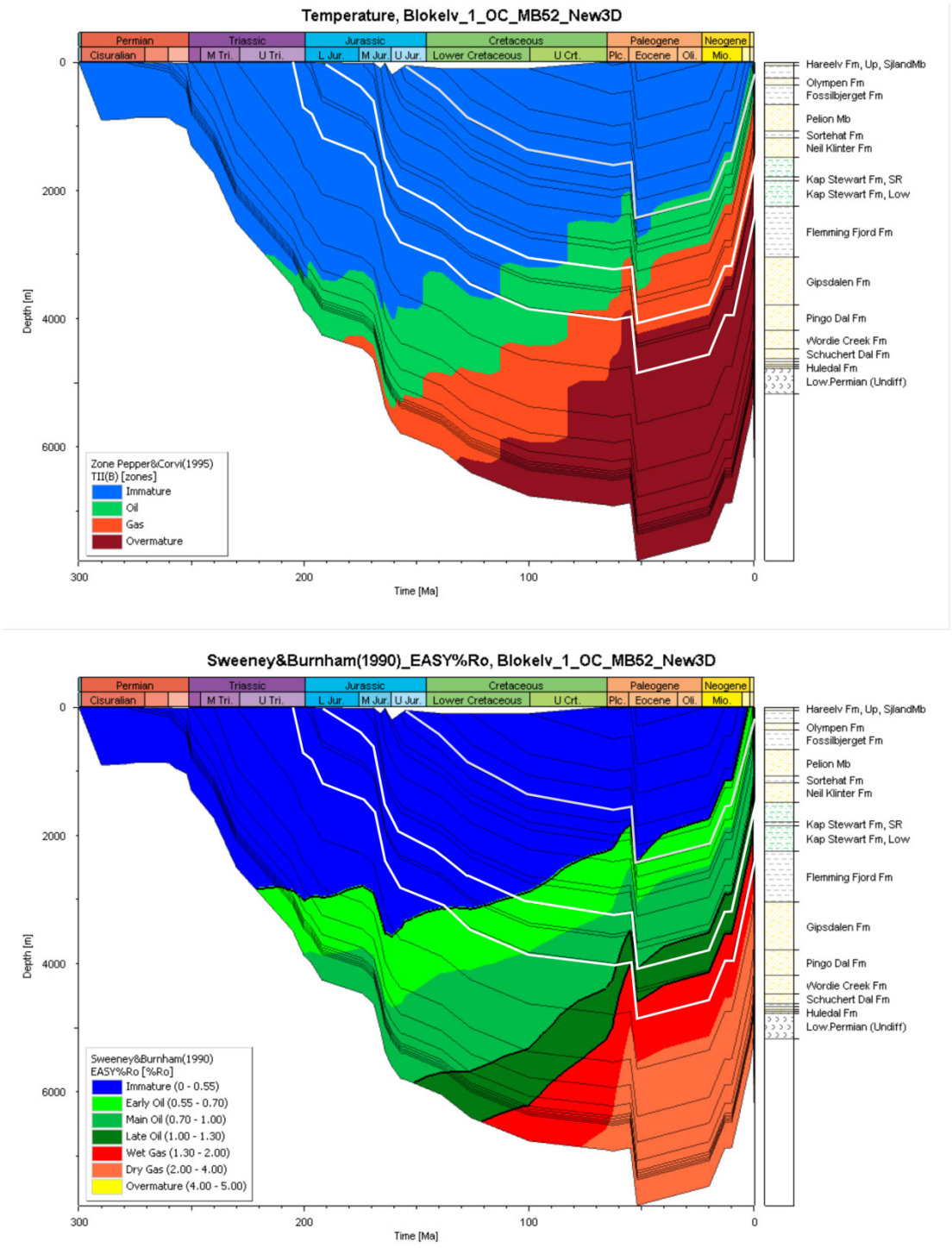

Figure 9.5a. Subsidence plot at the **Blokelv pseudo well location** with hydrocarbon generation zone based on Pepper & Corvi Type-II (1995) (top) and maturity zones (%Ro, bottom) against time based on the **updated model concept**. Notice that the potential Kap Stewart and Ravnefjeld source rock intervals (Kap Stewart Gr. highlighted in white) entered the oil window during Early Cretaceous and Middle-Late Triassic, respectively, and that the Kap Stewart source rock is in the late oil–gas window at present. Notice that the younger Upper Jurassic Hareelv source rock interval just reached the oil window at present.

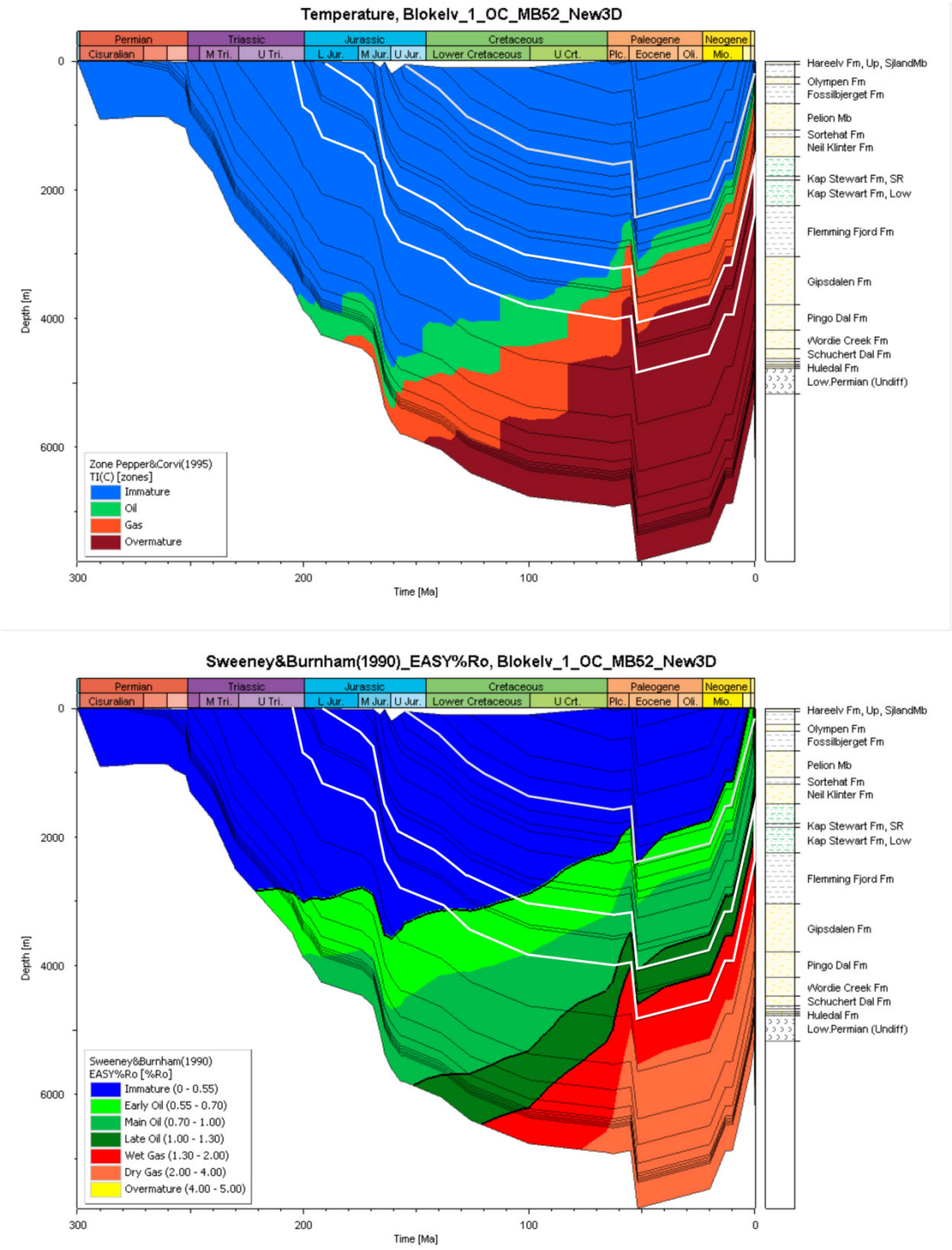

Figure 9.5b. Subsidence plot at the **Blokelv pseudo well location** with hydrocarbon generation zone based on Pepper & Corvi Type-I (1995) (top) and maturity zones (%Ro, bottom) against time based on the **updated model concept**. Notice that the potential Kap Stewart and Ravnefjeld source rock intervals (Kap Stewart Gr. highlighted in white) entered the oil window during Early Cretaceous and Middle-Late Triassic, respectively, and that the Kap Stewart source rock is in the gas-late oil window at present. Notice that the younger Upper Jurassic Hareelv source rock interval just reached the oil window at present.

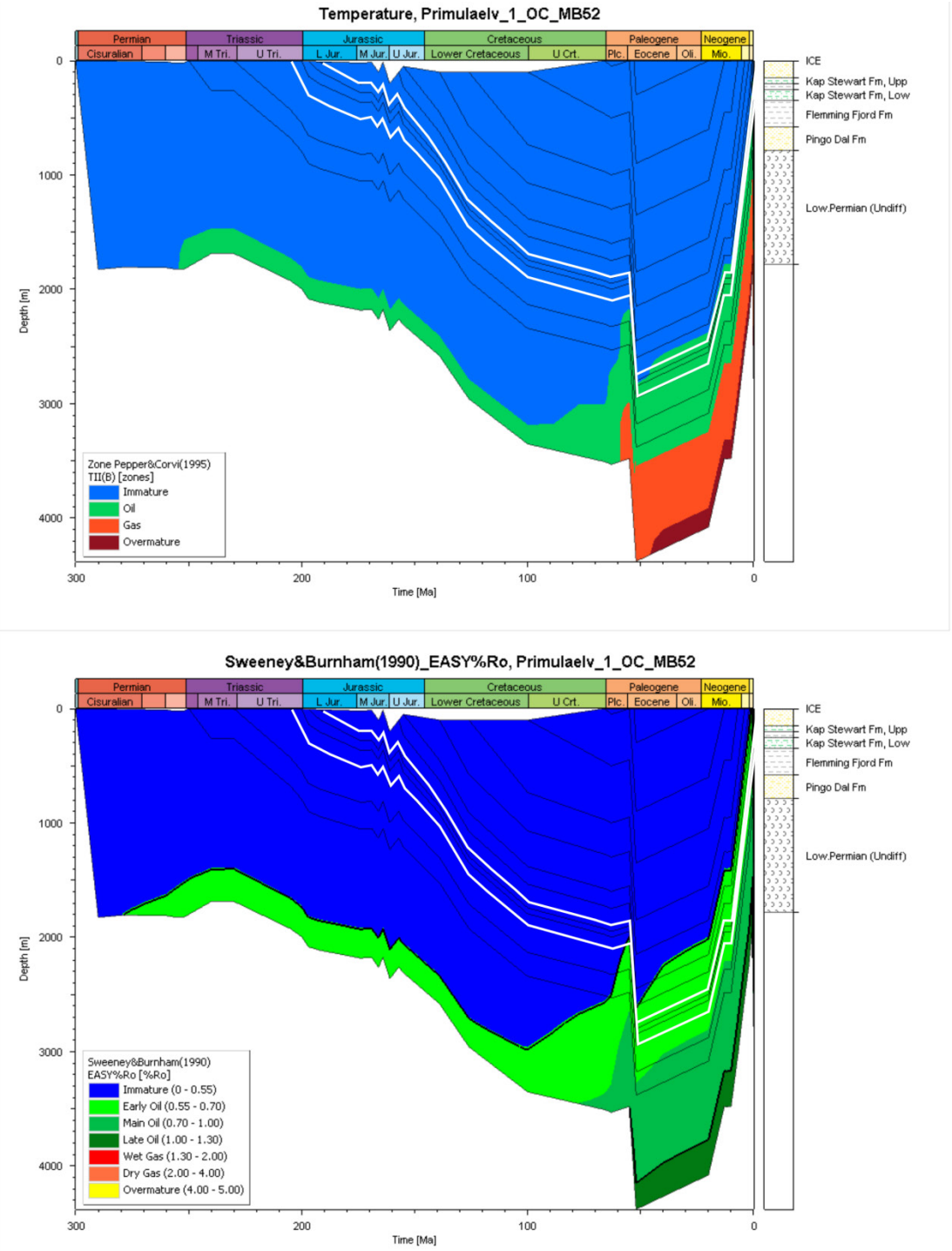

Figure 9.6. Subsidence plot at the **Primulaelv pseudo well location** with hydrocarbon generation zone based on Pepper&Corvi Type-II (1995) (top) and maturity zones (%Ro, bottom) against time based on the **updated model concept**. Notice that the potential Kap Stewart source rock interval (Kap Stewart Gr. highlighted in white) entered the oil window at c. 52 Ma during maximum burial due to extrusion of volcanics.

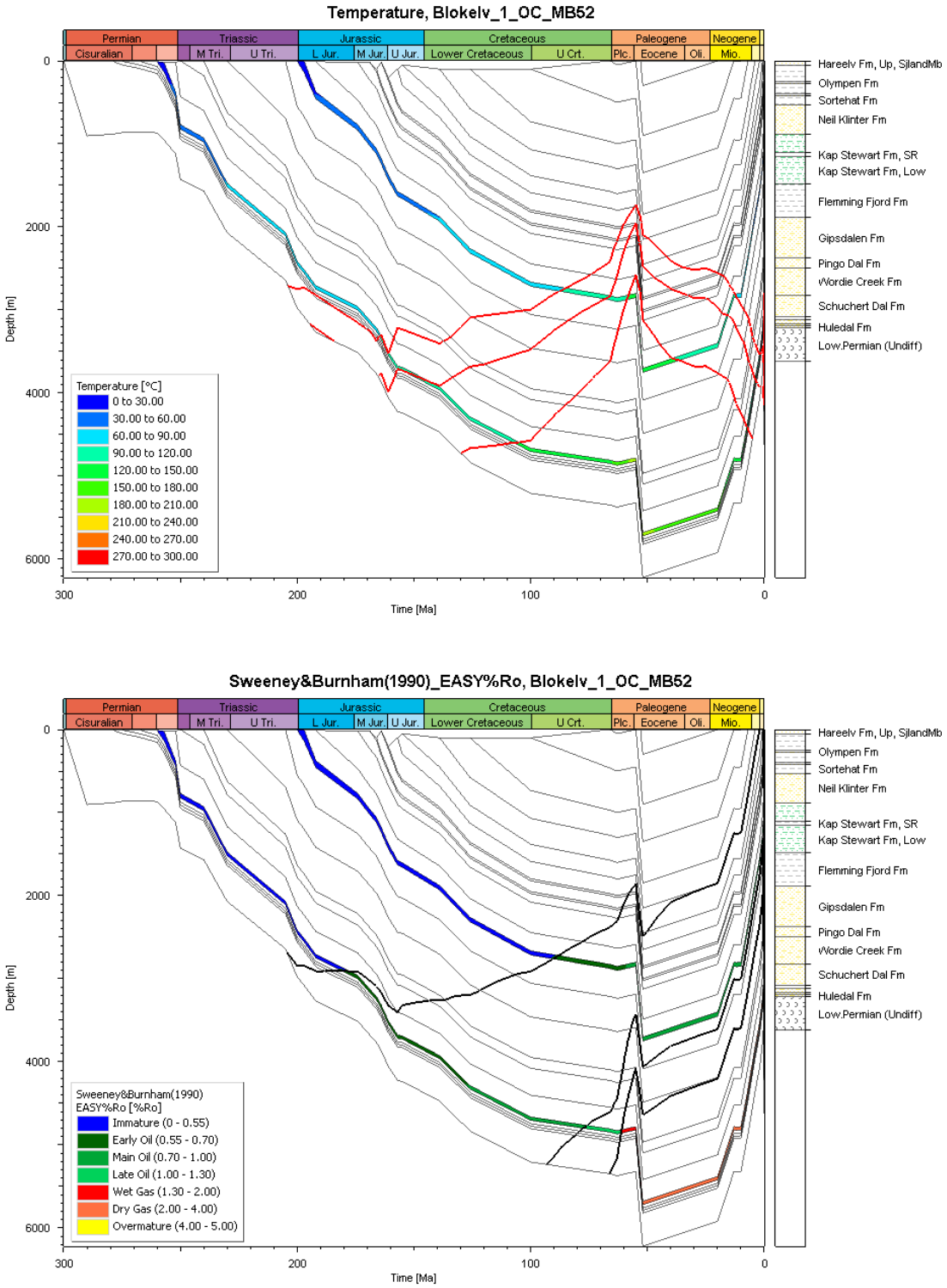

Figure 9.7. Subsidence plot at the **Blokelv pseudo well location** with temperature (top; isotherms at 90°C, 100°C, 120°C, respectively) and maturity (%Ro, bottom; isomaturity at 0.55%, 1.0%, 1.3%, respectively) against time, based on the **original model concept**. Notice the black isomaturity lines showing when the two potential source rock intervals entered the oil window during Late Cretaceous and Early Jurassic.

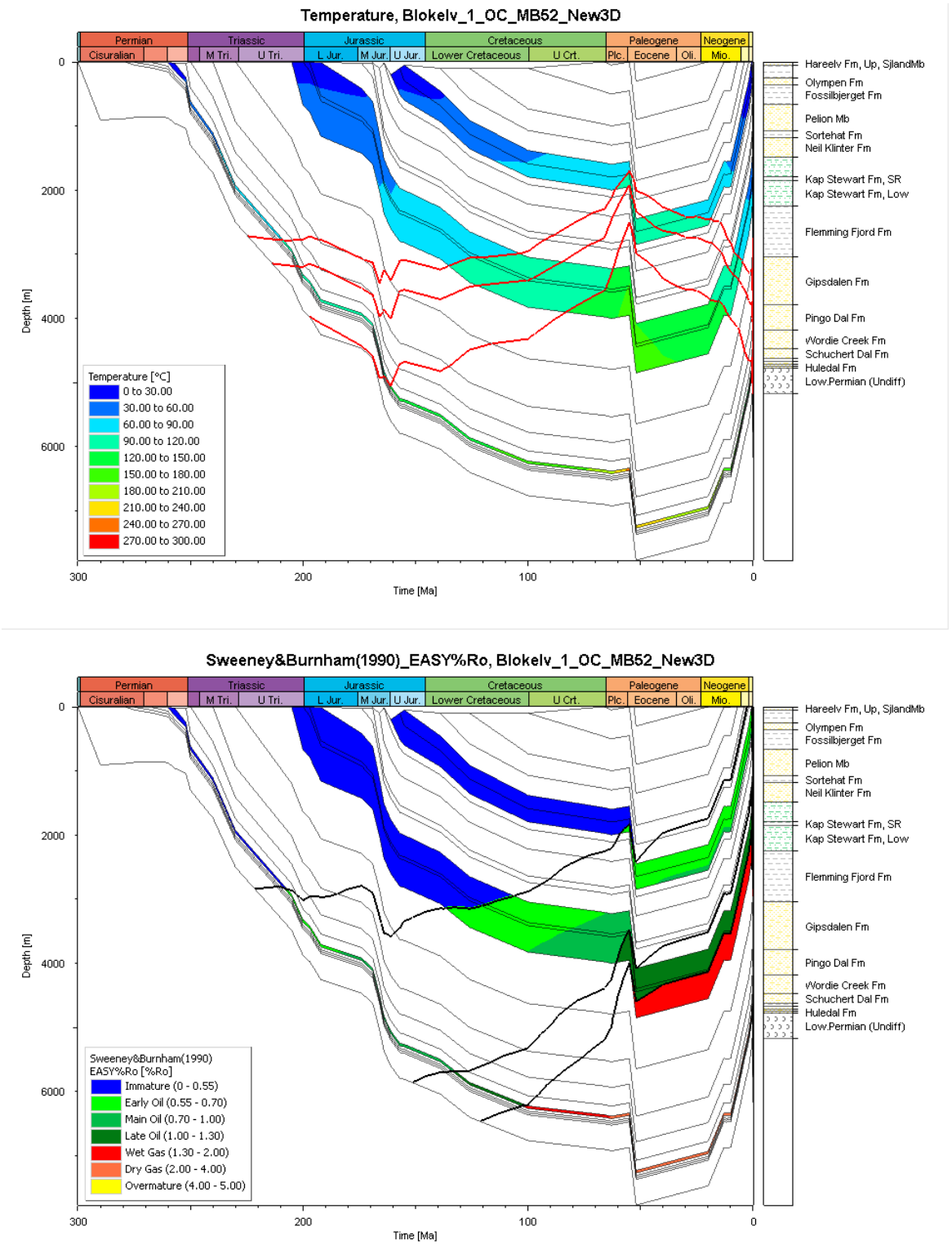

Figure 9.8. Subsidence plot at the **Blokelv pseudo well location** with temperature (top; isotherms at 90°C, 100°C, 120°C, respectively) and maturity %Ro, bottom; isomaturity at 0.55%, 1.0%, 1.3%, respectively) against time, based on the **updated model concept**. Notice the black isomaturity lines showing when the two potential source rock intervals entered the oil window during Early Cretaceous and Middle-Late Triassic, and that the younger Upper Jurassic Hareelv source rock interval just reached the oil window at present.

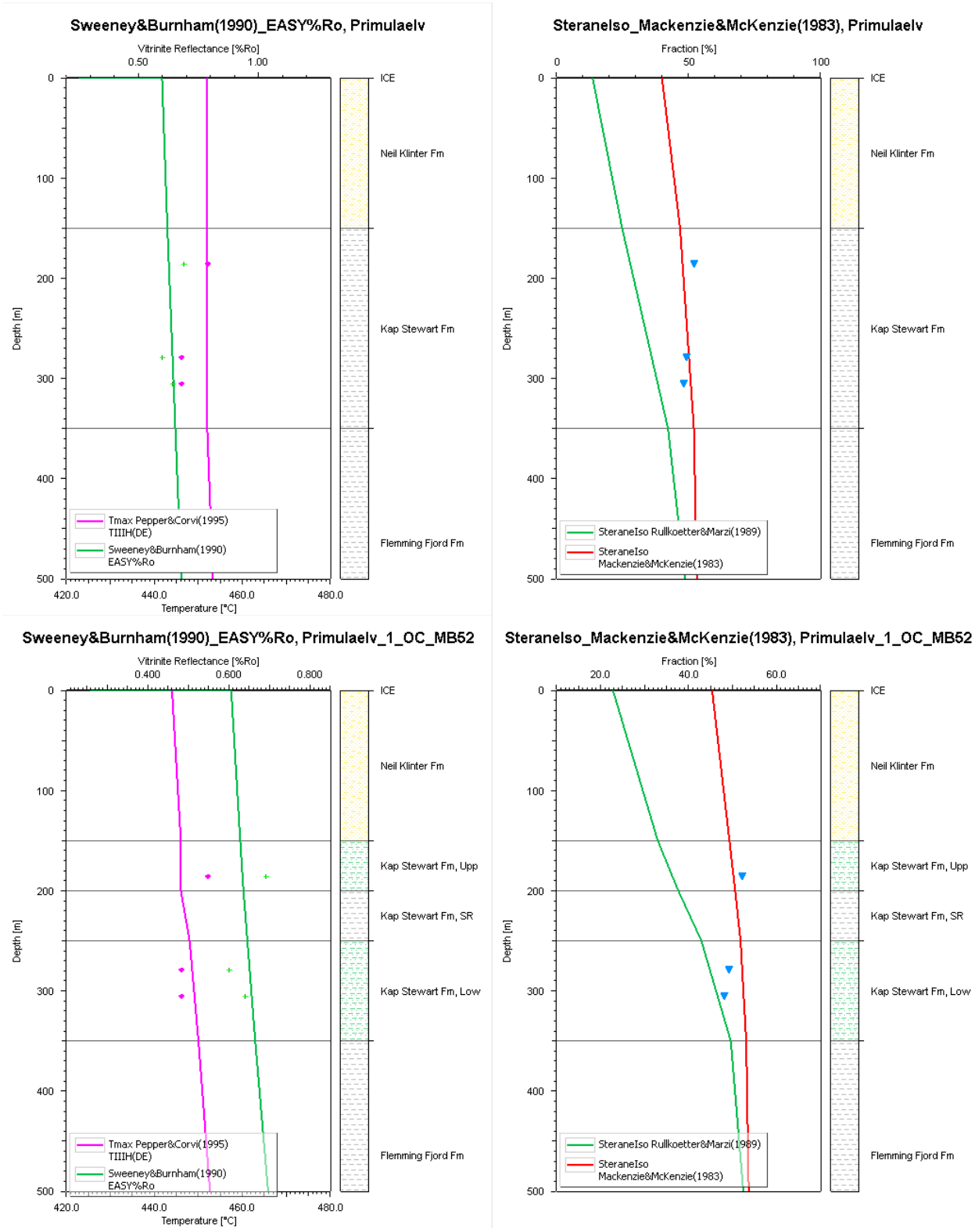

Figure 9.9. Plots at the **Primulaelv pseudo well location** with Primulaelv maturity data (symbols) showing matching of the updated 1D model maturity model, based on the **original model (top) and updated model concept (bottom)**. Modelled %Ro, Tmax and biomarker models are shown as solid lines.

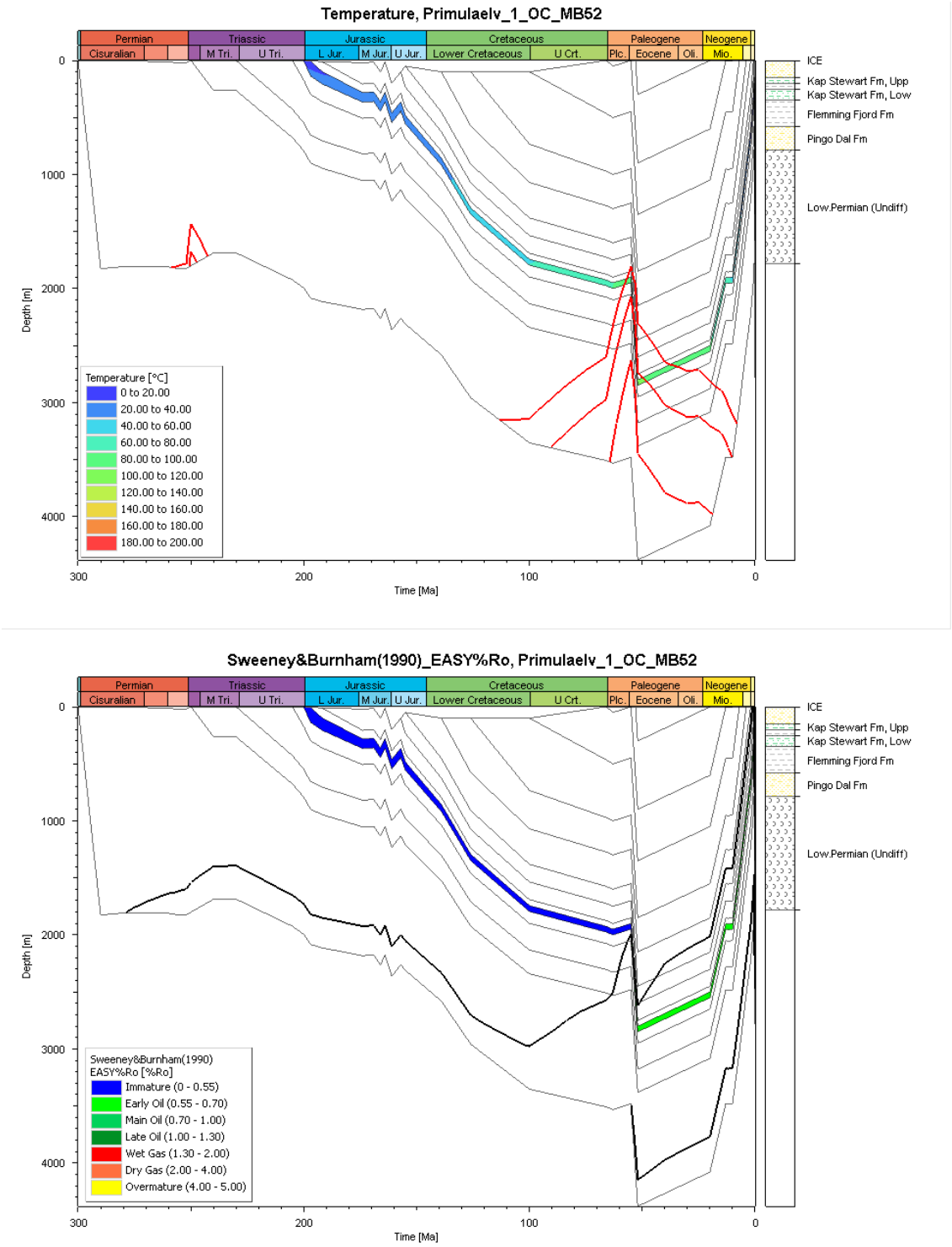

Figure 9.10. Subsidence plot at the **Primulaelv pseudo well location** with temperature (top; isotherms at 90°C, 100°C, 120°C, respectively) and maturity %Ro, bottom; isomaturity at 0.55%, 1.0%, 1.3%, respectively) against time, based on the **updated model concept**. Notice the temperature peak during the early-middle Triassic rifting and the black isomaturity lines showing when the potential Kap Stewart source rock intervals entered the oil window at c. 52 Ma during maximum burial due to extrusion of volcanics. The Ravnefjeld source rock is not expected to be present on the eastern margin of the Jameson Land Basin.

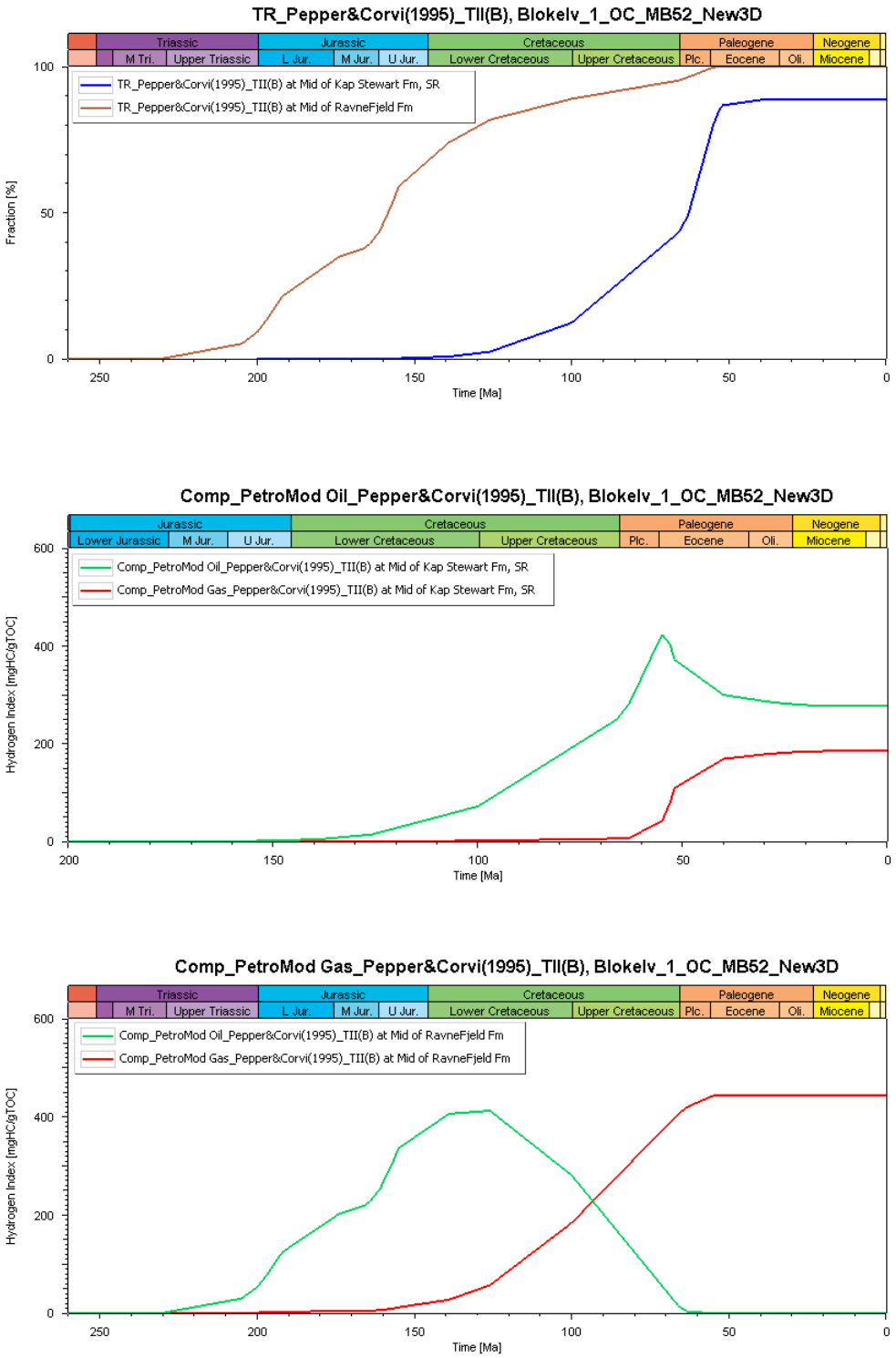

Figure 9.11. Combined plot showing the transformation ratio (TR, upper plot) and the oil and gas generation potential for the two potential source rocks at the **Blokelv pseudo well location** using Pepper&Corvi Type-II (1995) kinetics (Kap Stewart, middle plot and Ravnefjeld, lower plot). Notice the remaining kerogen transformation potential for the Kap Stewart source rock (middle plot) and that oil generation has continued since Paleocene (middle plot), while only gas is generating from the potential Ravnefjeld source rock at present (lower plot).

9.8 Maturity maps

The 1D maturity modelling of the 21 pseudo wells, using the new updated modelling concept based on the new seismic interpretation and depth-conversion, was applied to generate regional maturity maps.

To further support the 1D modelling results a preliminary 2D model of the W-E trending 86-6V seismic line was modelled to evaluate the general maturity from west to east, and a preliminary 3D regional model of the JLB based on the depth-converted seismic maps (Fig. 9.13). The results of the 2D modelling is not included in this report, but will together with other transects at a later stage be used to test possible scenarios/concepts to support potential play types. The 2D and 3D maturity modelling reflect levels of possible source rocks in the immature-, oil- and gas to overmature windows at the time just before (65 Ma) and after extrusion of volcanics (52 Ma).

The maturity maps are colour coded intervals from the isochore maps according to the following simple relation between vitrinite reflectance (VR) and depth:

- Immature:	**0–0.3 km**	**(0–0.55 %Ro);**
- Oil:	**0.3–2 km**	**(0.55–1.3 %Ro);**
- Gas to overmature:	**>2 km**	**(>1.3 %Ro).**

This simple maturity-depth relation is based on the available vitrinite reflectance data and basin modelling using Blokelv-1 data in the central part and Primulaelv-1 data in the eastern part of the Jameson Land Basin (Fig. 9.12)

For simplicity and lack of a more complete VR dataset, it is assumed that the same maturity levels can be used for all maturity maps, even though they are more optimistic than normally used levels, where the interval for the oil window is ~3000–4000 m. For this reason and because of many other uncertainties of the presumed source rock (e.g., presence, quality, thickness, etc.) the maps should be used with caution as they only provide rough and reginal simplistic maturity indications. Thus, the modelling results indicate that the upper part of Kap Stewart Group is in the oil window over most of the basin expect in the southwestern area where it has entered the late oil – gas window (Fig. 9.13a). At the level of the Early Triassic horizon (~Top Wordie Creek Fm) that confines the potential Ravnefjeld Fm below, the basin is generally in the gas–overmature window at present (Fig. 9.13b). However, the transition from gas to the late oil phase straddles the basin margin to the north and north-west, which raises the prospectivity in these parts.

The main uncertainty is associated with the presence, extent, quality and thickness of source rocks, but other factors, such as the depth conversion of the seismic maps (depth/time relations) (see Ch. 4) also have implications for the maturity maps. If depth conversion at a later stage is changed or updated, then the maturity maps should also be updated.

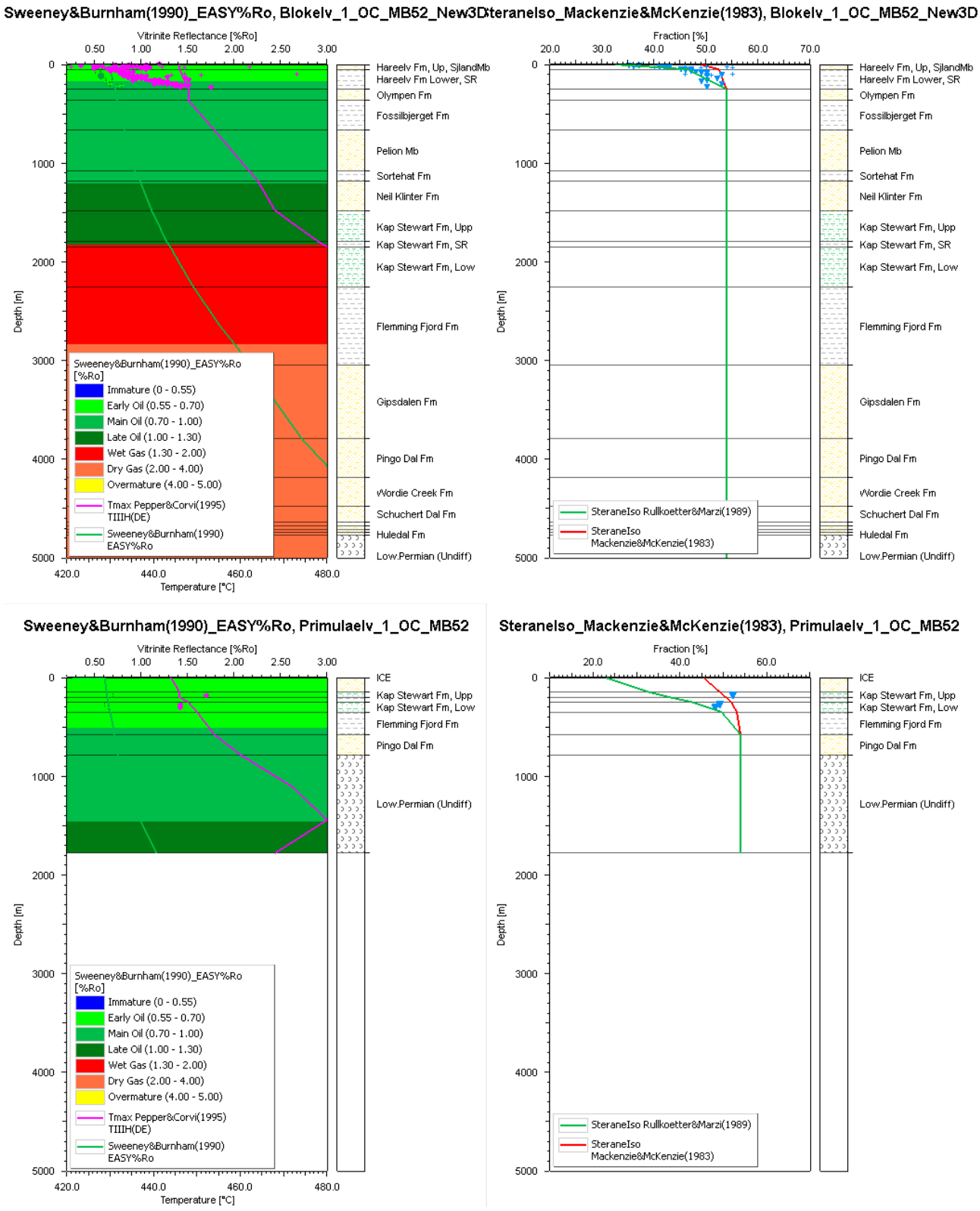

Figure 9.12. Plots comparing the results at the maturity modelling at the Blokelv and Primulaelv pseudo well locations, representing the central and the eastern margin of the Jameson Land Basin.

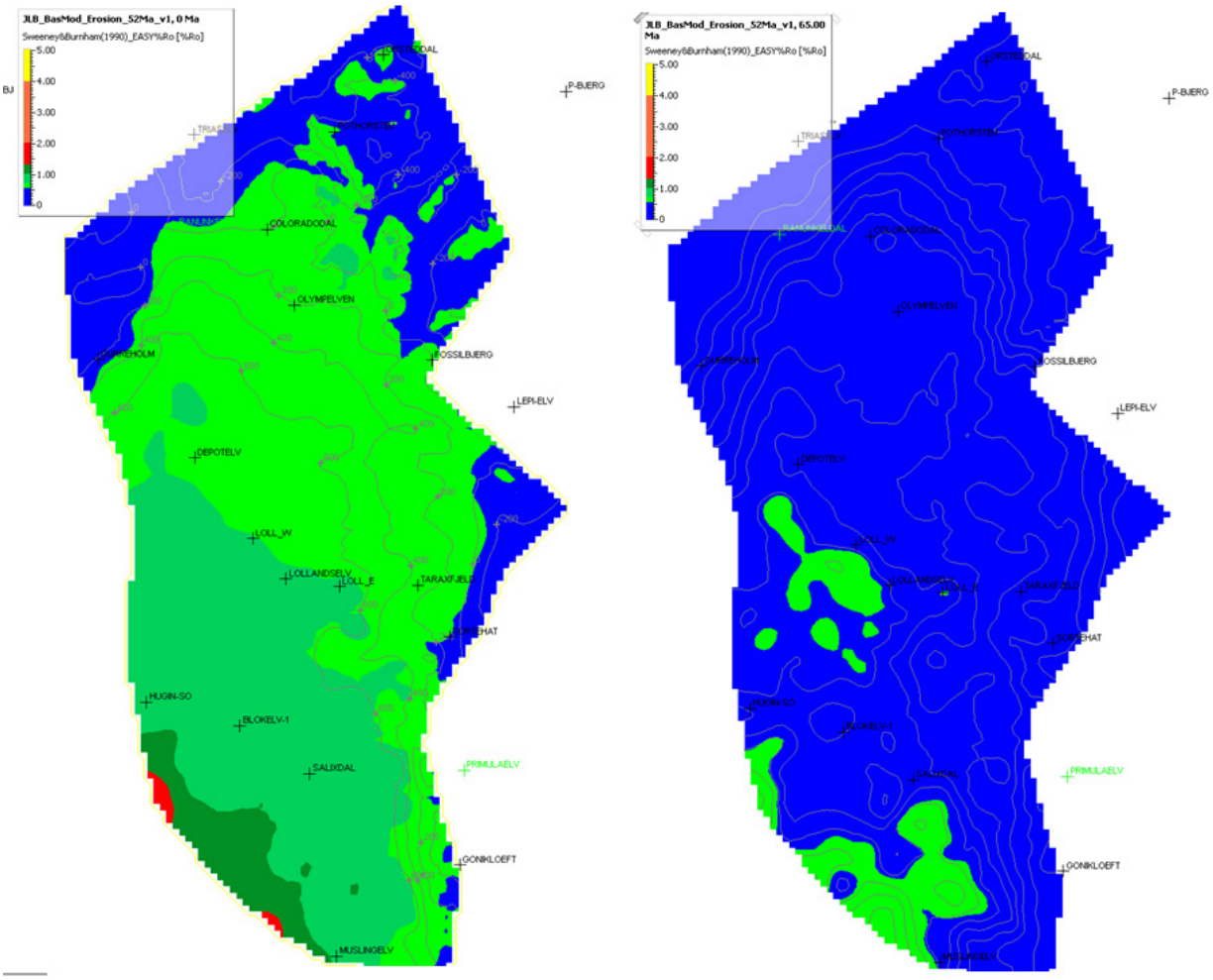

Figure 9.13a. Maturity map from the 3D model of the Top Kap Stewart source rock interval at present day (left) and at 65 Ma (right). At present the uppermost part of the Kap Stewart source rock is in the oil window over most of the Jameson Land region, except in the southwestern area where it has entered the late oil – gas window. The eastern margin of the JLB including the Primulaelv pseudo well location is not part of the map due to lack of seismic coverage.

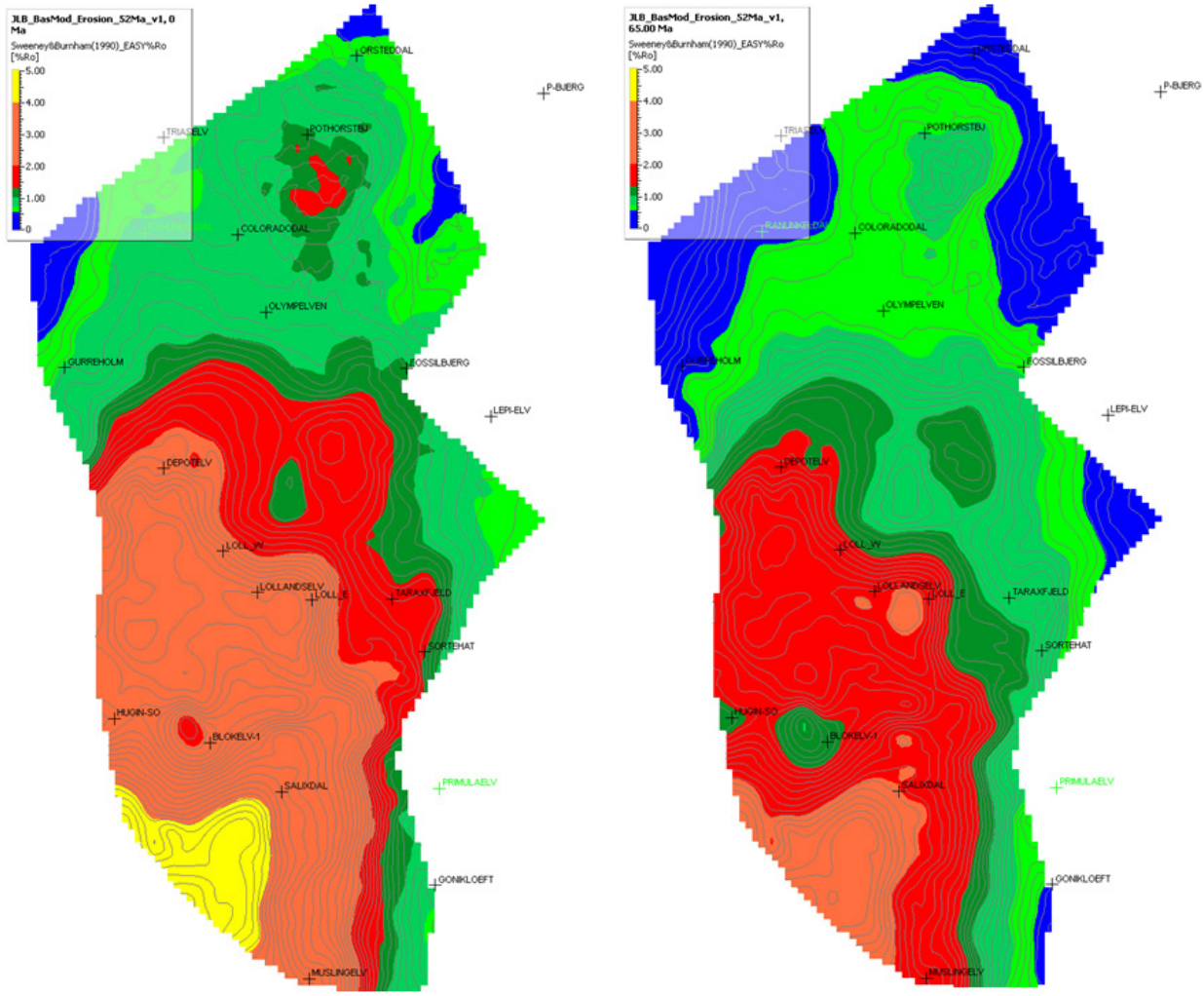

Figure 9.13b. Maturity map from the 3D model of the Top Wordie Creek horizon at present day (left) and at 65 Ma (right). Notice how the uppermost part of the Wordie Creek and deeper positioned Ravnefjeld source rock interval is gas- to overmature at present in central and southern part of the Jameson Land Basin, but is in the oil window and immature in the northern part of the Jameson Land area. The eastern margin of the JLB including the Primulaelv pseudo well location is not part of the map due to lack of seismic coverage.

9.9 Conclusions

The thickness of Upper Cretaceous sediments and Paleocene volcanics, as wells as enhanced heat flow during the Paleocene, are particular important factors for the thermal maturation of the source rocks. Other controls, such as post-volcanic uplift and erosion, are important for preservation of trapped hydrocarbons and possible later degradation or leakage.

The modelling concept used in the previous study has been revised based on new seismic interpretation and maturity data from the Blokelv-1 corehole (Ch.6) and AFTA data (Ch. 9.6). The new optimized results has been used to predict the depth of the oil-window defined oil window being defined as EASY %Ro= 0.55–1.3% and to calculate the timing of hydrocarbon generation.

The modelling does not show any significant difference when optimised against maturity data with burial at c. 52 Ma or later at c. 35 Ma, as inferred by the AFTA data and modelling (Ch. 8). However, an earlier maximum burial (100–90 Ma; ~Late Cretaceous), cannot be modelled to match the VR gradient and the revised model concept for JLB. This discrepancy between results from the new AFTA modelling and the maturity data is at present not fully understood. Based on the preliminary assumptions and maturity modelling, the timing of erosion subsequent to maximum burial at c. 52 Ma is, at present based on the general geological understanding and Late Paleocene and Neogene uplift and erosion with an increasing amount of erosion from 15–12 Ma.

Based on the revised model concept for the Jameson Land Basin the following conclusions are stipulated:

- The modelled thickness of the removed Cretaceous sediments decreases gradually, from approx. 1300 m (observed on seismic data in the Scoresby Sund fjord) to 500 m towards the margin of the basin in the northwest.

- The revised model concept requires a volcanic wedge thinning from more than 2 km (observed south of the Scoresby Sund fjord) to less than 100 m in northern Jameson Land, for the same heat flow history to be maintained across the area. The amount of erosion varies from ~4200 m in the northeastern part down to ~1600 in the central and northwestern part and increasing again to ~2900 m in southeastern part of the Jameson Land Basin.

- The Upper Permian Ravnefjeld Fm and older successions are post-mature over most of the Jameson Land Basin, corresponding to the Early Triassic horizon being positioned deeper than ~2500 m. However, along the northern and northeastern margin of the basin Ravnefjeld Fm is potentially located in a shallower position, thus raising the prospectivity of the Triassic in these parts. Generation started during early-middle Triassic and the main generation took place during Late Cretaceous and Early Tertiary during the volcanic event. The hydrocarbons generated were either thermally degraded or may have migrated into shallow stratigraphic and structural traps in the overlying succession during the Early Tertiary.

- The Lower Jurassic Kap Stewart Group is in the oil window over large parts of the basin except in the southwestern area where it has entered the late oil – gas window. Generation of hydrocarbons took place over a short time period during the Cretaceous (central basin) and shortly after the Early Tertiary volcanism (eastern margin).

- The new additional fission track data and models supports Cenozoic erosion of 2–3 km over most of the area. The erosion rate generally accelerated during the Neogene and Quaternary. The present depth interval of the oil window is strongly influenced by regional post-burial uplift/exhumation (most recently during Miocene), placing it in a shallower position that where it was during maximum burial.

- Following extrusion of the volcanic rocks, the basin was mainly uplifted and eroded and the temperature of the sediments decreased gradually resulting in a decrease or cessation of hydrocarbon expulsion from of the potential source rock intervals. However, small tectonic movements may generate or remove traps or they may change the direction of updip migration of the hydrocarbons generated. Understanding and assessing the uplift pattern of the region is therefore important for the evaluation of petroleum plays in the Jameson Land licence area.

- The revised basin modelling supports a high prospectivity in the Jameson Land Basin, although there are noticeable shortfalls in the knowledge of the petroleum system, e.g. source rock maturation, fluid migration, and reservoir/sealing capacities. Importantly, the results confirm the hydrocarbon potential of the Lower Jurassic Kap Stewart Group mudstones. Moreover, several other potential source rock intervals may have a significant potential for generating liquid hydrocarbons prior to the thermal alterations by volcanism.

- The basin modelling study stresses the critical need for more information on key aspects of the petroleum system: (a) original distribution, thickness and quality of source rocks, (b) maturation and fluid migration, (c) carrier and reservoir potential, (d) erosion/exhumation events, especially the Cenozoic uplift history (e) heat flow during and after Paleogene volcanism and (f) time-depth relationship of the strata units.

- The present study provides a framework for further modelling of the JLB that becomes applicable as new data is collected. A continuous revision of the basin model will provide important constraints on the key play types and facilitate the derisking of the petroleum system.

10. Play maps

Of the play types presented in chapter 7 the Jurassic post-rift and Triassic syn-rift plays are considered to the most relevant targets for further work. This is notably because of the present depth interval of the oil window, which is strongly influenced by regional post-burial uplift/exhumation (most recently during Miocene), placing it in a shallower position that where it was during maximum burial (Ch. 9). The depth level of the oil-gas transition, assumed to be around 2000-2500 m based on the maturation modelling, means that the Permian carbonate play is most at risk from being overmature. Conversely, the late Jurassic play with the Hareelv Fm exposed at terrain level over major parts and only covered by a veneer Cretaceous sediments in the south, is risked by insufficient burial and leakage. It is possible that the Hareelv Fm is buried deeper offshore into Scoresby Sund, thus increasing its potential toward south and southwest, but this notion needs further investigation. Considering the present limitations in understanding the JLB petroleum system, e.g. source rock maturation, fluid migration, reservoir and sealing capacities, time-depth relations, prospectivity of the Permian carbonate and the Late Jurassic clastic systems cannot be ruled out. It is, however, recommended that the Triassic rift and the Jurassic post-rift plays be tested first in the process of derisking. In this respect it is important to note that both the Permian carbonate play and the Triassic rift play relies on the same source rock, e.g. Ravnefjeld Fm, and thus it would make sense first to test the more shallow intervals (less risky) that could be sourced by the Ravnefjeld Fm.

10.1 Late Triassic – Lower Jurassic clastic play

Crucial for this play type is the presence of deltaic sandstone bodies that are underlain/interbedded by lacustrine anoxic mudstone of the Kap Stewart Group. The play type is mainly stratigraphic although faults on the eastern basin margin also suggest a structural component (Fig. 4.11). The thickness distribution and the seismic facies is suggestive of depocentres likely related to fluvial-deltaic progradation into the central parts of the Kap Stewart lake during regressional stages (Fig. 7.10). As described in Chapter 7 the seismic interpretation supports the conceptual sedimentological model based on outcrop studies. The outline of the play is defined by the depocentres of the KSG that are distributed in the southern part of the JLB (e.g. >700 m thickness) and located within the 500-2500 m depth contour of the Top Kap Stewart Group (Fig. 10.1). The charge is considered to be mainly intraformational with hydrocarbons having migrated over short distances from anoxic organic-rich lake sediments into interbedded deltaic sand-stone accumulations. The source rock quality probably increases towards the central parts of the basin, which were located farther away from clastic input sources. Additional reservoir potential may exist in the overlying Neill Klinter Group and Pelion sand where these formations are sufficiently buried in the central parts of the basin. The main sealing intervals comprise the KSG lacustrine mudstone and the internal marine mudstone units of the Neill Klinter Group. The play area constitutes about 40 % of the GGO's licence area although this may be larger due to the secondary reservoirs developed in the Middle Jurassic interval.

The interval deeper than 2000 m is risked by overmaturation while the eastern fringe of the play may be jeopardized by seal integrity due to truncation associated with uplift and erosion, including the effects of glaciations. Derisking studies should focus on narrowing the uncertainties, e.g. source rock quality/distribution, intra and extra-formational reservoir potential, overburden/seal properties (see “Further work” Ch. 11), which can add constraints to the play map and definition of prospective targets.

10.2 Triassic syn-rift play

The Triassic rift play concept is based on migration of hydrocarbons originating from Permian sources updip into structural-stratigraphic traps containing coarse-grained alluvial wedge sediments of the Pingo Dal Formation or more locally developed units of the late rift phase, e.g. Ørstedsdals Member (Fig. 10.2). Since the Ravnefjeld Fm. is probably overmature in the deep parts of the central and southern basins (Ch. 9) the play type requires that hydrocarbons migrated to shallow levels as maximum burial commenced. According to the basin modelling this most likely occurred during the early Cenozoic, although it is possible it may have occurred earlier, e.g. late Cretaceous (Ch. 8). Thus, the maturation history and migration pathways remain the key risk for the Triassic play. The crescent-shaped play area outlined in Fig. 10.2 cover both the early and late phases of the Triassic basin development represented by Pingo Dal Fm./Klitdal Mb. and Fleming Fjord/Ørsted Dal Mb., respectively. Additional traps or four-way closure may be associated with an intra-basinal ridge system expressed by the Early Triassic horizon (Fig. 10.2). At the level of Top Gipsdalen Fm. this area is likely to be in the oil-window mature interval but also in this case is the maturation and fluid history of critical importance. The strata contained in the northern Permian sub-basin may have significance for the Triassic play since, as discussed in 4.2.1, it is possible that marine source rocks of the Ravnefjeld Fm exists here at relatively shallow depths (e.g. 1300-1600 m) presently located in the oil window. In the southeastern parts of the JLB the Triassic rift play is considered less viable due to the enhanced presence of sills (and by implication poor seismic quality) and the risk of leakage along strata dipping westward at ~5°. This interpretation may, however, change as new data is collected.

An unknown factor that is particularly relevant for fluid migration of the Triassic rift play is the preservation of porosity with increasing burial depth. In general this will depend on mineralogical composition, diagenetic processes and overpressure development (Ramm & Bjørlykke, 1994). The quality of sandstone reservoirs is commonly linked with processes that hinder precipitation of quartz cement in pore spaces, such as the presence of intergranular clays or diagenetic coatings around quartz grains. Overpressure may play an important role in preserving porosity but it is difficult to predict pressure in basins that are both exhumed and/or contain rich source rocks such as those in the Barents Sea region, where the basin development may be highly influenced by dissequilibrium compaction. Under such conditions gas generation and expansion during exhumation may significantly increase pore pressure and facilitate updip migration of fluids (Edwards et al., 2013). These questions should be addressed by further work, for example pursued by a reservoir analyses study of the Avannaa cores.

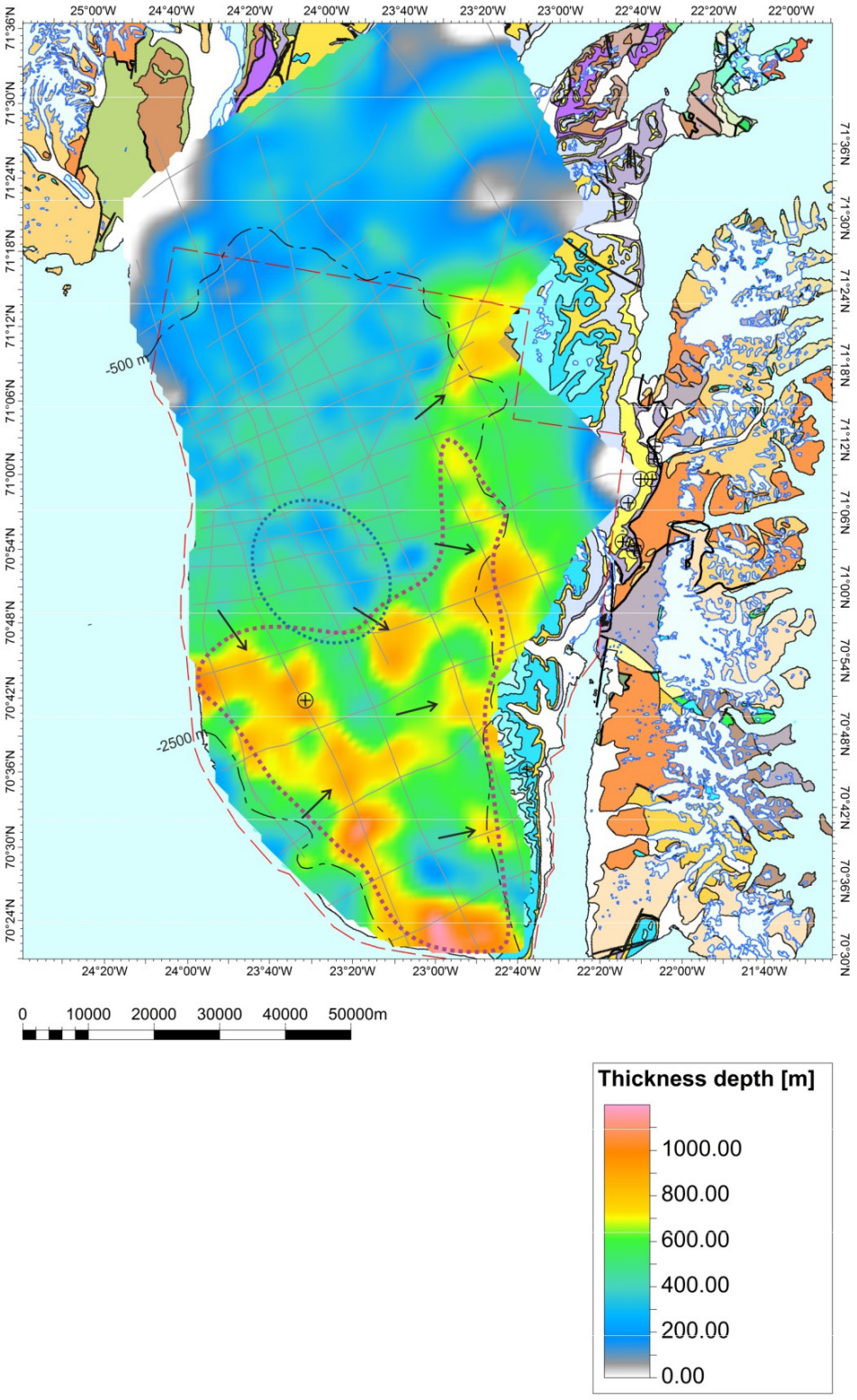

Figure 10.1. Map of the Late Triassic – Lower Jurassic clastic play. The map shows thickness distribution of the Kap Stewart Group. Depth isobars 500 and 2500 m below MSL of the Top Kap Stewart Group are indicated. Arrows illustrate possible fluid migration pathways. Secondary reservoirs may be present within the Neill Klinter Group (main depocentre demarcated by blue ellipse).

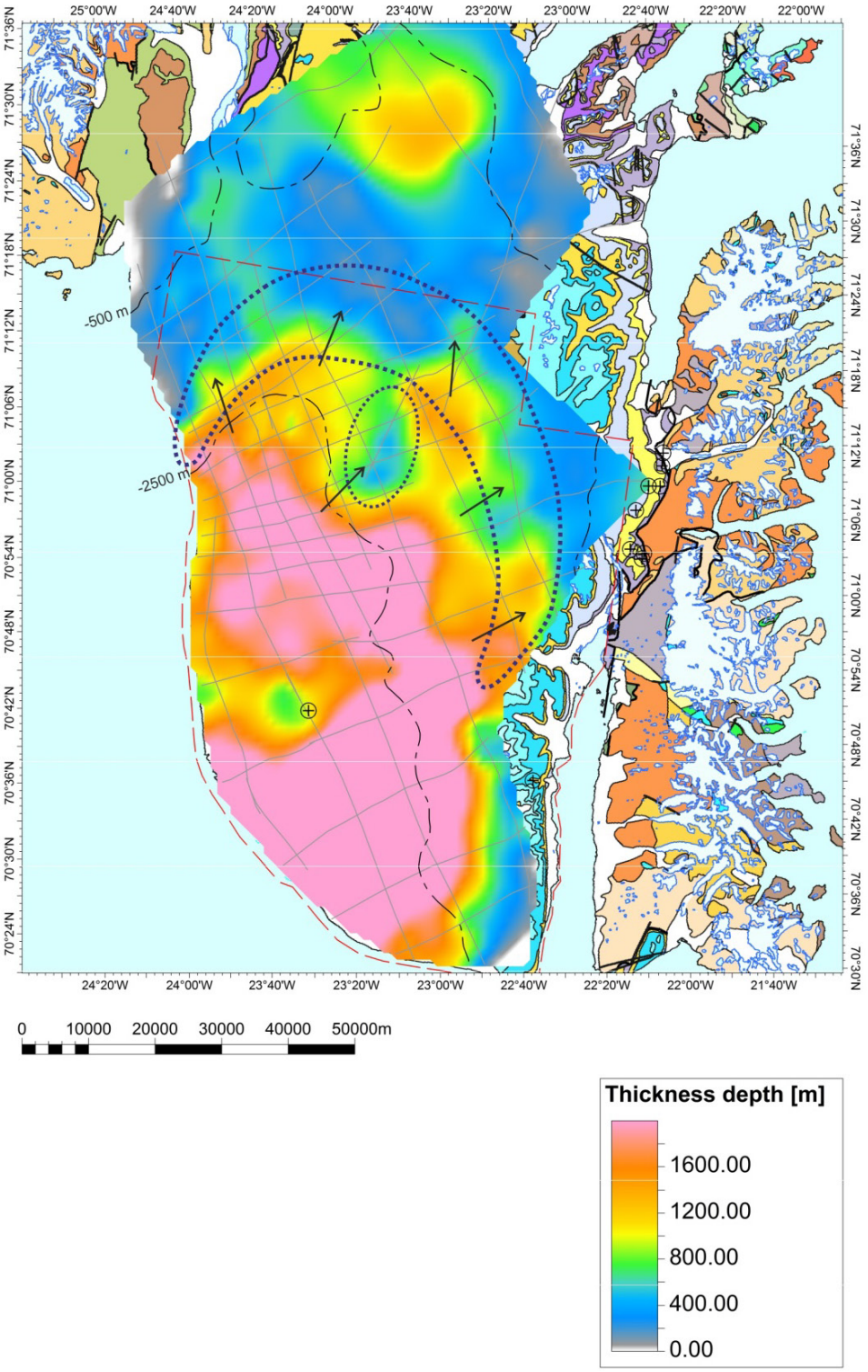

Figure 10.2. Map of the Triassic Rift play area. The crescent-shaped zone demarcates the north-northeastern margin of the rift basin that has potential for stratigraphic-structural traps developed updip from the Permo-Triassic central basin. The map is based on the thickness distribution of the Gipsdalen/Pingo Dal formations, representing the syn-rift depositional phase. The 500 and 2500 m depth isobars (below MSL) of the Top Gipsdalen horizon are indicated. Arrows illustrate possible fluid migration pathways from the basin interior toward the margins. Structural closures may also be associated with an intra-basinal ridge, defined by the Early Triassic horizon (A1.2), shown by ellipse.

11. Suggestions for further work

We recommend that further work is carried out in the licence area with focus on derisking and developing the key play types (Ch. 10). Firstly, to facilitate fieldwork and drilling in the JLB, analyses and studies can be carried out at GEUS based on available material. Secondly, once fieldwork/drilling has proceeded the results of the new data should be synthesized and integrated into working play models. As explained in the chapter on basin modelling there is a critical need for constraining source rocks levels, maturity gradients, carriers and reservoir properties within the key play types. Since many studies have been performed on outcrops and outcrop samples over the years, and the basin model is lacking critical information on the buried strata, e.g. age control, petroleum systems and time-depth relationships, stratigraphic coring would be the preferable and probably the most cost-effective way forward in derisking the basin.

11.1 Stratigraphic coring

The question is then which stratigraphic intervals and depths should be targeted by a stratigraphic coring campaign on Jameson Land? A focus on coring the late Triassic - early Jurassic interval is favoured by (1) the good evidence of a lacustrine source rock that appears to be close to generating oil, (2) occurrence of sand-prone deltaic systems on the eastern margin of JLB, forming both potential carriers and reservoirs, and (3) the possibility for stratigraphic traps based on the new seismic interpretation. In addition, the key source rock interval, the lacustrine deposits of the Kap Stewart Group (KSG), is located at depths that are potentially accessible by shallow drilling. Stratigraphic coring could also be used to provide more information on the Triassic rift play. However, the depths would require coring close to outcrops in eastern Jameson Land, which are located far from the central basin or “kitchen” region. Moreover, some of the Triassic strata in these parts have already been drilled by the Avannaa boreholes. Targeting the late Permian interval below is even more risky and may only be attempted on the northwestern fringe of the license area where the Permian unit is close to surface (Fig. 4.1). The most crucial factor for the Triassic rift play is the presence of hydrocarbons derived from Permo-Triassic source rocks below, e.g. the Ravnefjeld Fm. (Fig. 10.2). This structurally-controlled fluid migration may possibly be tested by drilling above fault structures in the northeastern part of the licence area (Fig. 4.6).

We suggest that the main objectives of a stratigraphic coring campaign should be to:

1. Recover a relatively complete sequence of anoxic lacustrine mudstone and interbedded sandstone of the late Triassic – early Jurassic Kap Stewart Group.
2. Recover middle-upper Jurassic strata of the Neill Klinter Group and Pelion Fm to test its sealing capacity and potential for secondary reservoirs.

As a secondary drilling objective we suggest:

3. Coring the Jurassic interval above Top Fleming Fjord Fm. at positions where the upper Triassic is closely connected to the main basin, and the seismic data reveal

show indications of hydrocarbons. The goal would be to gain information on possible hydrocarbon migration updip from the Permo-Triassic basin (Ravnefjeld Fm.) into lower Jurassic sandstone units.

To achieve the objective of penetrating the KSG westward of the basin margin (e.g. Hurry Inlet) it is necessary to drill deeper than the existing sites in the JLB (e.g. Blokelv-1, TD = 233 m). A concrete possibility is to use drilling equipment, which at the time of writing is present in eastern Jameson Land. This rig, according to information provided by MT Højgaard, has the capacity to drill to 1000 m (Fig. 11.1-A). Figure 11.1-B shows the gross area were the upper part of the KSG may potentially be captured by drilling to depths of 600-1000 m.

The results from this study indicate that drilling targets in the eastern JLB covered by seismic data have the best chance of successfully testing the late Triassic – middle Jurassic petroleum system. By selecting one or more sites within the eastern valley system (Katedralen/Uglelev) where overburden thicknesses are reduced by erosion, it may be possible to capture the major part of the Kap Stewart Group succession. Examples are shown in Fig. 11.2 of what recoveries might be expected for a 1000 m corehole. Sites targeting the KSG would also provide a test of the sealing units and secondary reservoirs (NKG, Pelion Fm). Attempts at drilling to the level of the Triassic rift phase, e.g. Pingo Dal Fm, would need to focus on localities were the KSG is wholly or partly truncated, e.g. eastward of the Hurry Inlet escarpment. A 1000 m stratigraphic corehole within the northeastern sector would likely reach the KSG above Top FFF (Fig. 4.6). Obviously the selection of targets and location will depend on the capacities of the drilling platform

In order to correlate corehole information with the seismic stratigraphy, drilling should be attempted along or close to one of the ARCO seismic profiles. On the other hand, to reach the Triassic targets may require that drilling is carried out in a position offset from the seismic lines. The problem facing such a strategy is the unknown continuation of strata and possible drilling hazards - notably the presence of sills away from outcrop localities. To address this issue one possibility is to carry out a SkyTEM survey across the selected sites prior to drilling. Generation of TEM profiles, as it was carried out in preparation for the Avannaa drilling operation (Fig. 4.8), would reduce the risk of drilling into large sill systems, and could provide a gross signature of strata continuation away from the seismic profiles. The SkyTEM survey could be designed to cover part of an ARCO profile or to link two seismic lines across a valley system.

To summarize, we recommend that stratigraphic coring is carried out in central-east Jameson Land, with objective to test the strata and prospectivity associated with the Jurassic lake-marine transgressional sequence of the Kap Stewart Group/Neill Klinter Group/Pelion Fm. In addition, we suggests that at least one site is selected in the northeastern part of licence area, which could provide information on pre-Jurassic source rocks, in support of the Triassic rift play. Depending on the scale of the operation it is suggested that a limited geophysical survey, e.g. TEM based, is carried out prior to drilling, This is not a requirement for coring the key KSG target based on ARCO seismic lines but it would reduce the risk of drilling hazards and facilitate drilling offset to the seismic lines.

The valley system of Katedralen/Ugleelv is located in a range of 15-20 km from the air landing strip at Constable Pynt, which reduces operational and logistical costs.

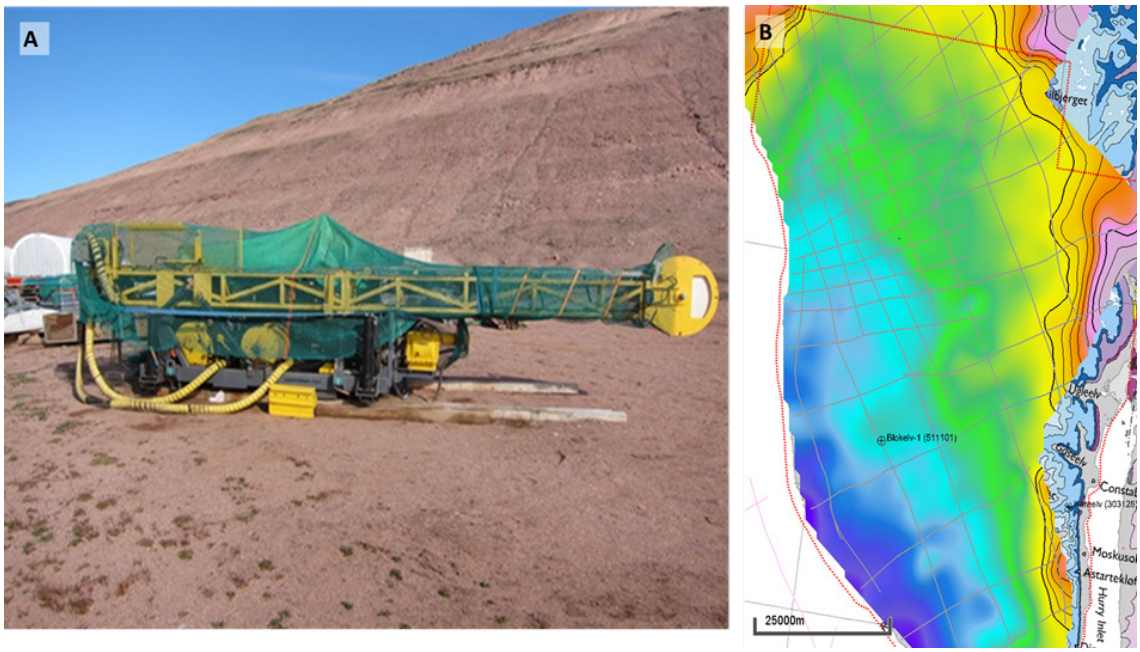

Figure 11.1. (**A**) Rig with drilling potential down to 1000 m, currently placed in north-east Jameson Land (MT Højgaard). (**B**). Depth-structure of the KSG with contours highlighting the eastern fringe (depth contours of top KSG down to 350 m below MSL) where it is likely that the upper part of Kap Stewart Group can be recovered by a 600-1000 m core hole.

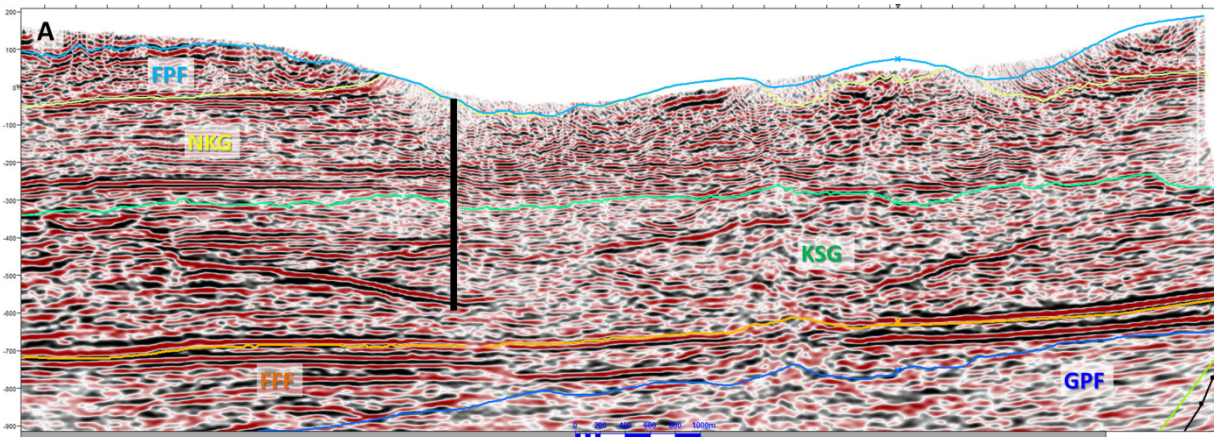

Figure 11.2. Seismic lines 88-13d (**A**) and 88-2d (**B**) shown with possible borehole locations. The indicated seismic penetrations are based on a 1000 m drilling depth and V_p of 3700 m/s. HEF = Hareelv Fm, FPF = Fossilbjerget/Pelion Fm, NKG = Neill Klinter Group, KSG = Kap Stewart Group, FFF = Fleming Fjord Fm, GPF = Gipsdalen/Pingo Dal Fm.

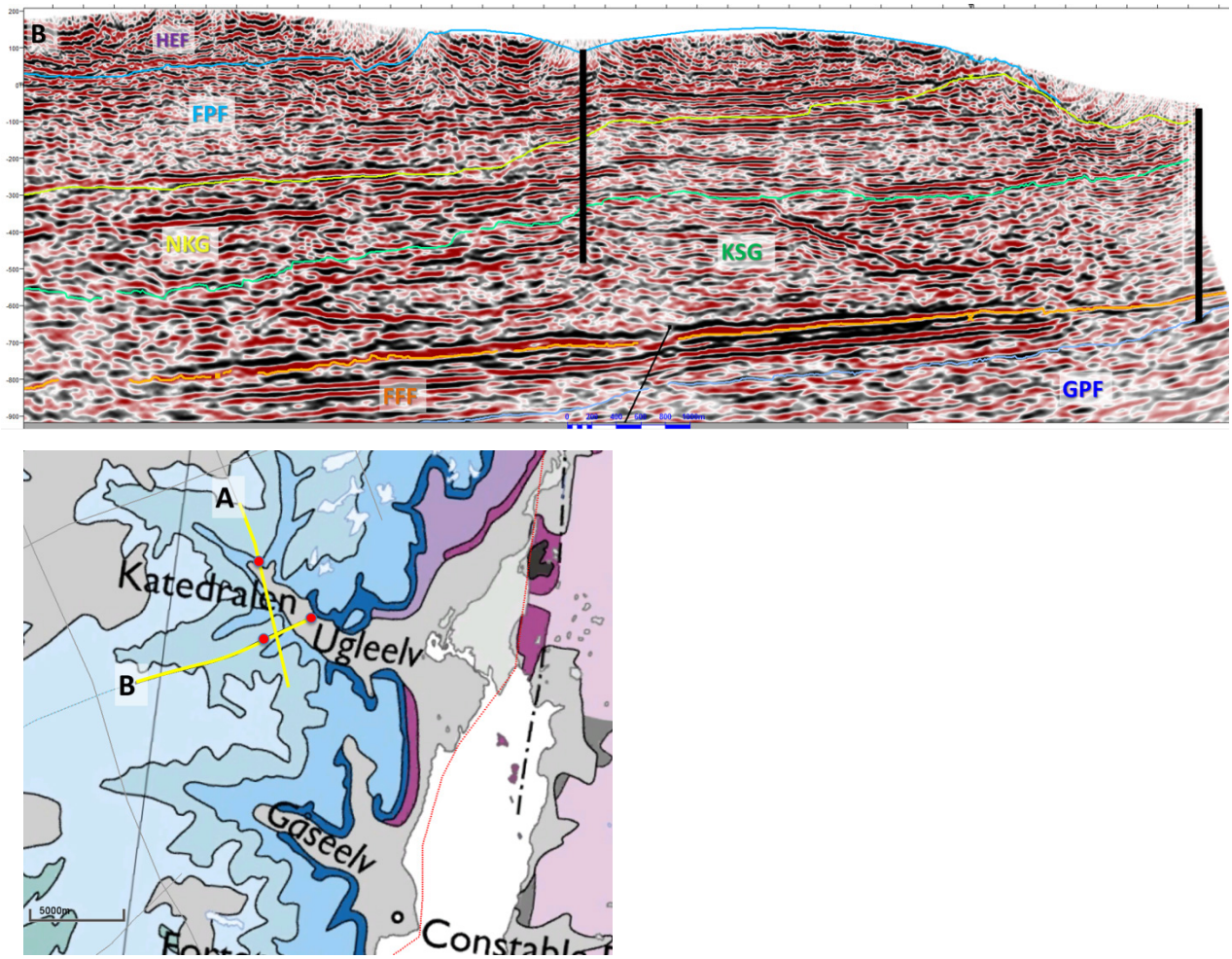

Figure 11.2. (continued from previous page).

11.2 Further work: In-house studies and fieldwork 2017

It is recommended that in-house studies are carried out that can support and constrain the key play concepts prior to drilling. With this goal in mind we suggest the following studies:

- Reprocessing and interpretation performed on selected seismic lines crossing the play types located in eastern part of the Jameson Land Basin. This will be valuable for constraining the seismic geometries, facies development, presence of DHI's and drilling hazards and establishing the seismic well-tie once drilling has ensued. Lines that are considered of particularly interest for further work are 88-13D, 87-1D (both plays); 86-10V, 89-38D (Triassic play); and 88-4D/4V, 88 2D/2V (Jurassic play).

- Sedimentological description and sampling on selected sections of the Avannaa cores to elucidate reservoir and source rock potential, e.g. Graaklint Member, of the Triassic rift play. The vast majority of the core material is stored in Jameson Land and will have to be transported to GEUS for analytical work.

It is essential that a fieldwork operation is carried out prior to stratigraphic coring. The primary aims are to (a) constrain (a) drilling risks e.g. sills/intrusions and hydrocarbon seeps, (b) placing exact drilling positions, and (c) mitigating challenges related to logistics, water supply and terrain/helicopter access. The fieldwork should include systematic mapping of possible seeps, sedimentary facies and fault structures in vicinity of the potential coring localities. Photo-flying could be applied to gain information on strata and structures over a wider area. The results of the fieldwork campaign will be used as a basis for formulating drilling prognosis and risk assessment reports.

Finally, in connection with a drilling operation in Jameson Land we recommend that an analytical programme be established that can provide the most effective way of maturing the play models to the level of exploration drilling. Cores and core-samples should be analysed aimed at reducing the risk associated with the key play types while also contributing to a better understanding of the JLB petroleum system. This new information will add value to the licence and facilitate the next exploration phase.

12. Final conclusions

New seismic processing and interpretation

1. The new seismic reprocessing has reinvigorated the ARCO data and significantly improved the interpretation potential of the Jameson Land Basin history. This is seen by enhanced recognition of major strata boundaries, e.g. unconformities, boundary faults, depositional geometries/facies and strata-cutting sill intrusions.

2. Seismic facies are recognised on the reprocessed seismic data above the Base Permian horizon, which are likely related to platform carbonate and build-ups. Further basinward onlapping strata is inferred as fine-clastic deposition, possible equivalent to the Ravnefjeld Fm. A more comprehensive identification of these features will require additional reprocessing of seismic lines.

3. The new interpretation differs substantially from the previous study reported in Christiansen et al. (1991). Development of major depocentres (>2 km thicknesses) within the Triassic interval displaying a NE-SW trend, similar to fault escarpments mapped in eastern Jameson Land, is linked to a continental rift phase occurring prior the Jurassic transgression. Active rifting was gradually replaced by more uniform thermal subsidence during the late Triassic (Fleming Fjord Formation).

4. The latest Triassic-early Jurassic Kap Stewart Group show multiple local depocentres of >700 m thickness with topographic reliefs of up to 200 m in the eastern and central-southern parts of the basin. The strata geometries are reminiscent of delta-fan deposits that prograde into the central parts of the basin, mainly from east and southeast. Parallel, semi-continuous seismic facies are commonly observed in between the depocentres and may reflect lacustrine mudstone deposits with possible source rock potential.

5. The Neill Klinter Group infills the central parts of the basin onlapping the Kap Stewart Group. Parallel strata at the base of this unit may indicate mudstone deposition (lacustrine-marine?) in the deepest part of the Jurassic basin, which may have additional source rock potential. The seismic strata patterns indicate that sediments generally filled the basin from east to west.

Basin modelling

1. The new apatite-fission track data and models supports Cenozoic erosion of 2–3 km over most of the area. The erosion rate generally accelerated during the Neogene and Quaternary. The present depth interval of the oil window is strongly influenced by regional post-burial uplift/exhumation (most recently during Miocene), placing it in a shallower position than where it was during maximum burial.

2. The revised basin modelling generally supports a high prospectivity in the Jameson Land Basin, and confirms the hydrocarbon potential of the Lower Jurassic Kap Stewart Group mudstones. Several other potential source rock intervals may have a significant potential for generating liquid hydrocarbons prior to the thermal alterations by volcanism but the present depth position and fluid migration history of these units is critical. The Late Permian Ravnefjeld Fm is post-mature over the central-southern parts of Jameson Land, but along the northern and northeastern basin margins potential source rocks of this interval may be located at prospective depths.

3. The basin modelling study stresses the critical need for more information on key aspects of the petroleum system: (a) original distribution, thickness and quality of source rocks, (b) maturation and fluid migration, (c) carrier and reservoir potential, (d) erosion/exhumation events, especially the Cenozoic uplift history (e) heat flow during and after Paleogene volcanism and (f) time-depth relationship of the strata units. The present study provides a framework for further basin modelling that becomes applicable as new data is collected. A continuous revision of the basin model will provide important constraints on the key play types and facilitate the derisking of the Jameson Land petroleum system.

Play development and further work

1. The new seismic study and basins modelling results advocates clastic systems of the (1) Early Jurassic post-rift and (2) Triassic syn-rift tectonic phases, as play types that should be developed in further exploration of the Jameson Land Basin. Other play types, e.g. Permian carbonate build-ups and deep marine sandstones of the Upper Jurassic, are not ruled out by this study but it is recommended that the above play types are tested first.

2. The Lower Jurassic play primarily focusses on deltaic sandstone bodies of the Kap Stewart Group stratigraphically underlain or interbedded by lacustrine anoxic mudstone units. The play area extends over the central-southern part of Jameson Land, covering about 40 % of the licence blocks, and is favoured by the sedimentological model of isolated low-stand sand-prone deposits. Additional reservoir potential may exist in sandstone intervals of the overlying Jurassic sequence, e.g. Neill Klinter Group. The main risk is related to sealing intervals comprising the KSG lacustrine mudstone and the internal marine mudstone units of the Neill Klinter Group.

3. The Triassic rift play, focussed along the north-northeastern basin margin, is based on migration of hydrocarbons originating from Permian sources updip into structural-stratigraphic traps containing coarse-grained alluvial wedge sediments (e.g. Pingo Dal Formation). Since the Ravnefjeld Fm. is presently overmature in the deep central and southern basins the play type requires that hydrocarbons migrated to shallow levels as maximum burial commenced. This likely occurred during the early Cenozoic, although it is possible it may have occurred earlier, e.g. late Cretaceous. Main seal is generated by mudstone units of Fleming Fjord Fm. Secondary reservoirs may be related to compartmentalized sands of the lower-middle Jurassic succession.

4. It is recommended that further work is carried out with focus on stratigraphic coring that can contribute to the development of the key play types and further derisking of the petroleum system. Possible drilling scenarios targeting the Lower – Middle Jurassic (Kap Stewart Group, Neill Klinter Group) in eastern Jameson Land are outlined.

5. The need for pre-drilling fieldwork, in order to reduce drilling risks and identify exact sites, is highlighted and in-house studies that can assists in the planning procedures are proposed. In particular these studies include further reprocessing of seismic data and reservoir analyses performed on existing Triassic cores. Finally, we recommend that once drilling has commenced the cores are subjected to an analytical programme aimed at constraining uncertainties identified in this study and maturing the play models to the level of exploration drilling

References

Andrews, S.D., Kelly, S.R.A., Braham, W. & Kaye, M., 2014: Climatic and eustatic controls on the development of a Late Triassic source rock in the Jameson Land Basin, East Greenland. Journal of the Geological Society, London. http://dx.doi.org/10.1144/jgs2013-075.

Birkelund, T., Callomon, J.H. & Fürsich, F.T. 1984: The stratigraphy of the Upper Jurassic and Lower Cretaceous sediments of Milne Land, central East Greenland. Bulletin Grønlands Geologiske Undersøgelse **147**, 56 pp.

Bjerager, M, Seidler, L., Stemmerik, L. & Surlyk, F. 2006: Ammonoid stratigraphy and sedimentary evolution across the Permian–Triassic boundary in East Greenland. Geological Magazine **143**, 635–656.

Bjerager, M., Alsen, P., Bojesen-Koefoed, J., Kjøller, C., Larsen L.M., Nytoft, H.P., Olivarius, M., Petersen H.I., Piasecki, S. & Schovsbo, N. 2009: Blokelv Corewell, GGU511101, Upper Jurassic Hareelv Formaton in Jameson Land, East Greenland. Danmarks og Grønlands Geologiske Undersøgelse Rapport 2009/86, Volume 1–3, 223 pp. 8 Appendices.

Bojesen-Koefoed, J.A., Alsen, P., Christiansen, F.G., Nytoft, H.P., Piasecki, S. & Stemmerik, L. 2009: Northeast Greenland Petroleum Systems. Report compiled as a part of the petroleum industry sponsored project: "Petroleum Geological Studies, Services and Data in East and North-East Greenland". GEUS rapport 2009/43, 342pp.

Bonow, J.M., Japsen, P. & Nielsen, T.F.D. 2014: High-level landscapes along the margin of East Greenland – a record of tectonic uplift and incision after breakup in the NE Atlantic. Global and Planetary Change **116**, 10–29.

Brooks, C.K. 2011: The East Greenland rifted volcanic margin. Geological Survey of Denmark and Greenland Bulletin Geological Survey of Denmark and Greenland Bulletin **2011/24**, 96 pp.

Bugge, T., Ringås, J. E., Leith, D. A., Mangerud, G., Weiss, H. M. & Leith, T. L., 2002: Upper Permian as a new play model on the mis-Norwegian continental shelf: Investigated by shallow stratigraphic drilling. AAPG Bulletin **86**, 107-127.

Cavanagh, A.J., di Primo, R., Scheck-Wenderoth, M., Horsfield, B., 2006: Severity and timing of Cenozoic exhumation in the southwestern Barents Sea. Journal of the Geological Society **163**, 761–774.

Christiansen, F. G., Dam, G., Piasecki, S. & Stemmerik, L. 1992: A review of Upper Palaeozoic and Mesozoic source rocks from onshore East Greenland. In: Generation, accumulation and production of Europe`s hydrocarbons II, Spencer, A. M. (ed.), Special Publication of the European Associaton Petroleum Geologists **2**, 151-161.

Christiansen, F. G., Piasecki, S. & Stemmerik, L. 1990: Thermal maturation history of the Upper Permian succession in the Wegener Halvø area, East Greenland. Rapp. Grønlands geol. Unders. **148**, 109-114.

Christiansen, F.G., Marcussen, C., Larsen, H.C. & Stemmerik, L. 1991: Petroleum potential of Jameson Land, East Greenland. Exploration report. Grønlands Geologiske Undersøgelse. 61 pp.

Christiansen, F.G., Piasecki, S., Stemmerik, L. & Telnæs, N. 1993: Depositional environment and organic geochemistry of the Upper Permian Ravnefjeld Formation source rock in East Greenland. American Association of Petroleum Geologists Bulletin **77**, 1519-1537.

Clemmensen, L.B. 1980a. Triassic rift sedimentation and palaeogeography of central East Greenland. Grønlands Geologiske Undersøgelse, Bulletin, **136**,1–72.

Clemmensen, L.B. 1980b. Triassic lithostratigraphy of East Greenland between Scoresby Sund and Kejser Franz Josephs Fjord. Grønlands Geologiske Undersøgelse, Bulletin, **139**, 1–56.

Clemmensen, L.B., Kent, D.V. & Jenkins, F.A.J. 1998. A Late Triassic lakesystem in East Greenland: Facies, depositional cycles and palaeoclimate. Palaeogeography, Palaeoclimatology, Palaeoecology, **140**, 135–159.

Dam, G. & Christiansen, F. G., 1990. Organic geochemistry and source potential of the lacustrine shales of the Upper Triassic – Lower Jurassic Kap Stewart Formation, East Greenland. Marine and Petroleum Geology **7**, 428-443.

Dam, G. & Surlyk, F. 1992: Forced regressions in a large wave and storm-dominated lake, Rhaetian–Sinemurian Kap Stewart Formation, East Greenland. Geology **20**, 749-752.

Dam, G. & Surlyk, F. 1993: Cyclic sedimentation in a large wave and storm-dominatedanoxic lake: Kap Stewart Formation (Rhaetian–Sinemurian), Jameson Land, East Greenland. In: Posamentier, H. W., Summerhayes, C. P., Haq, B. U. & Allen, G. P. (eds.): Sequence Stratigraphy and Facies Associations, IAS Spec. Publ. **18**, 419-448.

Dam, G. & Surlyk, F. 1998: Stratigraphy of the Neill Klinter Group; a lower – lower Middle Jurassic tidal embayment succession, Jameson Land, East Greenland. Geology of Greenland Survey Bulletin **175**, 80 pp.

Dam, G., Surlyk, F., Mathiesen, A. & Christiansen, F. G. 1995: Exploration significance of lacustrine forced regressions of the Rhaetian-Sinemurian Kap Stewart Formation, Jameson Land, East Greenland. In: Steel, R.J. et al. (eds): Sequence stratigraphy: Advances and Application for Exploration and Producing in North West Europe. Norwegian Petroleum Society, Elsevier, Amsterdam, 509-525.

Doré, A.G., Lundin, E.R., Birkeland, Eliassen, P.E. & Jensen, L.N. 1997: The NE Atlantic Margin: implications of late Mesozoic and Cenozoic events for hydrocarbon prospectivity. Petroleum Geoscience **3**, 117-131.

Edwards, J., Heller, S., Clancy, N., Whitfield, & O'Connor, S. 2013: Pressure Prediction in Exhumed Basins, GeoExpro **10**, No. 6.

Engkilde, M. & Surlyk, F. 2003: Shallow marine syn-rift sedimentation: Middle Jurassic Pelion Formation, Jameson Land, East Greenland. In: Ineson, J.R. & Surlyk, F. (eds): The Jurassic of Denmark and Greenland. Geological Survey of Denmark and Greenland Bulletin **1**, 813-863.

Green, P.F., Lidmar-Bergström, K., Japsen, P., Bonow, J.M. & Chalmers, J.A. 2013: Stratigraphic landscape analysis, thermochronology and the episodic development of elevated passive continental margins. Geological Survey of Denmark and Greenland Bulletin **2013/30**, 150 pp.

Hald, N., Tegner, C. 2000: Composition and age of tertiary sills and dykes, Jameson Land Basin, East Greenland: relation to regional flood volcanism. Lithos **54**, 207–233.

Hamann, N.E., Whittaker, R.C. & Stemmerik, L. 2005: Geological development of the Northeast Greenland Shelf. Geological Society, London, Petroleum Geology Conference, **6**, 887-902.

Holmes, P., Thomassen, B. & Stelter, S. 2014: Technical Report on Mineral Exploration 2014, Jameson Land and Liverpool Land, Central East Greenland - work carried out under exploration licence 2012/01. Avannaa Exploration Limited.

Ineson, J.R. & Surlyk, F. 2003: The Jurassic of Denmark and Greenland.

Japsen, P., Bonow, J.M., Green, P.F. & Guarnieri, P. 2012: Burial, uplift and exhumation history of North-East Greenland (70 to 78N) based on AFTA and VR data, the geological record and analysis of structures and landforms. 2nd edition. GEUS report 2012/87, 250 pp.

Japsen, P., Green, P.F., Bonow, J.M., Nielsen, T.F.D., & Chalmers, J.A. 2014: From volcanic plains to glaciated peaks: Burial and exhumation history of southern East Greenland after opening of the NE Atlantic. Global and Planetary Change **116**, 91–114.

Krabbe, H. 1996: Biomarker distribution in the lacustrine shales of the Upper Triassic –Lower Jurassic Kap Stewart Formation, Jameson Land, Greenland. Marine and Petroleum Geology **13**, 741-754.

Kreiner-Møller, M. & Dam, G., Surlyk, F., Mathiesen, A. & Christiansen, F. G. 1995: Exploration significance of lacustrine forced regressions of the Rhaetian–Sinemurian Kap Stewart Formation, Jameson Land, East Greenland. In: Steel, R. J. et al. (eds.): Sequence Stratigraphy on the Northwest European Margin. NPF Spec. Publ. 5. Elsevier, Amsterdam, 511-527.

Kreiner-Møller, M. & Stemmerik, L. 2001: Upper Permian lowstand fansof the Bredehorn Member, Schuchert Dal formation, East Greenland. In: Martinsen, O.J. & Dreyer, T.: Sedimentary Environments Offshore Norway – Palaeozoic to Recent. NPF Special Publication **10**, 51–65.

Larsen, H.C. & Marcussen, C. 1992: Sill-intrusion, flood basalt emplacement and deep crustal structure of the Scoresby Sund region, East Greenland. In: Storey, B.C., Alabaster, T. & Pankhurst, R.J. (eds): Magmatism and the Causes of Continental Break-up. Geological Society Special Publication **68**, 365-386.

Larsen, H.C. & Saunders, A.D. 1998: 41. Tectonism and volcanism at the southeast Greenland rifted margin: a record of plume impact and later continental rupture. In: Saunders, A.D., Larsen, H.C. & Wise, S.W., Jr. (Eds.): Proceedings of the Ocean Drilling Program, Scientific Results, 503–533.

Larsen, H.C., Saunders, A.D., Clift, P.D., et al. 1994: 13. Summary and principal results, Proceedings of the Ocean Drilling Program, Initial Reports. Ocean Drilling Program, College Station, TX, 279–292.

Larsen, M. & Surlyk, F. 2003: Shelf-edge delta and slope deposition in the Upper Callovian – Middle Oxfordian Olympen Formation, East Greenland. In: Ineson, J.R. & Surlyk, F. (eds.): The Jurassic of Denmark and Greenland. Geological Survey of Denmark and Greenland Bulletin **1,** 931–948.

Larsen, P-H., Olsen, H. & Clack, J.A. 2008: The Devonian basin in East Greenland—Review of basin evolution and vertebrate assemblages. GSA Memoirs, **202**, 273-292.

Lien, T. 2005: From rifting to drifting: effects on the development of deep-water hydrocarbon reservoirs in a passive margin setting, Norwegian Sea. Norwegian Journal of Geology / Norsk Geologisk Forening. Norsk Geologisk Forening **85**, 319-332.

Magoon, L.B., Dow, W.G., (Eds.) 1994: The petroleum system – From source to trap. AAPG Memoir, **60**, 655 pp.

Mathiesen, A., Christiansen, F.G., Bidstrup, T., Marcussen, C., Dam, G., Piasecki, S., Stemmerik, L. (1995): Modelling of hydrocarbon generation in the Jameson Land Basin, East Greenland. First Break **13**, 8, 329-341.

Mathiesen, A., Bidstrup, T. & Christiansen, F.G. 2000: Denudation and uplift history of the Jameson Land basin, East Greenland - constrained from maturity and apatite fission data. Global and Planetary Change **24**, 275–301.

Mitchum, R.M., Vail, P.R. & Sangree, J.B. 1977: Seismic stratigraphy and global changes of sealevel, Part 6: Stratigraphic interpretation of seismic reflection in depositional sequences Application of Seismic Reflection Configuration to Stratigrapic Interpretation Memoir, **26**, 117-133

Ohm, S.E.,Karlsen, D.A., Austin, T.J.F., 2008: Geochemically driven exploration models in uplifted areas: examples from the Morwegian Barents Sea. AAPG Buletin, **92**, 1191–1223.

Pepper, A.S., Corvi, P.J., 1995: Simple kinetic models of petroleum formation. Part 1: Oil and gas generation from kerogen. Marine and Petroleum Geology, **12**, 291–319.

Piasecki, S. & Stemmerik, L. 1991: Late Permian anoxia of central East Greenland. In: Modern and ancient shelf anoxia, Tyson, R. V. & Pearson, T. H. (eds.): Geological Society London Special Publication **58**, 275-290.

Piasecki, S., Christiansen, F. G. & Stemmerik, L. 1990: Depositional history of a Late Carboniferous organic-rich shale from East Greenland. Bulletin of Canadian Petroleum Geology **38**, 273-287.

Planke, S., Rasmussen, T., Rey, S.S. & Mycklebust, R. 2005: Seismic characteristics and distribution of volcanic intrusions and hydrothermal vent complexes in the Vøring and Møre basins. In: Doré, A.G. & Vining, B.A. (eds.) Petroleum Geology: North-West Europe and Global Perspectives. Geological Society, London, 833-844.

Ramm, M. & Bjorlykke, K. 1994: Porosity Depth Trends in Reservoir Sandstones - Assessing the Quantitative Effects of Varying Pore-Pressure, Temperature History and Mineralogy, Norwegian Shelf Data. Clay Minerals, **29**, 475-490, doi: DOI 10.1180/claymin.1994.029.4.07.

Scholle, P. A., Stemmerik, L. & Ulmer, D. S. 1991: Diagenetic history and hydrocarbon potential of Upper Permian carbonate buildups, Wegener Halvø area, Jameson Land basin, East Greenland. American Association of Petroleum Geologists Bulletin **75**, 701–725.

Scholle, P.A., Stemmerik, L., Ulmer, D.S., Di Liegro, G. & Henk, F.H. 1993: Paleokarst-influenced depositional and diagenetic patterns in Upper Permian carbonates, Karstryggen area, central East Greenland. Sedimentology **40**, 895–918.

Seidler, L. 2000: Incised submarine canyons governing new evidence of Early Triassic rifting in East Greenland. Palaeogeography, Palaeoclimatology, Palaeoecology **161**, 267–293.

Seidler, L., Steel, R.J., Stemmerik, L. & Surlyk, F. 2004: North Atlantic marine rifting in the Early Triassic: new evidence from East Greenland. Journal of the Geological Society, London **161**, 583–592.

Stemmerik, L. 1991: Reservoir evaluation of Upper Permian buildups in the Jameson Land basin, East Greenland. Rapport Grønlands Geologiske Undersøgelse **149**, 23 pp.

Stemmerik, L. 2001a: Stratigraphy of the Upper Permian Wegener Halvø Formation, Karstryggen area, East Greenland – A low productivity carbonate platform. Sedimentology **48**, 79–97.

Stemmerik, L. 2001b: Upper Permian lowstand fans of the Bredehorn Member, Schuchert Dal Formation, East Greenland. In: Martinsen, O.J. & Dreyer, T. (eds) Sedimentary Environments Offshore Norway - Palaeozoic to Recent. NPF Special Publication **10**, 51–65.

Stemmerik, L., Clausen, O.R., Korstgård, J., Larsen, M., Piasecki, S., Seidler, L., Surlyk, F. & Therkelsen, J. 1997: Petroleum geological investigations in East Greenland: project 'Resources of the sedimentary basins of North and East Greenland'. Geology of Greenland Survey Bulletin **176**, 29–38.

Stemmerik, L., Dam, G., Noe-Nygaard, N., Piasecki S., & Surlyk F. 1998: Sequence stratigraphy of source and reservoir rocks in the Upper Permian and Jurassic of Jameson Land, East Greenland. Geology of Greenland Survey Bulletin **180**, 43–54.

Stemmerik, L., Jensen, S. M. & Pedersen, M. 1997: Hydrocarbon-associated mineralisation of Upper Permian carbonate buildups, Wegener Halvø Formation, East Greenland. In J. P. Hendry, P. F. Carey, J. Parnell, A. H. Ruffell & R. H. Worden (eds) Contributions to the second International Conference on Fluid evolution, migration and interaction in Sedimentary Basins and Orogenic Belts. The Queens' University of Belfast, 485–487.

Stemmerik, L. & Piasecki, S. 1990: Post-Caledonian sediments in North-East Greenland between 76° and 78°30'N. Rapport Grønlands Geologiske Undersøgelse **148** , 123-126.

Stoker, M.S. & Ziska, H. 2011: Cretaceous. In: Ritchie, J.D., Ziska, H., Johnson, H. & Evans, D. (eds): Geology of the Faroe-Shetland Basin and adjacent areas, 123-150. British Geological Survey, Nottingham, UK. Jardfeingi, Tórshavn, Faroe Islands.

Surlyk, F. & Noe-Nygaard, N. 1991. Sand bank and dune facies architecture of a wide intracratonic seaway: Late Jurassic – Early Cretaceous Raukelv Formation, Jameson Land, East Greenland. In: *The three-dimensional facies architecture of terrigenous clastic sediments and its implication for hydrocarbon discovery and recovery.* Miall, A.D. and Tyler, N. (eds.). SEPM (Society for Sedimentary Geology). Concepts in Sedimentology and Paleontology **3**, 261–276.

Surlyk, F. & Noe-Nygaard, N. 2001: Cretaceous faulting and associated coarse-grained marine gravity flow sedimentation, Traill Ø, East Greenland. In: Martinsen,O.J. & Dreyer,T. (ed.) Sedimentary environments offshore Norway - Palaeozoic to Recent. NPF Special Publication **10**, 293-319.

Surlyk, F. 2003: The Jurassic of East Greenland: a sedimentary record of thermal subsidence, onset and culmination of rifting. In: Ineson, J.R. & Surlyk, F. (eds): The Jurassic of Denmark and Greenland. Geological Survey of Denmark and Greenland Bulletin **1**, 659–722.

Surlyk, F., Gjelberg, J. & Noe-Nygaard, N. 2007. The Upper Jurassic Hareelv Formation of East Greenland: A giant sedimentary injection complex. In: Hurst, A. and Cartwright, J. (eds.): *Sand injectites: implications for hydrocarbon exploration and production.* AAPG Memoir 87: 141–149.

Surlyk, F., Hurst, J. M., Piasecki, S., Rolle, F., Scholle, P. A., Stemmerik, L. & Thomsen, E. 1986: The Permian the western margin of the Greenland Sea – a future exploration target. In: Halbouty, M.T. (ed.) Future Petroleum Provinces of the World. American Association of Petroleum Geologists Memoir **40**, 629–659.

Sweeney, R.E. & Burnham, A.K. 1990: Evaluation of a simple model of vitrinite reflectance based on chemical kinetics, AAPG Bulletin, **74**, 1559–1570.

Upton, B.G.J., Rex, D.C., & Thirwall, M.F. 1995: Early magmatism in NE Greenland. Journal of the Geological Society of London, **152**, 959-964.

Vigran, J.O., Stemmerik, L. & Piasecki, S. 1999: Stratigraphy and depositional evolution of the uppermost Devonian - Carboniferous (Tournaisian-Westphalian) non-marine deposits in North-East Greenland. Palynology **23**, 115–152.

Whitham, A.G., Price, S.P., Koraini, A.M. & Kelly, S.R.A. 1999: Cretaceous (post-Valanginian) sedimentation and rift events in NE Greenland (71–77°N). Geological Society, London, Petroleum Geology Conference series, **5**, 325-336.

Wygrala, B.P. 1989: Integrated study of an oil field in the southern Po basin, northern Italy: Ph.D. dissertation, Köln University: Jülich, Research Centre Jülich, Jul-Rep. 2313, ISSN 0366-0885, 217p.

APPENDICES

A1: Depth converted seismic maps (m below MSL)

A2: Thickness maps (m)

A1.1 Base Permian_depth

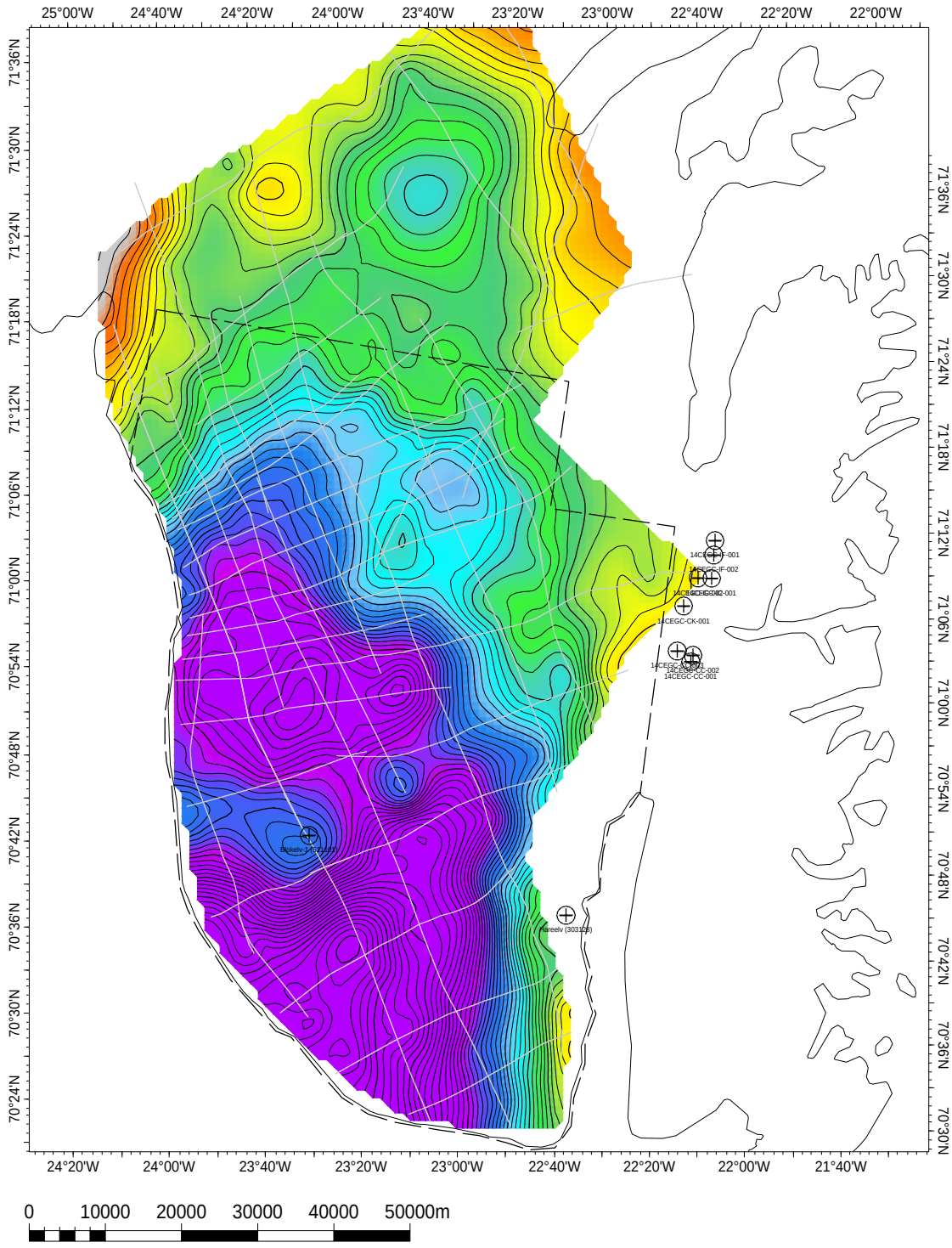

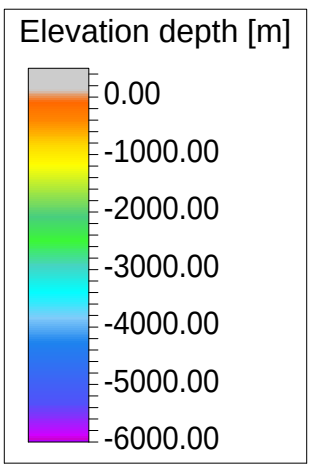

A1.2 Early Triassic_depth

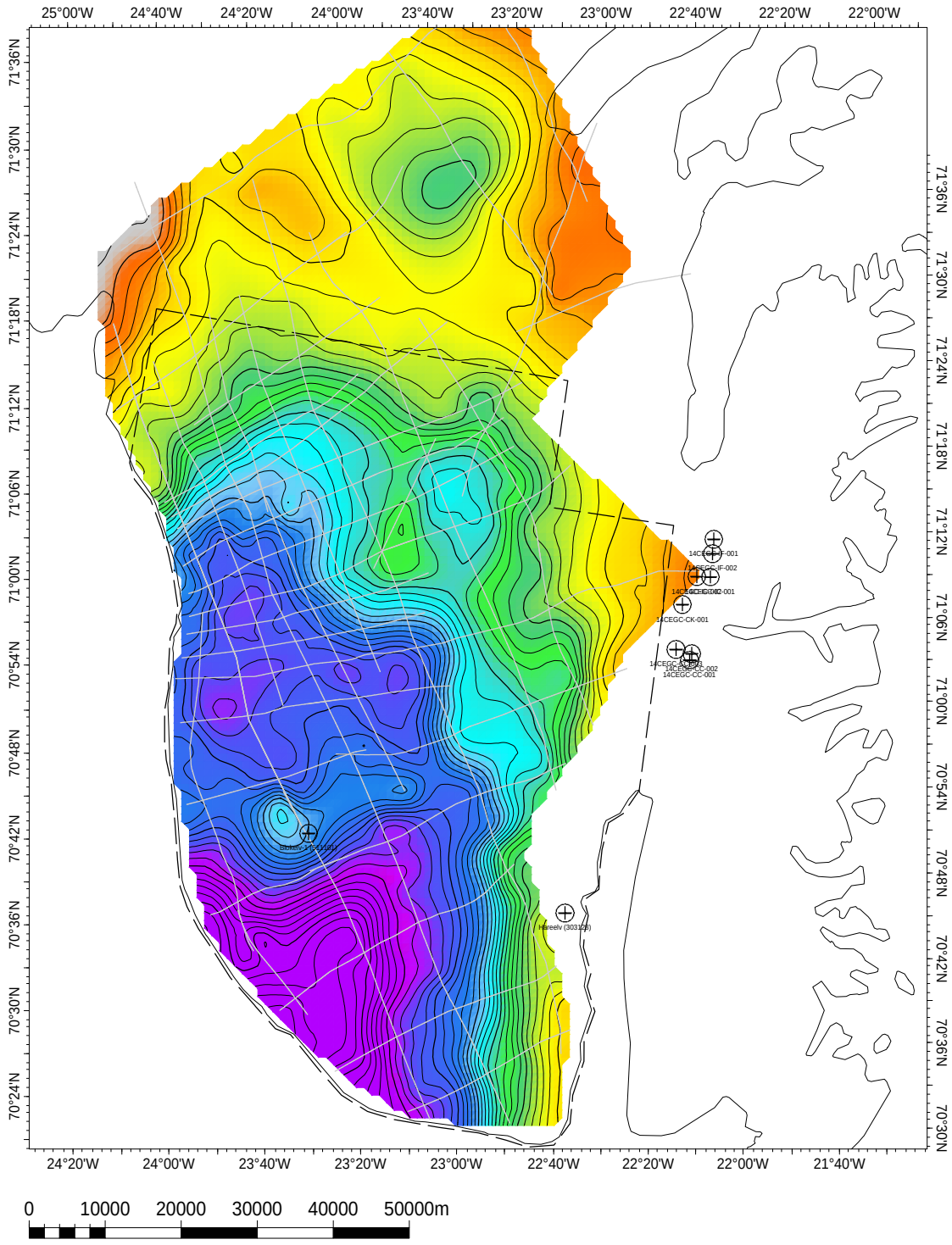

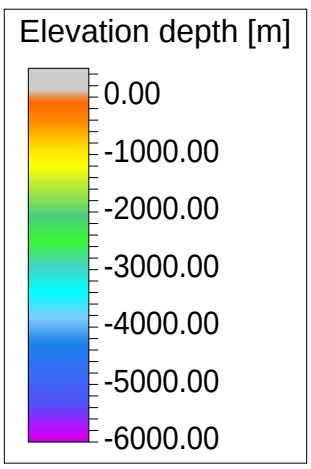

A1.3 Top GipsdalenFm_depth

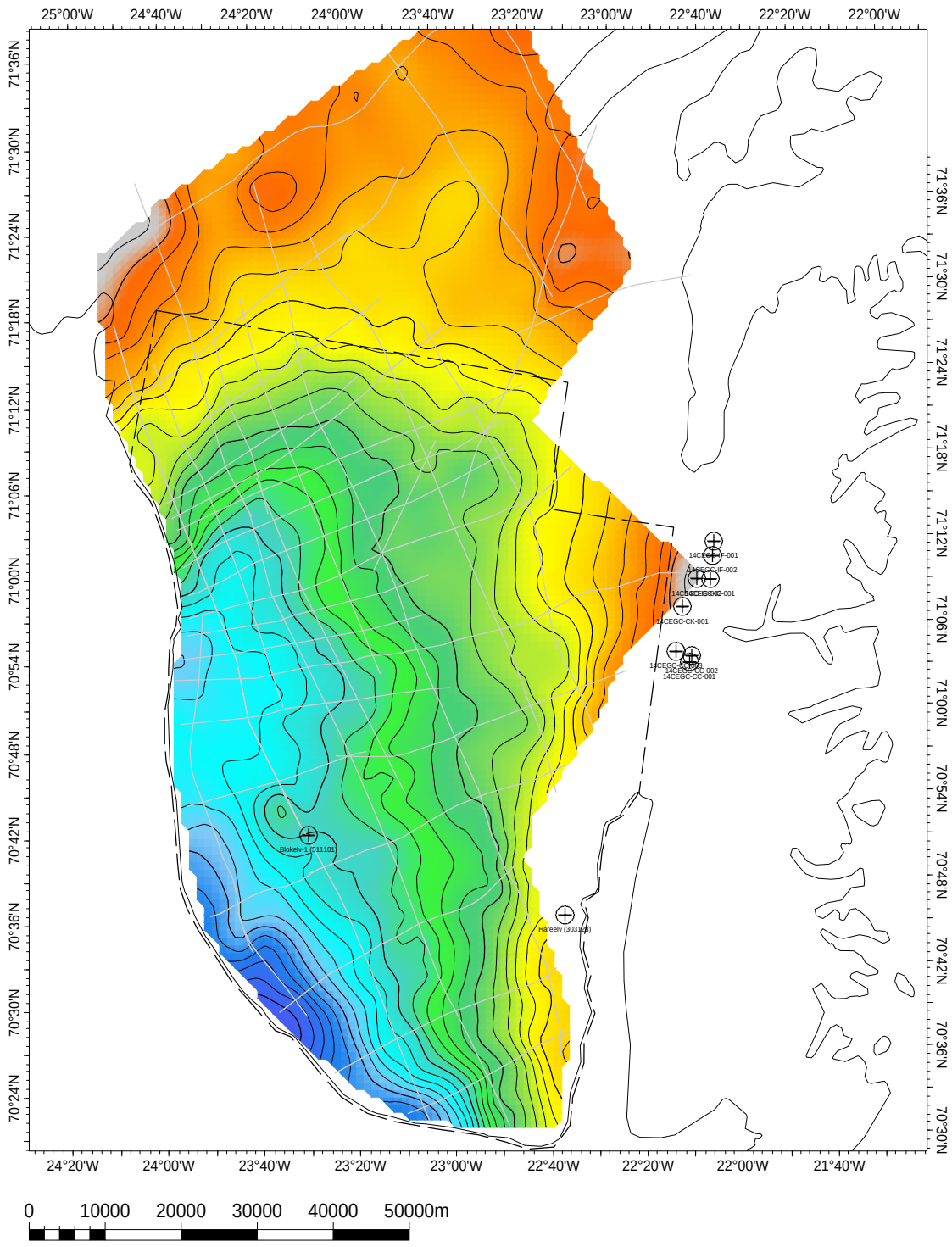

Elevation depth [m]

- 0.00
- -1000.00
- -2000.00
- -3000.00
- -4000.00
- -5000.00
- -6000.00

A1.4 Top FlemmingFjFm_depth

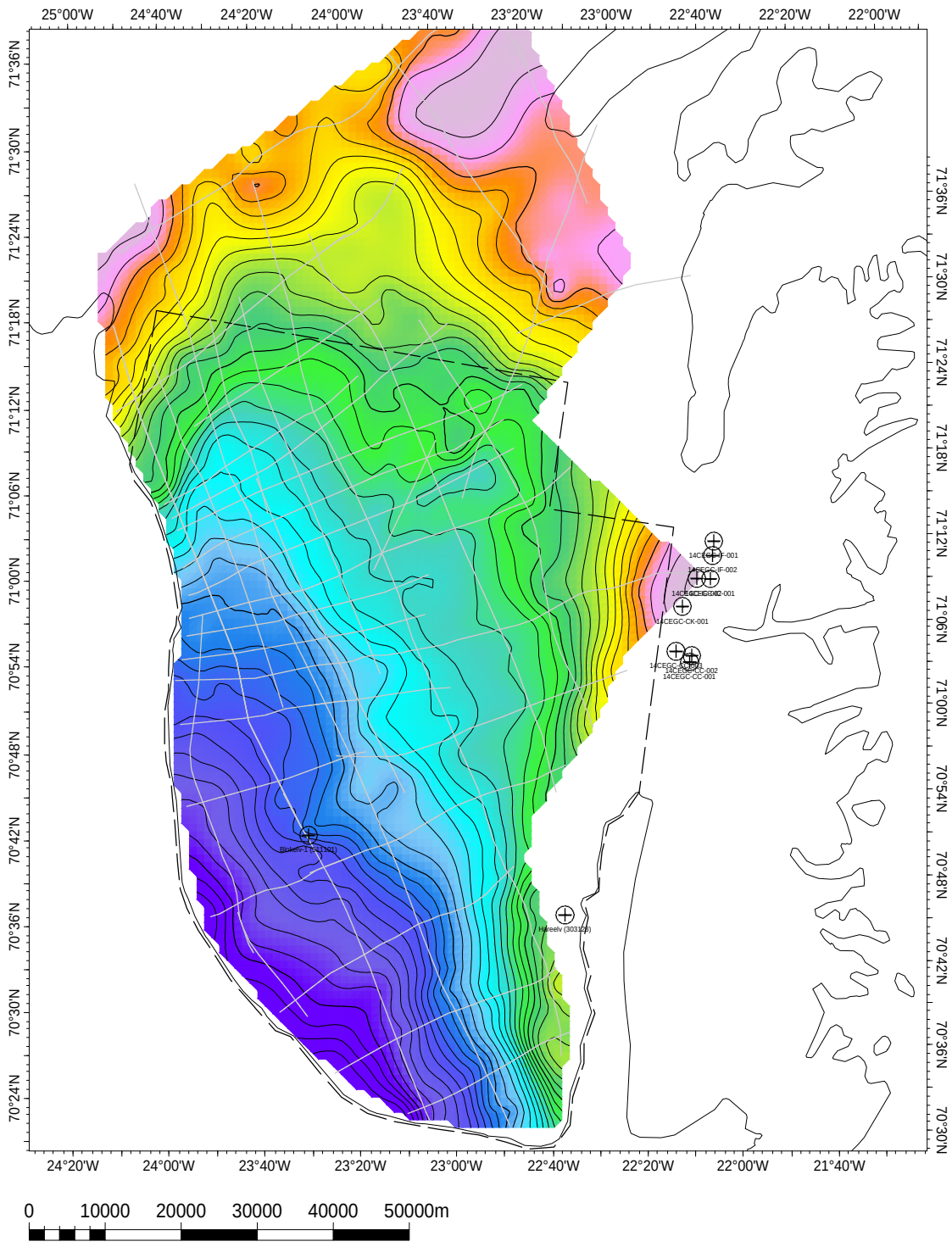

A1.5 Top KapStewartGr_depth

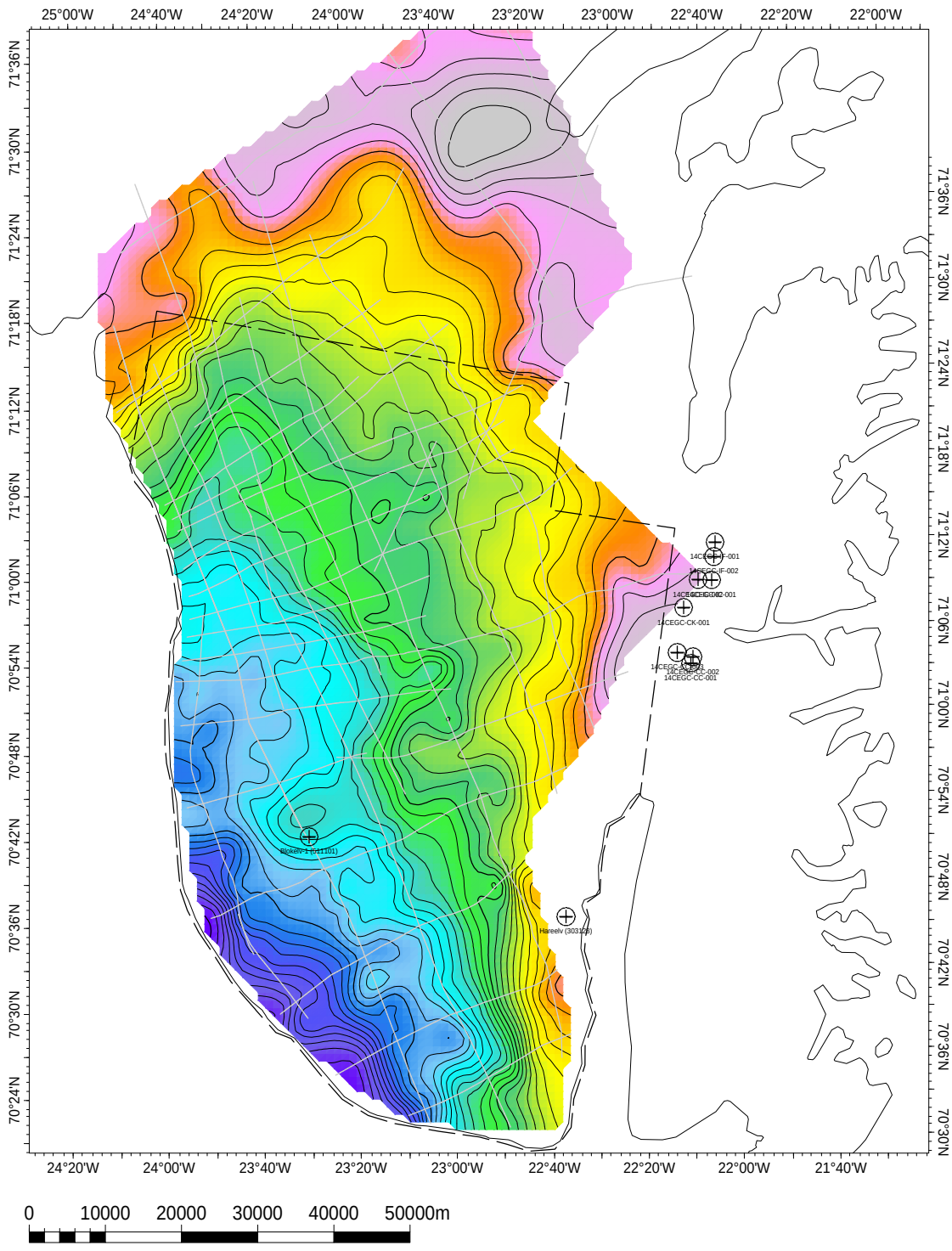

Elevation depth [m]

500.00
0.00
-500.00
-1000.00
-1500.00
-2000.00
-2500.00
-3000.00

A1.6 Top NeillKlinterGr_depth

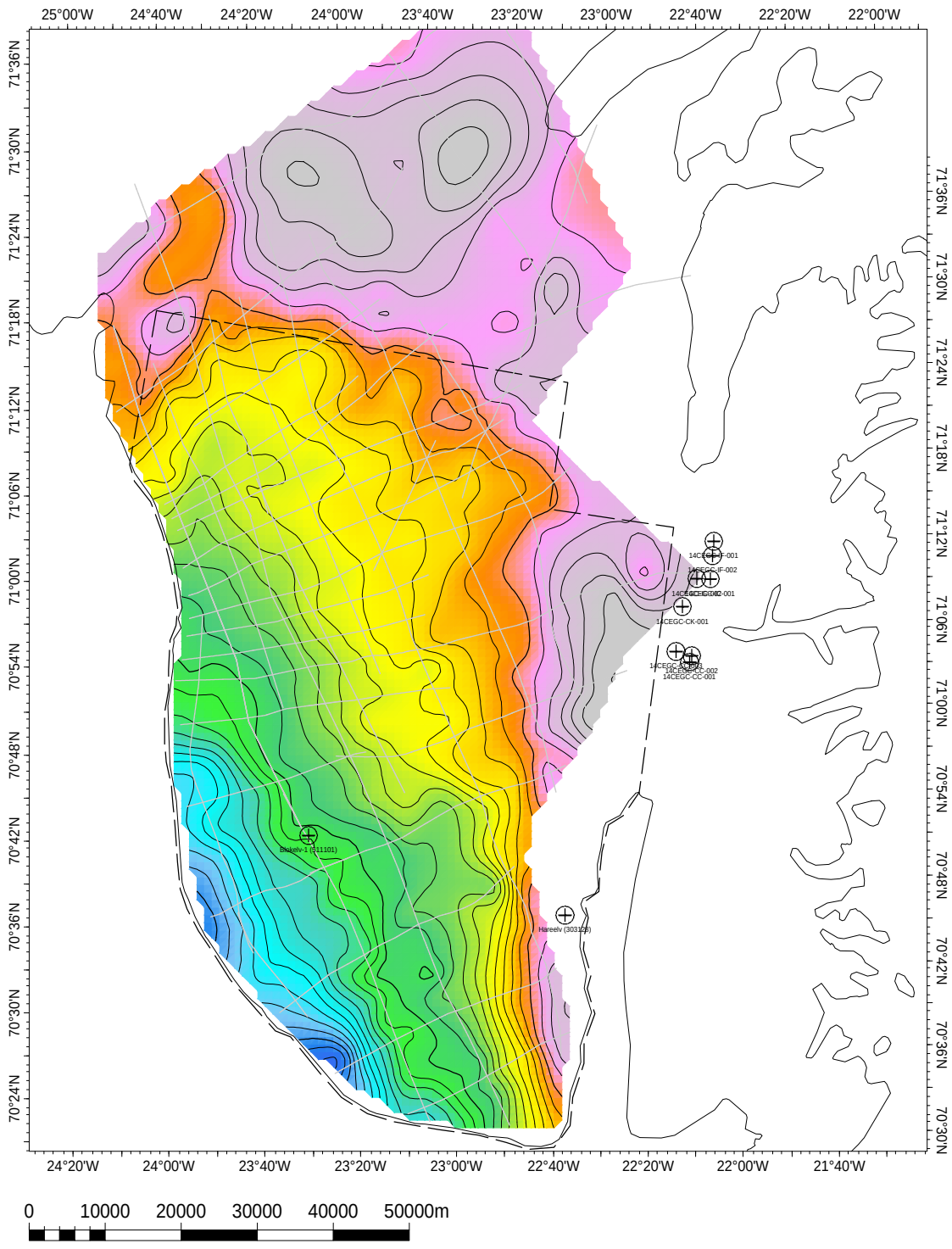

Elevation depth [m]

0.00
-500.00
-1000.00
-1500.00
-2000.00
-2500.00
-3000.00

A1.7 Top Fossilbjerg-PelionFm_depth

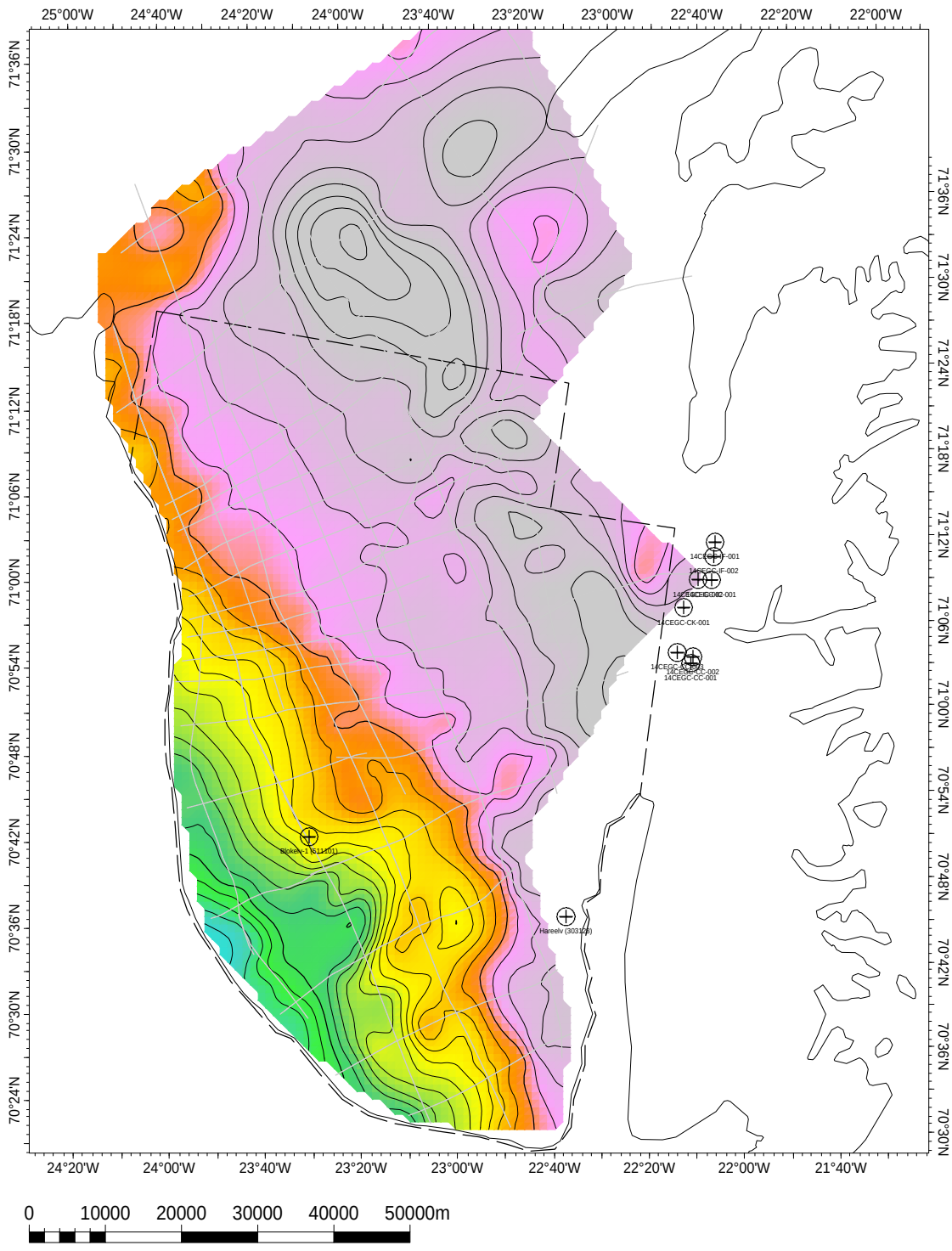

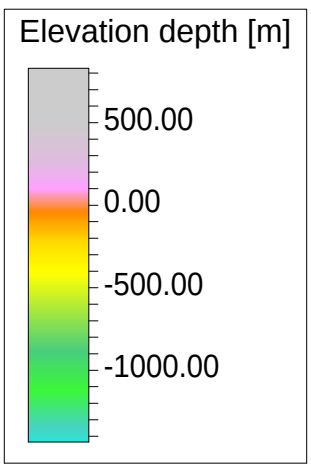

A2.1 Early Triassic - Base Permian horizon

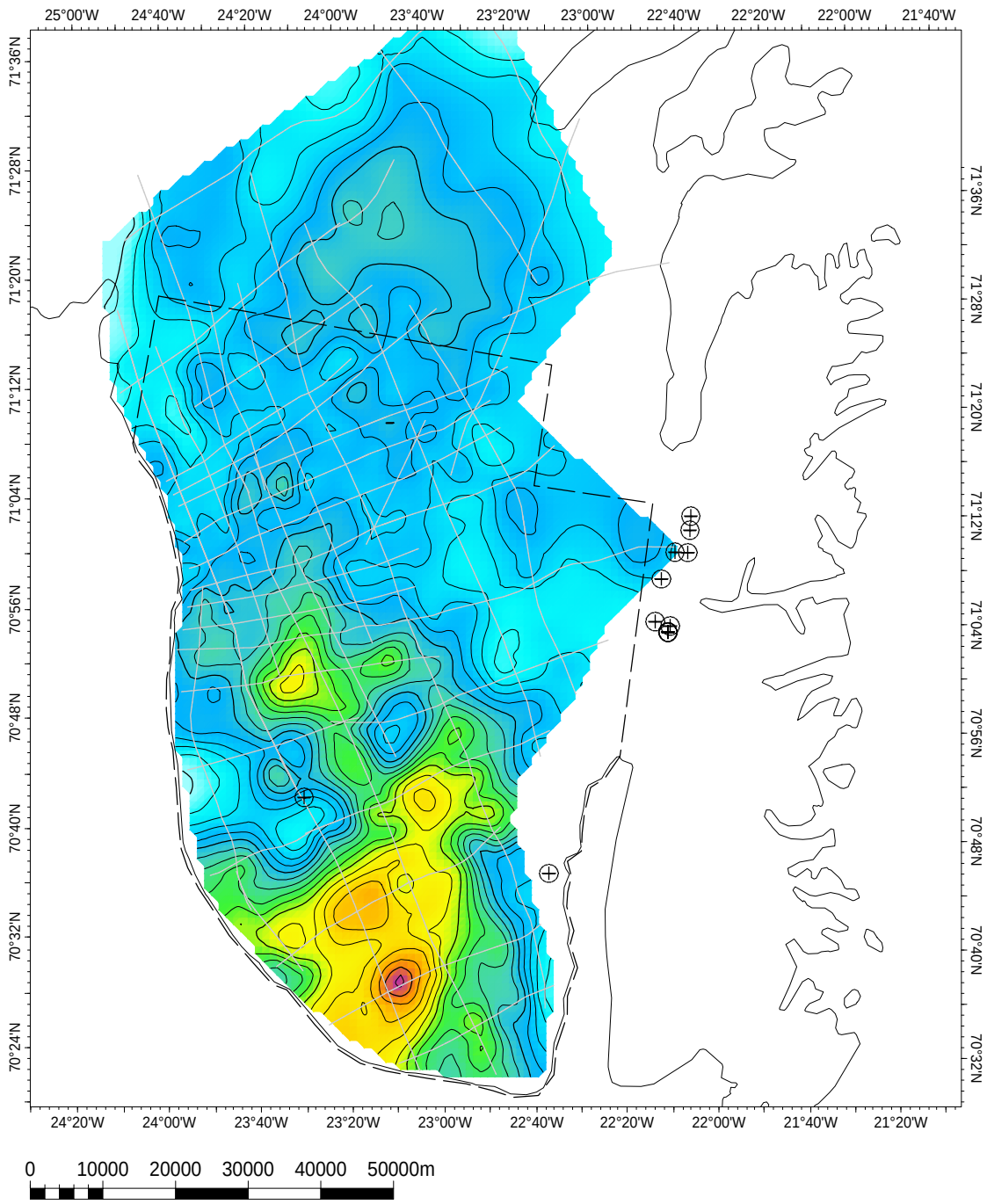

A2.2 Top GipsdalenFm - Early Triassic horizon

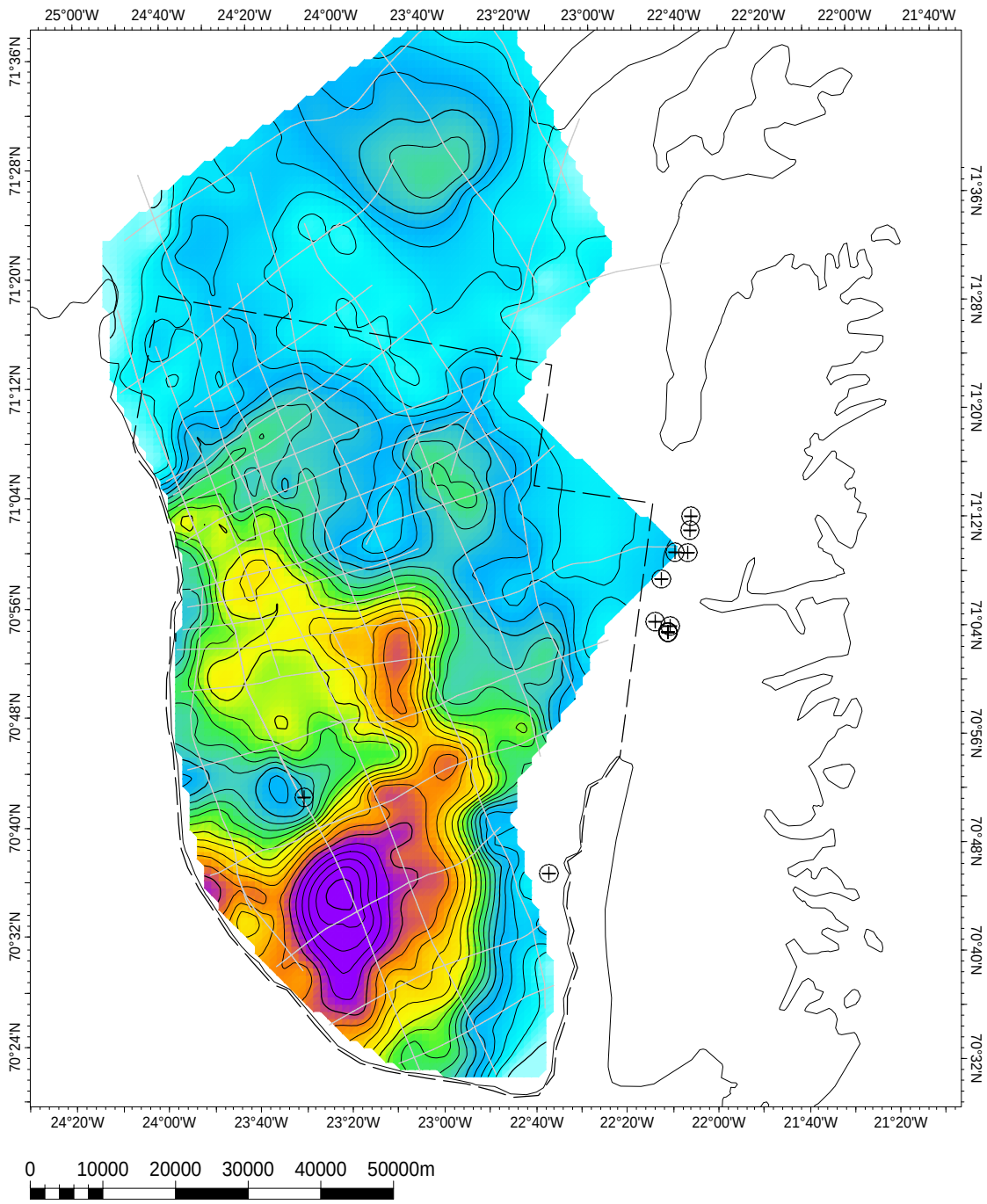

A2.3 Top FlemingFjordFm - Top GipsdalenFm

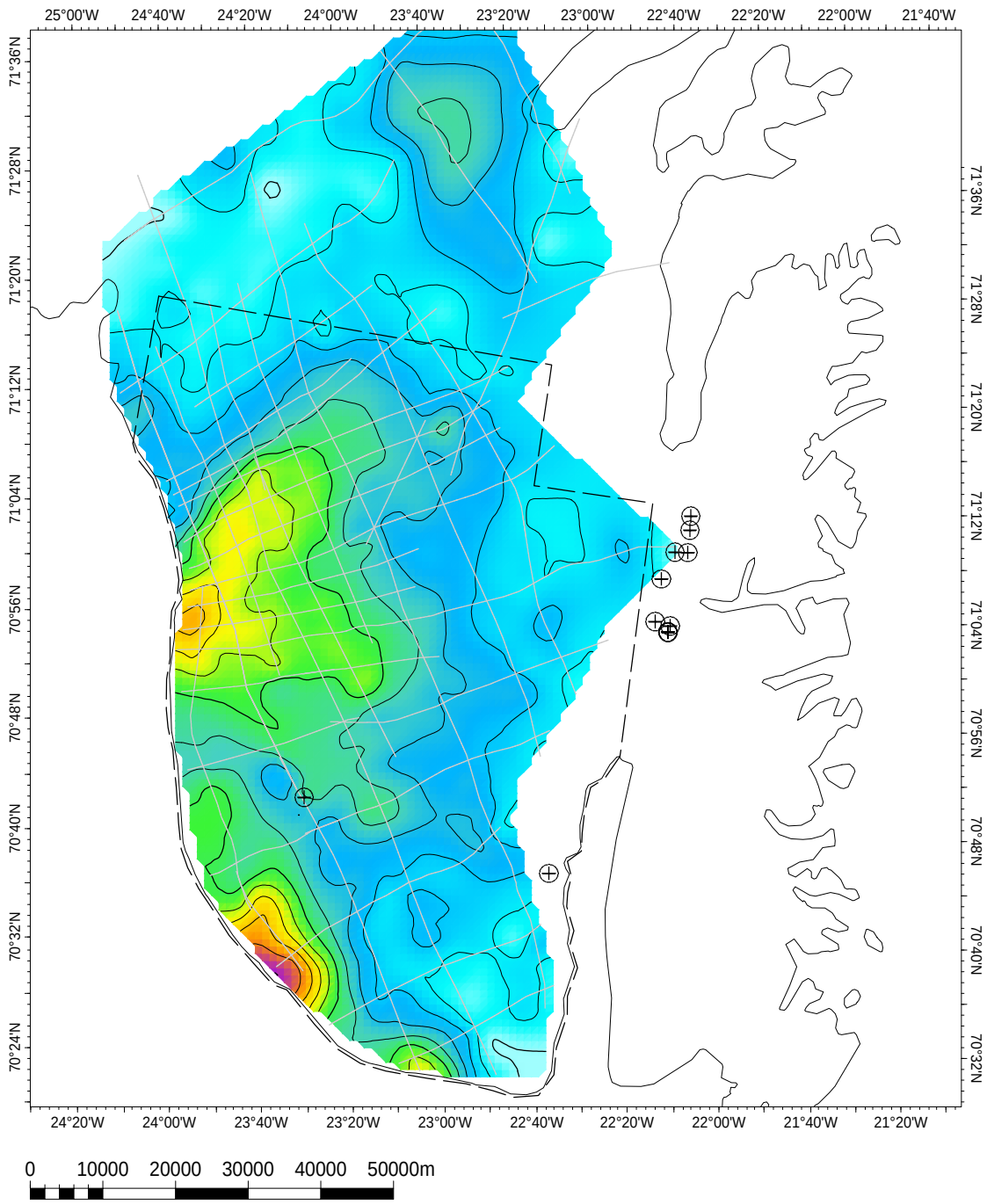

A2.4 Top KapStewartGr - Top FlemingFjordFm

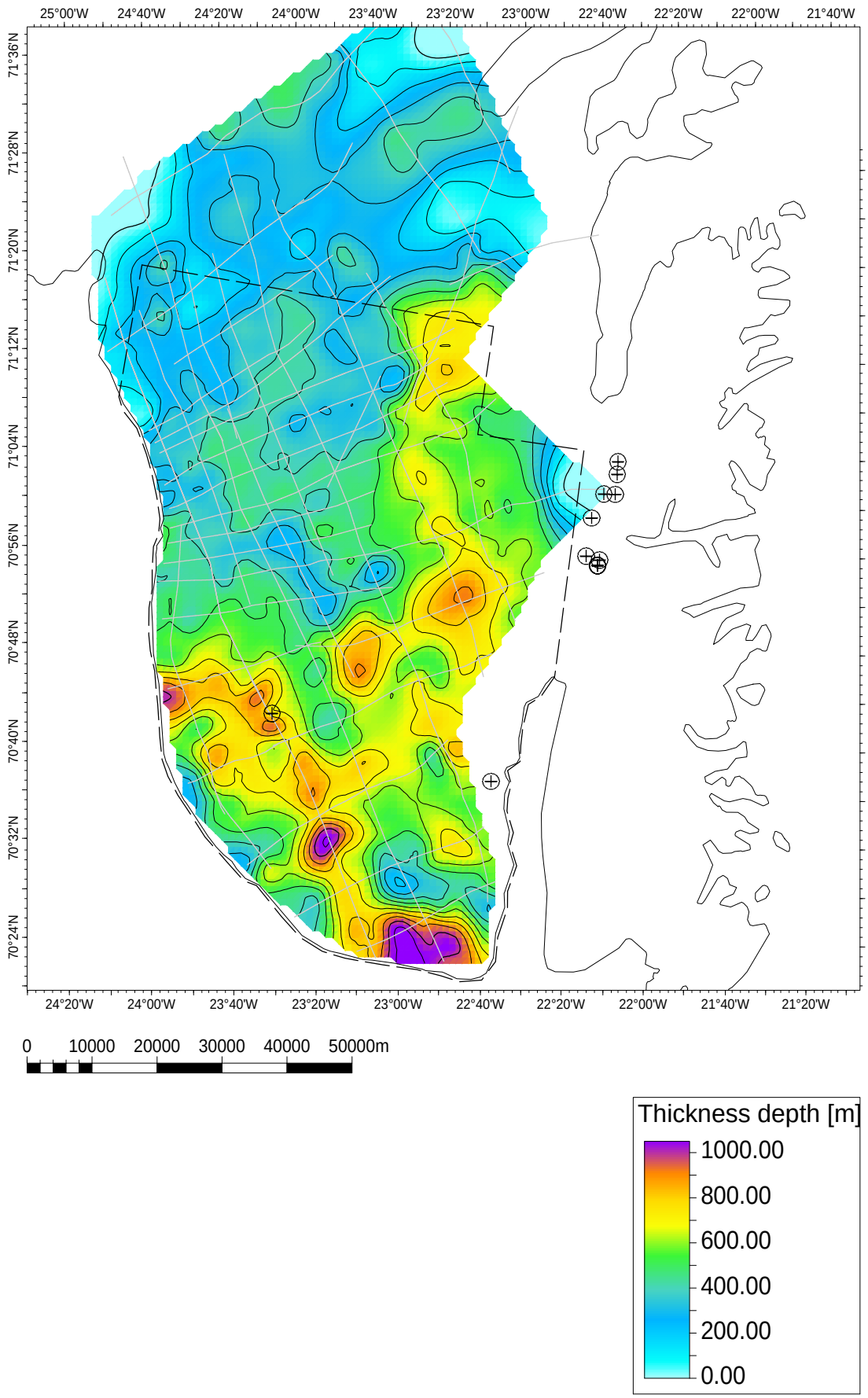

A2.5 Top NeillKlinterGr - Top KapStewartGr

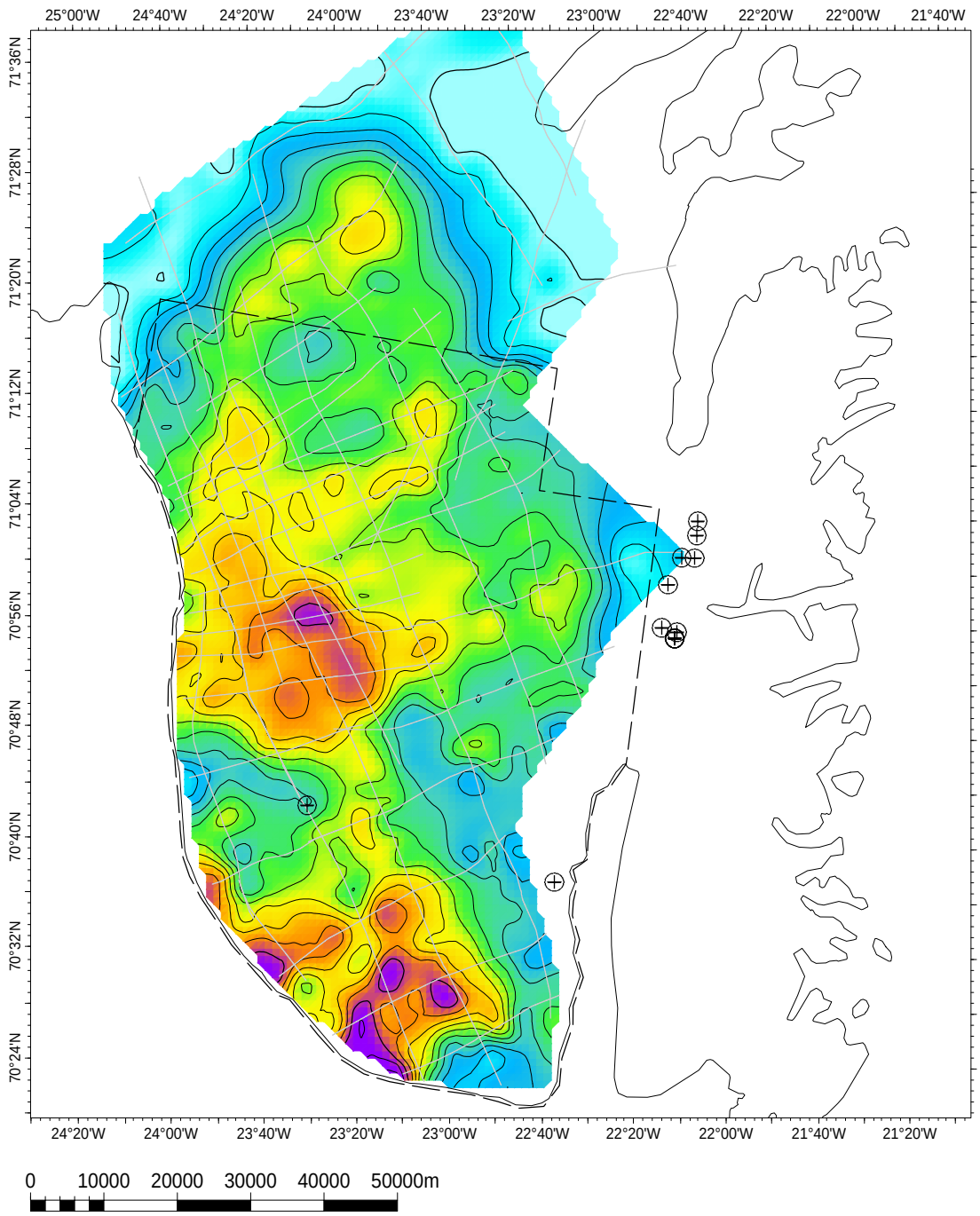

A2.6 Top Fossilbj/PelionFm - Top NeillKlinterGr